ISSN 2233-9485 (Print)
ISSN 2233-9574 (Online)

International Symposium on Magnetism and Magnetic Materials 2019

ABSTRACTS

Date	November 20-22 (Wed.-Fri.), 2019
Place	ICC JEJU, JEJU, Korea
Hosted by	The Korean Magnetics Society
Sponsored by	The Korean Federation of Science and Technology Societies (KOFST)

Digests of the International Symposium on Magnetism and Magnetic Materials 2019
The Korean Magnetics Society

International Symposium on Magnetism and Magnetic Materials 2019

ABSTRACTS

Date	November 20-22 (Wed.-Fri.), 2019
Place	INTERNATIONAL CONVENTION CENTER JEJU ICC JEJU, JEJU, Korea
Hosted by	The Korean Magnetics Society
Sponsored by	The Korean Federation of Science and Technology Societies (KOFST)

"This work was supported by the Korean Federation of Science and Technology Societies(KOFST) Grant funded by the Korean Government."

Notice

1. Presenters should follow the below guidelines.

1) The size of the board is 90cm(width) by 180cm(height).
2) The scheduled posters should be displayed from 09:00 to 18:00 on the day of their session. Poster Discussion will take place in the poster session room(Robby, 3rd Floor) from 17:00 to 18:00 and poster presenters must be present at their poster during this time.

2. Program at a Glance

<table>
<tr><td rowspan="4">Nov. 20(Wed.)</td><td>13:00~</td><td colspan="5">Registration</td></tr>
<tr><td>14:00~18:00</td><td colspan="5">Tutorial Program (Samda Hall, 3rd Floor)</td></tr>
<tr><td>18:00~19:00</td><td colspan="5">Dinner</td></tr>
<tr><td>19:00~21:00</td><td colspan="5">Ⓔ Special Session I (Samda Hall, 3rd Floor)</td></tr>
<tr><td rowspan="11">Nov. 21(Thu.)</td><td>08:30~</td><td colspan="5">Registration</td></tr>
<tr><td>09:00~12:00</td><td>Ⓔ Special Session II
(Samda Hall, 3rd Floor)</td><td>Oral Session I
(#301, 3rd Floor)</td><td colspan="2">Special Session III
(#303, 3rd Floor)</td><td rowspan="9">Poster Session
(Robby, 3rd Floor)</td></tr>
<tr><td>12:00~13:00</td><td colspan="4">Lunch</td></tr>
<tr><td>13:00~13:30</td><td colspan="4">Plenary Session I (Samda Hall, 3rd Floor)</td></tr>
<tr><td>13:30~15:30</td><td>Oral Session II
(Samda Hall, 3rd Floor)</td><td>Oral Session III
(#301, 3rd Floor)</td><td>13:30
~
14:50</td><td>Special Session IV
(#303, 3rd Floor)</td></tr>
<tr><td>15:30~15:40</td><td colspan="2">Coffee Break</td><td>14:50
~
14:55</td><td>Coffee Break</td></tr>
<tr><td>15:40~17:00</td><td>Oral Session IV
(Samda Hall, 3rd Floor)</td><td>Oral Session V
(#301, 3rd Floor)</td><td>14:55
~
17:00</td><td>Special Session V
(#303, 3rd Floor)</td></tr>
<tr><td>17:00~18:00</td><td colspan="3">Poster Discussion (Robby, 3rd Floor)</td></tr>
<tr><td>18:00~18:30</td><td colspan="5">Plenary Session II (Samda Hall, 3rd Floor)</td></tr>
<tr><td>18:30~19:00</td><td colspan="5">KMS Regular General Meeting & KMS Awards (Samda Hall, 3rd Floor)</td></tr>
<tr><td>19:00~20:30</td><td colspan="5">Banquet (Ocean View, 5th Floor)</td></tr>
<tr><td rowspan="4">Nov. 22(Fri.)</td><td>09:00~</td><td colspan="5">Registration</td></tr>
<tr><td>09:20~12:00</td><td colspan="3">Special Session VI (Samda Hall, 3rd Floor)</td><td>Special Session VII (Closed Session)
(#301, 3rd Floor)</td></tr>
<tr><td>12:00~13:00</td><td colspan="2">Closing Ceremony (Samda Hall, 3rd Floor)</td><td>12:00
~
14:00</td><td>Lunch</td></tr>
<tr><td colspan="3"></td><td>14:00
~
17:00</td><td>Special Session VII (Closed Session)
(#301, 3rd Floor)</td></tr>
</table>

3. The Poster Awards Ceremony will take place in the main room (Samda Hall, 3rd Floor) from 18:30 to 19:00 on November 21.
(If the winner (presenter) does not attend that time, the awards will be cancelled.)

Nov. 20 (Wed.)

Time	PROGRAM	
13:00 ~	**Registration**	
	Tutorial Program (Samda Hall, 3rd Floor) Chair : SungKyun Park(Pusan Nat'l Univ.)	
14:00 ~ 15:15	14:00 ~ 14:25	T-1. Soft Magnetic Materials: From Fundamentals to Applications Sang-Im Yoo(Seoul Nat'l Univ.)
	14:25 ~ 14:50	T-2. Soft Magnetic Materials and Their Application Derac Son(Hannam Univ.)
	14:50 ~ 15:15	T-3. Way for developing new high performance permanent magnet materials Hae-Woong Kwon(Pukyong Nat'l Univ.)
15:15 ~ 15:20	**Coffee Break**	
15:20 ~ 16:10	T-4. How neurons communicate to each other Chi Hye Chung(Konkuk Univ.)	
16:10 ~ 16:20	**Coffee Break**	
16:20 ~ 18:00	T-5. When topology meets strong interaction Sang-Jin Sin(Hanyang Univ.)	
18:00 ~ 19:00	**Dinner**	
	Ⓔ Special Session I (Samda Hall, 3rd Floor) **'Spin-Orbit Coupling Effects'** Chair : Hyun-Woo Lee(POSTECH)	
19:00 ~ 19:30	(Invited)S-I-1. Skyrmions, Antiskyrmions, Bobbers: New Particles for Information technology Stefan Blügel(Forschungszentrum Jülich and JARA)	
19:30 ~ 20:00	(Invited)S-I-2. Demonstration of Topological Stability of Magnetic Skyrmions Soong-Geun Je(Chonnam Nat'l Univ.)	
20:00 ~ 20:30	(Invited)S-I-3. Hydrodynamics of Spin Textures in Insulators Yaroslav Tserkovnyak(Univ. of California)	
20:30 ~ 21:00	(Invited)S-I-4. Optical spin-orbit torque in heavy metal/ ferromagnet heterostructures Gyung-Min Choi(Sungkyunkwan Univ.)	

Nov. 21 (Thu.)

Time	PROGRAM						
08:30 ~	**Registration**						
09:00 ~ 12:00		**Ⓔ Special Session II (Samda Hall, 3rd Floor) 'Spin-Orbit Coupling Effects'** Chair : Sug-Bong Choe (Seoul Nat'l Univ.)		**Oral Session I (#301, 3rd Floor) 'Soft/Hard Magnetics'** Chair : Haein Yim (Sookmyung Women's Univ.)		**Special Session III (#303, 3rd Floor) 'Magnetism in strongly correlated oxides and exotic materials'** Chair : Changhee Sohn (UNIST)	**Poster Session (Robby, 3rd Floor)** [1] Magnetic theory and calculation [2] Magnetization dynamics [3] Hard-magnetic Material [4] Soft-magnetic Material [5] Semiconductor spintronic [6] Spin orbit coupling and related phenomena [7] Nano-structured materials [8] Spin transfer torque for magnetic memory [9] Nanoscale Magnetics [10] Magnetic Oxides and Multiferroic [11] Biomedical Magnetic [12] Sensor and Application [13] 회원 참여 스페셜 세션 (자성소재, 부품, 장비핵심기술개발, 자기센서, 양자컴퓨팅, 산화물자성체, 의료장비 및 소재 등) [14] Others
	09:00 ~ 09:30	(Invited)S-II-1. Tracking the angular momentum flow of spin-orbit torques — Paul Haney (National Institute for Standards and Technology)	09:00 ~ 09:20	O-I-1. Fabrication and magnetic properties of Fe rich compound with a tetragonal $ThMn_{12}$ structure — Hui-Dong Qian (KIMS)	09:00 ~ 09:30	(Invited)S-III-1. Coupled spin-charge transport in oxide interface — Jung-Woo Yoo (UNIST)	
	09:30 ~ 10:00	(Invited)S-II-2. Semi-realistic tight-binding approach to spin-orbit physics at interfaces — Aurelien Manchon (KAUST)	09:20 ~ 09:40	O-I-2. Two-dimensional systems in curved geometry — Minkyu Park (Univ. of Ulsan)	09:30 ~ 10:00	(Invited)S-III-2. NMR investigation of a field-induced quantum spin liquid in α-$RuCl_3$ — Seung-Ho Baek (Changwon Nat'l Univ.)	
			09:40 ~ 10:00	O-I-3. Hot-deformation behavior of NdFeB magnet with Ce/La substitution — Ga-Yeong Kim (KIMS)			
	10:00 ~ 10:30	(Invited)S-II-3. Bulk-Boundary Correspondence for Spin Transport: Equivalence between Intrinsic Spin Hall Effect and Rashba-Edelstein Effect — Dongwook Go (POSTECH)	10:00 ~ 10:20	O-I-4. Effect of Initial Alloy on Coercivity Enhancement of Hot-deformed Magnet using Nd-Fe-B HDDR Powder — Jae-Gyeong Yoo (KIMS)	10:00 ~ 10:30	(Invited)S-III-3. A new quasi-one-dimensional $S = 1$ chain $NiTe_2O_5$ and its intriguing critical behavior — Yoon Seok Oh (UNIST)	
			10:20 ~ 10:40	O-I-5. Effect of post-sintering annealing conditions on the magnetic and microstructural properties of the multi main phase Nd-Ce-Fe-B sintered magnets — Kyoung-Hoon Bae (KIMS)			
	10:30 ~ 11:00	(Invited)S-II-4. Influences of interfacial oxidization on magnetic damping and spin-orbit-torques in Pt / ferromagnet / capping structures — Ouk Jae Lee (KIST)	10:40 ~ 11:00	O-I-6. A Study of Soft Magnetic Materials for Development of Economic Ignition Coil — Shin Gyu Kim (Hyundai Motor Company)	10:30 ~ 11:00	(Invited)S-III-4. Exotic phases and phase transitions in quantum magnets — Eun-Gook Moon (KAIST)	
	11:00 ~ 11:30	(Invited)S-II-5. Ferrimagnetic spintronics — Teruo Ono (Kyoto Univ.)	11:00 ~ 11:20	O-I-7. CFSM Design for EV Traction Comparing Vehicle System Efficiency — Kyoung-Soo Cha (Hanyang Univ.)	11:00 ~ 11:30	(Invited)S-III-5. Tunable real- and reciprocal-space topological properties in $SrRuO_3$ ultrathin films — Lingfei Wang (Seoul Nat'l Univ.)	
	11:30 ~ 12:00	(Invited)S-II-6. Magnetotransport and Magnetization Dynamics in Ferrimagnetic Alloys — Kab-Jin Kim (KAIST)	11:20 ~ 11:40	O-I-8. Effect of iron deficiency and La-Co substitution on the magnetic properties of Sr M-type hexaferrites — Kang Hyuk Lee (Seoul Nat'l Univ.)	11:30 ~ 12:00	(Invited)S-III-6. Magnetic field and thermal Hall effect in a pyrochlore U(1) quantum spin liquid — Sungbin Lee (KAIST)	
			11:40 ~ 12:00	O-I-9. Enhancement of magnetic properties of Fe-rich $Sm(Fe_{0.8}C_{0.2})_{11}Ti$ compounds by grain boundary diffusion process — Jung Tae Lim (KIMS)			

Nov. 21 (Thu.)

Time	PROGRAM						
12:00 ~ 13:00	**Lunch**						
	Plenary Session I (Samda Hall, 3rd Floor) Chair : Jongil Hong(Yonsei Univ.)						
13:00 ~ 13:30	(Invited)P-I-1. Recent Development Status of MTJ with TEL PVD EXIM™ Chang Man Park(Tokyo Electron U.S. Holdings, Inc.)						
13:30 ~ 15:30		**Oral Session II (Samda Hall, 3rd Floor) 'Spintronics I'** Chair : Sanghoon Kim (Univ. of Ulsan)		**Oral Session III (#301, 3rd Floor) 'Nano Magnetism'** Chair : June Seo Kim (DGIST)		**Special Session IV (#303, 3rd Floor) 'Mössbauer Session'** Chair : Young Rang Uhm (KAERI)	**Poster Session (Robby, 3rd Floor)** [1] Magnetic theory and calculation [2] Magnetization dynamics [3] Hard-magnetic Material [4] Soft-magnetic Material [5] Semiconductor spintronics [6] Spin orbit coupling and related phenomena [7] Nano-structured materials [8] Spin transfer torque for magnetic memory [9] Nanoscale Magnetics [10] Magnetic Oxides and Multiferroic [11] Biomedical Magnetic [12] Sensor and Application [13] 회원 참여 스페셜 세션 (자성소재, 부품, 장비핵심기술개발, 자기센서, 양자컴퓨팅, 산화물자성체, 의료장비 및 소재 등) [14] Others
	13:30 ~ 13:50	O-II-1. Strengths and angular dependence of spin-orbit torques in ferromagnet/normal metal heterostructures Hyung Keun Gweon (Korea Univ.)	13:30 ~ 13:50	O-III-1. Upshift of MnBi magnetic properties via process optimizations Yang Yang (KIMS)	13:30 ~ 13:50	(Invited)S-IV-1. Effects of In^{3+} site occupancy on the magnetic properties of M-type strontium hexaferrites Sunghyun Yoon (Gunsan Nat'l Univ.)	
	13:50 ~ 14:10	O-II-2. Magnetic Domain Wall Motion due to AC Bias-Driven Resonances Duck-Ho Kim (KIST)	13:50 ~ 14:10	O-III-2. The effect of Sn substitution on magnetic properties of MnBi Jong-Woo Kim (KIMS)	13:50 ~ 14:10	(Invited)S-IV-2. Analyses of Nano-Crystalline Structure in Precipitated Iron-Based Catalysts for Fischer-Tropsch Synthesis Dong Hyun Chun (KIER)	
	14:10 ~ 14:30	O-II-3. Static and dynamic modes of magnetic skyrmions in magnetic nanotubes Jaehak Yang (Seoul Nat'l Univ.)	14:10 ~ 14:30	O-III-3. W Thickness-Dependent Perpendicular Magnetocrystalline Anisotropy of Pt/Co/W(111) Superlattices Ho Huynh Thi (Univ. of Ulsan)	14:10 ~ 14:30	(Invited)S-IV-3. Study on Multiferroic materials using Mössbauer Spectroscopy Sung Baek Kim (Konyang Univ.)	
	14:30 ~ 14:50	O-II-4. Influence of vanadium incorporation on spin-orbit torque efficiency in W/W-V/CoFeB/MgO structures Gyu Won Kim (Korea Univ.)	14:30 ~ 14:50	O-III-4. Spin-orbit-induced field in GaMnAs/Bi_2Se_3 bilayer system Kyung Jae Lee (Korea Univ.)	14:30 ~ 14:50	(Invited)S-IV-4. Introduction of In-beam Mössbauer spectroscopy and its application of Heritage analysis Young Rang Uhm (KAERI)	
	14:50 ~ 15:10	O-II-5. Observation of Positive and Negative Spin-Transfer Torques in Chiral Domain-Wall Motion Dae-Yun Kim (KIST)	14:50 ~ 15:10	O-III-5. Zn substituted Strontium W-type hexaferrite in Ka band (26.5–40 GHz) for microwave absorber Sungjoon Choi (Seoul Nat'l Univ.)	14:50 ~ 14:55	**coffee break**	
						Special Session V (#303, 3rd Floor) ' Magnetic Materials and Components Related to Japan's Export Restrictions' Chair : Jung-Goo Lee (KIMS)	
			15:10 ~ 15:30	O-III-6. Ferromagnetic resonance effect in superparamagnetic iron oxide nanoparticles and its application for hyperthermia Jae-Hyeok Lee (Seoul Nat'l Univ.)	14:55 ~ 15:20	(Invited)S-V-1. Amorphous Soft Magnetic Powders for High-Frequency Inductors Jae Won Jeong (KIMS)	
					15:20 ~ 15:45	(Invited)S-V-2. Recent Developments of Electrical Steel in Korea Eonbyeong Park (RIST)	
15:30 ~ 15:40	**coffee break**						

Nov. 21 (Thu.)

<table>
<tr><th>Time</th><th colspan="6">PROGRAM</th></tr>
<tr><td rowspan="5">15:40
~
17:00</td><td></td><td>Oral Session IV
(Samda Hall, 3rd Floor)
'Spintronics II'
Chair : Chun-Yeol You
(DGIST)</td><td></td><td>Oral Session V
(#301, 3rd Floor)
'Magnetics Theory/Oxide'
Chair : Eun-Gook Moon
(KAIST)</td><td rowspan="2"></td><td rowspan="2"></td></tr>
<tr><td>15:40
~
16:00</td><td>O-IV-1.
Coexisting and strongly interacting spin torque driven free and reference layer magnetic droplet solitons
Sunjae Chung
(Korea Nat'l Univ. of Education)</td><td>15:40
~
16:00</td><td>O-V-1.
Magnetic parameter estimation using Deep learning techniques
Heeyoung Kwon
(KIST)</td></tr>
<tr><td>16:00
~
16:20</td><td>O-IV-2.
Tunable magnetic properties via interface engineering
June-Seo Kim
(DGIST)</td><td>16:00
~
16:20</td><td>O-V-2.
The Intrinsic Spin Hall Conductivity of α-Ta and α-W: first principles study
Do Duc Cuong
(Univ. of Ulsan)</td><td>15:45
~
16:10</td><td>(Invited)S-V-3.
Perspective and prospects for rare earth permanent magnets
Dong-Hwan Kim
(STARGROUPIND.CO.,LTD)</td></tr>
<tr><td>16:20
~
16:40</td><td>O-IV-3.
Control of the skyrmion Hall effect via external magnetic fields
Seungmo Yang
(KRISS)</td><td>16:20
~
16:40</td><td>O-V-3.
First principles study on magnetic anisotropy mechanism in tetragonal distorted structural phases of Fe_2YZ based Heusler alloys (Y= Mn, Pt; Z = Ge,Sn)
Thu Thuy Hoang
(Univ. of Ulsan)</td><td>16:10
~
16:35</td><td>(Invited)S-V-4.
High frequency magnetic material technologies and related industrial issues in the EMC industry
Kyung-sub Lee
(NOPION Co. Ltd)</td></tr>
<tr><td>16:40
~
17:00</td><td>O-IV-4.
Influences of Co-substitution on Magnetic Properties of Tetragonal $D0_{22}$-Mn_3Ga
Thi Quynh Anh Nguyen
(Univ. of Ulsan)</td><td>16:40
~
17:00</td><td>O-V-4.
SrFeOx: discovery of ReRAM and spectroscopic study on its unique switching mechanism
Chang Uk Jung
(Hankuk Univ. of Foreign Studies)</td><td>16:35
~
17:00</td><td>(Invited)S-V-5.
Study on the Design of Power Density Improvement for Reducing Material Using Motor-Generator
Dong-Woo Kang
(Keimyung Univ.)</td></tr>
<tr><td>17:00
~
18:00</td><td colspan="6">Poster Discussion (Robby, 3rd Floor)
Chairs : Jung-Goo Lee(KIMS) / S. H. Sonny Rhim(Univ. of Ulsan) / Haein Yirn(Sookmyung Women's Univ.)</td></tr>
<tr><td></td><td colspan="6">Plenary Session II (Samda Hall, 3rd Floor)
Chair : Jong-Ryul Jeong(Chungnam Nat'l Univ.)</td></tr>
<tr><td>18:00
~
18:30</td><td colspan="6">(Invited)P-II-1.
Present of MRAM development in Samsung
D. S. Kim(Samsung Electronics Corp.)</td></tr>
<tr><td>18:30
~
19:00</td><td colspan="6">KMS Regular General Meeting & KMS Awards (Samda Hall, 3rd Floor)</td></tr>
<tr><td>19:00
~
20:30</td><td colspan="6">Banquet (Ocean View, 5th Floor)</td></tr>
</table>

Nov. 22(Fri.)

Time	PROGRAM			
09:00 ~	**Registration**			
09:20 ~ 12:00	**Special Session VI** **(Samda Hall, 3rd Floor)** **'Medical Magnetics'** Chair : Woo Sang Ahn(Univ. of Ulsan College of Medicine) / Man-Seok Han(Kangwon Nat'l Univ.)			**Special Session VII** **(#301, 3rd Floor)** **'High Clarke number element based Supermagnet'** **(Closed Session)** Chair : Chul Jin Choi(KIMS)
	09:20 ~ 09:40	(Invited)S-VI-1. Investigation of transverse magnetic field induced dose effects in inhomogeneous medium on small fields of medical linear accelerator Woo Sang Ahn (Univ. of Ulsan College of Medicine)	09:20 ~ 10:00	(Invited)S-VII-1. The Practical Energy Product of Hard- and Soft-magnetic Core/Shell Cylinder Ki-Suk Lee(UNIST)
	09:40 ~ 10:00	(Invited)S-VI-2. Fundamental Study on Optimization and Measurement Protocols of Alanine/ESR System Ki Tek Han (Korean Association for Radiation Application)		
	10:00 ~ 10:20	(Invited)S-VI-3. Metal artifact reduction of silicon material in head and neck cancer with metal So Hyun Park (Jeju Nat'l Univ. Hospital)	10:00 ~ 10:40	(Invited)S-VII-2. First-Principles Materials Design of Rare-Earth Free Permanent Magnets with High Energy Product and Good Thermal Stability D. Odkhuu(Incheon Nat'l Univ.)
	10:20 ~ 10:40	**coffee break**		
	10:40 ~ 11:00	(Invited)S-VI-4. A Feasibility Study of Fan-beam DEXA detector based LYSO and GAPD Jingyu Yang (Chonnam Nat'l Univ.)	10:40 ~ 11:20	(Invited)S-VII-3. The effect of grain size, grain boundary materials, and grain boundary thickness on the magnetic properties of Fe-based magnetic materials Ho-Sup Kim(KERI)
	11:00 ~ 11:20	(Invited)S-VI-5. Changes according to the lead thickness for Shielding evaluation Dong Hee Han (Kangwon Nat'l Univ.)		
	11:20 ~ 11:40	(Invited)S-VI-6. The effects of motor imagery combined with functional electrical stimulation on cerebral cortex excitability in stroke patients Jong-Bae Choi (KyungHee Univ. Medical Center)	11:20 ~ 12:00	(Invited)S-VII-4. Synthetic methods for magnetically enhanced rare-earth free MnBi magnets Jong-Woo Kim(KIMS)
	11:40 ~ 12:00	(Invited)S-VI-7. Interplay Effect in Proton Scanning Therapy by Magnetic Scanner Jeongmin Seo (Catholic Univ. of Pusan)		
12:00 ~ 13:00	**Closing Ceremony** **(Samda Hall, 3rd Floor)**		12:00 ~ 14:00	**Lunch**

Nov. 22(Fri.)

Time	PROGRAM	
	Special Session VII **(#301)** **'High Clarke number element based Supermagnet'** **(Closed Session)** Chair : Chul Jin Choi (KIMS)	
	14:00 ~ 14:40	(Invited)S-VII-5. Fabrication of Powder Making and Bulk Process for Fe Rich Magnetic Compound with $ThMn_{12}$ Structure Jihoon Park (KIMS)
	14:40 ~ 15:20	(Invited)S-VII-6. Synthesis and Characterization of $ThMn_{12}$-type by nitridation reaction Sang-Im Yoo (Seoul Nat'l Univ.)
	15:20 ~ 16:00	(Invited)S-VII-7. Control of morphology in hard magnetic Sm-Co nanofibers Jongryoul Kim (Hanyang Univ.)
	16:00 ~ 17:00	Discussion of current issues

CONTENTS

Nov. 21(Thu.), 09:00~12:00
Ⓔ Special Session II 'Spin-Orbit Coupling Effects'

Samda Hall, 3rd Floor

Chair : Sug-Bong Choe(Seoul Nat'l Univ.)

Nov. 21(Thu.), 09:00~12:00
Oral Session I 'Soft/Hard Magnetics'

#301, 3rd Floor

Chair : Haein Yim(Sookmyung Women's Univ.)

Nov. 21(Thu.), 09:00~12:00
Special Session III 'Magnetism in strongly correlated oxides and exotic materials'

#303, 3rd Floor

Chair : Changhee Sohn(UNIST)

Nov. 21(Thu.), 13:00~13:30
Plenary Session I

Samda Hall, 3rd Floor

Chair : Jongil Hong(Yonsei Univ.)

Nov. 21(Thu.), 13:30~15:10
Oral Session II 'Spintronics I'

Samda Hall, 3rd Floor

Chair : Sanghoon Kim(Univ. of Ulsan)

Nov. 21(Thu.), 13:30~15:30
Oral Session III 'Nano Magnetism'

#301, 3rd Floor

Chair : June Seo Kim(DGIST)

Nov. 21(Thu.), 13:30~14:50
Special Session IV 'Mössbauer Session'
#303, 3rd Floor

❀ Chair : Young Rang Uhm(KAERI)

Nov. 21(Thu.), 15:40~17:00
Oral Session IV 'Spintronics II'
Samda Hall, 3rd Floor

❀ Chair : Chun-Yeol You(DGIST)

Nov. 21(Thu.), 15:40~17:00
Oral Session V 'Magnetics Theory/Oxide'

#301, 3rd Floor

Chair : Eun-Gook Moon(KAIST)

Nov. 21(Thu.), 14:55~17:00
Special Session V 'Magnetic materials and Components related to Japan's export restrictions'

#303, 3rd Floor

Chair : Jung-Goo Lee(KIMS)

Nov. 21(Thu.), 17:00~18:00
Poster Session

Robby, 3rd Floor

❀ Chairs : Jung-Goo Lee(KIMS) / S. H. Sonny Rhim(Univ. of Ulsan) / Haein Yim(Sookmyung Women's Univ.)

○ Session MT[Magnetic theory and calculations]

○ **Session MD[Magnetization dynamics]**

○ Session SM[Soft-magnetic Materials]

○ Session SS[Semiconductor spintronics]

○ Session SO[Spin orbit coupling and related phenomena]

○ **Session NS[Nano-structured materials]**

○ Session SA[Sensor and Applications]

Nov. 21(Thu.), 18:00~18:30 Plenary Session II

Samda Hall, 3rd Floor

Chair : Jong-Ryul Jeong(Chungnam Nat'l Univ.)

Nov. 22(Fri.), 09:20~12:00 Special Session VI 'Medical Magnetics'

Samda Hall, 3rd Floor

Chairs : Woo Sang Ahn(Univ. of Ulsan College of Medicine) / Man-Seok Han(Kangwon Nat'l Univ.)

Nov. 22(Fri.), 09:20~17:00

Special Session VII 'High Clarke number element based Supermagnet' (Closed Session)

#301, 3rd Floor

Chair : Chul Jin Choi(KIMS)

International Symposium on Magnetism and Magnetic Materials 2019

Tutorial Program

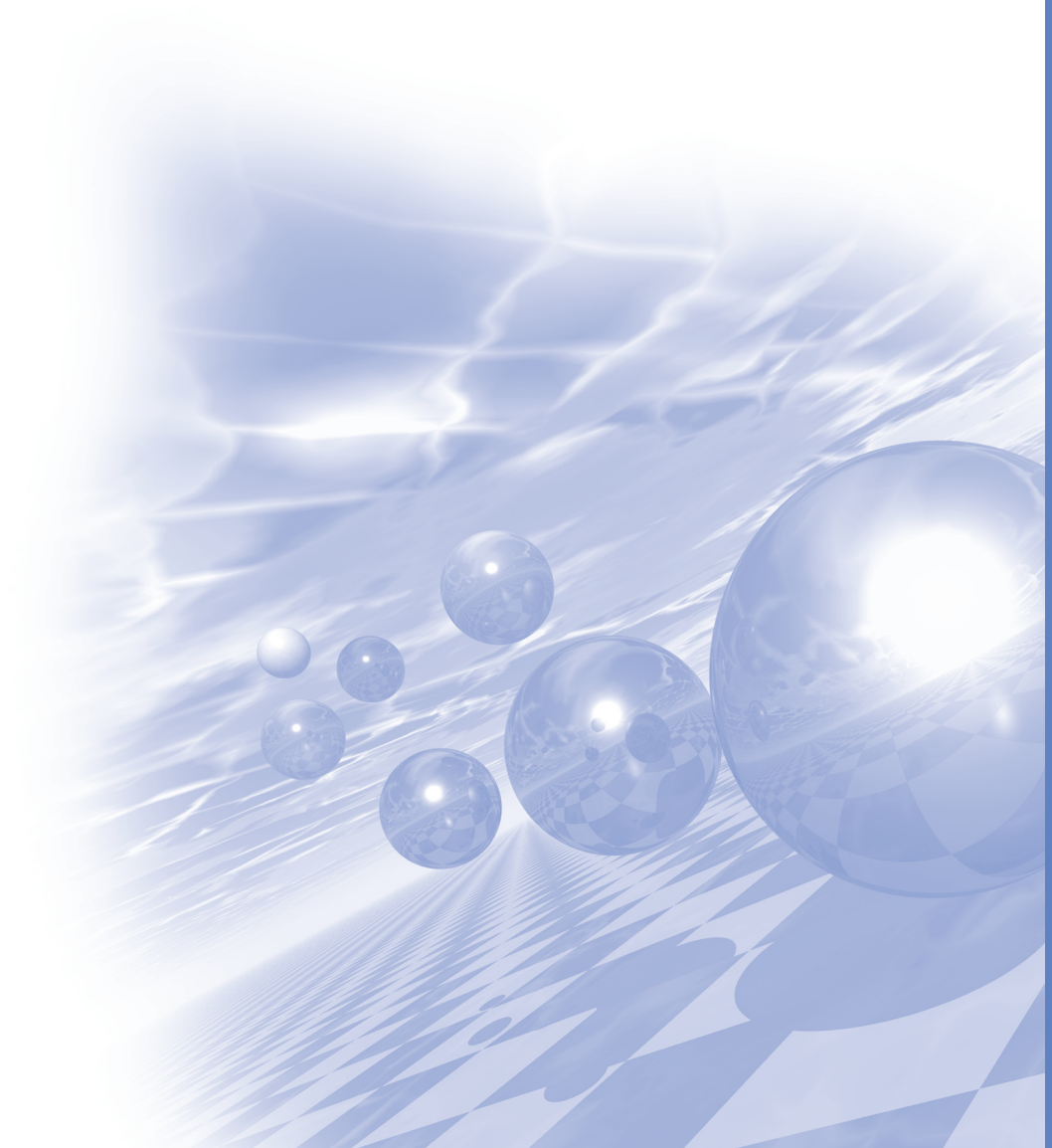

Soft Magnetic Materials: From Fundamentals to Applications

Sang-Im Yoo*
Department of Materials Science and Engineering & Research Institute of Advanced Materials,
Seoul National University, Seoul 151-744, Korea

In this tutorial lecture, I will explain the soft magnetic materials by dividing into two different parts of fundamentals and applications. In the part of fundamentals, after a brief explanation for material classification between soft and hard magnets, I will explain important characteristics of soft magnets required for real applications, including permeability, coercivity, saturation magnetization, remanence, hysteresis loss, and microwave absorbance. In the part of applications, I will review soft magnetic materials and their production technologies for real applications. Typical materials include electrical steels like low-carbon steel and silicon steel, Fe-Ni permalloy, Fe-Co permendur, amorphous/nanocrystalline alloys, and soft ferrites. Real applications include both DC and AC applications.

T-2

Soft Magnetic Materials and Their Application

Derac Son*
Department of Optics and Electromagnetics, Hannam University, Korea

Soft magnetic materials are classified as coercivity of ferromagnetic or ferrimagnetic materials lower than 1 000 A/m in IEC standard IEC60404-1. Soft magnetic materials have been traditionally used for electromagnets, transformers and electric motors. Nowadays in forth industrial evolution and unmanned technology, compact and high facility of electric machines become more and more important because of easy control by means of electric power with power semiconductor device and micro-processor technology. LED lighting and adopter of smart phone need also a lot of high frequency chip inductors. Diverse use of soft magnetic materials in many electric devices requires various magnetic properties.

In this presentation, soft magnetic materials used for AC and DC electromagnet, transformer cores used for line frequency, audio frequency, and SMPS. Also inductor used for line frequency and PWM power supplies.

Quantity of magnetic materials used for sensors and actuators are small but it`s economic effect is very high. Some magnetic materials used in sensors also introduced.

Way for developing new high performance permanent magnet materials

Hae-Woong Kwon*
Pukyong National University, Busan, Republic of Korea 48513

Current high performance Nd-Fe-B-type magnet has chronic apprehension of limited supply and volatile price of raw materials (rare-earth metals) and poor thermal stability (in particular, large temperature coefficient of coercivity(b)) due to low Curie temperature, but is otherwise almost a perfect permanent magnet. As demand of the Nd-Fe-B-type magnet for various industries such as HEV and EV has increased, limited supply and volatile price of rare-earth metals have become more of a concern. Therefore, now more than ever, finding new materials containing no rare-earth metals is in urgent and constant demand. To address the growing demand for new permanent magnet materials, an extensive effort has been made for finding new rare-earth-free permanent magnet materials. Most of the activities have been focused upon finding materials based on abundant transition metals. Among technical quandaries with the transition metal based materials is difficulty of achieving sufficient coercivity, and researchers seemingly have thrown everything at the achieving coercivity. When it comes to developing transition metal based permanent magnet materials, the importance of achieving sufficient coercivity can't be overstated. But the fact of the matter is that, together with sufficient coercivity, good texture would also be as crucial for achieving high magnetic performance in the new materials. Achieving good texture in the transition metal based materials could be more difficult than getting coercivity. The leading-edge technologies of achieving coercivity and texture in the conventional permanent magnets are reviewed, and take full advantage of them for developing new rare-earth-free permanent magnet materials such as transition metal based materials.

T-4

How neurons communicate to each other

Chi Hye Chung*
Neurophysiology laboratory, Department of Biological Sciences, Konkuk University, Seoul, Korea

Neurons are communicating by using both electrical and chemical signals. Within a single neuron, information passes through by electrical forms although the nature of electrical signal differs depending on where in a neuron. When information transfers between two neurons, the electrical signal is converted into a chemical signal at the end of presynaptic terminal, which in turn evokes electrical signals in the next (postsynaptic)neuron. In this tutorial, I will describe the basic characteristics and working principles of neurons and synapses and explain how electrical and chemical signals are generated and integrated.

When topology meets strong interaction

Sang-Jin Sin*
Dept. of Physics, Hanyang University

After discussing Topology in real space using kink and Skyrrmion (20 min), we move to Topology in momentum space which is so called topological band theory (20min).

After discussing Topological invariant. Z vs. Z2 (20min), we discuss the Dirac and Weyl Semi-metals(20min).

Finally, we discuss the effects of interaction and temperature against stability of the topological matter using the holographic principle (20min).

International Symposium on Magnetism and Magnetic Materials 2019

Special Session I

'Spin-Orbit Coupling Effects'

Skyrmions, Antiskyrmions, Bobbers: New Particles for Information technology

Stefan Blügel*, Juba Bouaziz, Sergii Grytsiuk, Jan-Phillip Hanke, Markus Hoffmann, Hongying Jia, Gideon P. Müller, Bernd Zimmermann, Gustav Bihlmayer, Samir Lounis, Nikolai S. Kiselev, Yuriy Mokrousov

Peter Grünberg Institute and Institute for Advanced Simulation, Forschungszentrum Jülich and JARA, Germany

Chiral magnets are an emerging class of topological matter harboring localized and topologically protected vortex-like magnetic textures called skyrmions, which are currently under intense scrutiny as a new entity for information storage and processing. It is an important mosaic stone of the bigger field of spin-orbitronics. The real-space topology of the magnetization texture offers interesting dynamical and transport properties. Chirality in magnetism is introduced through the chiral symmetry breaking Dzyaloshinskii-Moriya interaction (DMI), which arizes through the spin-orbit interaction in magnets with structural bulk and interface inversion asymmetry. We have shown that chiral magnets cannot only host skyrmions but also antiskyrmions and chiral bobbers as localized magnetization particles.

We discuss the stability of skyrmions on the level of a micromagnetic energy functional elucidating the role of the DMI. The energy and size of the skyrmions is determined by the competition between the Heisenberg, Dzyaloshinskii-Moriya (DMI), and Zeeman interaction together with the magnetic anisotropy energy (MAE). We discuss examples of bulk and interface stabilized skyrmions. With respect to future applications, interfaces offer a great variety of options for optimizing and controlling magnetic parameters of the various interactions. We will present some selected examples where the variation of the interface composition [1, 2], of the interface crystal symmetry [3], as well as the fabrication of interlayers [4] and multilayers [5,6] are chosen such as to obtain skyrmions with sizes and temperature stability suitable for technology, e.g. in the context of the race track memory.

We will report about a recent work [3] were we extended the scope of skyrmions to antiskyrmions and introduced a classification scheme partitioning chiral magnets into isotropic rank-three DM bulk and rank-two DM film magnets, described by an isotropic DM interaction expressed by a single DMI constant in the micromagnetic theory, for which antiskyrmions are stable only for bulk crystals with certain point group symmetries. Newly introduced are the anisotropic rank-two DMI film magnets, where skyrmions and antiskyrmions can coexist, while the sign of the determinant of the micromagnetic DM matrix determines which of the two has the lower energy. Finally, zero determinant indicates a rank-one DMI material, for which skyrmions and antiskyrmions have the same energy. Employing the methodology introduced above we conjecture that a Fe double on W(110) provides a possible system that hosts antiskyrmions.

Recently, we were able to extend the scope of skyrmions to a second class of particles, the chiral magnetic bobber (CB), first through theoretical analysis [7] and then veryfied experimentally by the direct observation in thin films of B20-type FeGe by means of quantitative off-axis electron holography [8]. The CB is a localized three-dimensional hybrid particle on the nanoscale composed of both the smooth magnetization texture of skyrmions and a Bloch point, singularity in the micromagnetic theory of smooth magnetizations textures playing

the role of a monopole. The interaction of electrons with such hybrid-objects. e.g. to understand how to move CB by spin currents is subject to ongoing investigations.

We acknowledge funding from Deutsche Forschungsgemeinschaft (DFG) through SPP 2137 “Skyrmionics” the CRC 1238 (C1), and SFB/TRR 173 (MO 1731/5-1), the Icelandic Research Fund (grant no. 152483-052), the DARPA TEE program (#HR0011831554) from DOI, and ERC-consolidator grant 681405 – DYNASORE, as well as computing time from HLRN and Jülich Supercomputing Centre (projects jias1a and jias1f) and JARA-HPC of RWTH Aachen University.

References

[3] S. Heinze et al., Nature Phys. **7,** 713 (2011).

[1] A. Belabbes, G. Bihlmayer, F. Bechstedt, S. Blügel, A. Manchon, Phys. Rev. Lett **117,** 247202 (2016).

[2] B. Zimmermann, W. Legrand, D. Maccariello, N. Reyren, V. Cros, S. Blügel, A. Fert, Appl. Phys. Lett. **113,** 232403 (2018).

[3] M. Hoffmann, B. Zimmermann, G. P. Müller, D. Schürhoff, N. S. Kiselev, C. Melcher, S. Blügel, Nat. Commun. **8**, 308 (2017).

[4] A. Nandy, N. S. Kiselev, S. Blügel, Phys. Rev. Lett. **116**, 177202 (2016).

[5] B. Dupé, G. Bihlmayer, M. Böttcher, S. Blügel, S. Heinze, Nature Commun. **7**, 11779 (2016).

[6] H. Jia, B. Zimmermann, S. Blügel, Phys. Rev. B **98**, 144427 (2018).

[7] F. N. Rybakov, A. B. Borisov, S. Blügel, N. S. Kiselev, Phys. Rev. Lett. **115**, 117201 (2015), ibid New J. Phys. **18**, 045002 (2016).

[8] Fengshan Zheng et al., Nature Nanotechnology **13**, 451 (2018).

Demonstration of Topological Stability of Magnetic Skyrmions

Soong-Geun Je[1,2,3*], Hee-Sung Han[4], Se Kwon Kim[5], Sergio A. Montoya[6], Weilun Chao[1], Ik-Sun Hong[7], Eric E. Fullerton[8,9], Ki-Suk Lee[4], Kyung-Jin Lee[7,10], Mi-Young Im[1], Jung-Il Hong[2]

[1]Center for X-ray Optics, Lawrence Berkeley National Laboratory, Berkeley, CA, USA.
[2]Department of Emerging Materials Science, DGIST, Daegu, Korea.
[3]Department of Physics, Chonnam National University, Gwangju, Korea
[4]School of Materials Science and Engineering, Ulsan National Institute of Science and Technology, Ulsan, Korea.
[5]Department of Physics and Astronomy, University of Missouri, Columbia, MO, USA.
[6]Space and Naval Warfare Systems Center Pacific, San Diego, CA, USA.
[7]KU-KIST Graduate School of Converging Science and Technology, Korea University, Seoul, Korea.
[8]Center for Memory and Recording Research, University of California – San Diego, La Jolla, CA, USA.
[9]Department of Electrical and Computer Engineering, University of California – San Diego, La Jolla, CA, USA.
[10]Department of Materials Science and Engineering, Korea University, Seoul, Korea.

Topological concept, initially introduced in particle physics, brought new excitements to many other fields of physics such as topological insulators, ultracold atoms, and topological lasers to unveil various robust states therein. In nanomagnetism, the most prominent example governed by topology is the magnetic skyrmion. The magnetic skyrmion is topologically nontrivial spin texture. Therefore, it has sparked considerable interest due to the academical interest and the prospect of employing the skyrmions as the nanometer-scale non-volatile information carriers.

Although profound the concept is, the realistic situation that magnetic moments are localized in a discrete atomic lattice raises an immediate question of whether the topological concept is still viable in the real system. Despite the fundamental importance, the thorough assessment has remained elusive due to the challenge of controlling topology, and thereby directly comparing the topologically nontrivial skyrmions and trivial bubbles in a single specimen.

Here we report how to manipulate topology and how robust the magnetic skyrmion structure in comparison with the stability of topologically trivial bubbles for the first time. By measuring the lifetimes of both skyrmions and bubbles in the same specimen, we found that magnetic skyrmion exhibit far longer lifetime (Fig.1), directly evidencing the topological effect in a real discrete system.

Our results corroborate the physical importance of the topology in the magnetic materials and open up a versatile route towards the topology manipulation, which will facilitate the implementation of ever-stable nanometer-scale magnetic devices.

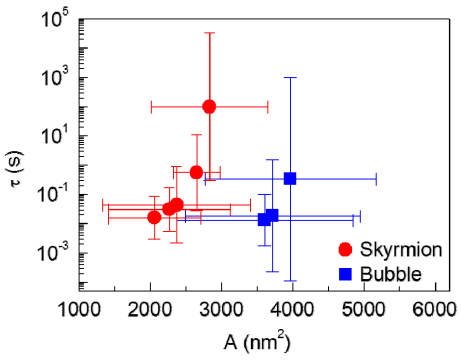

Fig. 1. Lifetimes of the magnetic skyrmion and the bubbles as a function of the size of the spin textures.

Hydrodynamics of Spin Textures in Insulators

Yaroslav Tserkovnyak*
Department of Physics and Astronomy, University of California, Los Angeles, CA 90095 USA

I will discuss recent progress on understanding and harnessing novel collective transport phenomena in magnetic insulators. Central to this talk will be conservation laws that are rooted in topological invariants associated with magnetic textures, irrespective of the existence of any global symmetries. In one example, the emergent hydrodynamics closely mimics neutral superfluidity, which may allow to establish and utilize superflows in solid-state devices at room temperature. Other examples will include magnetic films harboring skyrmionic textures and, surprisingly, disordered glassy spin systems. Recently developed magnetoelectric and thermoelectric techniques are now allowing us to explore this physics in a range of materials, both old and new.

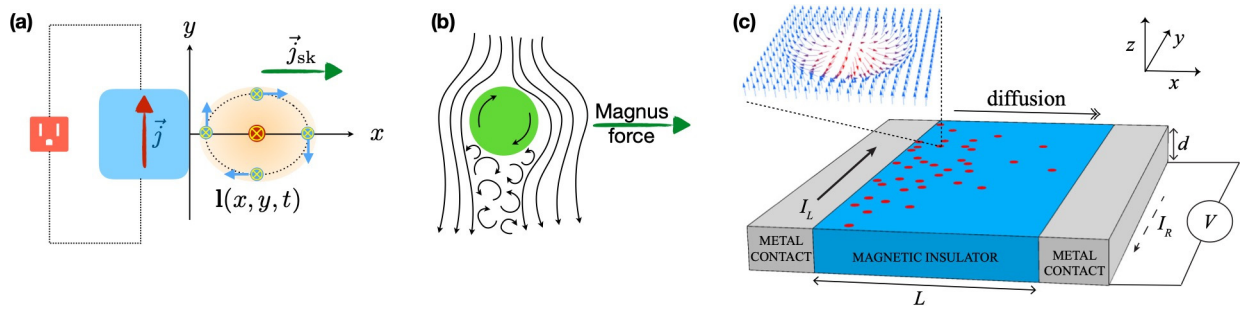

Optical spin-orbit torque in heavy metal/ ferromagnet heterostructures

Gyung-Min Choi[1,2,3†*], Jung Hyun Oh[4†], Dong-Kyu Lee[4], Seo-Won Lee[4], Kun Woo Kim[5], Mijin Lim[6], Byoung-Chul Min[3], Kyung-Jin Lee[4,7*], and Hyun-Woo Lee[6*]

[1]Department of Energy Science, Sungkyunkwan University, Suwon 16419, Korea
[2]Center for Integrated Nanostructure Physics, Institute for Basic Science (IBS), Suwon 16419, Korea
[3]Center for Spintronics, Korea Institute of Science and Technology, Seoul 02972, Korea
[4]Department of Materials Science and Engineering, Korea University, Seoul 02841, Korea
[5]Center for Theoretical Physics of Complex Systems, Institute for Basic Science (IBS), Daejeon 34051, Korea
[6]Department of Physics, Pohang University of Science and Technology, Pohang 37673, Korea
[7]KU-KIST Graduate School of Converging Science and Technology, Korea University, Seoul 02841, Korea

Spin current generation through the spin-orbit interaction in non-magnetic materials lies at the heart of spintronics. Electrically generated spin currents through the spin Hall effect produce spin-orbit torques when injected to a ferromagnet, and manipulate its magnetization efficiently. Optically generated spin currents are expected to be superior to their electrical counterpart in terms of the manipulation speed. Here we report optical spin-orbit torques in heavy metal/ferromagnet heterostructures. The strong spin-orbit coupling of heavy metals induces photo-excited carriers to be spin polarized, and their spin-polarized transport from heavy metals to ferromagnets generates a torque on magnetization. Our results demonstrate that heavy metals can generate spins not only electrically but also optically.

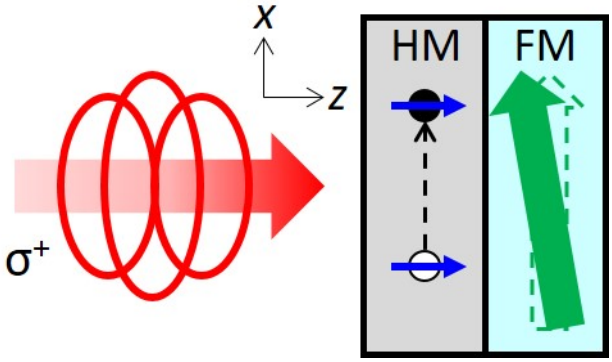

Fig. 1. Schematics for optical spin-orbit torque. A light produces spin polarization on heavy metal (HM). A spin current from heavy metal to ferromagnetic metal (FM) produces a torque on magnetization.

International Symposium on Magnetism and
Magnetic Materials 2019

Special Session II

'Spin-Orbit Coupling Effects'

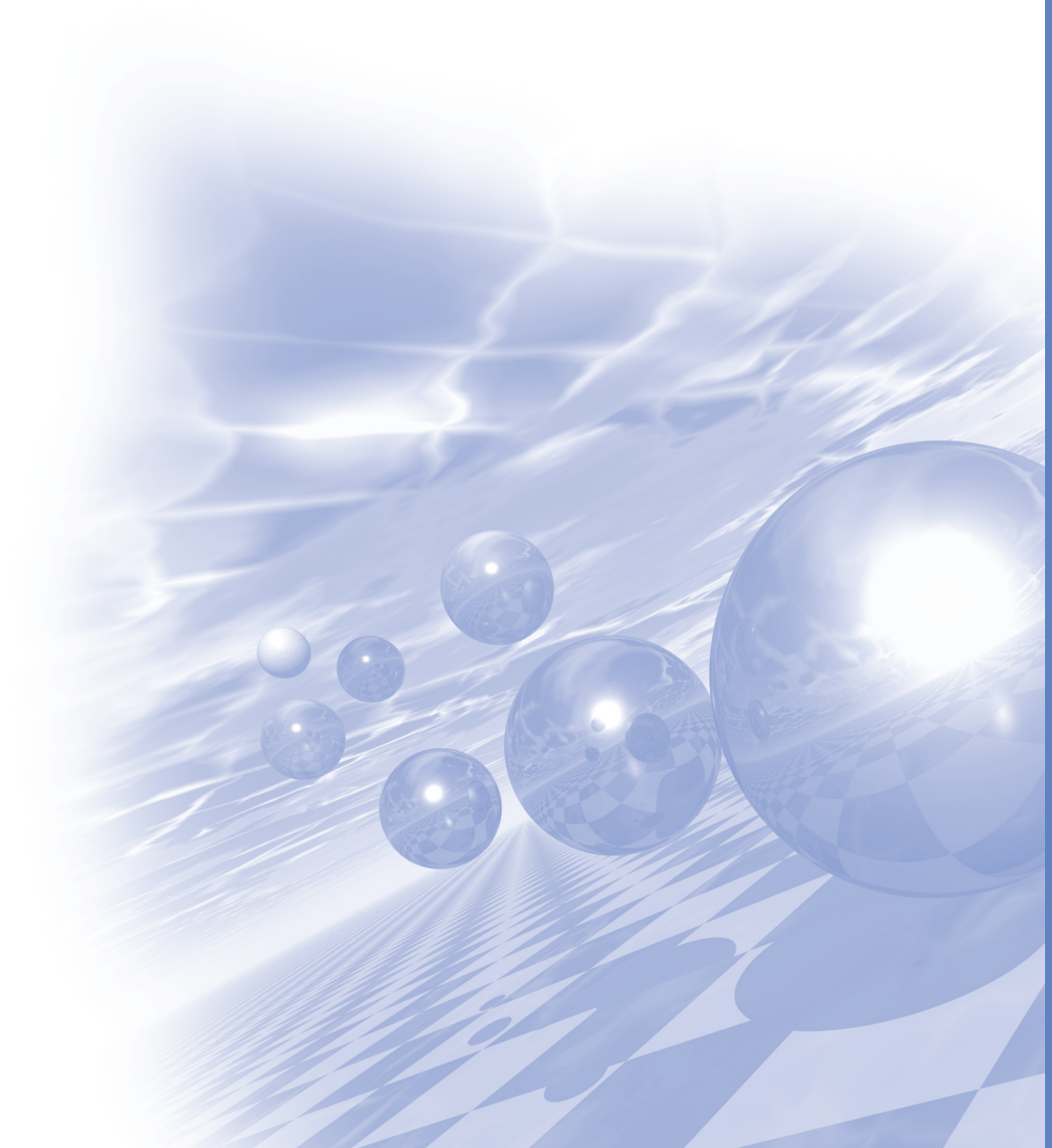

Tracking the angular momentum flow of spin-orbit torques

Paul Haney[1*], Fei Xue[1,2], Vivek Amin[1,2], Mark Stiles[1]
[1]National Institute for Standards and Technology, Physical Measurement Laboratory
[2]Maryland NanoCenter, University of Maryland at College Park

Magnetic systems with broken inversion symmetry exhibit a wide array of phenomena that enable the electrical control of magnetization. Tracking the electric-field induced flow of angular momentum responsible for magnetic torques provides insight into the origin and properties of these torques. In this talk, I'll discuss recent work on the intrinsic response of ferromagnets and bilayer systems. For bulk ferromagnets, we compute the full spin current conductivity tensor [1]. We find spin current flowing transverse to the applied field, with substantial components of the spin direction perpendicular to the magnetization. This bulk spin current contributes to interfacial torque, consistent with recent optical measurements of the electrical response of single ferromagnetic layers [2]. We also consider the origin of the anomalous Hall charge current, and propose that the intrinsic Hall effect can be understood in terms of the interference between the orbital and Bloch components of the electronic wave function in the presence of a symmetry-breaking potential.

In bilayer systems composed of thin films of heavy metal and ferromagnets, applying an in-plane electric field leads to torques on the ferromagnetic layer. These torques arise from multiple effects (e.g. spin Hall effect and spin transfer torque, Rashba-Edelstein effect, and others), some of which have identical symmetry. Disentangling the different contributions to the final torque is therefore very challenging. Theoretically, we use the Kubo formalism and a pseudo-steady state analysis to determine contributions to the electric field-induced magnetic torques from various sources, including: spin currents, Berry curvature of the electronic band structure, and direct flows of angular momentum from the lattice via spin-orbit coupling. We perform this analysis for Co-Pt bilayers and ferromagnet-transition metal dichalcogenide (TMD) bilayer systems. The latter systems exhibit torques with novel symmetry properties due to the reduced in-plane symmetry of the TMD interface, and are of particular interest because they enable spin-orbit torque switching of perpendicularly magnetized layers.

Semi-realistic tight-binding approach to spin-orbit physics at interfaces

A. Manchon*, S. Ghosh, G. Manchon, A. Hajr, A. Hariri
Physical Science and Engineering Division (PSE), King Abdullah University of Science and Technology (KAUST), Thuwal 23955-6900, Kingdom of Saudi Arabia

Spin-orbit physics in transition metal heterostructures is one of the most promising topics in modern magnetism. Such interfaces are the platform of novel mechanisms such as spin-transfer torque, Dzyaloshinskii-Moriya interaction and chiral magnetic damping that are currently being investigated for future applications in data storage and manipulation. However, most theoretical approaches produced to date either use oversimplified models (Rashba spin-orbit coupling, drift-diffusion transport etc.) or comprehensive density functional theory. Whereas the former lacks realism, the latter lacks transparency. In this talk, I will present a multi-orbital tight-binding model of a W/Fe bcc heterostructure. In this approach, the spin-orbit coupling is modeling under Russel-Saunders scheme, which enables us to treat interfacial and bulk spin-orbit transport on equal footing. The two components of the spin-orbit torque, as well as Dzyaloshinskii-Moriya interaction are computed within Kubo linear response theory. We identified several features worth noticing. First, the spin-orbit torque displays four sizable components: the field-like and damping-like torques, as well as two planar components that vanish when the magnetization lies out-of-plane. The planar field-like torque decreases smoothly with the normal metal thickness, whereas the planar damping-like torque increases with the normal metal thickness. Second, we investigate the self-torque exerted on the ferromagnet when spin-orbit coupling of the normal metal is turned off. Our results suggest that the spin accumulation that builds up inside the ferromagnet can be large enough to induce magnetic excitations. Finally, I will also present our calculations of the Dzyaloshinskii-Moriya interaction in this heterostructure and discuss its connection with the damping-like spin-orbit torque.

Bulk-Boundary Correspondence for Spin Transport: Equivalence between Intrinsic Spin Hall Effect and Rashba-Edelstein Effect

Dongwook Go[1,2,3*], Hyun-Woo Lee[1]

[1]Department of Physics, Pohang University of Science and Technology, Pohang 37673, Korea
[2]Basic Science Research Institute, Pohang University of Science and Technology, Pohang 37673, Korea
[3]Peter Grünberg Institut and Institute for Advanced Simulation,
Forschungszentrum Jülich and JARA, 52425 Jülich, Germany

In topological insulators, inverted band structure gives rise to nontrivial topological invariant of the system in the bulk. Such nontrivial topology results in metallic states at the boundary of the system, which is called bulk-boundary correspondence (BBC). Typically, a topological invariant is defined for a Hall-like response of a quantum number protected by the symmetry, such as time-reversal symmetry and crystalline symmetries. In reality, however, experimental apparatus measures projection of an observable, which is not conserved in general. Spin is one example, which is not conserved in solids due to spin-orbit coupling (SOC), which complicates spin transport studies. Here we show that the BBC can be generalized to describe excitation of nonconserved quantities like spin, and covers not only insulators but also metals. Motivated by recent advances in spintronics, we find that the generalized BBC implies equivalence of the Rashba-Edelstein effect (REE) arising from the Fermi surface and intrinsic spin Hall effect (SHE) arising from the Fermi sea, which have been considered to be independent mechanisms for the spin accumulation. Our result not only resolves controversies over the mechanism of the spin accumulation but also enrich our understanding on the geometry of the electronic structure and its relation to bulk and boundary excitations that are intricately entangled.

Influences of interfacial oxidization on magnetic damping and spin-orbit-torques in Pt / ferromagnet / capping structures

Dong Joon Lee[1,2], Wonmin Jeong[1,2], Deokhyun Yun[1,2], Seung Young Park[3], Byeong-Kwon Ju[1], Hyun Cheol Koo[1,2], Byoung-Chul Min[2], Kyung-Jin Lee[1], Ouk Jae Lee[2*]

[1]Korea University, Seoul (the Republic of Korea)

[2]Korea Insutitute of Science and Technology, Seoul (the Republic of Korea)

[3]Korea Basic Science Institute, Daejeon, (the Republic of Korea)

Current induced spin-orbit torques (SOTs) have attracted a lot of attention because the mechanism can efficiently reverse the magnetization in multilayers of heavy metal(HM)/ferromagnet(FM)/insulator with strong spin-orbit coupling (SOC). Although most of the research to date has focused on the HM/FM interface at which the generation of spin-current ($J_{s)}$ and the enhancement in magnetic damping (α) occur, several recent works have suggested that the physical and chemical properties of the capping (CAP) can also change the characteristics of SOTs. In addition, our previous work [1] showed that the insertion of an ultrathin (< 1 nm) magnetic dusting layer between FM and MgO layers can play an important role in the determination of magnetic damping. Nevertheless, there is still a dearth of experimental work studying how the FM/CAP interface contributes to surface magnetic energy (Ks), damping (α), and SOT efficiencies (θ_{DL} and θ_{FL}) in HM/FM/CAP heterostructures.

In this presentation, we present our experimental results [2] that investigate how a naturally formed magnetic oxide at the FM/oxide interface influences the magnetic and spintronic properties. We examined six different series of layer stacks consisting of Pt / FM(Co or Py) / CAP (MgO, HfO and TaN) by utilizing X-ray photoelectron spectroscopy (XPS) and spin-torque ferromagnetic resonance (ST-FMR) measurements. Our results show that the SOTs originate primarily from the Pt/FM interface with some modulations by the FM/oxide interface. On the other hand, the perpendicular magnetic anisotropy (PMA) and the magnetic damping can be significantly influenced by the FM/CAP interface, especially with an extra magnetic damping for Co/MgO, which must be related to the interfacial formation of antiferromagnetic (AF) oxides. This implies that the interfacial AFM-oxide is a decent spin-current conductor, for instance, by incoherent magnon generation at the interfacial CoO, even above its magnetic ordering temperature (T_N). Our results facilitate a better understanding of the interfacial oxide contributions on the PMA, magnetic damping, and SOTs in Pt/FM/CAP systems.

References

[1] D. J. Lee, J. H. Kim, H. G. Park, K.-J. Lee, B.-K. Ju, H. C. Koo, B.-C. Min, and O. J. Lee, “Spin-Orbit Torque and Magnetic Damping in Tailored Ferromagnetic Bilayers”, Phys. Rev. Applied 10, 024029 (2018).

[2] D. J. Lee, W. M. Jeong, D. H. Yun, S. Y. Park, B.-K. Ju, K.-J. Lee, H. C. Koo, B.-C. Min, and O. J. Lee, Influences of interfacial oxidization on surface magnetic energy, magnetic damping and spin-orbit-torques in Pt / ferromagnet / capping structures, arXiv:1901.05777 (2019).

Ferrimagnetic spintronics

Teruo Ono[1,2*]
[1]Institute for Chemical Research, Kyoto University
[2]Center for Spintronics Research Network, Osaka University

Antiferromagnetic spintronics is an emerging research field which aims to utilize antiferromagnets as core elements in spintronic devices. Antiferromagnets are expected to show much faster spin dynamics than ferromagnets because they have higher resonance frequencies than ferromagnets. However, experimental investigations of antiferromagnetic spin dynamics have remained unexplored mainly because of the immunity of antiferromagnets to magnetic fields.

We show that fast field-driven antiferromagnetic spin dynamics is realized in ferrimagnets at the angular momentum compensation temperature T_A. Using rare-earth–3d-transition metal ferrimagnetic compounds where net angular moment is nonzero at T_A, the field-driven DW mobility remarkably enhances up to 20 km s−1T^{-1}. The collective coordinate approach generalized for ferrimagnets and atomistic spin model simulations show that this remarkable enhancement is a consequence of antiferromagnetic spin dynamics at T_A. Correlation between T_A, the magnetization compensation temperature, and the Curie temperature has been investigated [2]. Vanishing the skyrmion Hall effect at T_A has been also demonstrated [3]. We also found bulk Dzyaloshinskii-Moriya interaction in amorphous ferrimagnets materials [4]. Our finding allows us to investigate the physics of antiferromagnetic spin dynamics and highlights the importance of tuning of the angular momentum compensation point of ferrimagnets.

This work was partly supported by JSPS KAKENHI Grant Numbers 15H05702, 26870300, 26870304, 26103002, 25220604, 2604316, Collaborative Research Program of the Institute for Chemical Research, Kyoto University, and Cooperative Research Project Program of the Research Institute of Electrical Communication, Tohoku University.

References

[1] K.-B. Kim et al., Nature Materials 16, 1187 (2017).
[2] Y. Hirata et al., Phys. Rev. B 97, 220403(R) (2018).
[3] Y. Hirata et al., Nature Nanotechnology14, 232 (2019).
[4] Duck-Ho Kim et. al., Nature Materials 18, 685 (2019).

Magnetotransport and Magnetization Dynamics in Ferrimagnetic Alloys

Kab-Jin Kim*
Department of Physics, Korea Advanced Institute of Science and Technology, Daejeon 34141, Korea

Antiferromagnetic spintronics is an emerging research field which aims to replace the conventional ferromagnetic core elements by the antiferromagnetic ones. However, the experimental investigations on antiferromagnets have been hampered by difficulties in exciting and detecting the antiferromagnetic spin dynamics and transport due to field-immunity of antiferromagnet. Recent reports have shown that the ferrimagnets can be alternative platform to study the antiferromagnetic properties, especially in the vicinity of compensation points [1-3]. In this talk, we will briefly introduce the concept of ferrimagnetic spin dynamics and transport, and will discuss how the ferrimagnetic properties are related to the antiferromagnetic ones. In particular, we will show our recent experimental result of unidirectional magnetoresistance (UMR) in heavy metal/ferrimagnet bilayers, in which we found that the UMR is much enhanced in ferrimagnetic bilayers compared to the conventional ferromagnetic bilayers. The study of spin wave across the compensation points will also briefly presented.

References

[1] Kab-Jin Kim et al. Nat. Mater. **16**, 1187 (2017).
[2] Duck-Ho Kim et al. Phys. Rev. Lett. **122**, 127203 (3019).
[3] T. Okuno et al. Nat. Electron. **2**, 389 (2019).

International Symposium on Magnetism and
Magnetic Materials 2019

Oral Session I

'Soft/Hard Magnetics'

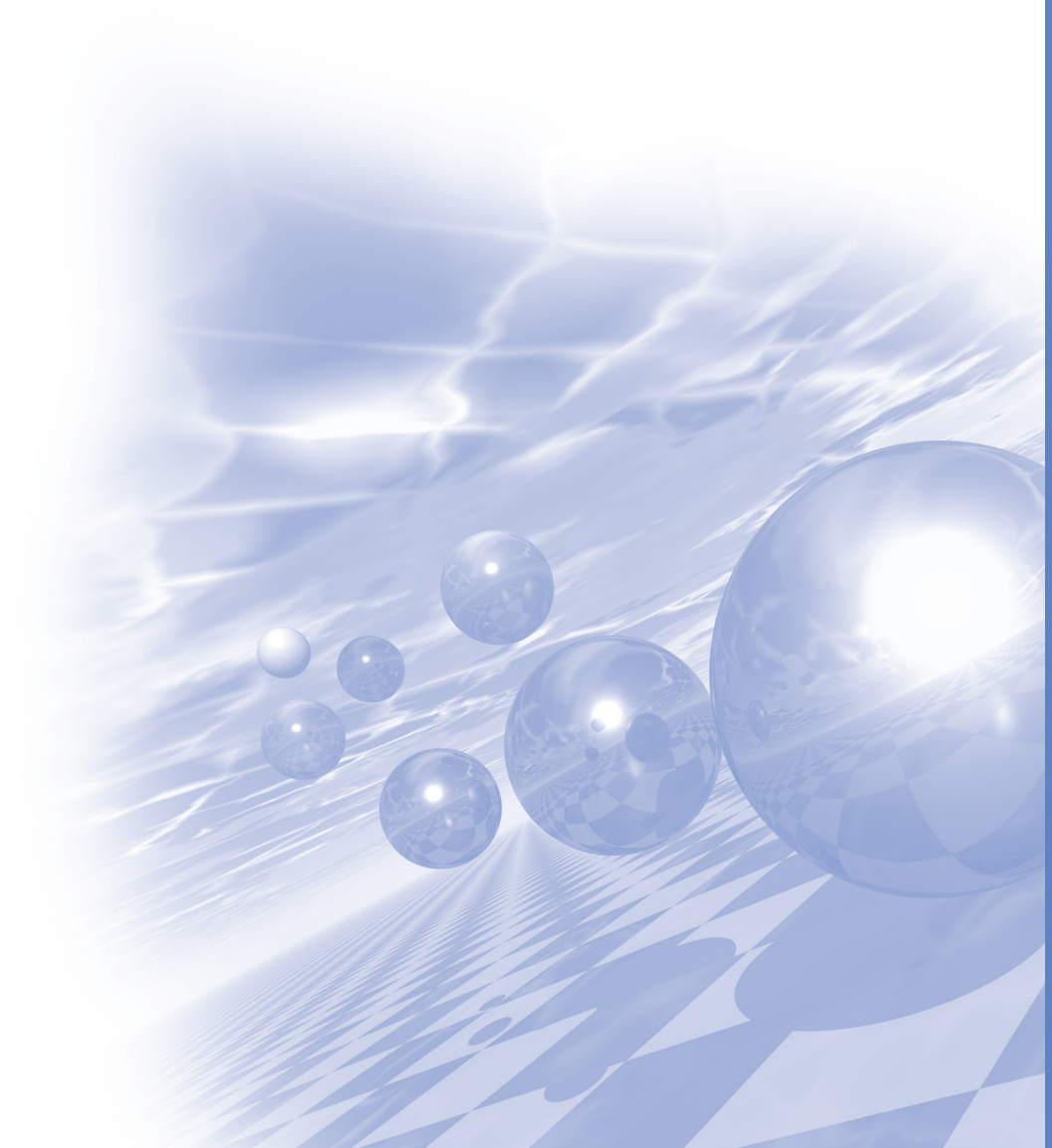

Fabrication and magnetic properties of Fe rich compound with a tetragonal $ThMn_{12}$ structure

Hui-Dong Qian[1,2*], Jung Tae Lim[1], Yang Yang[1,2], Jong-Woo Kim[1],
Kyung Mox Cho[2], Jihoon Park[1†], Chul-Jin Choi[1†]

[1]Powder & Ceramic Division, Korea Institute of Materials Science, Changwon, Gyeongnam, 51508, South Korea
[2]School of Materials Science and Engineering, Pusan National University, Busan, 46241, South Korea

Iron-rich rare-earth (RE) alloys with tetragonal $ThMn_{12}$ structure have been extensively studied as a potential high performance permanent magnetic material due to its high saturation magnetization of 1.43 T, anisotropy field of 10.9 T and Curie temperature of 800 K [1]. In order to diverse the usage of light rare earth elements, the iron rich RFe_{12} compounds with the $ThMn_{12}$ structure has recently received interest for potential permanent magnet applications with respect to maximizing the saturation magnetization with minimum Ti addition and optimum substitution of Co for Fe [2]. Although there have been several reports of the production of the $Sm(Fe,T)_{11}Ti$ phase, this has been in the form of powder, ribbon or thin film [3]. In this work, we have developed a complete process to prepare a fully dense(>99%) $Sm(Fe_{0.8}Co_{0.2})_{11}Ti$ bulk magnet.

Amorphous $Sm(Fe_{0.8}Co_{0.2})_{11}Ti$ ribbons were prepared by arc-melting raw material pieces and melt-spinning. The melt-spun ribbons were ground and pressed to produce green bodies, and the green bodies were annealed at 800°C for various times ranging from 10 to 30 min, followed by quenching as shown in Fig. 1. Here, the purity, density, and magnetic properties were controlled by optimizing pressing, annealing, and quenching conditions.

The fabricated high density $Sm(Fe_{0.8}Co_{0.2})_{11}Ti$ bulk sample (7.72 g/cc; 99.3%) exhibits high purity $ThMn_{12}$ phase of higher than 93 %. The saturation and remanent magnetizations are higher than the reported data, which results in greater maximum energy product $(BH)_{max}$ of 8.65 MGOe than the reported 5 MGOe [3]. To the best of our knowledge, this $(BH)_{max}$ is the highest value with composition of Sm(Fe-Co)Ti bulk magnet without doping of any Zr, La, Ce, V, etc. The details of the fabrication procedure, microstructure and magnetic properties will be discussed.

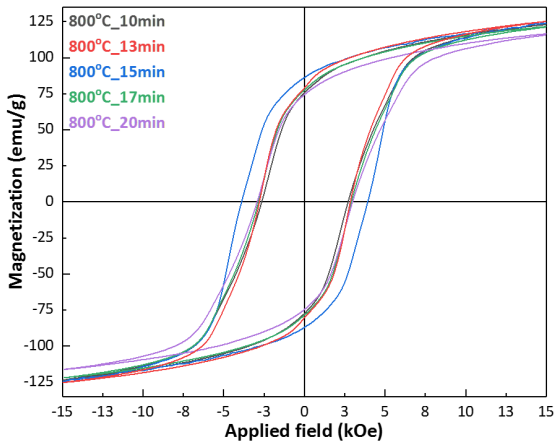

Fig. 1. Magnetic hysteresis loops of $Sm(Fe_{0.8}Co_{0.2})_{11}Ti$ bulk magnets

References

[1] Y. Hirayama, Y. K. Takahashi, S. Hirosawa, and K. Hono, Scr. Mater. **138**, 62 (2017).

[2] P. Tozman, H. Sepehri-Amin, Y. K. Takahashi, S. Hirosawa, and K. Hono, Acta Mater. **153**, 354 (2018).

[3] Tetsuji Saito, Fumiya Watanabe, and Daisuke Nishio-Hamane, J. Alloys Compd. **773**, 1018 (2019)

Two-dimensional systems in curved geometry

Minkyu Park[1*] and Sung Hyon Rhim[2]
[1]Research Institute of Basic Sciences, University of Ulsan
[2]Department of Physics and Energy Harvest Storage Research Center, University of Ulsan

Two-dimensional systems in curved geometry is investigated. We adopt the continuum model explored in graphene, fullerene, and so forth. Curved geometry inevitably introduces the spin connection, a spacetime driven gauge eld not accessible in at geometry. The spin connection turns out to be the origin of a pseudo-magnetic eld that actually is the curvature. Time reversal or inversion symmetry may be preserved depending on the system. By evaluating the leading order curvature correction to Green function, we assert that the local band gap can be modulated by controlling the curvature.

O-I-3

Hot-deformation behavior of NdFeB magnet with Ce/La substitution

Ga-Yeong Kim[1,2*], Hee-Ryoung Cha[1], Dong-Hwan Kim[3], Yang-Do Kim[2†], and Jung-Goo Lee[1†]

[1]Powder&Ceramics Division, Korea Institute of Materials Science, Changwon, Korea

[2]Department of Materials Science and Engineering, Pusan National University, Busan, Korea

[3]Research Center of SG Tech., Star Group Ind. Co., Daegu, Korea)

Nd-Fe-B magnets are technologically important materials for the applications in the wind turbines, traction motors of electric/hybrid vehicles, acoustics devices, etc.. In general, 30–33 wt.% of rare earth elements (Nd, Dy) are consumed to produce Nd-Fe-B magnets. With the increasing demand for Nd-Fe-B magnets, interest in decreasing the use of Nd by substituting with light rare earth elements is increasing. Ce and La are the most abundant elements in the natural rare earth resources and its price is much cheaper than Nd, Pr and Dy. The price of Ce metal is currently about 1/10 of that of Nd metal. However, the intrinsic hard magnetic properties of $Ce_2Fe_{14}B$ ($4\pi M$ = 11.7 kG, H_a = 26 kOe) and $La_2Fe_{14}B$ ($4\pi M$ = 13.8 kG, H_a = 20 kOe) are much inferior to those of $Nd_2Fe_{14}B$ ($4\pi M$ = 16 kG, H_a = 73 kOe). Furthermore, there exists secondary phase of $CeFe_2$ with high melting point in Ce-Fe-B magnet. It has been also considered that the $CeFe_2$ phase inevitably forms in the Nd-Ce-Fe-B component with high Ce content. The curie temperature and melting temperature of $CeFe_2$ are 235K and 1198K respectively. Therefore, $CeFe_2$ phase is paramagnetic at room temperature and has a weaken wettability compared with low melting point RE-rich phase during low-temperature deformation. Previous study has reported that the formation of $CeFe_2$ phase can be suppressed by addition of La. Although Nd-lean RE-Fe-B magnets have attracted great attention, most of the studies has been concerned with conventional sintered magnets and studies on hot-deformed Nd-lean RE-Fe-B magnet are quite limited. In this study, therefore, hot-deformation process was employed to fabricate the anisotropic ultrafine-grained Nd-lean RE-Fe-B magnet using melt-spun powder, and the effect of Ce/La substitution for Nd on hot deformation behavior was investigated. Initial ribbons with the nominal compositions of $(Nd_{1-x}M_x)_{13.6}Fe_{bal}B_{5.6}Ga_{0.6}Co_{6.6}$ (x=0, x=0.2/M=Ce, x=0.3/M=Ce and x=0.3/M=Ce+La, wt.%, named as ND, CE0.2, CE0.3 and CELA0.3, respectively) were prepared by a single-roller melt-spinning machine with a wheel speed of 28m/s in an argon atmosphere and then pulverized into powders. The powders were hot-pressed at 700℃ under 100 MPa in a vacuum and then subjected to die-upsetting at 700℃ with a deformation rate of $\dot{\varepsilon}$ = 0.1 s^{-1}. As increase of Ce and La content, the stress for deformation should be increased for the same strain during hot-deformation process, which indicates that deformation is difficult with increasing the addition of Ce and La content. It was also confirmed that the degree of alignment and density was decreased with increasing Ce and La content. TEM observation showed that triple junction phase increased with Ce and La content. Another point to be noted in TEM observation is the fact that the RE-rich phase distribution along grain-boundaries is quite different between CE0.3 and CELA0.3 magnets. The grain boundary phase of CELA0.3 hot-deformed magnets was quite indistinct in almost area, whereas the grain boundary phase of CE0.3 was continuous and homogeneous. Therefore, CE0.3 magnet shows the better magnetic properties than CELA0.3 magnet. Based upon these results, the effect of Ce and La substitution on hot-deformation behavior and magnetic properties of Nd-Fe-B magnet will be discussed.

Keywords: Nd-lean, RE-Fe-B, melt-spun powder, Hot-deformation, triple-junction

Effect of Initial Alloy on Coercivity Enhancement of Hot-deformed Magnet using Nd-Fe-B HDDR Powder

Jae-Gyeong Yoo[1,2*], Hee-Ryoung Cha[1], Youn-Kyoung Baek[1],
Dong-Hwan Kim[3], Yang-Do Kim[2], Jung-Goo Lee[1†]

[1]Powder & Ceramics Division, Korea Institute of Materials Science, Changwon, Korea
[2]Department of Materials Science and Engineering, Pusan National University, Busan, Korea)
[3]Research Center of SG Tech., Star Group Ind. Co., Daegu, Korea

High performance Nd-Fe-B permanent magnet has been used for generator of wind turbines and traction motor of electric/hybrid vehicles due to their excellent magnetic property. For these applications, however, quite high coercivity is required at room temperature due to the high operating temperature. The conventional sintering process of magnetically aligned monocrystalline powders is well established as a fabrication approach of anisotropic bulk magnet. However, in order to achieve high coercivity with conventional sintering process, addition of heavy rare earth element such as Dy is necessary despite of scarce resources problem and high cost of Dy. On the other hand, hot-deformation process is alternative method to produce the high coercive anisotropic bulk magnet without the Dy, which use the polycrystalline powders with isotopically aligned ultra-fine grains such as melt-spun or isotropic hydrogenation–disproportionation–desorption–recombination (HDDR) powder. However, the coercivity of hot-deformed magnets is still too low to be used for traction motor of hybrid vehicles. Therefore, post-treatment such as grain boundary diffusion process (GBDP) is essential for coercivity enhancement. On the other hands, the grains of hot-deformed magnet made from melt-spun powder can be easily grown at the higher temperature than 700℃ due to the ultrafine grain size, decreasing coercivity of magnet. However, the hot-deformed magnet made from HDDR powder has relatively coarser-grains compared to that of melt-spun powder. Therefore, it could be subjected to heat-treatment at the higher temperature than 700℃ without significant grain growth. Thus, the HDDR powder could be a good candidate to produce high-performance hot-deformed magnets.

In this study, the anisotropic Nd-Fe-B bulk magnets were produced by hot-deformation process using HDDR powders. And as-produced and annealing-treated strip-casting (SC) alloy, which have different microstructure, are employed as initial alloy to produce HDDR powders. For coercivity enhancement, the hot-deformed magnets made from two different HDDR powder were subjected to GBDP using NdHx-Cu. The coercivity of hot-deformed magnet made from as-produced SC alloy is higher than that of annealing-treated SC alloy. After GBDP, however, the coercivity of hot-deformed magnet made from annealing-treated SC alloy significantly increased to 14 kOe, whereas that made from as-produced SC alloy slightly increased to 12 kOe. Based upon these results, effect of distribution and composition of Nd-rich phases at grain boundaries on microstructure and magnetic properties of hot-deformed magnet will be discussed.

O-I-5

Effect of post-sintering annealing conditions on the magnetic and microstructural properties of the multi-main phase Nd-Ce-Fe-B sintered magnets

Kyoung-Hoon Bae[1*], Sang-Sun Yang[1], Ji-Hun Yu[1], Jung-Goo Lee[1], Dong-Hwan Kim[2]
[1]Powder & Ceramics Division, Korea Institute of Materials Science, Changwon, Korea
[2]R&D center, Star Group, Daegu, Korea

Recently, reducing the amount of Nd without sacrificing the coercivity (H_c) is the most important issue in the development of Nd-Ce-Fe-B sintered magnets. However, the H_c of the magnets could be drastically deteriorated after replacing Nd with Ce due to the poor intrinsic magnetic properties of $Ce_2Fe_{14}B$ phase compared with $Nd_2Fe_{14}B$ phase. Developing a multi-main phase (MMP) microstructure by a mixture of Ce-rich and Ce-lean powders is known to be the most effective way to enhance the H_c, and reduced the Nd content in the magnets. However, the H_c of MMP Nd-Ce-Fe-B (45 wt.% Ce substituting for Nd, 6.2 kOe) sintered magnet is remarkably low, which is a problem to be solved. The roughness of the rare-earth (RE)-rich grain boundary phase (GBP) is enhanced during post-sintering annealing. In addition, a continuous and uniform RE-rich GBP is formed during PSA, resulting in the suppression of the reverse domain nucleation and enhancing the magnetic isolation. However, the optimum PSA temperature for the MMP magnets have not yet been clarified. In this study, we investigated the effects of PSA conditions on the microstructural and the magnetic property changes of the MMP sintered Nd-Ce-Fe-B magnets as a function of the Ce/Nd mixing ratio and clarified the optimum PSA temperature for the MMP process. Ce-free and Ce-containing magnetic powders with nominal compositions of $(Pr,Nd)_{31.0}Fe_{bal.}M_{1.90}B_{1.0}$ and $[(Pr,Nd)_{19}Ce_{12}]_{31.0}Fe_{bal.}M_{1.90}B_{1.0}$ M (wt.%, M=Al, Ga, Nb, Cu, and Co) were prepared using the powder metallurgical method. Ce-free and Ce-containing powders, with a mean particle size of less than 3.0 ㎛, were mixed (ratio of 20:80 and 70:30). The green compacts were sintered at 1030°C for 2h. The PSA temperatures were varied from 850 to 600°C to optimize the PSA temperature. The microstructure, phase identify and magnetic properties of samples were investigated by using EPMA, HRTEM, DSC, and BH-tracer. When the magnet has a low Ce content (70:30), the H_c was not changed with decreasing PSA temperature (850 → 650 °C). However, when the magnet had a high Ce content (20 : 80), the highest H_c were obtained at the 650°C-PSA temperature. It was well known that the eutectic temperature of $Ce_2Fe_{14}B$ phase was lower than that of the $Nd_2Fe_{14}B$ phase. Thus, when the magnet had a high Ce content, the GBP could be formed continuously and homogeneously even at low PSA temperature (650°C). In addition, the core-shell microstructure was also effectively maintained by decreasing the PSA temperature. Consequently, as the content of Ce in a Ce/Nd mixed powder was increased, it was effective for the magnetic properties to decrease the PSA temperature.

Keywords: Nd-Ce-Fe-B sintered magnet, Coercivity, Core-shell microstructure, Grain boundary phase, Post-sintering annealing

A Study of Soft Magnetic Materials for Development of Economic Ignition Coil

Shin Gyu Kim[1], Hyungsuk Kim[1], Yeon Jun Chung[1], Seong Gwan Bae[2], Su Dong Kim[3]
[1]Materials Development Center ,Hyundai Motor Company, Korea
[2]Powertrain Performance Development Center, Hyundai Motor Company, Korea
[3]Yuratech, Korea

During the past several years, a great deal of attention has been paid to lean-burn combustion, which reduces the amount of fuel in the mixed gases in engine combustion chambers, in order to improve the fuel economy of cars. High energy ignition coil application is essential for stable ignition in lean combustion conditions. Ignition coils are automotive electric parts that form sparks for fuel ignition by converting a battery's low 12V to a high voltage of tens of kV by the principle of mutual induction between the primary and secondary coils. The development of high energy ignition coils requires the optimal combination of the magnetic core design and the development of materials. In this study we compare the performance of ignition coils with two different core materials; one with magnetically improved electrical steel sheets, the other with soft magnetic powders.

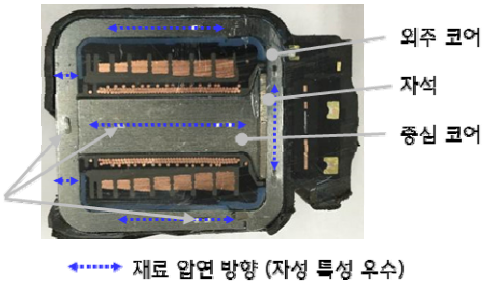

Fig. A cross section of ignition coil

CFSM Design for EV Traction Comparing Vehicle System Efficiency

Kyoung-Soo Cha[1*], Young-Hoon Jung[1], Chung-Seong Lee[2], Myung-Seop Lim[1†]
[1]Department of Automotive Engineering, Hanyang University, Korea
[2]Central R&D Center, Mando Inc., Seongnam 13486, Korea

Due to environmental regulations, the eco-friendly vehicle industry is growing noticeably. The eco-friendly vehicles include hybrid electric vehicle (HEV), plug-in hybrid electric vehicle (PHEV), battery electric vehicle (BEV), and fuel cell electric vehicle (FCEV). Recently, various studies on EVs have been conducted. The majority of research on EV traction motors aims at improving efficiency and increasing power density. Improving motor efficiency and power density can improve mileage because it reduces energy consumption. The most suitable motor that meets these requirements is interior permanent magnet synchronous motor (IPMSM) using Neodymium (Nd) magnets. Therefore, many studies on IPMSM are performed. However, Nd magnets, which are rare earth magnets, have disadvantages of price instability. Therefore, in order to replace IPMSM, the researchers discuss various non-rare-earth motors.

Wound field synchronous motor (WFSM) and concentrated flux synchronous motor (CFSM) are representative non-rare earth motors. However, WFSM has a low power density. Also, it is not suitable as a traction motor because of the brush and slip ring. CFSM is suitable as a traction motor because it can have a power density similar to that of IPMSM. CFSM is spoke type motor using non-rare earth magnet. Ferrite magnets, which are non-rare earth magnets, have a residual magnetic flux density of about 30% compared to Nd magnets. Therefore, in order to increase air-gap flux density, magnets are arranged in the shape of the spoke.

In this paper, CFSM is designed to have the same power density as IPMSM. These motors are designed for EV traction. As a result of 2-dimensional finite element analysis, the performance of IPMSM and CFSM is compared. Finally, vehicle simulations are used to compare system efficiencies for vehicles using CFSM and IPMSM as traction motors. For vehicle simulation, the target driving cycle is urban dynamometer driving schedule (UDDS).

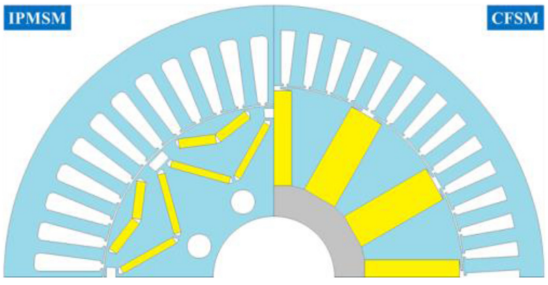

Fig. 1. Shape of IPMSM and CFSM

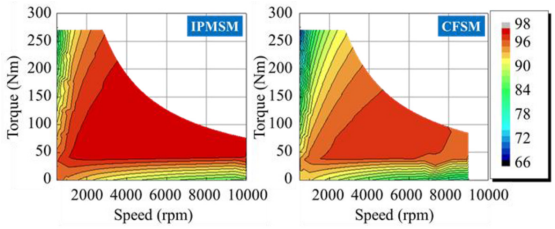

Fig. 2. Efficiency map of IPMSM and CFSM

Table 1. System Efficiency for vehicle using IPMSM and CFSM

Items	IPMSM	CFSM	Unit
System Efficiency	43.5	42.3	%

Effect of iron deficiency and La-Co substitution on the magnetic properties of Sr M-type hexaferrites

Kang-Hyuk Lee*, Junho Park, Sang-Im Yoo†
Department of Material Science and Engineering, Research Institute of Advanced Materials (RIAM),
Seoul National University, Seoul, Korea

Recently, La-Co substituted Sr M-type hexaferrites ($Sr_{1-x}La_xFe_{12-y}Co_yO_{19,}$ Sr-La-Co M-type) have been reported to possess higher crystalline anisotropy without reducing its saturation magnetization (M_s), resulting in higher coercivity (H_c). Previous reports have been mainly focused on La^{3+}substitution for the Sr^{2+} site and transition metals substitution for the Fe^{3+} sites of M-type hexaferrites. However, the effect of iron deficiency on magnetic properties of the Sr-La-Co M-type hexaferrites remains unexplored. In this study, therefore, we tried to investigate La-Co substituted Sr M-type hexaferrites $Sr_{1-x}La_xFe_{12-x}Co_xO_{19,}$ ($0 \leq x \leq 0.3$) and the effect of iron deficiency on the magnetic properties of $Sr_{0.7}La_{0.3}Fe_yCo_{0.3}O_{19-\delta}$ ($10 \leq y \leq 11.7$) hexaferrites prepared by solid state reaction. The raw materials were ball-milled for 24 h and calcined at 1280 ℃ for 2 h in air. as-calcined powder was pressed into pellets and sintered at 1230 ℃ for 1 h in air. Samples were characterized by powder X-ray diffraction (XRD), vibrating sample magnetometer (VSM), and scanning electron microscope (SEM). In case of Iron deficient Sr-La-Co M-type hexaferrties, Powder XRD analyses revealed that M-type single phase were obtained with all Fe contents at sintering temperature. The saturation magnetization (M_s) of the Sr-La-Co M-type hexaferrite samples was around 72 emu/g. The maximum M_s was obtained for Fe content of 11.7 at 73.5 emu/g. However, the coercivity (H_c) decreased with higher Fe content because the grain size was larger than the single domain size. Detailed microstructures and magnetic properties of Sr-La-Co M-type hexagonal ferrites will be presented for a discussion

Keywords: Hexaferrite, magnetic property, iron deficiency, M-type hexaferrite

Enhancement of magnetic properties of Fe-rich $Sm(Fe_{0.8}C_{0.2})_{11}$ Ti compounds by grain boundary diffusion process

Jung Tae Lim*, Hui-Dong Qian, Jihoon Park, Jong-Woo Kim, and Chul-Jin Choi†
Powder & Ceramic Division, Korea Institute of Materials Science, Changwon 51508, Korea

Recently, among rare earth (R)-Fe-X compounds, the Fe-rich compounds with tetragonal $ThMn_{12}$ structure have shown potential as next generation permanent magnet materials, since the ratio of the rare earth elements is very small as about 8%. In addition, the $Sm(Fe_{0.8}Co_{0.2})_{12}$ thin film was reported to have excellent properties of saturation magnetization of 1.78 T and magnetic anisotropy field of 12 T[1]. However, Fe-rich compounds with $ThMn_{12}$ structure, which exhibit theoretically superior properties, present only about 40% of the theoretically predicted coercivity, and the full potential of the magnet is not yet realized. Grain refinement and grain boundary control are well-known methods to achieve high coercivity[2]. Therefore, in this study, grain boundary diffusion was investigated Fe-rich $Sm(Fe_{0.8}Co_{0.2})_{11}Ti$ compounds by using non-magnetic grain boundaries diffusion materials. The crystalline and magnetic properties by using x-ray diffractometer (XRD) with Cu-Kα radiation source, scanning electron microscopy (SEM), electron probe micro analysis (EPMA) and vibrating sample magnetometer (VSM). The $Sm(Fe_{0.8}Co_{0.2})_{11}Ti$ compounds and grain boundaries diffusion materials were prepared by using arc-melting and melt spinning methods. Then, the as-prepared sample was mixed with a grain boundary diffusion material using ultra-sonication in ethanol and annealed at different temperatures. From the analyzed XRD patterns by using Rietveld refinement method, the crystal structure of all sample was determined to be tetragonal structure with the space group *I4/mmm*. The hysteresis curves of grain boundary modified $Sm(Fe_{0.8}Co_{0.2})_{11}Ti$ compounds were measured under 20 kOe at 295 K, showing their intrinsic coercivity increases and magnetization decreases. Details of the microstructure and magnetic properties of $Sm(Fe_{0.8}Co_{0.2})_{11}Ti$ compounds will be discussed.

References

[1] Y. Hirayama, Y. K. Takahashi, S. Hirosawa, and K. Hono, Scr. Mater. **138**, 62 (2017).
[2] K. Hono and H. Sepehri-Amin, Scr. Mater. **67**, 530 (2012).

International Symposium on Magnetism and
Magnetic Materials 2019

Special Session III

'Magnetism in Strongly Correlated Oxides and Exotic Materials'

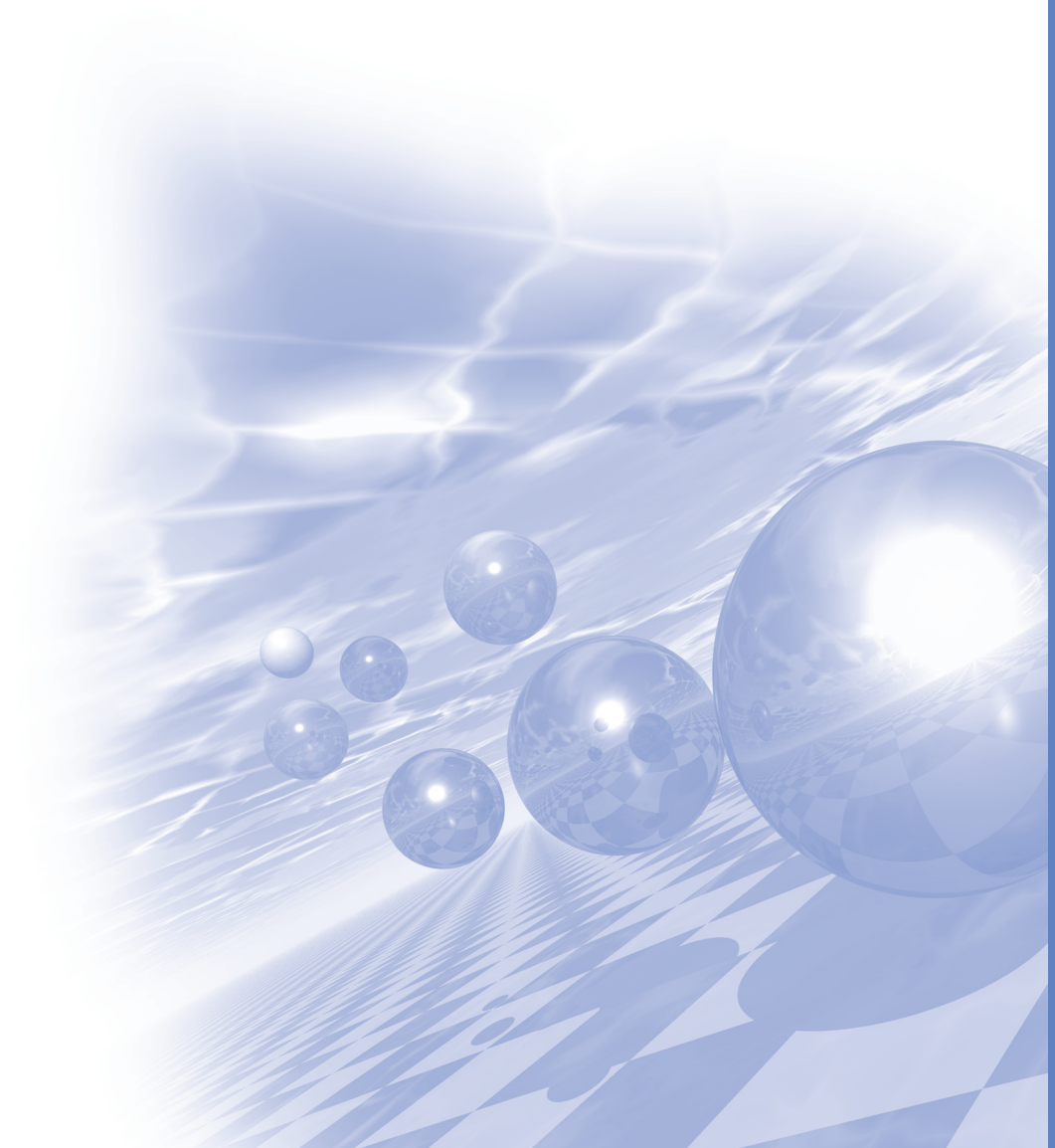

Coupled spin-charge transport in oxide interface

Jung-Woo Yoo*
School of Materials Science and Engineering, Ulsan National Institute of Science and Technology, Republic of Korea

A two-dimensional (2D) electron gas emerged at a $LaAlO_3/SrTiO_3$ (LAO/STO) interface is an interesting electronic platform as the structure itself has broken inversion symmetry. This noncentrosymmetric 2D conductor retains Rashba-type spin-orbit interaction, which ties spin and momentum of electrons in the band structure leading to coupled spin and charge transport. In this talk, I will present coupled spin-charge transport in LAO/STO interface evidenced in various experimental platforms. We demonstrated the non-local spin diffusion in conducting interface of LAO/STO using H-bar type structure, where the spin Hall and its inverse effect function as the spin injector and detector [1]. The inherent structural asymmetry in the conductive oxide interface can induce further intriguing transport properties. When the time-reversal symmetry is further broken, the system could exhibit directional propagation of itinerant electrons, i.e. the rightward and leftward currents differ from each other. In addition, the Rashba spin-orbit interaction can be further tuned by applying gate bias, so does the nonreciprocal charge transport [2].

References

[1] Nonlocal Spin Diffusion Driven by Giant Spin Hall Effect at Oxide Heterointerfaces, Nano Lett. **17**, 36−43 (2017)

[2] Gate-tunable giant nonreciprocal charge transport in noncentrosymmetric oxide interfaces, Nat. Comm. **10**, 1-8 (2019)

NMR investigation of a field-induced quantum spin liquid in α-$RuCl_3$

Seung-Ho Baek[1*], Hyeon Woo Yeo[1], Seung-Hwan Do[2], Kwang-Yong Choi[2], and Bernd Büchner[3]
[1]Changwon National University, Changwon, Korea
[2]Chung-Ang University, Seoul, Korea
[3]IFW Dresden, Helmholtzstr. 20, 01069 Dresden, Germany

In this talk, I will present an NMR investigation in the field-induced quantum spin liquid phase of the Kitaev honeycomb lattice, α-$RuCl_3$ [1] by substituting Ru^{3+} with non-magnetic Ir^{4+} (S=0) ions[2]. With increasing dilution or spin vacancy toward a percolation limit of 0.22, we find that the spin gap behavior which appears at fields above the critical field Hc is rapidly suppressed, in exact parallel with the suppression of Hc itself. This strongly suggests that the spin gap originates from neither Kitaev nor Heisenberg interaction alone, but rather from their subtle combination. Our NMR results imply that, while a gapless (Abelian) Kitaev QSL may emerge above a critical spin vacancy, a non-Abelian QSL is realized only in the presence of Heisenberg interactions in α-$RuCl_3$.

References

[1] S.-H. Baek et al, Physical Review Letters, **119**, 037201 (2017)
[2] S.-H. Baek et al, unpublished

A new quasi-one-dimensional $S = 1$ chain $NiTe_2O_5$ and its intriguing critical behavior

Yoon Seok Oh*

Department of Physics, Ulsan National Institute of Science and Technology, Ulsan 44919, Republic of Korea

In this presentation, we introduce a new quasi-one-dimensional $S = 1$ chain compound $NiTe_2O_5$. Recently, we found $NiTe_2O_5$ has one-dimensional chain structure through NiO_6 octahedra's edge-sharing. Although spin-1 of Ni^{2+} ion undergoes a long-range antiferromagnetic (AFM) order at T_N = 30.5 K where the DC magnetic susceptibility shows an archetypical anisotropic AFM anomaly, the AFM order parameter develops with intriguing unconventional critical exponents as a function of temperature. We present magnetic and structural properties of $NiTe_2O_5$ and discuss its unconventional critical behavior.

Exotic phases and phase transitions in quantum magnets

Eun-Gook Moon*
KAIST, Daejeon, Korea

Quantum magnets may host exotic phases and their transitions, characterized by massively entangled ground and excited states. Strong quantum fluctuations may melt orderings of quantum spins and give rise to unexpected phenomena. Prime examples include quantum spin liquids with Majorana fermions, which have been suggested as a future platform of quantum entanglement control. In this talk, we discuss properties of exotic phases and phase transitions in quantum magnets, focusing on how to detect and characterize the phases theoretically and experimentally.

Tunable real- and reciprocal-space topological properties in $SrRuO_3$ ultrathin films

Lingfei Wang[1,2*], Han Gyeol Lee[1,2], Eun Kyo Ko[1,2], and Tae Won Noh[1,2]
[1]Center for Correlated Electron Systems, Institute for Basic Science, Seoul, Republic of Korea
[2]Department of Physics and Astronomy, Seoul National University, Seoul, Republic of Korea
[*]E-mail: lingfei.wang@outlook.com

Perovskite-structured $SrRuO_3$ is a prototypical ferromagnetic metal with a Curie temperature of ~ 160 K. Because of its high electrical conductivity and structural stability, SRO epitaxial film has been widely used as an electrode layer for perovskite oxide-based heterostructures and devices.[1] Furthermore, a fine balance between the electron-electron correlation and spin-orbit coupling in $SrRuO_3$ gives rise to a variety of exotic physical properties, including itinerant ferromagnetism, non-Fermi liquid electrical transport, magnetic monopoles in momentum space, and tunable magnetic skyrmions.[1-3]

Here, we will show our recent results about tunable real-space and reciprocal-space topological properties in $SrRuO_3$ ultrathin films. In the first part, we will report the discovery of ferroelectrically tunable skyrmions in ultrathin $BaTiO_3/SrRuO_3$ bilayer heterostructures. In this epitaxial system, ferroelectric proximity effect at the $BaTiO_3/SrRuO_3$ heterointerface can trigger a sizable Dzyaloshinskii-Moriya interaction, thus stabilizing a real-space topological spin texture: magnetic skyrmion with a diameter of ~100 nm.[4] Thanks to the strong coupling between ferroelectric distortion and Dzyaloshinskii-Moriya interaction, we can achieve local, switchable, and nonvolatile control of both skyrmion density and thermodynamic stability. In the second part, we will focus on the highly tunable anomalous Hall effect in $SrRuO_3$ single layers. We found the anomalous Hall coefficient exhibit a clear sign change as the $SrRuO_3$ film thickness decreases to 4 unit-cells. This behavior is dominated by the non-trivial topology and large Berry curvature at the avoided crossing points in $SrRuO_3$ band structure. By harnessing the step-flow growth of SRO ultrathin film and artificially inducing a thickness non-uniformity, we can further modulate such a reciprocal-space topology-dominated magnetotransport. At last, we will propose several experimental methods for identifying the differences between the skyrmion-induced topological Hall effect and thickness inhomogeneity induced anomalous Hall effect.

References

[1] Koster, G. et al. Structure, physical properties, and applications of $SrRuO_3$ thin films. Review of Modern Physics, **84,** 253-298 (2012).
[2] Fang, Z. et al. The Anomalous Hall Effect and Magnetic Monopoles in $SrRuO_3$. Science, **302,** 92 (2003).
[3] Ohuchi, Y. et al. Electric-field control of anomalous and topological Hall effects in oxide bilayer thin films. Nature Communications, **9,** 213 (2018).
[4] Wang, L. et al. Ferroelectrically tunable magnetic skyrmions in ultrathin oxide heterostructures. Nature Materials, **17,** 1087 (2018).

Magnetic field and thermal Hall effect in a pyrochlore U(1) quantum spin liquid

Sungbin Lee*
KAIST, Daejeon, Korea

The antiferromagnetic system on a rare-earth pyrochlores has been focused as a strong candidate of U(1) quantum spin liquid. Here, we study the phase transitions driven by external magnetic field and discuss the large thermal Hall effect due to emergent spinon excitations with staggered gauge fields. Despite the spinons, the charge excitations of the effective action that carry spin-1/2 quantum number, do not couple to the external field, the emergent U(1) gauge field is influenced in the presence of external magnetic field. Especially along [111] and [110]-directions, we discuss the possible phase transitions between U(1) spin liquids with different gauge fluxes are stabilized in fields. Beyond the cases where gauge flux per plaquette are fixed to be either 0 or π, there exists a regime where the staggered gauge fluxes are stabilized without time reversal symmetry. In such a phase, the large thermal Hall conductivity κxy /T ∼ 4.2 × 10−3 W/(K2 · m) is expected to be observed below 1K.

International Symposium on Magnetism and
Magnetic Materials 2019

Plenary Session I

Recent Development Status of MTJ with TEL PVD EXIM™

Chang Man Park*
Director of Advanced Technology, Corporate Marketing, Tokyo Electron U.S. Holdings, Inc.
2859 Bayview Drive, Fremont, California 94538, USA

STT-MRAM (Spin Transfer Torque-Magnetic RAM) has been demonstrated in globe with many technical breakthrough as next generation emerging memory this year. Despite the steep demands to use the memory as embedded memory, cache memory, standalone memory, storage-class memory and so on, challenges in process, material, and circuit technology still remain. The author will update the latest development of TEL EXIM™ PVD tools for STT-MRAM p-MTJ stack deposition process.

From device characteristic perspective, major targets are to accomplish small write current, high MR ratio / low RA product, and high thermal stability. The first demand for PVD tools in STT-MRAM fabrication are to set the basis of such properties, as they are highly decided by the engineered stacks and actual PVD processes. Another important aspect of PVD tool is flexibility, to deposit stacks with perpendicular magnetization, and also stacks using unknown future technologies that lie ahead, which makes the Spintronics device more appealing. Finally, depositing complex multi-layer MTJs with stableness, from within wafer uniformity to tool marathon run performance, is essential to take STT-MRAM into high volume manufacturing.

In this presentation, the latest MTJ film properties deposited with high throughput on EXIM™, along with read/write characteristics with patterned MTJ elements will be discussed.

International Symposium on Magnetism and
Magnetic Materials 2019

Oral Session II

'Spintronics I'

Strengths and angular dependence of spin-orbit torques in ferromagnet/normal metal heterostructures

Hyung Keun Gweon[1*], Kyung-Jin Lee[1,2], Sang Ho Lim[1†]
[1]Department of Materials Science and Engineering, Korea University, Seoul 02841, Korea
[2]KU-KIST Graduate School of Converging Science and Technology, Korea University, Seoul 02841, Korea

Spin-orbit torques (SOTs) are investigated for various elements of X (Pt, Ru, Pd, Cu, Mo, W, and Ta) in Pt/Co/X heterostructures. We find that both angle-independent and angle-dependent torque components are strongly dependent on the choice of X. Large negative anisotropic SOTs are observed for the elements showing high SOT efficiencies (such as X = Ta or W), the behaviour of which is detrimental for device applications. Our careful analysis shows that the angle-dependent torques are closely correlated with the work-function difference between Co and X, indicating that the interfacial Rashba spin-orbit coupling plays a role in the anisotropy of SOTs.

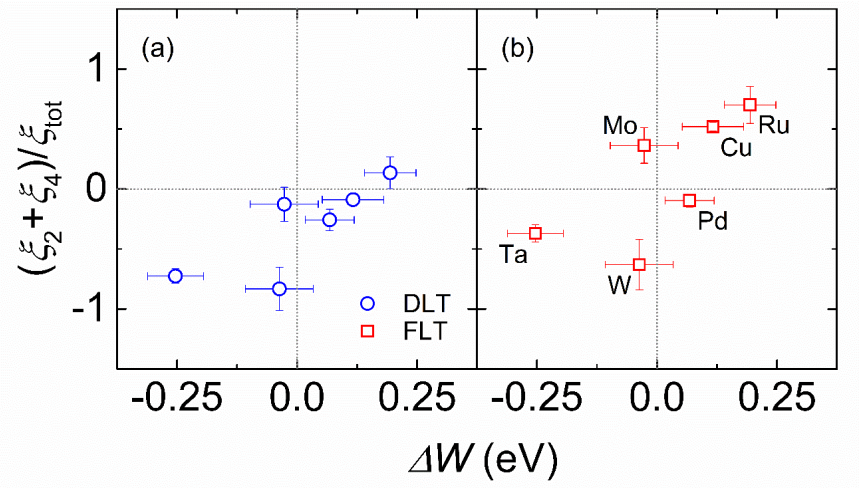

Fig. 1. (a) Anisotropic damping-like torque (circles) and (b) anisotropic field-like torque (squares) for Pt/Co/X structures as a function of work-function difference at the Co/X interface (ΔW). Both the ΔW values and their error bars were taken from Ref. [1].

This research was supported by the Creative Materials Discovery Program through the National Research Foundation of Korea (No. 2015M3D1A1070465) and by the Samsung Electronics' University R&D program.

Reference

[1] H. K. Gweon, H.-J. Park, K.-W. Kim, K.-J. Lee, and S. H. Lim, arXiv: 1906.08450 (2019).

O-II-2

Magnetic Domain Wall Motion due to AC Bias-Driven Resonances

Duck-Ho Kim[1,2*], Dong-Hyun Kim[3], Dae-Yun Kim[1,4], Sug-Bong Choe[4], Teruo Ono[2,5], Kyung-Jin Lee[3,6,7], and Se Kwon Kim[8]

[1]Center for Spintronics, Korea Institute of Science and Technology, Seoul 02792, Republic of Korea
[2]Institute for Chemical Research, Kyoto University, Uji, Kyoto 611-0011, Japan
[3]Department of Semiconductor Systems Engineering, Korea University, Seoul 02841, Republic of Korea
[4]Department of Physics and Institute of Applied Physics, Seoul National University, Seoul 08826, Republic of Korea
[5]Center for Spintronics Research Network (CSRN), Graduate School of Engineering Science, Osaka University, Osaka 560-8531, Japan
[6]Department of Materials Science & Engineering, Korea University, Seoul 02841, Republic of Korea
[7]KU-KIST Graduate School of Converging Science and Technology, Korea University, Seoul 02841, Republic of Korea
[8]Department of Physics and Astronomy, University of Missouri, Columbia, Missouri 65211, USA

Most of the existing researches on the dynamics of a domain wall (DW) have focused on the effect of DC biases, where the induced velocity is determined by the bias strength. Here we show that AC biases such as a field or a current are also able to move a DW via synchronization between the DW angle and the phase of the AC bias. The resulting DW velocity is proportional to the driving frequency of the AC bias, but independent of the bias strength, offering potentially low-power operations of DW devices. The AC-bias-driven DW motion is shown to exhibit a phase locking-unlocking transition, a critical phenomenon akin to the Walker breakdown of a DC-bias-driven DW motion. Our work shows that a DW can be driven resonantly by synchronizing its angle to AC biases, shedding a light on hitherto overlooked utility of internal degree of freedom for driving magnetic textures.

Static and dynamic modes of magnetic skyrmions in magnetic nanotubes

Jaehak Yang[1*], Junhoe Kim[1], Claas Abert[2], Dieter Suess[2], and Sang-Koog Kim[1†]

[1]National Creative Research Initiative Center for Spin Dynamics and Spin Wave Devices, Nanospinics Laboratory, Research Institute of Advanced Materials, Department of Materials Science and Engineering, Seoul National University, Seoul 151-744, Republic of Korea

[2]Christian Doppler Laboratory - Advanced Magnetic Sensing and Materials, University of Vienna, Austria

[*]Corresponding author: sangkoog@snu.ac.kr

Magnetic skyrmions are among the topologically protected magnetization textures that are promisingly applicable to information processing devices [1] owing to their nanosize and low-power-consumption motions. Fundamental dynamic modes of skyrmions for two-dimensional (2D)-geometry elements have been demonstrated theoretically by M. Mochizuki [2] and experimentally by Y. Onose et al. [3]; these modes include skyrmion-core gyrations in either the clockwise (CW) or counter-clockwise (CCW) rotation sense, as excited by in-plane ac magnetic fields or currents, as well as the breathing mode excited by out-of-plane ac magnetic fields or currents. To date, there have been no reports of skyrmion dynamic modes in curved-geometry structures.

Since the dynamic behaviors of skyrmions in 3D elements are expected to differ from their known dynamic modes in 2D elements, we investigated, as reported herein, skyrmions' dynamic modes and motions in short-length nanotubes. The model nanotubes were assumed to have the magnetocrystalline anisotropy axis and the Dzyaloshinskii-Moriya Interaction (DMI) vector in the direction normal to their surface. Unlike the case in 2D flat systems, the skyrmions formed in the nanotubes had rather an elliptical shape and asymmetry between the longitudinal and transverse directions. This geometrical asymmetry results in an additional curvature-induced interaction terms. The long axis of elliptical shape is parallel (perpendicular) to the tube's longitudinal axis for the positive (negative) DMI constant.

For in-plane applications of resonant ac magnetic fields, there exist either CCW or CW gyration motions. For the CCW gyration, the skyrmion's core rotates in a vertical oval orbit. In the case of CW gyration, the core of the skyrmion rotates in a nearly circular orbit. The breathing mode, as in 2D elements, is also excited by out-of-plane application of resonant ac magnetic fields. Unlike the case in 2D elements, with increasing strength of in-plane ac field above its critical strength, the CCW gyration motion becomes a periodic translational motion in the circumferential direction. The critical field strength is about 400 Oe for a given dimension, and the velocity of the skyrmion is about 22.9 m/s irrespective of ac magnetic field strength. The rotation sense of this periodic translational motion is determined by the skyrmion helicity that is governed by the sign of the interfacial DMI constant. This work provides a new physical insight into skyrmion dynamics in curved-geometry systems and also might prove applicable to potential skyrmion-based 3D racetrack memories.

References

[1] Fert, A., Cros, V., and Sampaio, J. Skyrmions on the track. Nature Nanotech. 8, 152 (2013).

[2] Mochizuki, M. Spin-wave modes and their intense excitation effects in skyrmion crystals. Phys. Rev. Lett. 108, 017601 (2012).

[3] Onose, Y. et al. Obervation of magnetic excitations of skyrmion crystal in a helimagnetic insulator. Phys. Rev. Lett. 109, 037603 (2012).

This research was supported by the Basic Science Research Program through the National Research Foundation of Korea (NRF) funded by the Ministry of Science, ICT & Future Planning (NRF-2018R1A2A1 A05078913).

Influence of vanadium incorporation on spin-orbit torque efficiency in W/W-V/CoFeB/MgO structures

Gyu Won Kim*, Yong Jin Kim, In Ho Cha, Taehyun Kim,
Min Hyeok Lee, and Young Keun Kim
Department of Materials Science and Engineering, Korea University, Seoul 02841, Korea

For the realization of magnetic random-access memory (MRAM) which operated by spin-orbit torque (SOT), it is crucial to find out the materials combinations for lowering write current density.

In the typical normal metal (NM)/Ferromagnet (FM)/oxide heterostructures, we adopted the tungsten (W) as an NM layer, because it is known to have the largest spin-Hall angle among the single metallic materials. Thus, we utilized the W/CoFeB/MgO structure and modified the W/CoFeB interface with 1 nm thickness of the W-V alloyed layer. The composition changing in W-V alloyed layer affects both magnetic anisotropy and spin-orbit torque efficiency. In the case of magnetic anisotropy, they showed a limited composition range from 0 to 70 atomic% for developing perpendicular magnetic anisotropy. Next, the SOT efficiency, we obtained the spin-Hall angle about 0.5, which is 40% enhanced value compared to that of ordinary W/CoFeB/MgO structure, which is 0.36.

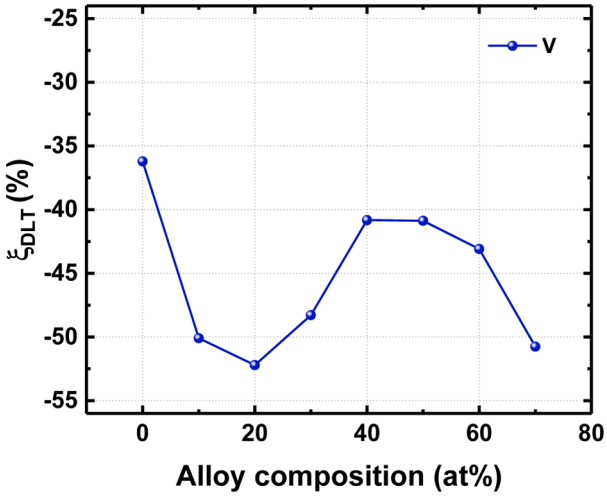

Fig. 1. Damping-like SOT efficiency with different W-V alloyed layer compositions

Observation of Positive and Negative Spin-Transfer Torques in Chiral Domain-Wall Motion

Dae-Yun Kim[1,2*], Qurat ul Ain[3], Yune-Seok Nam[1], Seonghyub Lee[1], Jun-Young Chang[1], Ji-Sung Yu[1], Byoung-Chul Min[2], Sung-Hyon Rhim[3], and Sug-Bong Choe[1]

[1]Department of Physics and Astronomy, Seoul National University, Korea

[2]Center for Spintronics, Korea Institute of Science and Technology, Korea

[3]Department of Physics, University Of Ulsan, Korea

We report observation of positive and negative spin-transfer torque (STT) in ultra-thin magnetic films. Spin-torque measurement reveals that opposite sign of the STT comes into the chiral domain-wall (DW) motion for Pt/Co/Pt and Pd/Co/Pd films; the STT moves the chiral DW into the electron flow (current flow) for Pt/Co/Pt films (for Pd/Co/Pd films). The first principle calculation finally demonstrated that the opposite sign of STT is attributed to the inversion of spin polarizations between two films.

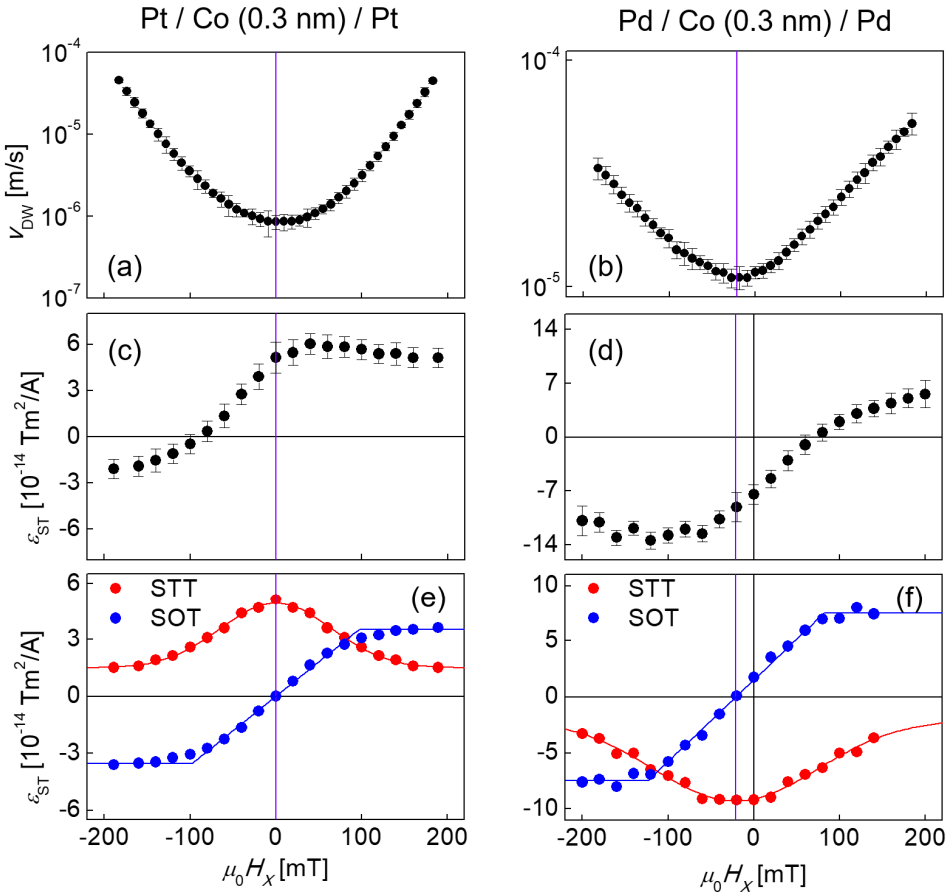

Fig. 1. (a), (b) Plots of DW speed as a function of H_x. (c), (d) Plots of spin-torque efficiency as a function of H_x. (e), (f) Plots of decomposed STT and SOT as a function of H_x. Purple vertical lines indicate DMI-induced effective longitudinal magnetic field.

International Symposium on Magnetism and
Magnetic Materials 2019

Oral Session III

'Nano Magnetism'

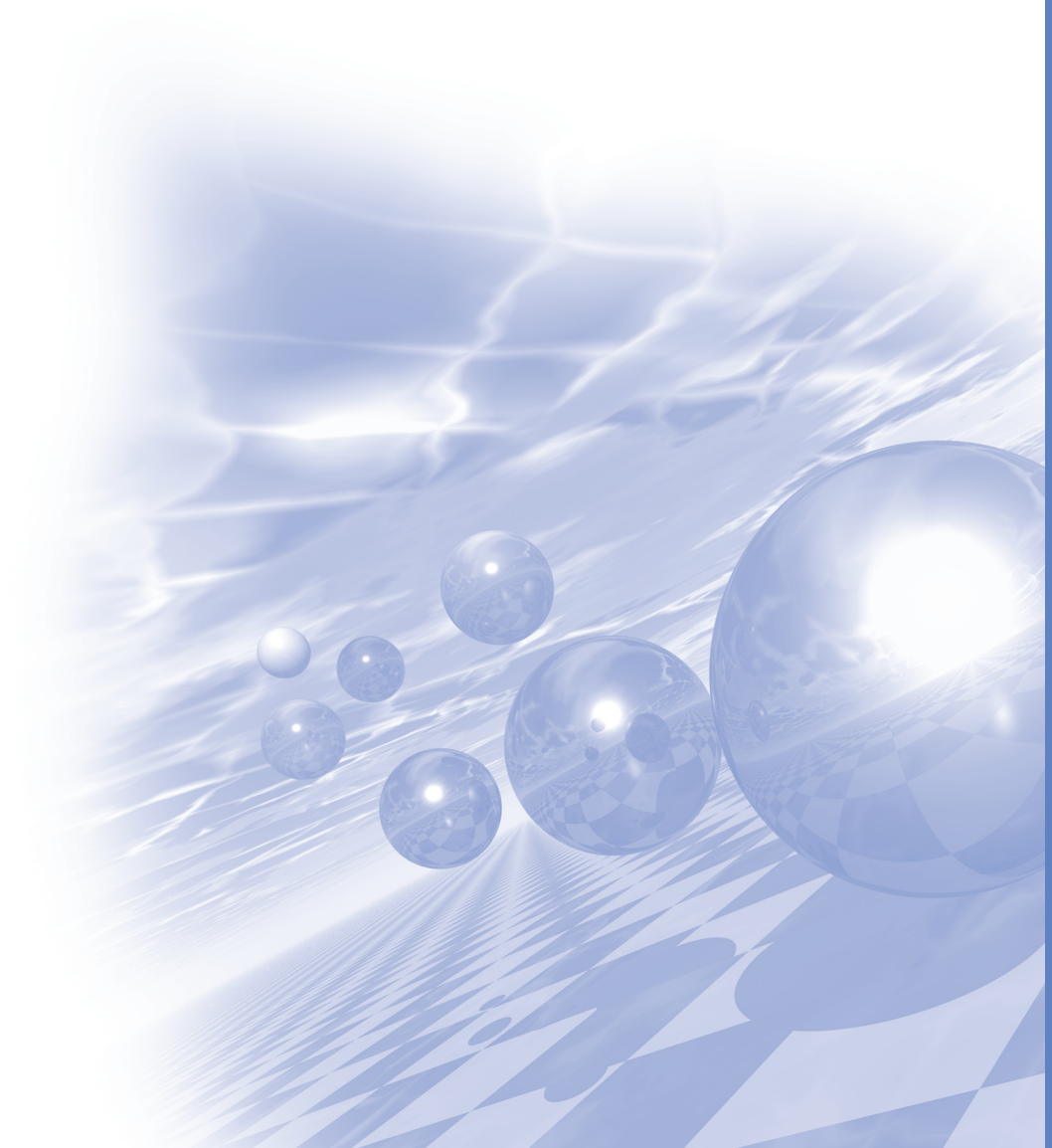

Upshift of MnBi magnetic properties via process optimizations

Yang Yang[1,2*], Jong-Woo Kim[1†], Jihoon Park[1], Hui-Dong Qian[1],
Jung Tae Lim[1], Oi Lun Li[2], Chul-Jin Choi[1†]

[1]Powder & Ceramics Division, Korea Institute of Materials Science, Changwon 51508, Republic of Korea
[2]School of Materials Science and Engineering, Pusan National University, Busan 46241, Republic of Korea

MnBi has attracted attention because of its appreciable coercivity, high crystalline anisotropy and, especially, reverse temperature coefficient of magnetic properties. In this work, high purity low temperature phase (LTP) MnBi powders were prepared via induction melting followed by heat treatment and low energy ball milling processed. The effects of heat treatment and ball milling conditions on purity and magnetic properties were systematically investigated. A prolonged homogenization process was employed to increase the purity of the LTP MnBi in the alloy, which shows remarkably enhanced saturation magnetization (M_s) of up to 71.4 Am^2/kg and purity of 97 *wt.*% LTP MnBi. An optimized composition was found to be in the vicinity of $Mn_{56}Bi_{44}$. After low energy ball milling for 3 h, the optimum $Mn_{56}Bi_{44}$ powder displays the maximum energy product $(BH)_{max}$ of 11.7 MGOe under applied magnetic field of 1.5 T at room temperature as shown in Fig. 1. Based on this qualified MnBi powder, bulk sintered magnet was prepared. Recently, the $(BH)_{max}$ of 6.4 MGOe and a cercivity (H_c) higher than 1 T were obtained at room temperature. In this presentation, fabrication and optimization processes for MnBi powder and bulk will be discussed in detail.

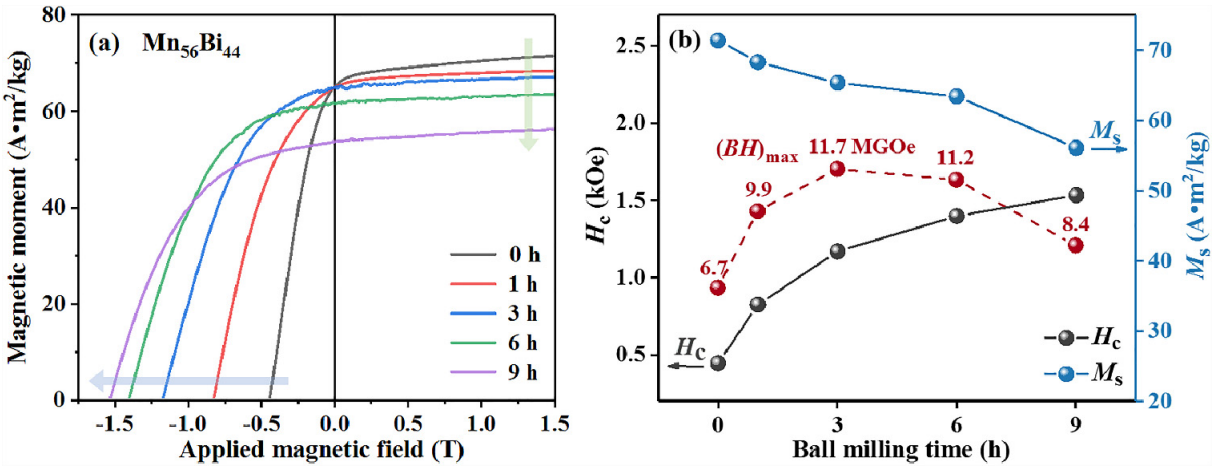

Fig. 1. (a) The demagnetization curves and (b) magnetic properties of the $Mn_{56}Bi_{44}$ ball-milled powders for 1 h,3 h, 6 h, and 9 h, respectively.

The effect of Sn substitution on magnetic properties of MnBi

Yang Yang[1,2], Jong-Woo Kim[1*], Jihoon Park[1], Jung Tae Lim[1],
Hui-Dong Qian[1], Oi Lun Li[2], Chul-Jin Choi[1†]

[1]Powder & Ceramics Division, Korea Institute of Materials Science, Changwon 51508, Republic of Korea
[2]School of Materials Science and Engineering, Pusan National University, Busan 46241, Republic of Korea

MnBi intermetallic compound, known as low-temperature phase (LTP) MnBi is a magnetic material with many attractive features of interests for industrial applications such as rare-earth-free permanent magnets, spintronics and magnetic refrigeration. In this work the effects of Sn addition on the magnetic and physical properties of MnBi magnetic materials are investigated systematically in both powder and bulk forms. At first, high quality LTP MnBi powder was prepared by induction melting, followed by post processes. The obtained MnBi powder was then mixed with Sn submicron powder using low energy ball milling. Bulk sintered Sn-doped MnBi magnet was prepared by hot press at relevant temperature and pressure. Fig. 1(a). shows the Sn *wt.*% dependence on the density for the Sn-doped LTP MnBi bulk magnet. The density increases with increasing Sn 0 *wt.*% up to 5 *wt.*%. Meanwhile, the phase fraction of LTP MnBi is getting higher according to the Sn contents. In this presentation, an optimized experimental procedures and analysis of physical and magnetic properties of Sn addition to MnBi alloy will be discussed in detail.

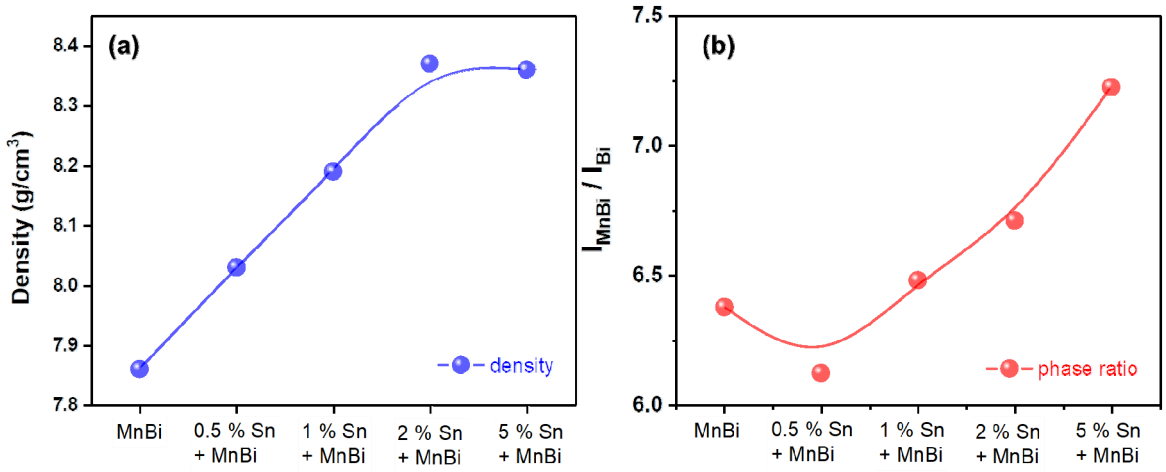

Fig. 1. (a) Sn wt.% dependence of the density for MnBi/Sn bulk magnetic materials and (b) phase ratio variation of LTP MnBi according to Sn contents.

W Thickness-Dependent Perpendicular Magnetocrystalline Anisotropy of Pt/Co/W(111) Superlattices

Thi Huynh Ho*, Sanghoon Kim, S. H. Rhim, S. C. Hong
Department of Physics and Energy Harvest Storage Research Center,
University of Ulsan, Ulsan 44610, Republic of Korea

Pt/Co/W trilayers structure reveals strong perpendicular magnetocrystalline anisotropy (PMA), which raises great interests for promising spintronics applications[1,2]. Despite of its potentials, the effects of W-capping on PMA of Pt/Co have not been fully identified. In this study, the influence of W thickness on PMA of Pt/Co/W(111) is explored using density functional theory calculations. Pt/Co and W/Co superlattices for various in-plane lattice constants are first compared to clarify the effects of heavy metal-capping on Co: PMA of W/Co is much greater than Pt/Co. For Pt/Co/W superlattice, PMA exhibits the maximum value at W thickness of 0.6 nm. Our analysis indicates that W and Co interfacial layers play major role in PMA. Moreover, k-resolved PMA demonstrates the origin of contribution is mostly from Γ point.

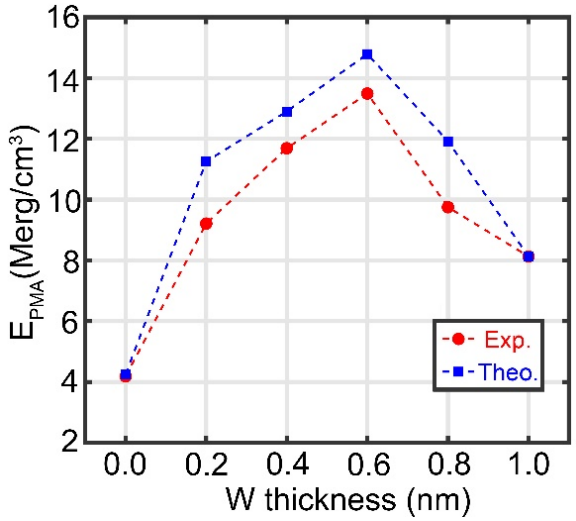

Fig. 1. PMA energy of Pt/Co/W superlattices as a function of W thickness.

Keywords: perpendicular magnetocrystalline anisotropy, superlattices, thickness dependence.

References

[1] Z. A. Bekele et al., Solid State Commun. **274**, 41 (2018).
[2] S. Mendisch et al., J. Magn. Magn. Mater. **485**, 345 (2019).

Spin-orbit-induced field in GaMnAs/Bi_2Se_3 bilayer system

Kyung Jae Lee[1*], Seul-Ki Bac[1], Seonghoon Choi[1], Phunvira Chongthanaphisut[1], Seongjin Park[1], Sanghoon Lee[1†], Xinyu Liu[2], M. Dobrowolska[2], and Jacek K. Furdyna[2]

[1]Physics Department, Korea University, Seoul 02841, Republic of Korea

[2]Physics Department, University of Notre Dame, Notre Dame, IN 46556, USA

We report observation of spin-orbit-induced (SOI) field on GaMnAs/Bi_2Se_3 bilayer structure. The magneto-transport measurement was carried out in order to detect SOI field of the system. The magnetization reversal process was monitored during the application of current along the [110] and the [1-10] crystalline directions. We are able to detect asymmetry of planar Hall resistance (PHR) hysteresis between positive and negative current directions even with small current density of 1.4 x 10^5 A/cm^2 during the magnetization reversal process (see Fig. 1). The asymmetry of hysteresis systematically increases with increasing current density. The asymmetry in the hysteresis was caused by the combination of Dresselhaus-type SOI field in GaMnAs and effective field induced by the spin polarized surface state of Bi_2Se_3 topological insulator. Since the directions of these fields depend on the direction of applying current (i.e., either along the [110] and the [1-10] crystalline direction) we carefully analyze the current polarity dependence of the asymmetry in the PHR hysteresis in order to identify the contribution of the Dresselhaus-type SOI field in GaMnAs and the spin polarized surface state of Bi_2Se_3 topological insulator in our GaMnAs/Bi_2Se_3 bilayer structure.

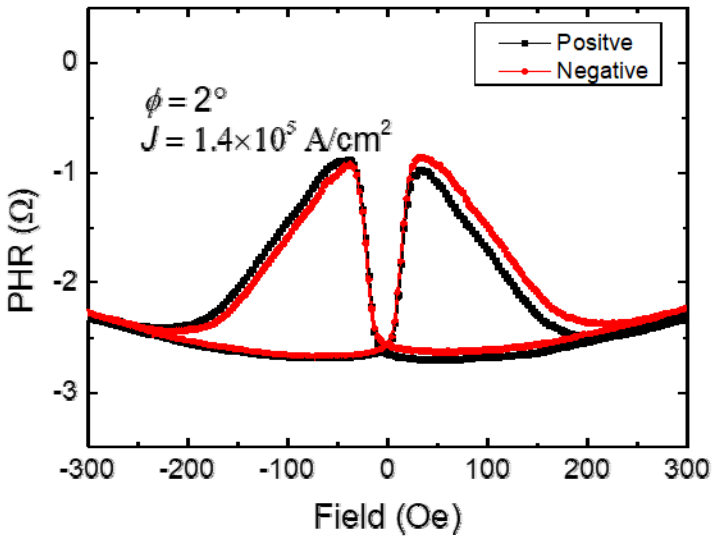

Fig. 1. PHR data measured at 3 K with a current density of 1.4 x 10^5 A/cm^2. Black and Red data indicate positive and negative current, respectively.

Zn substituted Strontium W-type hexaferrite in Ka band (26.5 – 40 GHz) for microwave absorber

Sungjoon Choi[1*], Jae-Hyoung You[1], Seung-Young Park[2], Seong Jin Choi[3], and Sang-Im Yoo[1]

[1]Department of Materials Science and Engineering, and Research Institute of Advanced Materials, Seoul National University, Seoul 151-744, Korea

[2]Spin Engineering Physics Team, Division of Scientific Instrumentation, Korea Basic Science Institute, Daejeon 34133, Korea

[3]Chang Sung Co Ltd, R&D Ctr, 11-9 Namdong Ind Area, Inchon 405100, Republic of Korea

Strontium W-type hexaferrite ($SrMe_2Fe_{16}O_{27}$; $SrMe_2W$, where Me is a divalent transition metal ion), have been widely studied for microwave absorber as they exhibit uniaxial anisotropy along the c-axis, and thus high ferromagnetic resonance frequency. Also, Zn^{2+} is known to increase real and imaginary permittivity of $SrMe_2W$, we tried to synthesize and identify the microwave absorbing property of partially Zn^{2+}-substituted $SrMe_2W$ hexaferrites ($SrZn_xFe_{2-x}W$, where $0.0 \leq x \leq 2.0$). For this purpose, the composites having epoxy resin as a matrix, and $SrZn_xFe_{2-x}W$ (x=0.0, 0.5, 1.0, and 2.0) as magnetic fillers were fabricated with the ferrite volume factions of 30, 60, 90 vol%, with different x values were annealed at the temperature region of 1000–1350 ˚C for 2 h in the PO_2 of 10^{-3} atm. The complex permittivity and permeability of $SrZn_xFe_{2-x}W$ in Ka band (26.5–40 GHz) were measured, and the reflection losses were calculated based on the obtained permittivity and permeability spectra. Detailed results will be presented for discussion.

This work was supported by a Grant from Chang Sung CO.

Ferromagnetic resonance effect in superparamagnetic iron oxide nanoparticles and its application for hyperthermia

Jae-Hyeok Lee[1*], Jaegun Sim[1], Yongjun Lim[2], Seung-hyun Noh[2], Seung Ho Moon[2], Jinwoo Cheon[2] and Sang-Koog Kim[1†]

[1]Seoul National University, Korea

[2]Yonsei University, Korea

Corresponding author: sangkoog@snu.ac.kr

For a new paradigm of bio-applications of magnetic nanoparticles, the robust resonant dynamic characteristics of spin-precession motions [1] can be utilized with the advantage of the ultra-high sensitivity. In cases where the frequency of AC magnetic fields equals the Larmor precession frequency to a given DC magnetic field, individual magnetic moments efficiently absorb energies that are transferred from externally applied AC magnetic fields, after which those energies dissipate into other forms due to their intrinsic damping of given magnetic materials. Such energy dissipations of magnetic nanoparticles are of crucial importance in hyperthermia bio-applications for high specific loss power (SLP). [2] Larmor precession motions of individual spins in magnetic particles excited by relatively high-frequency (several hundred MHz) AC magnetic fields can give rise to a higher efficiency of energy dissipation than those by Brownian rotation of nanoparticles and/or by Néel relaxation of nanoparticles' magnetizations.

Dynamic response of isolated superparamagnetic iron oxide (15 nm in diameter) nanoparticles of spherical shape were analyzed by the vector network analyzer to observe the Larmor precession of the nanoparticles. We obtained microwave absorption spectra as a function of frequency at each static magnetic field varied up to 3 kOe. For a given magnetic field strength, the collective Larmor precession motions in nanoparticles exhibit its resonant peaks where strong absorption and dissipation of microwaves occur. The resonant frequencies as a function of field strength were well fitted to a linear curve according to the Larmor equation with a specific gyromagnetic ratio. Further we experimentally observed the heat generation from the ferromagnetic resonance in superparamagnetic nanoparticles. The superparamagnetic iron oxide nanoparticles are deposited on the microstrip where a few Watts RF fields applied. In our present system, temperature increases up to 10 degrees were observed purely due to ferromagnetic resonance of superparamagnetic nanoparticles under the applied RF frequency between 1-3 GHz and certain DC magnetic fields. This work would open a new horizon in the field of high-frequency magnetic nanoparticle-based bio-applications.

References

[1] S.-K. Kim et al., Sci. Rep. 5, 11370 (2015); S.-K. Kim et al., Sci. Rep. 6, 31513 (2016).

[2] M.-K. Kim and S.-K. Kim et al., Phys. Rev. Applied 9, 054037 (2018); M.-K. Kim and S.-K. Kim et al., J. Appl. Phys. 125, 063901 (2019)

This research was supported by the Basic Science Research Program through the National Research Foundation of Korea (NRF) funded by the Ministry of Science, ICT & Future Planning (NRF-2018R1A2A1A05078913).

International Symposium on Magnetism and Magnetic Materials 2019

Special Session IV

'Mössbauer Session'

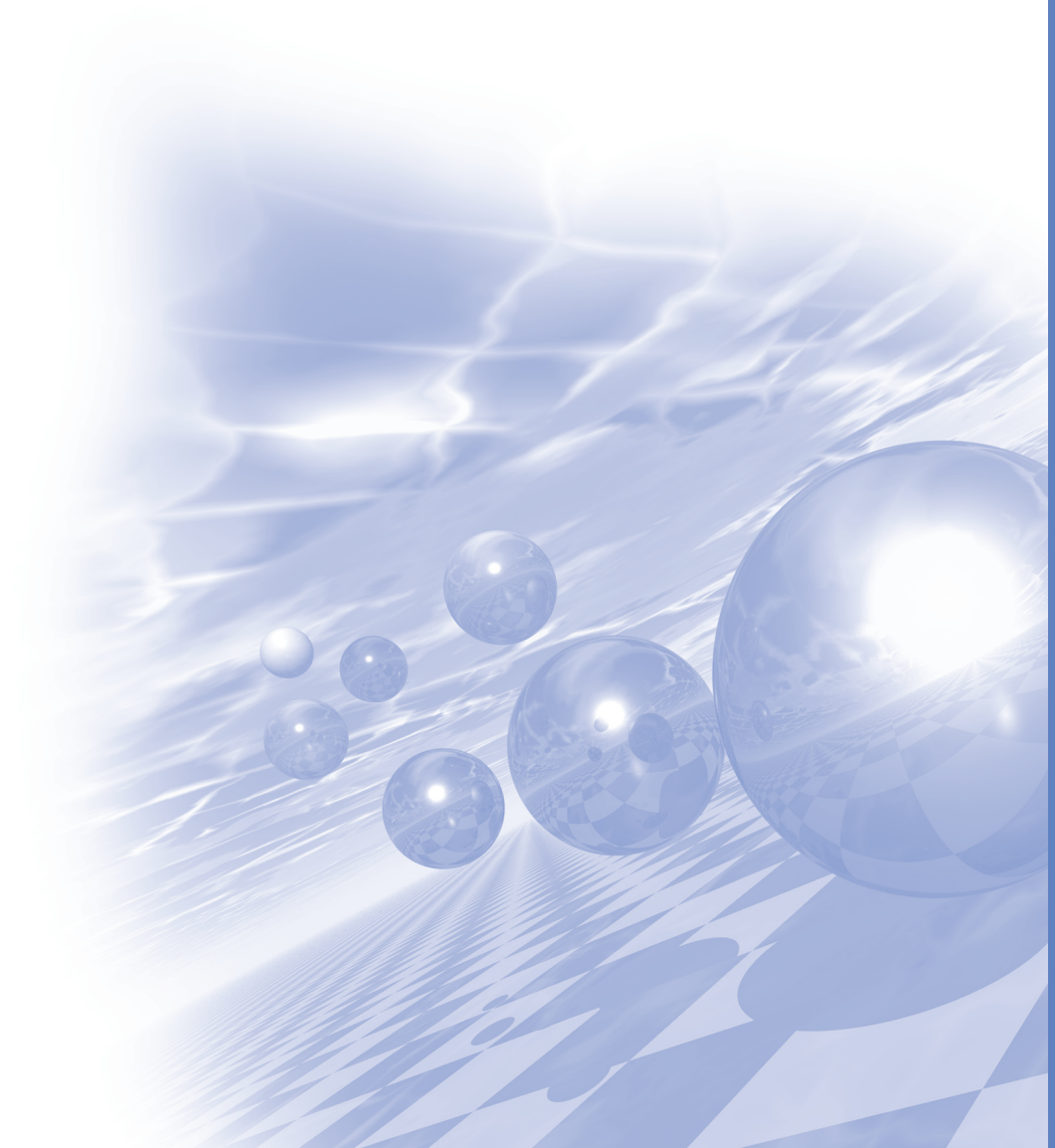

Effects of In^{3+} site occupancy on the magnetic properties of M-type strontium hexaferrites

Chul Sung Kim[1], and Sunghyun Yoon[2*]
[1]Department of Physics, Kookmin University, Seoul 02707, Rep. of Korea
[2]Department of Physics, Gunsan National University, Gunsan 54150, Rep. of Korea

Effects of non-magnetic indium substitution on magnetic properties of M-type Strontium hexaferrites has been studied by first-principle calculation and crystallographic and magnetic measurements. The Indium doped samples SrFe12-xInxO19 (x=0.25, 0.5, 0.75, 1.0) have been prepared by the auto-combustion method using metal nitrates and citric acid, followed by annealing at 1100 ℃ for 12 hours.

Scanning electron microscopy images show that the samples have hexagonal plate-like shape with the particle size ranging from 500~1000 nm and that the apparent size decrease with addition of indium. Lattice parameters show linear increase with increasing indium content, meaning the uniform solid solution is formed throughout the doping range (Fig 1).

The variations of saturation magnetization M_S and the coercivity H_C with indium content x were obtained from room temperature vibrating sample magnetometer. Whereas the H_C decreased monotonically with indium addition, the M_S first increase until x=0.5 reaching maximum but decrease thereafter. Effective magnetic anisotropy constants K are calculated as well from hysteresis curves using the Law of approach to saturation method, and are 3.79´105, 3.70´105, 2.95´105, and 2.87´105 J/m^3 for x= 0.25, 0.5, 0.75 and 1.0, respectively.

Mössbauer spectra showed that In^{3+} mainly replaced Fe^{3+} ions in $4f_2$ sites and that 12k subspectra split into two distinct components 12k1 and 12k2. This behavior was explained by the existence of two competing interactions in terms of nonmagnetic indium substitution.

Analyses of Nano-Crystalline Structure in Precipitated Iron-Based Catalysts for Fischer-Tropsch Synthesis

Dong Hyun Chun*
Clean Fuel Laboratory, Korea Institute of Energy Research (KIER)

FTS (Fischer-Tropsch synthesis) is a process invented by two German researchers, Franz Fischer and Hans Tropsch, in the 1920s, which catalytically convert syngas (H_2 + CO) into hydrocarbon products: $nCO + \{2n(+1)\}H_2 \rightarrow C_nH_{2n(+2)} + nH_2O$. Iron-based catalysts are highly promising for the FTS due to their high activity and low cost. A precipitation technique is one of the commercially proven methods for preparation of iron-based FTS catalysts as this technique can easily generate nano-crystalline particles. In general, the as-prepared precipitated iron-based catalysts are known to be composed of hematite (α-Fe_2O_3) that are inactive for the FTS. Thus, the as-prepared catalysts must be subjected to a proper activation treatment to change the as-prepared catalysts into active phases such as Fe_5C_2 and Fe_2C. This means that the crystal structure of as-prepared catalysts and their reduction and carburization behavior can critically influence the catalytic performance of precipitated iron-based FTS catalysts. But, it is very difficult to reveal the exact relationship among the crystal structure of as-prepared catalysts, their reduction and carburization behavior, and the catalytic performance for FTS because high-performance iron-based FTS catalysts are usually composed of a mixture of several iron species with nano-crystalline structure. In this presentation, the crystal structure of precipitated iron-based FTS catalysts was analyzed in detail by X-ray diffraction and Mössbauer spectroscopy. It was found that a significant amount of ferrihydrite ($FeOOH \cdot nH_2O$, $0 < n < 1$) can coexist with hematite in the as-prepared catalysts, which depends on the precipitation conditions. Furthermore, it was revealed that the ferrihydrite plays a crucial role in determining the catalytic performance as well as the reduction and carburization behavior of the catalysts.

Study on Multiferroic materials using Mössbauer Spectroscopy

Sung Baek Kim*
Humanity College, Konyang University, Korea

Mössbauer spectroscopy provides a unique measurement that probes magnetically fine phenomena occurring within 10^{-7} sec time interval and 10^{-12} eV energy scale. It is useful to examine the magnetic hyperfine field, electric-field gradient tensor, and spin state of magnetic ions in a variety of magnetic materials. Here we present interesting results of Mössbauer spectroscopy experiments, especially for multiferroic materials. The multiferroic material is the one in which both magnetic order and ferroelectric are simultaneously expressed. Most of these materials are magnetic materials containing Fe or lanthanide (rare earth) ion, and research using Mössbauer spectroscopy is being actively conducted.

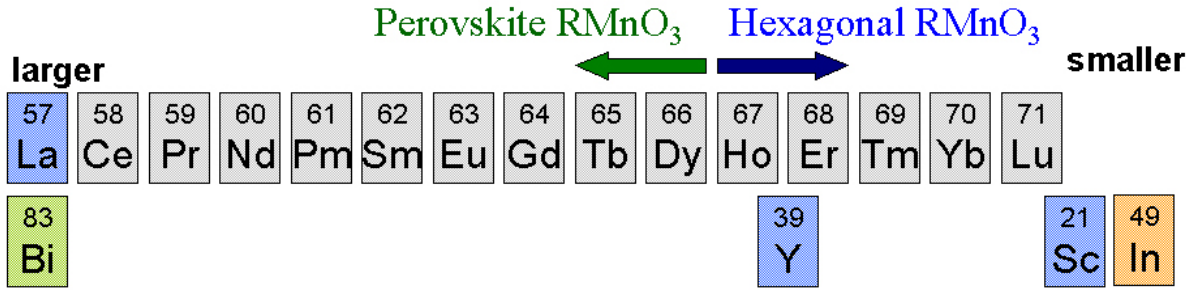

Fig. 1. Changes in the crystallographic structure of $RMnO_3$ materials by the size of R^{3+} ions

In the materials with perovskite structures (ABO_3; A = rare earth ion), as the atomic number of A-site ions increases, the ionic radius decreases, increasing the crystallographic distortion, resulting in a hexagonal structure from Ho ions. It has been studied by Mössbauer spectroscopy that the ferroelectric correlation of the material is expressed from the change in magnetic structure due to crystallographic properties. In addition, the study of double perovskite structure ($A_2BB'O_6$) materials has resulted in Mössbauer spectroscopic studies, where the causes of the multiferroic properties of these materials are explained by the anisotropic magnetic hyperfine field fluctuation due to crystallographic properties.

Introduction of In-beam Mössbauer spectroscopy and its application of Heritage analysis

Young Rang Uhm[1*], Gwang Min Sun[1], and Chul Sung Kim[2]
[1]Neutron& Radioisotope Application Research Division,
Korea Atomic Energy Reasearch Institute(KAERI), Daejeon, Rep.of Korea
[1]Nano-Electro Physics, Koomin univercity, Seoul Rep.of Korea
[*]E-mail: uyrang@kaeri.re.kr

In-situ irradiated radioisotope (RI) beam by positrons and neutrons in heavy ion accelerator and research reactor is played a roll of Mössbauer source for in-beam Mössbauer spectroscopy. These instruments are one of the most powerful techniques to observe the site occupations, dynamic atomic jump processes, and exotic chemical states of extremely diluted atoms in a material. The Mössbauer technique offers unique information of the probe atoms under non-equilibrium or metastable conditions in the Mössbauer lifetime. Here, the outlines of recent developed the facilities in RIKEN RI-beam Factory and in Budapest research reactor are explained. Mössbauer spectroscopy using ^{57}Co as a source is able to apply analyses of reproducing chromaticity of Celadon and Dancheong which is traditional multicolored paintwork on wooden buildings. The greenish colored celadon is determined by the condition of kiln and valence state of iron in glaze. The traditional multicolor of Dancheong is also restored using mineral pigment. Its reddish base color results in the ocher soil in Ulleong-do, Korea. The valence state of iron and its ratio can be accurately analyzed using Mössbauer spectrometer. Recently, development of the potable Mössbauer spectrometer is also focused in our research to apply in-situ detection of heritages. Also, in-beam spectrometer will be set up for analyzing golden relics, near future.

International Symposium on Magnetism and
Magnetic Materials 2019

Oral Session IV

'Spintronics II'

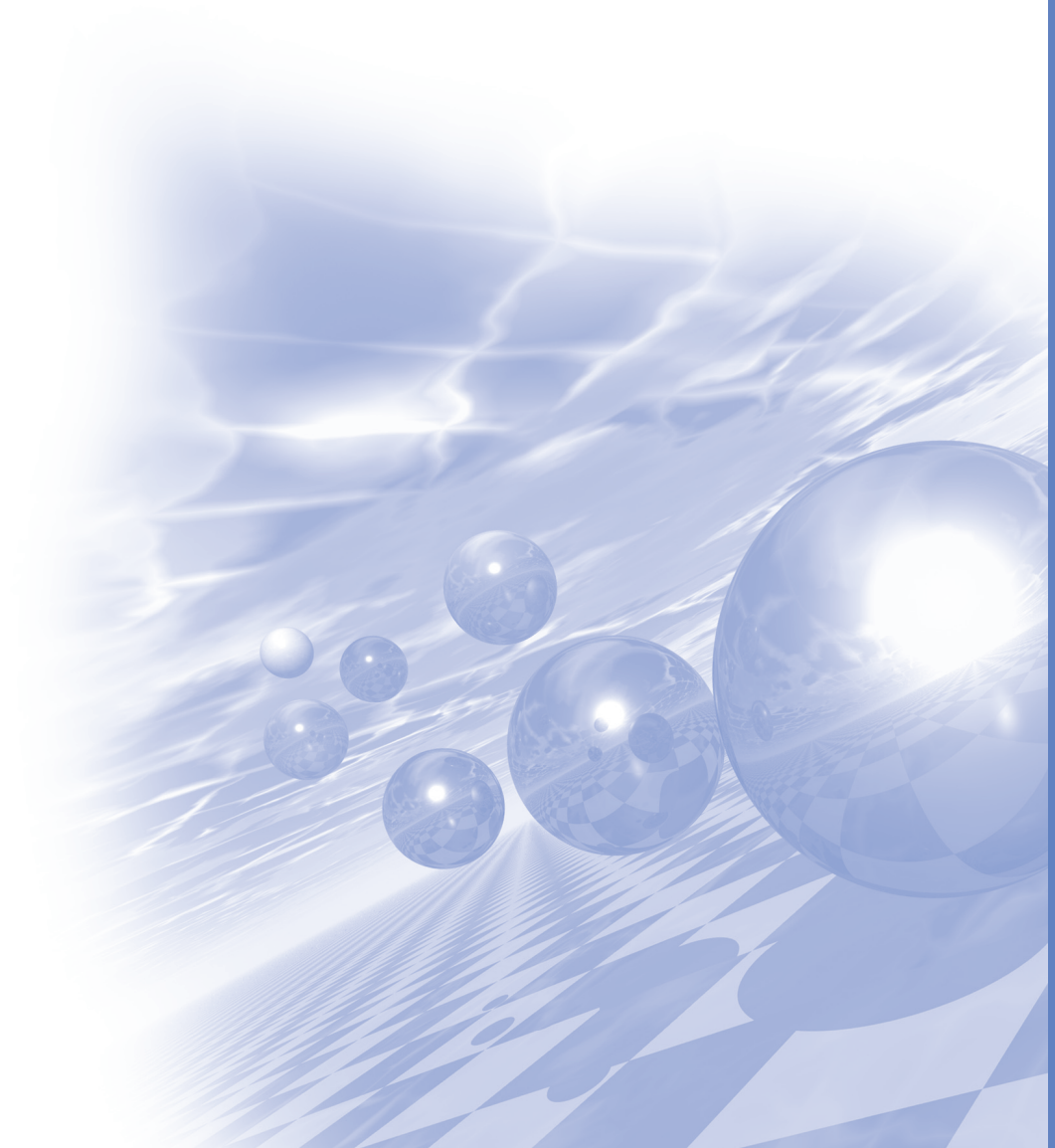

Coexisting and strongly interacting spin torque driven free and reference layer magnetic droplet solitons

S. Chung[1,2*], S. Jiang[2,3], M. Ahlberg[2], A. A. Awad[2], Q. Tuan Le[2,3], H. Mazraati[3], A. Gangwar[2], A. Houshang[2], O. Heinonen[4], and J. Åkerman[2,3]

[1]Department of Physics Education, Korea National University of Education, Cheongju 28173, Korea

[2]Physics Department, University of Gothenburg, 412 96, Gothenburg, Sweden

[3]Department of Applied Physics, School of Engineering Sciences,
KTH Royal Institute of Technology, Electrum 229, SE-16440 Kista, Sweden

[4]Materials Science Division, Argonne National Laboratory, Lemont, IL 60439, USA

Magnetic droplets are nanoscale magneto-dynamical solitons that can be nucleated and sustained underneath nano-contact (NC) using spin transfer torque. So fat, all theoretical, numerical, and experimental droplet has been studied on the free layer (FL), and any additional dynamics in the reference layer (RL) has not been considered. Here, we show, using experiments and micromagnetic simulations of all-perpendicular [CoPd]/Cu/[CoNi] based

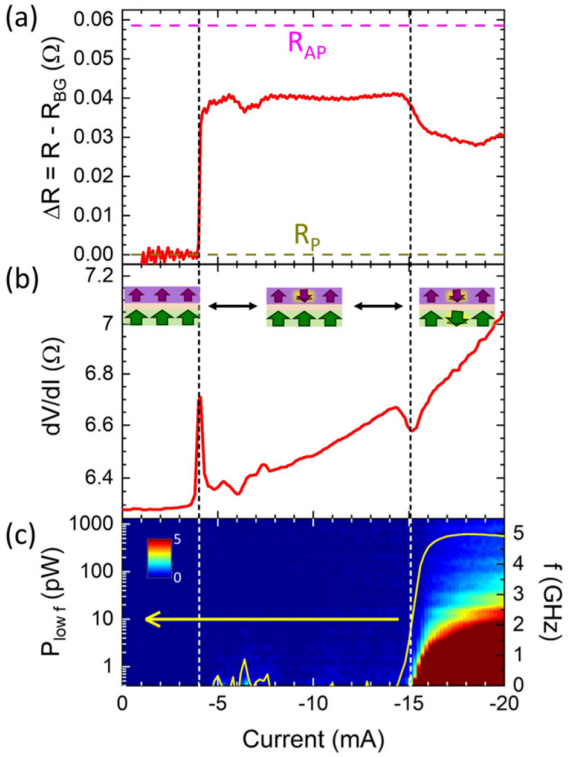

Fig. 1. (a) Device resistance vs. applied current (I) after a background subtract: Three different states corresponding to no droplet (left), FL droplet (middle), both FL and RF droplets (right) distinguished by dashed lines. R_P and R_{AP} are the value of resistance from fully parallel and anti-parallel of both FL and RL. (b) Differential resistance (dV/dI) measurement vs. I: two large peaks of dV/dI are well correlated with a resistance transition in (a) and each states are described in cartoons. (c) Power spectral density (PSD) and integrated power (yellow line): Large power at above -14 mA indicates strong and chaotic behavior of both FL and RL droplets.

nano-contact spin torque nano-oscillators (STNOs), that there is not only significant magneto-dynamics in the RL but that the RL itself can host another droplet coexisting with the FL droplet. The RL droplet can be nucleated by the spin polarized current from the reversed core of the FL droplet at a current substantially higher than that required for a FL droplet. Both the FL and RL droplets are observed experimentally as step-wise changes of the STNO resistance and as sharp peaks with opposite sign in the STNO differential resistance. In addition, whereas the FL droplet is highly stable when alone, the state of coexisting FL and RL droplets exhibits high-power broadband microwave noise. Micromagnetic simulations corroborate the experimental results and reveal a strong interaction between the droplets. Depending on simulation parameters, the coexisting droplets have their own uncoupled intrinsic precession frequencies, they interact strongly leading to an intense chaotic lower-frequency dynamics underneath NC, consistent with the experimentally measured broadband microwave noise. Our first demonstration of strongly interacting and closely spaced droplets can offer a unique platform for fundamental studies of highly non-linear soliton pair dynamics.

Tunable magnetic properties via interface engineering

June-Seo Kim[1*], Jinyong Jung[2], Chun-Yeol You[2]
[1]Division of Nanotechnology, DGIST, Daegu, 42988 Republic of Korea
[2]Department of Emerging Materials Science, DGIST, Daegu, 42988 Republic of Korea

The interfacial Dzyaloshinskii-Moriya interaction (iDMI) based on an inversion symmetry breaking structure has been widely investigated because of its various physical roles in the dynamics of the non-colinear spin structure. Especially, topologically stable skyrmion state for future non-volatile memory and logic devices including neuromorphic applications is dependent on the iDMI and perpendicular magnetic anisotropy (PMA) energy. Many studies of skyrmion state have been carried out using bulk DMI and ferromagnet and heavy metal superlattice structures. However, the skyrmion state via interfacial spin-orbit coupling at room temperature has been challenging to achieve and has not been reported yet for ultrathin magnetic trilayer systems such as heavy metal/ferromagnet/heavy metal structure. Manipulating the iDMI and PMA energy can lead to a new pathway to control the topologically stable skyrmions. Not only changing the materials but also the inversion symmetry changes can be used to control and vary the iDMI and PMA energy density. In this study, we investigate the iDMI and PMA for Pt/Co/Pd and Pd/Co/Pt systems by performing Brillouin light scattering (BLS) spectroscopy and vibrating sample magnetometer (VSM). As shown in Fig. 1(a), the anisotropy field with Pd underlayer, which is directly proportional to PMA, is suppressed approximately 80% (compare with Pt underlayer systems). However, the iDM energy density is almost identical for Pd and Pt underlayer (See Fig. 1(b)). It can be emphasized that by engineering the Pd underlayer, we achieve a reduction of PMA energy and large value of iDMI energy density, despite the nominal identical interface materials. We strongly anticipate through our experimental observations that a topologically stable skyrmion state at room temperature on a trilayer system via Pd underlayer is possible and it can open a new path to fabricate new type non-volatile spintronic devices.

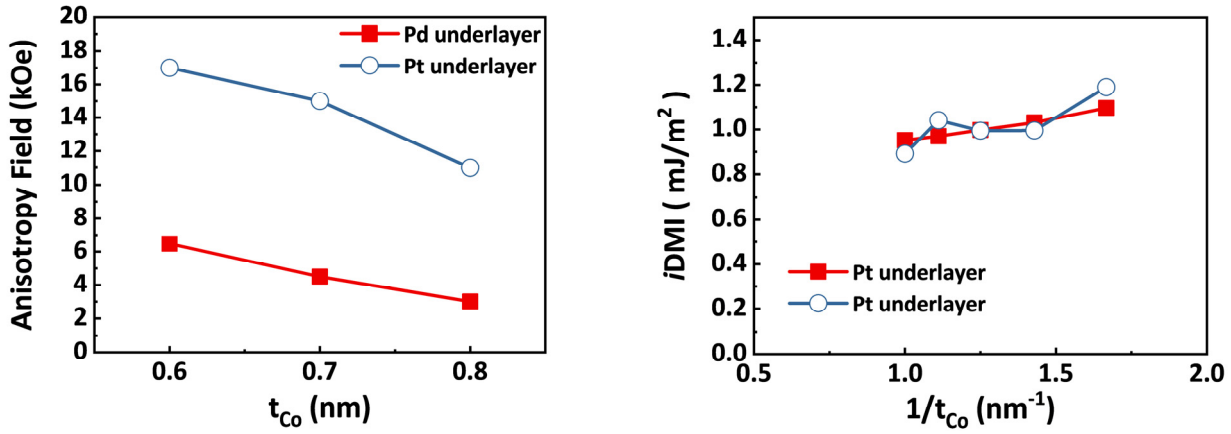

Fig. 1. (a) Anisotropy measurement (by using VSM) and (b) determined iDMI energy density for Pt and Pd underlayer systems

Control of the skyrmion Hall effect via external magnetic fields

Seungmo Yang[1*], Kyoung-Woong Moon[1], Changsoo Kim[1], Duck-Ho Kim[2], Jeonghun Shin[3], Byong Sun Chun[1], Jinpyo Hong[3], Se Kwon Kim[4], Chanyong Hwang[1†]

[1]Quantum Technology Institute, Korea Research Institute of Standards and Science, Daejeon, Korea

[2] Center for Spintronics, Korea Institute of Science and Technology, Seoul, Korea

[3]Nanoscale semiconductor engineering, Hanyang University, Seoul, Korea

[4]Department of Physics and Astronomy, University of Missouri, Columbia, MO, United States

The topological chiral spin textures, skyrmions, have been significant interest due to their novel topological phenomena including emergent electromagnetism, the topological Hall effect and the skyrmion Hall effect (SkHE) [1]. In addition, magnetic skyrmions have also become one of the most promising candidates as robust information carriers in the next-generation spintronic devices. However, the skyrmions motion is deflected from the direction of the force by SkHE [2,3]. Therefore, it is essential to understand and manipulate the SkHE not for only unveiling the underlying physics but also for making the best use of skyrmions in spintronics applications.

Here, we address a novel method to control the skyrmion Hall angle (SkHA) using both out-of-plane and in-plane external magnetic fields, and an efficient way to achieve the straight motion of magnetic skyrmions by completely suppressing the SkHE. Manipulation of the SkHA via the external magnetic fields is experimentally confirmed by studying chiral stripe shooting with the half-skyrmion end as shown in Fig.1. The observed field dependence of the SkHA is explained by generalizing the existing theory for the elongated chiral bubbles [4] to the cases with the simultaneous presence of external magnetic fields and spin-orbit torques. Finally, based on the demonstrated precise control of the SkHA, extremely simple SUM operation devices are fabricated where the direction of the current-induced elongation of skyrmions is determined by the external magnetic field.

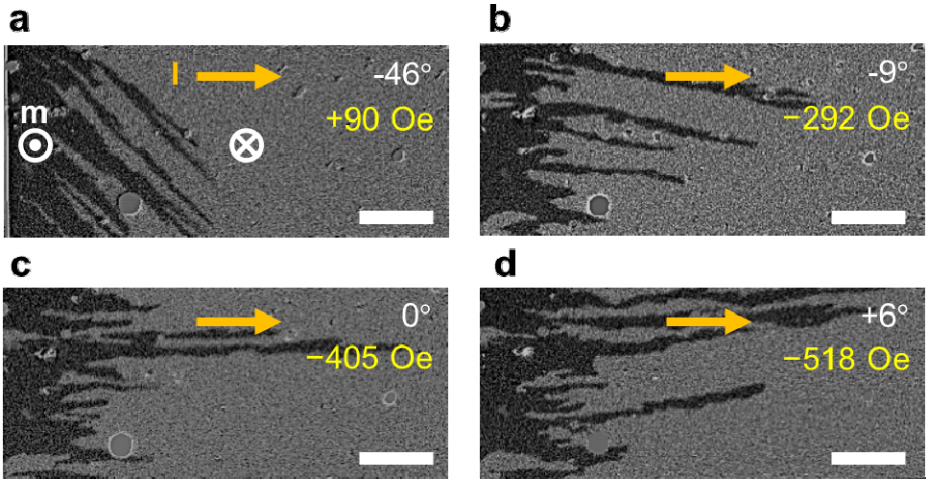

Fig. 1. The current-induced stripe shooting angle as a function of the y-axis external magnetic field (H_y). Current-driven stripe shooting under 1.78 Oe of H_z and **a,** +90 Oe, **b,** -292 Oe, **c,** -405 Oe, **d,** -518 Oe of H_y with 6.38 MA/cm^2 of current along the x-axis. The white numbers indicate the stripe shooting angle, that is, the skyrmion Hall angle (SHA). The angle is defined as positive counter clockwise from the x-axis.

References

[1] N. Nagaosa & Y. Tokura. **Nature Nanotechnology**. Vol. **8**, p. 899 (2013).

[2] W. Jiang, X. Zhang, G. Yu et al. **Nature Physics**. Vol. **13**, p. 162 (2016).

[3] K. Litzius, I. Lemesh, B. Krüger et al. **Nature Physics**. Vol. **13**, p. 170 (2016).

[4] Y. Hirata, D.-H. Kim, S. K. Kim et al. **Nature Nanotechnology**. Vol. **14**, p. 232 (2019).

Influences of Co-substitution on Magnetic Properties of Tetragonal $D0_{22}$-Mn_3Ga

Thi Quynh Anh Nguyen*, Thi H. Ho, S. C. Hong, S. H. Rhim
Department of Physics and Energy Harvest Storage Research Center,
University of Ulsan, Ulsan 44610, Republic of Korea

Mn-based Heusler compounds have drawn special attention because of rich physics and diverse applications in spintronic and permanent magnet. Among them, Mn_3Ga is a potential candidate with combinations of high spin polarization, high Curie temperature (~750 K), low magnetic moment, and high perpendicular magnetic anisotropy [1,2], which are useful for spin transfer torque (STT) devices. In this study, influences of Co-substitution on electronic structure and magnetic properties of $Mn_{3-x}Co_xGa$ (x = 0~1) is presented by first-principles calculations. Mn_3Ga possesses two inequivalent Mn sites, octahedral and tetrahedral ones denoted as Mn-I and Mn-II, respectively, where Mn-II site is energetically favored [3]. Notably, structural phase transition from tetragonal to cubic is found at x = 0.6. In particular, tetragonal and cubic phases exhibit different magnetic behaviors governed by different Co moment. In tetragonal case, magnetic moment decreases from 1.73 μ_B to 0.72 μ_B with x due to nearly vanishing Co moment. In contrast, magnetic moment increases from 1.00 μ_B to 2.00 μ_B with Co concentration, where Co moment (~1.00 μ_B) is almost unchanged. Furthermore, half-metallicity in cubic phase occurs when x = 0.5 and x = 1.0. The underlying reason are strong ferromagnetic Co-Mn(II) and week antiferromagnetic Co-Mn(I) couplings obtained from Heisenberg model.

Keyword: Heusler compounds, structural phase transition, first-principles calculations, half-metallicity, Heisenberg exchange interaction.

References

[1] B. Balke et all, Appl. Phys. Lett. **90**, 152504 (2007)
[2] Y. You, G. Xu, F. Hu, Y. Gong, E. Liu, G. Peng, and F. Xu, J. Magn. Magn. Mater. **429**, 40 (2017)
[3] Schadow et al, Phys. Rev. B **91**, 094203 (2015)

International Symposium on Magnetism and
Magnetic Materials 2019

Oral Session V

'Magnetics Theory/Oxide'

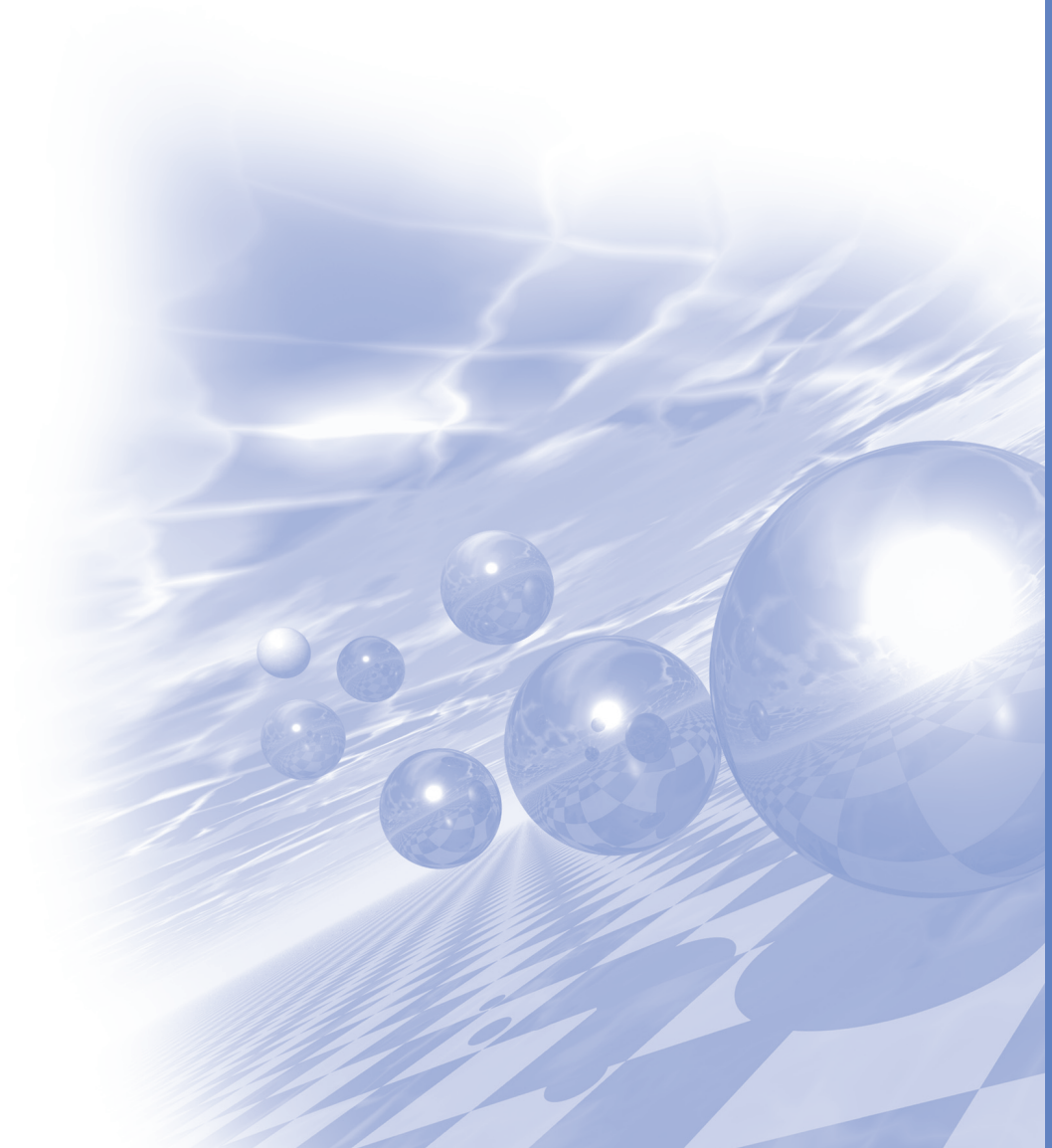

Magnetic parameter estimation using Deep learning techniques

Heeyoung Kwon[1*], Jun Woo Choi[1], Changyeon Won[2]
[1]Korea Institute of Science and Technology
[2]Kyunghee University

We performed a study for estimating magnetic Hamiltonian parameter values from magnetic domain images through machine learning techniques using deep learning techniques. The Monte-Carlo simulated annealing method was used to generate magnetic domain configurations which are used for the training, validation and testing process of machine learning techniques. Using statistical analysis methods, we analyzed the error amount of the estimated values. Most notably we found that the network learned the relationship between the magnetic Hamiltonian parameters determining the characteristics of the magnetic domain, although not directly informed in the algorithm. To verify the effectiveness of this method, we used the directly observed magnetic domain images through the spin-polarized low-energy electron microscopy (SPLEEM) as the input data of the trained network to estimate magnetic Hamiltonian parameters of the images, and confirmed that the estimated results are consistent with the experimentally observed results which were published in the previous study.

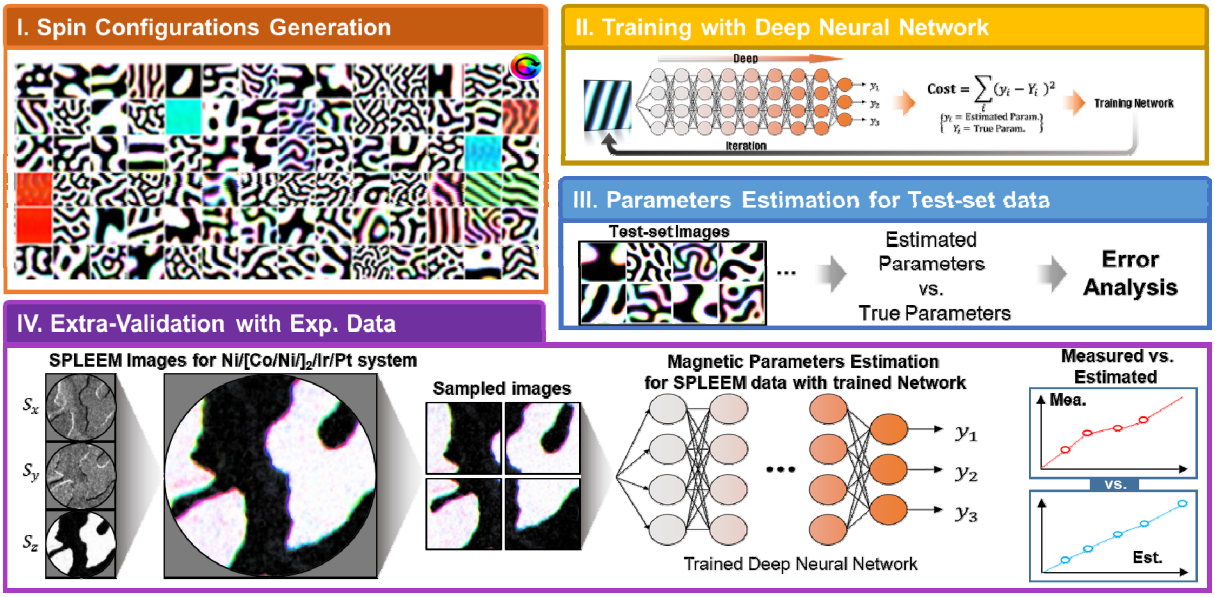

The Intrinsic Spin Hall Conductivity of α-Ta and α-W: first principles study

Do Duc Cuong[1*], Jinwoong Kim[2], Nicholas Kioussis[2], Soon Cheol Hong[1†], and S. H. Rhim[1†]
[1]Department of Physics and Energy Harvest Storage Research Center, University of Ulsan, Ulsan 44610, South Korea
[2]Department of Physics and Astronomy, California State University, Northridge, California 91330, USA
[†]email : schong@ulsan.ac.kr , sonny@ulsan.ac.kr

Spin Hall effect (SHE) is a generation of transverse spin current by applying a longitudinal electric field in the absence of external magnetic field. In recent years, SHE has received a lot of interests for the magnetization switching due to its potentially fast switching and low power consumption. For this purpose, large spin Hall conductivity (SHC) is explored to achieve desirable performance. In this study, SHC of α−Ta and α−W are studied using first-principles calculations in the context of band structure. Due to the same *bcc* structure and similar strength of spin orbit coupling (SOC), band structures of α−Ta and α−W are relative shift to each other. Therefore, spin Berry curvature of both materials exhibit similar magnitudes, where some large values stem from SOC induced energy splitting. The SHC of α−Ta and α−W are different showing -121 $\hbar/e$ $(\Omega \cdot cm)^{-1}$ and -783 $\hbar/e$ $(\Omega \cdot cm)^{-1}$, respectively, which results from occupation change in spin Berry curvature owing to one electron difference. More specifically, spin Hall conductivities of individual band are exhaustively investigated, indicating that sign change of those SHCs is evident in W, which is washed out in Ta because of different electron occupation.

First principles study on magnetic anisotropy mechanism in tetragonal distorted structural phases of Fe_2YZ based Heusler alloys (Y = Mn, Pt; Z = Ge, Sn)

Hoang Thu Thuy*, Qurat ul Ain, S. H. Rhim, and S. C. Hong
Department of Physics and Energy Harvest-Storage Research Center, University of Ulsan, Republic of Korea
schong@ulsan.ac.kr, sonny@ulsan.ac.kr

Due to limited resource and high cost of rare-earth elements, demand of finding rare-earth-free permanent magnets is becoming greater and greater. Among several material classes, Heusler alloys have drawn recently attentions thanks to the flexibilities of crystal structure and magnetic property, which can be tailored by changing chemical compositions. In this work, using *ab-initio* calculation, we reveal that Heusler alloys Fe_2YZ (Y = Mn and Pt; Z = Ge and Sn) have some desirable properties for permanent magnets as listed in Table 1, except Fe_2MnGe. Firstly, Fe_2PtGe, Fe_2PtSn, and Fe_2MnSn are more stable in a tetragonal structure, compared to a cubic phase. Induced K_u values (see Table 1) by tetragonal distortion are large enough for the Heusler alloys to be hard magnets. Being combined with their saturation magnetizations $\mu_o M_s$, the large K_u values result in magnetic hardness parameters k of larger than one, which is a necessary condition for a rare-earth-free permanent magnet [1]. Therefore, we suggest Fe_2PtGe, Fe_2PtSn, and Fe_2MnSn as possible rare-earth-free permanent magnets. We will discuss origin of the strong uniaxial MCA of Fe_2YZ with variations of atomic-orbital contribution to MCA and electronic structure driven by tetragonal distortion.

Table 1. Calculated Physical Properties of Heusler Alloys of Fe_2YZ

	Lattice constants (Å)		$\mu_o M_S$ (T)	K_u (MJm^{-3})	$(BH)_{MAX}$ (MGOe)	κ
	a	*c*				
Fe_2PtGe	5.19	8.15	1.11	4.69	31	2.19
Fe_2PtSn	5.44	8.19	1.01	1.95	25	1.39
Fe_2MnGe	5.68	5.68	0.75	-	-	-
Fe_2MnSn	5.56	7.23	2.75	2.19	58	1.09

Reference

[1] R.W. McCallum et al., Annu. Rev. Mater. Res. **44**, 451 (2014).

SrFeOx: discovery of ReRAM and spectroscopic study on its unique switching mechanism

Venkata Raveendra Nallagatla, Umasankar Dash, and Chang Uk Jung*
Department of Physics and Oxide Research Centre, Hankuk University of Foreign Studies, Yong-in 17035, Korea

Resistance switching memory (ReRAM) has long been considered to be next stage non-volatile memory and hundreds of researchers (at university or at company) on perovskite oxide (CMR and HTSC) has published thousands of papers and hundreds of patents. However, the rather random nature of switching mechanism resulted in unacceptable non-uniformity in the switch parameters, which bothered its commercialization. Thus an escape from ReRAM field has occurred. Here we will introduce 1) our strategy to find novel material (naturally layered oxide with brownmillerite structure) to overcome such problems and 2) spectroscopic evidence of the switching material. We found a novel ReRAM phenomena at SrCoOx for the first time. Here the forming voltage was quite

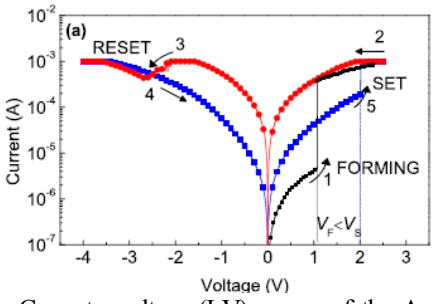

Fig. 1. Current – voltage (I-V) curves of the Au/BM-SCO/SRO crosspoint cell. The arrows indicate the direction of the voltage sweep. APPLIED PHYSICS LETTERS. (2014) 105, 063507.

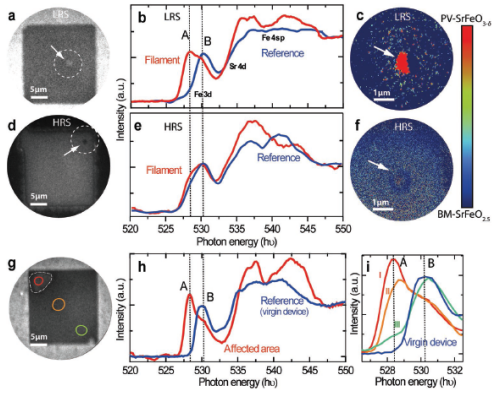

Fig. 3. SrFeOx 111 device and SrFeOx 001 device, PEEM image. Adv. Mater. (2019) 1903391.

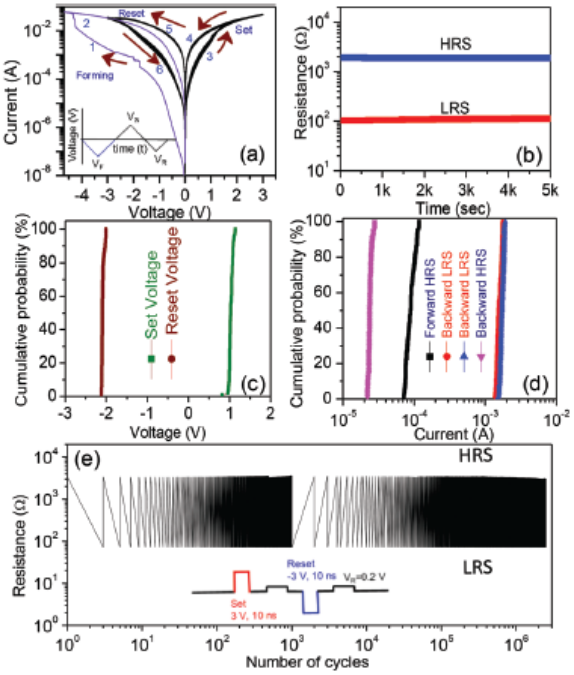

Fig. 2. (a) I-V switching curves of the Au/BM-SFO (111)/SRO/STO (111) device for 100 consecutive cycles of the switching process. The arrows indicate the directions of the voltage sweeps. (b) Retention data for the LRS and HRS after the "set" and "reset" steps, respectively. (c) Cumulative plots of the set and reset voltages in the device. (d) Cumulative probability graphs of the HRS and LRS currents for the forward and reverse biases. (e) Resistance variation with repeated electrical cycles. Switching was carried out with a (3 V, 10 ns) pulse for set and a (-3 V, 10 ns) pulse for reset. Nanoscale, (2017) 9, 10502.

small. Then we found a novel ReRAM phenomena at SrFeOx for the first time and surprisingly, by controlling the crystal orientation, the switching parameters improved quite drastically, almost up to commercial lever. Finally we found that the switching is based on topotactic phase transition between insulating SrFeO2.5 and conducting SrFeO3-d. Depending on the crystal orientation, the nature of the conducting filament consisting of SrFeO3-d was quite different. Together with other application suggested to these oxides, brownmillerite oxides should be ideal material platform for various functionality and application.

International Symposium on Magnetism and Magnetic Materials 2019

Special Session V

'Magnetics Materials and Components Related to Japan's Export Restrictions'

Amorphous Soft Magnetic Powders for High-Frequency Inductors

Jae Won Jeong*, Kyoung-Hoon Bae, Young Gyun Nam, Min-Sun Jang, Sangsun Yang, Jung-Goo Lee, and Yong-Jin Kim
Powder & Ceramics Research Division, Korea Institute of Materials Science, Changwon, Korea

As the working frequency of electronic devices is continuously increasing (10 ~ 10^4 kHz), development of reliable and low-loss soft magnetic core materials for inductors has become an important work. Recently, soft magnetic amorphous powders are gaining great attention due to their excellent soft magnetic properties including high permeability and extremely low loss especially at high frequency. In this work, ultra-fine soft-magnetic micro-powders having amorphous phase were prepared by high-pressure gas atomization and their soft-magnetic properties were examined. First we designed alloys having high glass forming ability, and demonstrated fabrication of fine soft magnetic powders at pilot-scale through process-controlled gas-atomization. Obtained powders were classified, and characterized through SEM, XRD, DSC, and VSM. For the examination of permeability and core loss, toroid-shaped inductor cores were fabricated through powder compaction approach, and characterization was performed using LCR meter and BH analyzer. As a result, we successfully designed and fabricated Fe-B-Si-P-M alloy powders with fully amorphous phase having saturation magnetization above 1.2 T. The performance of obtained powders was also compared with that of commercially available amorphous soft magnetic powders (Epson Atmix, Japan).

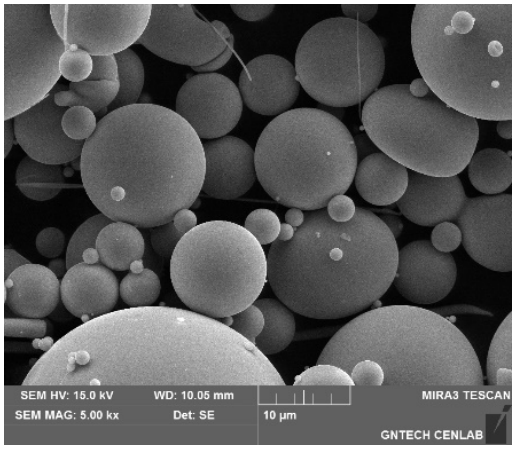

Fig. 1. A SEM image of amorphous soft magnetic powders

Recent Developments of Electrical Steel in Korea

Eonbyeong Park*, Yongchan Kim
Research Institute of Industrial Science and Technology, Materials & Processing Research Laboratory, Korea

Electrical steel known as silicon steel shows excellent magnetic properties such as low core loss, high permeability and so on. Electrical steel manufactured with the process of cold strip rolling, has 2 types such as non grain-oriented electrical steel(NO) and grain-oriented electrical steel(GO). NO electrical steel is usually applicable to core material in rotating machines and GO electrical steel is useful to essential material for manufacturing many kinds of transformers and generators. In recent years, due to the global trend towards energy saving, environmental protection and noise reduction, the electrical steel market is expected to grow considerably and the demand for lower core loss, lower magnetostriction material with high performance is increasing.

POSCO starts to produce the electrical steels in 1979, and produces over 1 million tons of high quality electrical steel every year. GO electrical steel produced by POSCO is classified into Hyper GO(≤0.85W/kg) and High GO(≤1.05W/kg) according to core loss value. It is used for various sized transformers, distribution transformers and reactors because of the excellent magnetic properties along the rolling direction. NO electrical steel from POSCO is also named Hyper NO(≤3.5W/kg) and High NO(≤6.0W/kg) according to core loss value. Because of the homogeneous magnetic properties regardless of the direction, it has an extensive range of applications from large scale power generators to small precision motors and cores in rotators. Nowadays, there has been growing demand for less loss of electricity for higher efficiency in the traction motor of EV, and Hyper NO can meet that requirement with low core loss and high magnetic saturation.

In the last two decades, POSCO has made great efforts to improve the magnetic properties of electrical steel such as high permeability, lower core loss, lower magnetostriction and high induction. Through the highly developed technologies such as employing grain growth inhibitor, magnetic domain refinement, texture control, coating, surface roughness controll and precision rolling, POSCO has marketed electrical steel sheets with excellent magnetic properties. More technical details will be presented at the conference.

Perspective and prospects for rare earth permanent magnets

Dong-Hwan Kim*
STARGROUPIND.CO.,LTD 8-Holim-Dong, Dalseo-Gu, Daegu City, Korea

Recently, with the development of industry, the demand for highly efficient/miniaturized parts has been increasing.

Especially, the hybrid/electric vehicle market is rapidly growing because of environmental problems and the need to save energy. The Nd-Fe-B magnet, which determines the efficiency and the performance of traction motors, is one of the most important materials in the automobile industry. However, issues with the availability and the price of heavy rare-earth (HRE) metals, which are used to improve the thermal stability of the magnet, are constantly emerging. In addition, as the demand for Nd-Fe-B magnets has been increasing rapidly with the growth of the electric vehicle market, Nd is also expected to be in short supply to meet the demand. Thus, the interest in research to replace Nd/Pr with Ce/La, which is more abundant and cheaper than Nd, along with the development of HRE lean/free magnets, has been growing. The present article introduces the trend in research and development on a Nd-reduced rare-earth magnet to solve the problem of limited rare-earth resources.

High frequency magnetic material technologies and related industrial issues in the EMC industry

Kyung-sub Lee*
NOPION Co. Ltd, 84, Jangan-ro 309 Jangan-gu Suwon Korea

Electromagnetic suppression materials, which are being used to solve the electromagnetic noise problem occurring in smart phones and various digital devices, are steadily increasing in the form of films or sheets. Korean manufacturers' electromagnetic wave suppressing material technology has reached the highest level in the world. However, only a few companies have the technology related to high performance magnetic powder, which is a key raw material. Most electromagnetic wave absorbing film manufacturers rely on imports of foreign ingredients from abroad, which are closely related to the performance of the final product. This presentation introduces the technology and industrial structure of the current electromagnetic wave suppression material and discusses the direction of the development of electromagnetic wave absorption in the industry for 5G mobile communication devices and mm wave band.

Study on the Design of Power Density Improvement for Reducing Material Using Motor-Generator

Dong-Woo Kang[1*], Sung Gu Lee[2]
[1]Dept. of Electrical Energy Engineering, Keimyung University, Korea
[2]ADept. of Electrical Engineering, Dong-A University, Korea

This study contains the results of research conducted for the purpose of reducing the consumption of major materials used in motors. Recently, research on electric power propulsion systems to replace existing internal combustion engines is being actively conducted due to issues such as carbon reduction and eco-friendliness and high efficiency. In particular, the electric motor-driven system is typical of the use of the synchronous electric motors. In order to reduce the overall weight and to increase efficiency of the system, synchronous motors with permanent magnets are being actively applied. In general, permanent magnet synchronous motors use rare earth magent as NdFeB magnets and SmCo magnets. In the past, through the Chinese government's rare earth weaponization policy, the design of electric motors has been improved to reduce the use of rare earth as much as possible. In this regard, the authors hope that through this study, the authors will consider the rare earth consumption reduction technology applied to electric motors, and the countermeasures of current export regulations in Japan.

Increasing the number of poles of the motor or blocking the leakage circuit inside the rotor is a typical design that increases the power density. Recently, with the industry's activation of eco-friendly vehicles, automobile manufacturers are promoting the design of automotive electric motors to improve output density and light weight. The typical method is to design permanent magnets inside the rotor in a V-shape to concentrate the magnetic flux and increase the diameter of the rotor to increase the number of poles. In addition, to reduce the weight, a portion of the rotor core that is not affected by the magnetic path is drilled to reduce the weight. In addition, the design method of reducing the overall size of the motor by increasing the current density by improving the cooling method of the motor and the stator winding method is applied. All these methods also contribute to reducing the amount of material used in the motor.

In addition, in the case of motors for robots which have packages of gears and motors, it is developed to reduce the system weight. The driving part for the robot requires low speed and high torque characteristics, and the motor generally has a shape in which the large diameter of the rotor in order to generate high speed and low torque. In this case, if the gear ratio is very large, the rotor size can be reduced and more various motor types can be applied. In this paper, the authors analyzed the domestic supply and demand situation and development status of motors and motor-related parts due to Japan's export regulations, including permanent magnets, gear reducers, etc.

International Symposium on Magnetism and Magnetic Materials 2019

Poster Session

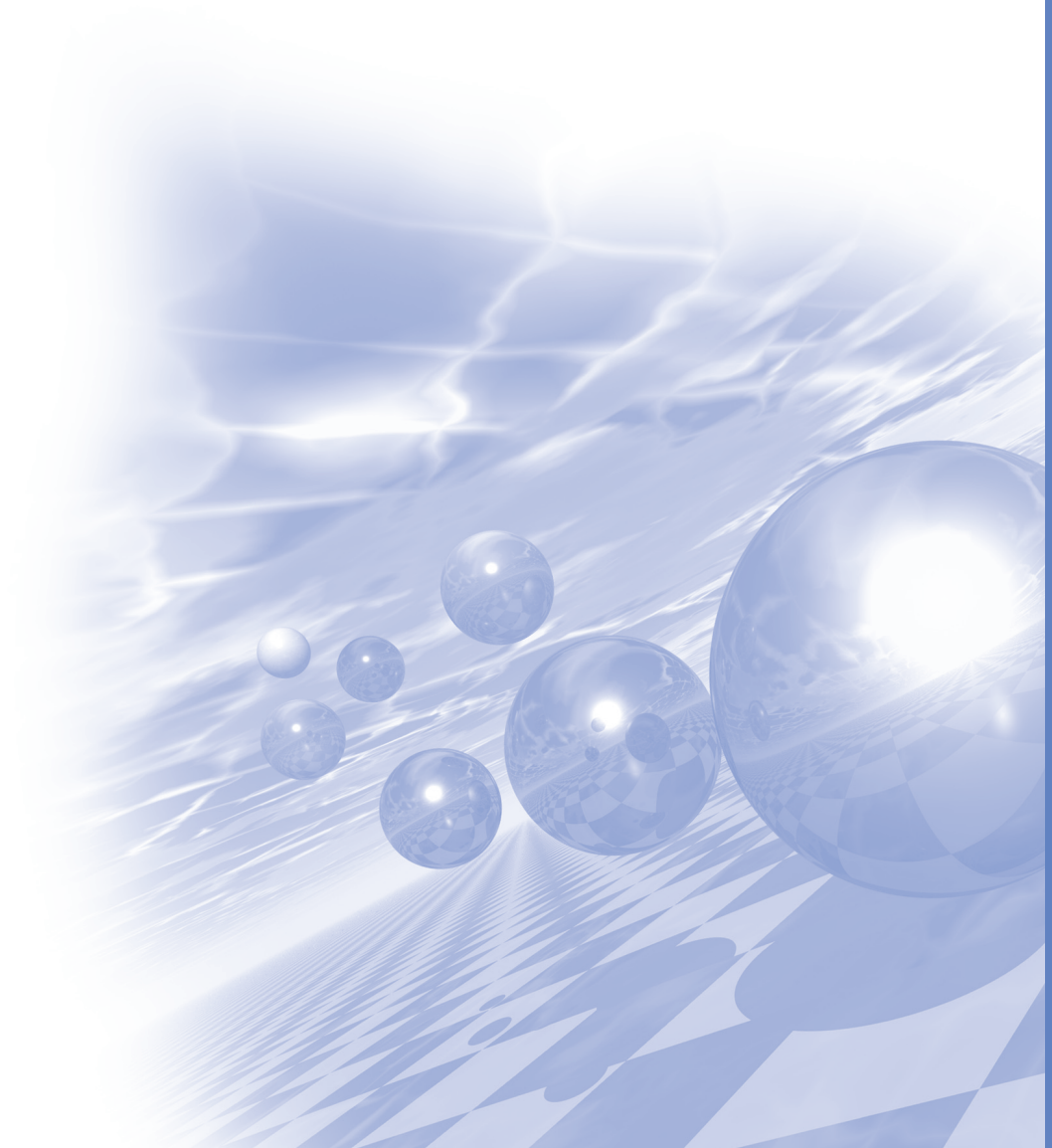

Conservative skyrmion guiding using domain wall

Moojune Song[1*], Kyoung-Woong Moon[2,a], Chanyong Hwang[2], and Kab-Jin Kim[1,b]
[1]Department of Physics, Korea Advanced Institute of Science and Technology, Daejeon 34141, Republic of Korea
[2]Spin Convergence Research Team, Korea Research Institute of Standards and Science,
Daejeon 34113, Republic of Korea
[a]kwmoon@kriss.re.kr, [b]kabjin@kaist.ac.kr.

A magnetic skyrmion is believed to be robust in magnetic materials because of its topological property. However, in conventional skyrmion nanotracks, the skyrmion can be easily annihilated near a physical boundary during its current-driven motion, leading potential information loss in skyrmion memory devices. In order to prevent the skyrmion annihilation in physical boundary, we suggest a skyrmion guiding structure using magnetic domain wall. By imitating Pt/Co system on micromagnetic simulations, we found that the skyrmion can be stably guided by domain wall during its spin-orbit torque-driven motion. A threshold current density of skyrmion annihilation is remarkably enhanced to 5.6×10^{11} A/m^2, compared to that in conventional physical boundary (1.1×10^{11} A/m^2). As a maximum current density can be higher using domain wall guide, the skyrmion speed can also be improved. As applications, we show that a multi-skyrmion transmission using highly-narrow domain wall channel within 40 nm is possible. In addition, we suggest skyrmion sorting devices such as a skyrmion funnel and skyrmion track switch, which can control paths of skyrmions without any annihilation. As the suggested structures can be realized by a technique of planar patterning by ion irradiation, our idea can be easily applied to real skyrmion memory or computing devices.

Enhancement of a spin-wave self-focusing effect by a pulsed flat-top excitation field in a multi-domain state

H. S. Kim*, I. H. Choi, and J. S. Lee†
Department of Physics and Photon Science, Gwangju Institute of Science and Technology (GIST), Gwangju 61005, Republic of Korea

Spin-wave (SW) or its quantum, magnon, is studied with renewed interest as a basis for wave-based classic information processing instead of using an electric charge. Like other physical waves, SWs also have wave-like properties, such as focusing, reflection, refraction, and so on, and these properties have been extensively investigated to manipulate SWs. For example, there have been several methods successfully demonstrated to focus the SW via the nonlinearity of SWs, interference of multiple SW-modes, a graded refractive index of SWs, a phase-controlled SW sources, and so on. In this work, we propose another efficient way of the SW focusing by using the spatially and temporally tailored magnetic field excitations. Using a micro-magnetic simulation, we investigate how the spin-wave propagates and is focused in a ferromagnetic thin film with a perpendicularly magnetized anisotropy (PMA) after its excitation by a pulsed magnetic field having a flat-top amplitude distribution. In particular, we observe that the self-focusing effect appears more efficiently in the multi-domain state divided by Bloch walls compared to that in the single-domain state, as illustrated in Fig. 1. Based on these results, we can propose the flat-top excitation of the magnetostatic spin wave as a new efficient way to create magnetic droplets in a multi-domain state of a perpendicularly magnetized system.

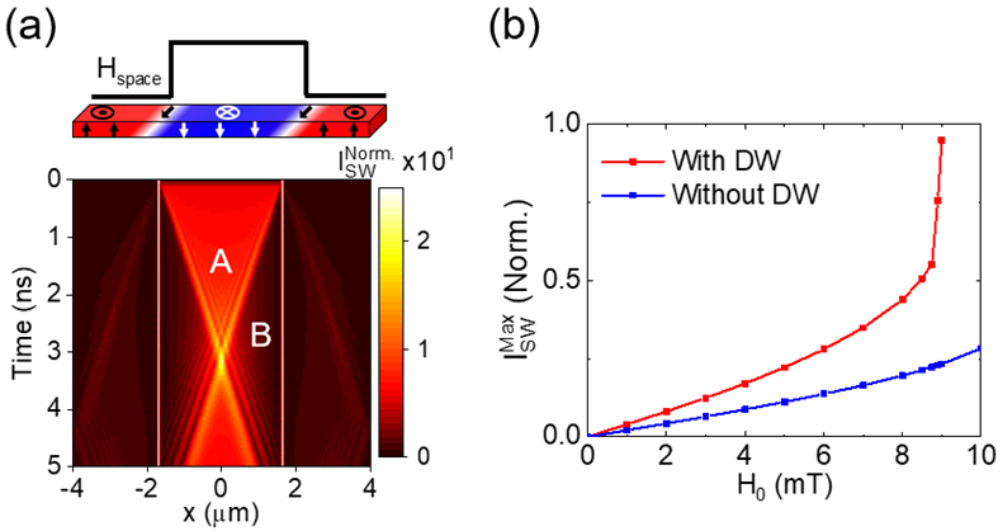

Fig. 1. (a) The spatiotemporal image of the SW propagation induced by a pulsed Flat-top excitation in the presence of DWs, (b) The graph for the maximized SW intensities at the focusing point depending on the strength of the Flat-top excitation fields with and without DWs

First Principles Calculation on Magnetic Properties and Magnetocrystalline Anisotropy of an Fe_3Mn alloy

Mun Bong Hong*, S. H. Rhim, and S. C. Hong†
Department of Physics and Energy Harvest Storage Research Center University of Ulsan,
Ulsan 44610, Republic of Korea

Many efforts have been paid to find new rare-earth-free permanent magnet materials because of the scarcity of rare-earth elements. Mn is one of cheap magnetic elements. We investigate magnetism and magnetocrystalline anisotropy (MCA) of Fe_3Mn whose structure is assumed to be tetragonal by combining of a B2 FeMn alloy with a bcc Fe. Doping effects of 2p elements is checked further for that the Fe_3Mn alloy can have strong enough MCA to be applicable for a cheap permanent magnet.

In this presentation, calculated MCA of Fe_3Mn and Fe_3MnX (X= B, C, N, O) will be presented and discussed origin of the MCA energy enhanced by the 2p elements. The lattice constants of Fe_3Mn are calculated as a= 2.805 Å and c= 5.692 Å. There two type Fe atoms in Fe_3Mn, Fe_{I} and Fe_{II} with different environments. Calculated magnetic moments are 2.31 μ_B for Fe_{I}, 1.93 μ_B for Fe_{II}, and 1.08 μ_B for Mn, respectively. Saturation magnetization deduced from the magnetic moments is 1.89 T and MCA energy of Fe_3Mn is 0.46 MJ/m^3. The hardness parameter κ obtained from the MCA energy and saturation magnetization is 0.41, which is a little bit smaller than the value required to be a semihard permanent magnet. As seen in Table 1(b), dopings of the 2p elements except N are detrimental to uniaxial MCA: N enhances the uniaxial MCA energy of Fe_3Mn to 0.79 MJ/m^3, but reduces the saturation magnetization significantly to 1.17 T. The hardness parameter κ obtained from the MCA energy and saturation magnetization is 0.85, which indicates the N-doped Fe_3Mn to be a semihard permanent magnet.

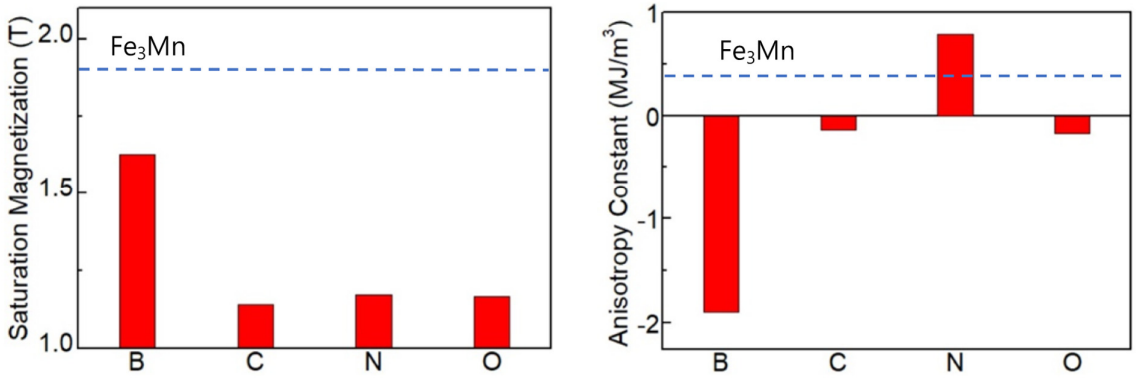

(a) (b)

Fig. 1. (a) Saturation magnetization and (b) magnetocrystalline anisotropy energy of Fe_3Mn doped by the 2p elements. The horizontal dashed lines are the corresponding values of undoped Fe_3Mn alloy.

First-Principles Prediction of High Energy Product of Pt-reduced FePt Alloys

Chang Geun Park[1*], S. C. Hong[2†], and D. Odkhuu[1†]
[1]Department of Physics, Incheon National University, Incheon 22012, South Korea
[2]Department of Physics and EHSRC, University of Ulsan, Ulsan, South Korea
E-mail: ckdrms7410@naver.com, schong@ulsan.ac.kr, odkhuu@inu.ac.kr

As information storage and high-speed motor technologies have evolved, hard magnetic properties, including large saturation magnetization (M_s) and uniaxial magnetic anisotropy (K_u), have become critical in high performance permanent magnet research field. The market for permanent magnet is now divided into two categories: rare-earth magnet and ferrite. Numerous research studies have been drawn into exploring magnetic materials that do not include rare-earth or heavy metal elements. In this perspective, the FePt alloys are out of scopes because of their prices although they have large M_s and K_u. In this study, we perform first-principles calculations to search a potential replacement of 3d and 4d transition metal (TM) elements for Pt-site in $L1_0$-FePt without depressing magnetic properties. We found that, among TM replacements, Sc and Y exhibit highest K_u of 10.8~12.8 MJ/m^3 while improving the thermal stability, which are more than 2 times that (5MJ/m^3) of the typical permanent magnet $Nd_2Fe_{14}B$. We thus expect that Sc and Y doped FePt alloys have a potential in high performance permanent magnet applications.

This research was supported by Future Materials Discovery Program through the National Research Foundation of Korea (NRF) funded by the Ministry of Science and ICT (2016M3D1A1027831).

Potential Usage of Fe-rich Heusler Alloys for High-Performance Permanent Magnet

Tuvshin Dorjsuren[1*], Ochirkhuyag Tumentsereg[1], Chang Geun Park[1], Soon Cheol Hong[2†], and Dorj Odkhuu[1]

[1]Department of Physics, Incheon National University, Incheon 22012, South Korea

[2]Department of Physics and EHSRC, University of Ulsan, Ulsan, South Korea

The recent research direction of high-performance permanent magnet is devoted into developing a potential magnetic material with at least 40% energy product of slate-of-art magnet $Nd_2Fe_{14}B$ while being more than 10 times cheaper in cost. The other prerequisites, including high saturation magnetization (M_S), Curie temperature (T_C), thermal stability and coercivity (H_c), are also crucial. Fe-rich Heusler alloys, which have been mainly referred to as a candidate in thin-film spintronics, usually have cubic symmetries in bulk form that prevent them from having a substantial uniaxial magnetic anisotropy (K_u) required for permanent magnet applications. In this work, we used first-principles calculations to reveal possibilities of an existence of tetragonal symmetry and thus desirable permanent magnetic properties in Heusler Fe_2YZ compounds (Y = Mn to Zn; Z = Al, Si, Ga, Ge, Sn and Sb). It is found that Fe_2YZ compounds can stabilize in tetragonal inverse structure, rather than the cubic phase, especially when Y = Cu and Zn for all Z. More remarkably, we predict a large K_u up to ~2 meV/cell for Fe_2ZnAl and Fe_2ZnSi compounds. We will also discuss on how to enhance K_u further by tuning the partial substitution of Z elements; for example, K_u of 3 meV/cell can be achieved for $Fe_2ZnAl_{0.5}Si_{0.5}$. These results suggest that Heusler compounds have great potential for rare-earth free permanent magnets with the high energy product and cheap cost.

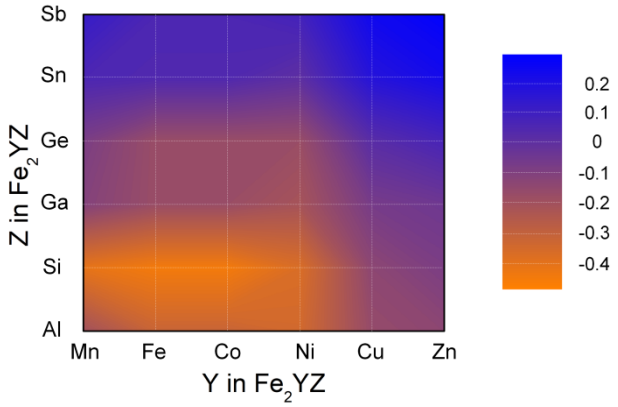

Fig. 1. Schematic diagram of the formation energy of Heusler alloys

This research was supported by Future Materials Discovery Program through the National Research Foundation of Korea (NRF) funded by the Ministry of Science and ICT (2016M3D1A1027831).

First-Principles Prediction of Thermodynamically Stable α"-$Fe_{16}N_2$ with High Energy Product

Tumentsereg Ochirkhuyag[1*], Chang Geun Park[1], Dorjsuren Tuvshin[1], Soon Cheol Hong[2†], and Dorj Odkhuu[1†]

[1]Department of Physics, Incheon National University, Incheon 22012, South Korea

[2]Department of Physics and EHSRC, University of Ulsan, Ulsan, South Korea

[†]schong@ulsan.ac.kr, [†]odkhuu@inu.ac.kr

High-performance permanent magnetic materials require large uniaxial magnetic anisotropy (K_u) and high saturation magnetization (M_s) at the same time. While α"-phase $Fe_{16}N_2$ exhibits largest M_s ever, practical usage of α"-$Fe_{16}N_2$ is quite limited due to its thermally unstable phase and small K_u. Herein, employing first-principles calculations and rigid-band analysis, we demonstrate a five times enhancement of K_u up to 3 MJ/m^3 in $Fe_{16}N_2$ by replacing Fe with Zn while improving the thermal stability. We attribute such a supreme K_u to the mutual mechanisms of the Jahn-Teller orbital splitting and excess electron-induced energy level changes in the rigid-band selection rule. Moreover, we show that the further replacement by Ti in addition to Zn can improve the thermal stability further by a factor of several times of the formation enthalpy without suppressing K_u. Our results provide an useful guideline for the simultaneous improvement of the thermal stability and energy product in 3d-only permanent magnets without RE or heavy metal elements.

This research was supported by Future Materials Discovery Program through the National Research Foundation of Korea (NRF) funded by the Ministry of Science and ICT (2016M3D1A1027831).

First principles calculation of magnetism of Mn_3Al in bulk and in films

Su Yeon An*, Qurat ul Ain, S. H. Rhim, and Soon C. Hong
Department of Physics and EHSRC, University of Ulsan, Ulsan 44610, Republic of Korea
E-mail: sonny@ulsan.ac.kr, schong@ulsan.ac.kr

Heusler compounds have been widely explored in the field of spintronics for their rich physics and various chemical compositions. Recently, antiferromagnetic materials are also extensively studied, where total moment is fully compensated by local moments. Here, we present our study on magnetism of Mn_3Al, a Heusler alloy, using density functional theory (DFT) calculations. In DFT calculations, GGA is used for treating exchange-correlation effects. The Brillouin zone is integrated by using 8 × 8 × 8 k-point mesh and wave functions are expanded by plane waves with 450 eV cutoff energy. Mn_3Al has two inequivalent Mn-types, Mn(X) and Mn(Y). The moment of Mn(X) is -2.32 μ_B and Mn(Y) is 1.16 μ_B. Interestingly the moment of Mn(X) is exactly twice of that of Mn(Y), which results in vanishing moment similar to antiferromagnet. The ferrimagnetic phase is energetically lower than ferromagnetic counterpart. We extend to 5-layer film, where moment of the top surface is greatly enhanced to -3.23 μ_B with respect to bulk while those of inner layers are almost the same as in bulk. The electronic structure of bulk and film geometry is more explored and discussed using density of states, charge density, and band plot.

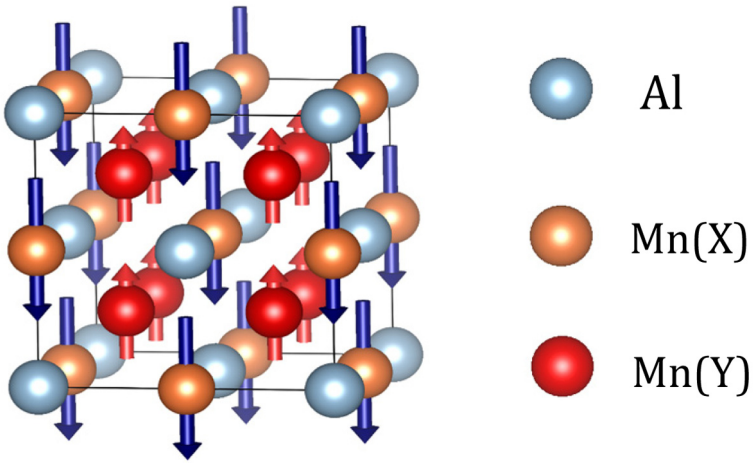

Magnetic Structure of Mn_3Al

Enhanced magneto-electricity and magneto-elastic switching of FePt/$BaTiO_3$

Qurat ul Ain[1*], D. Odkhuu[2], S. H. Rhim[1†], and S. C. Hong[1]

[1]Department of Physics and Energy Harvest-storage Research Center, University of Ulsan, Ulsan, Republic of Korea

[2]Department of Physics, Incheon National University, Incheon, Republic of Korea

The magneto-electricity (ME) and magneto-elasticity (MEL) effects on FePt/$BaTiO_3$ is investigated using first-principles calculations. We predict the interfacial ME coefficient, a_I = 35.6x10^{-10} G·cm^2/V, two times larger than Fe/$BaTiO_3$ interface [1]. The large a_I results from considerable difference in magnetization under the polarization (P) reversal. Furthermore, strain (η) strongly modifies the electronic structure. At η =1.75%, magnetization switches from out-of-plane (P<0) to in-plane (P>0). The rearrangement of atomic orbitals, a response to electric field, emerges as a consequence of spontaneous polarization at interfaces. In particular, out-of-plane (*xz*, *yz*) and in-plane (*xy*, x^2-y^2) orbitals, odd and even under reflection with respect to *z*-plane, show different behavior under the polarization reversal. The magnetization direction is mainly governed by $\langle xy,\downarrow | L_z | x^2-y^2,\downarrow \rangle$ and $\langle xz,\downarrow | L_z | yz,\downarrow \rangle$ matrices.

Reference

[1] C.-G. Duan, S.S. Jaswal, and E. Y. Tsymbal, Phys. Rev. Lett. **97**, 047201 (2006).

SMR based spin Hall measurement technique for in-plane magnetization

Dongseuk Kim[1], Jiho Kim[2*], Changjin Yun[2], Sungjung Joo[1], B. C. Lee[3], and Kungwon Rhie[2]

[1]Center for Nanometrology, Korea Research Institute of Standards and Science, Daejeon, 34113, Korea

[2]Department of Display and Semiconductor Physics, Korea University, Sejong, 30019, Korea

[3]Department of Physics, Inha University, Incheon, 22212, Korea

Spin Hall angle measurement technique is well developed at heavy metal/ ferromagnet which has perpendicular magnetic anisotropy (PMA). However, a DC current based spin Hall angle measurement for in-plane anisotropy (IPA) has not been yet developed. We present a simple spin hall magnetoresistance (SMR) technique that measures spin Hall angle without any worry of artifacts which could be introduced in RF based spin Hall measurement. SMR signal is measured with applied field transverse to current. SMR peak shifts its maximum as applied current is increased, since spin Hall torque is added to the torque induced by transverse field. This shift yields spin Hall angle of heavy metal layer. For a Pt/CoFeB bilayer, we obtained θ_{SH}^{eff} = 0.045, l_s = 2.49 nm, which is a reasonable value.

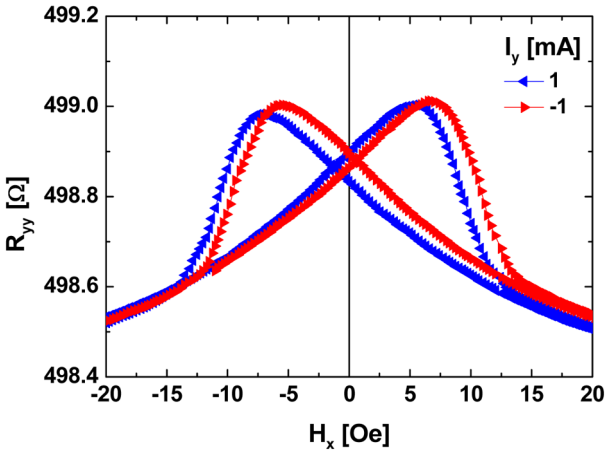

Fig 1. The R-H curve measured with two direct current flow in the Pt/CoFeB bilayer.

The Limitation of Anticipation by First Order Reversal Curve Method

Namkyu Kim*, Hee-Sung Han, Soo Seok Lee, and Ki-Suk Lee†
School of Materials Science and Engineering, Ulsan National Institute of Science and Technology, Ulsan 44919, Republic of Korea

The magnetic hysteresis loops have been mathematically interpreted by the classical Preisach model assuming that the magnetic materials are composed of many of hysterons. The hysteron is defined as hysteresis elements having bistable state. The distribution of switching field of these hysterons gives information of the interaction in the system. First order reversal curve (FORC) analysis proposed by Mayergoyz [1] is successive tool to understand reversal mechanism, and interactions in magnetic system by extracting switching distributions from additional reversal curves. Because of the convenience of extracting switching distributions, FORC method has been utilized for investigating the magnetic materials such as permanent magnets [2-3] and their temperature dependence [4], or alloy structure [5]. However, there is a clear limitation for investigating magnetic materials by using FORC methods based on classical Preisach model. This is arising from the basic assumption, there are only bistable states of each hysteron, even though most of magnetic systems are comprised of vector magnetic moments. In this presentation, we will clearly show the limitation anticipation by FORC method by comparing the switching field distributions from FORC method with the switching field obtained from full hysteresis loops of all grains in micromagnetic simulations [6]. There is a broad distinction between two kinds of the switching distributions not only displacement of the loops, but also the coercivity.

References

[1] I. D. Mayergoyz, Phys. Rev. Lett. 56, 1518 (1986).
[2] H. Chiriac et al., J. Magn. Magn. Mater. 316, 177 (2007).
[3] T. Schrefl et al., J. Appl. Phys. 111, 07A728 (2012).
[4] T. Yomogita et al., J. Magn. Magn. Mater. 447, 110 (2018).
[5] B. C. Dodrill, Advanced Materials: TechConnect Briefs, 1, 173-176 (2017).
[6] A. Vansteenkiste et al., AIP advances 4, 107133 (2014)

Stoner-Wohlfarth Model at Multi-Domain System

Changjin Yun[1*], Mingu Kim[1], Jiho Kim[1], Kungwon Rhie[2], and B. C. Lee[3]
[1]Department of Applied physics, Korea University, Sejong, 30019, Korea
[2]Department of Display and Semiconductor Physics, Korea University, Sejong, 30019, Korea
[3]Department of Physics, Inha University, Incheon, 22212, Korea

Magnetization reversal in multi domain structure by spin-torque has not been well studied in spite of its application possibility. Systematically measured magnetization reversal of multi-domain Pt/Co/Pt spin Hall structure with perpendicular magnetic anisotropy is compared with a modified Stoner-Wohlfarth (SW) model for multi-domain. For multi domain magnetization reversal, we adopted a simple phenomenological model of H_K contraction (contraction factor $\gamma \equiv H_K/H_C$) along the easy axis [1]. DC magnetic fields were applied on a sample in y (current direction) and z direction (easy axis) at the same time. To generate SW asteroid for a given current, y-directional magnetic field is varied from –3000Oe to 3000Oe with 3 degree, while z-directional magnetic field is fixed with a Helmholtz coil. After that, induced magnetic fields by 3 degree were compensated. SW astroid is obtained for each applied current, and is compared with the modified SW theory. It is turned out that the experimentally reduced SW asteroid follows the shape change which was predicted by the theory.

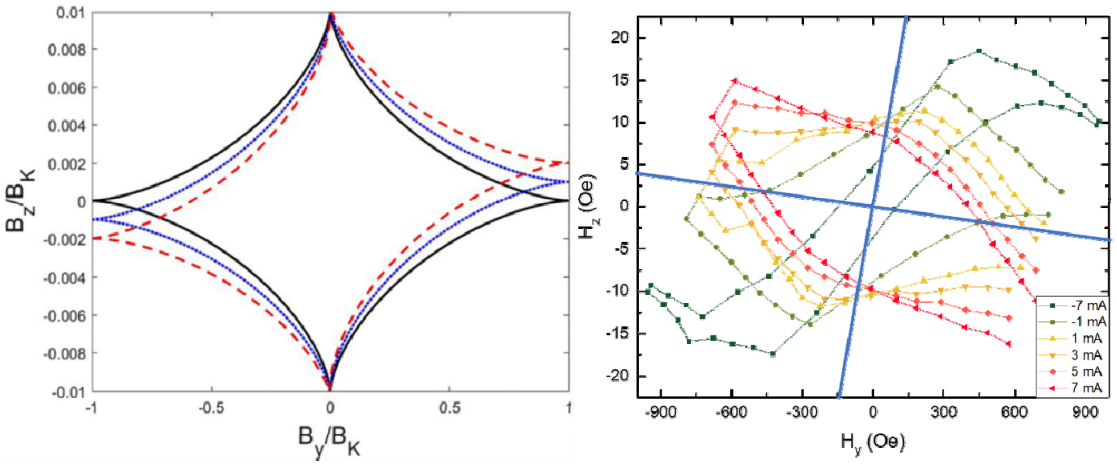

Fig. 1. (a) Astroid following our phenomenological theory. The solid, dotted and dashes lines are for spin Hall torque = 0, 1, and 2 mT, respectively. (b) Experimentally measured astroid for several currents through a Pt/Co/Pt sample. The rotation of astroid is clearly seen. The solid blue lines are expected to be Hy and Hz when there is no misalign in angle.

Reference

[1] Dongseuk Kim, Bumjin Kim, Jimin Kim, Chang-Jin Yun, Chanyong Hwang, B. C. Lee, Sungjung Joo, and K. Rhie Phys. Rev. B 100, 014433 (2019)

Effect of Rashba interaction at normal metal/insulator interface on spin-orbit torque of ferromagnet/normal metal/insulator trilayers

Eun-Sang Park[1,2*], Byoung-Chul Min[2], Hyun Cheol Koo[2], Kyoung-Whan Kim[2], Kyung-Jin Lee[1,2,3]

[1]KU-KIST Graduate School of Converging Science and Technology, Korea University, Seoul 02841, Korea

[2]Center for Spintronics, Korea Institute of Science and Technology, Seoul 02792, Korea

[3]Department of Materials Science and Engineering, Korea University, Seoul 02841, Korea

Based on a spin drift-diffusion model, we theoretically investigate the spin-orbit torque in ferromagnet/normal metal/insulator trilayers with considering the Rashba interfacial spin-orbit coupling at the normal metal/insulator interface. We find that the spin-orbit torque shows the opposite normal-metal-thickness dependences for the bulk spin-orbit coupling effect in the normal metal layer and for the interfacial spin-orbit coupling effect at the normal metal/insulator interface, offering a way to disentangle these two spin-orbit coupling effects. Moreover, we show that the conventional interpretation based on the bulk spin-orbit coupling effect overestimates the spin Hall angle and underestimates the spin diffusion length of the normal metal layer, when the interfacial contribution is non-negligible. Our result, a concise analytic expression of the spin-orbit torque considering both bulk and interface spin-orbit coupling effects, will be useful to design and interpret experiments on spin-orbit torque experiments in ferromagnet/normal metal/insulator trilayers.

Role of orbital hybridization in anisotropic magnetoresistance

Hye-Won Ko[1*], Hyeon-Jong Park[1], Gyungchoon Go[2], Jung Hyun Oh[2], Kyoung-Whan Kim[3], and Kyung-Jin Lee[1,2]

[1]KU-KIST Graduate School of Converging Science and Technology, Korea University, Seoul 02841, Korea
[2]Department of Materials Science and Engineering, Korea University, Seoul 02841, Korea
[3]Center for Spintronics, Korea Institute of Science and Technology, Seoul 02972, Korea

Based on tight-binding model, we demonstrate that longitudinal orbital currents in ferromagnets depend on the magnetization direction, which contribute to the anisotropic magnetoresistance (AMR). We call this orbital contribution to the AMR as the *orbital anisotropic magnetoresistance* (OAMR). The orbital degrees of freedom effectively correlates with the magnetization via a concerted action of the spin-orbit coupling and exchange coupling. This correlation gives rise to OAMR when momentum-dependent orbital splitting is present, which is generally achieved by typical properties of multi-orbital system: orbital anisotropy [1] and orbital hybridization. We highlight the latter as the unrecognized origin of AMR and also as the common origin of OAMR and orbital Hall effect [2,3].

References

[1] J. Velev, R. F. Sabirianov, S. S. Jaswal, and E. Y. Tsymbal, Phys. Rev. Lett. **94**, 127203 (2005).
[2] H. Kontani, T. Tanaka, D. S. Hirashima, K. Yamada, and J. Inoue, Phys. Rev. Lett. **102**, 016601 (2009).
[3] D. Go, D. Jo, C. Kim, and H. –W. Lee, Phys. Rev. Lett. **121**, 086602 (2018).

Current-Induced Spin Wave Dynamics in Ferrimagnets

Dong-Hyun Kim[1*], Se Kwon Kim[2], Se-Hyeok Oh[3], Dong-Kyu Lee[4], and Kyung-Jin Lee[1,3,4,5]

[1]Department of Semiconductor Systems Engineering, Korea University, Seoul 02841, Korea

[2]Department of Physics and Astronomy, University of Missouri, Columbia, Missouri 65211, USA

[3]Department of Nano-Semiconductor and Engineering, Korea University, Seoul 02841, Korea

[4]Department of Materials Science and Engineering, Korea University, Seoul 02841, Korea

[5]KU-KIST Graduate School of Converging Science and Technology, Korea University, Seoul 02841, Korea

For ferromagnets, spin wave (SW) Doppler shift by the adiabatic spin-transfer torque (STT) and manipulation of SW attenuation length by the non-adiabatic torque have been established theoretically and experimentally [1-3]. However, STT effects on ferrimagnetic SWs have remained unexplored. In this work, we theoretically and numerically study STT-induced SW Doppler shift and control of the SW attenuation length in ferrimagnets.

Figure 1(a) and (b) show STT-induced Doppler shift of right-handed and left-handed SWs at the angular momentum compensation point, respectively. Symbols are numerical results and solid lines are theories, which are in good agreement. We find that the sign of the Doppler shift of left-handed SW is opposite to that of the right–handed SW, which originates from the opposite spin polarizations carried by left- and right-handed SWs.

Figure 2(a) and (b) show SW attenuation length as a function of the current density for $\beta = 10\alpha$, where β is the non-adiabaticity and α is the damping constant. Theoretical and numerical results are shown in the vicinity of the angular momentum compensation temperature (T5 = T_A) and T4 (T6) is the temperature which is below (above) T_A. We find that the SW attenuation length of both right- and left-handed SWs increase when electrons flow in the same direction with the SW propagation. In addition, when sufficiently large non-adiabatic torque is applied, the SW amplitude exponentially increases from the SW source.

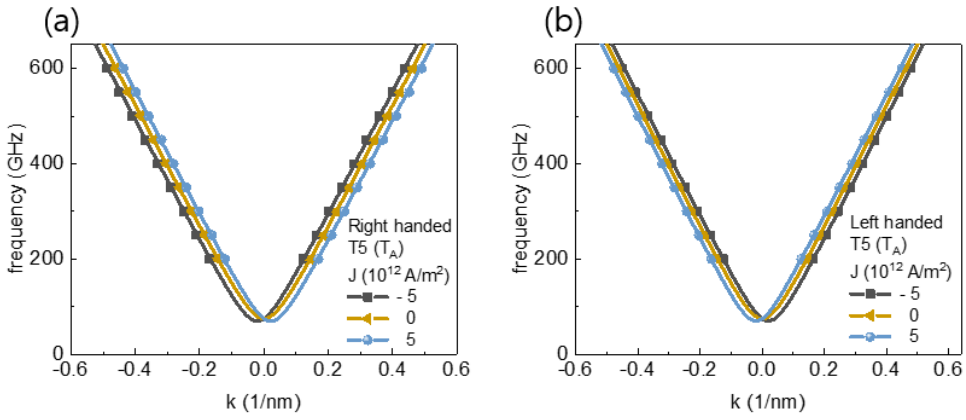

Fig. 1. Doppler shift of (a) right- and (b) left-handed SWs in a ferrimagnet at the angular momentum compensation temperature.

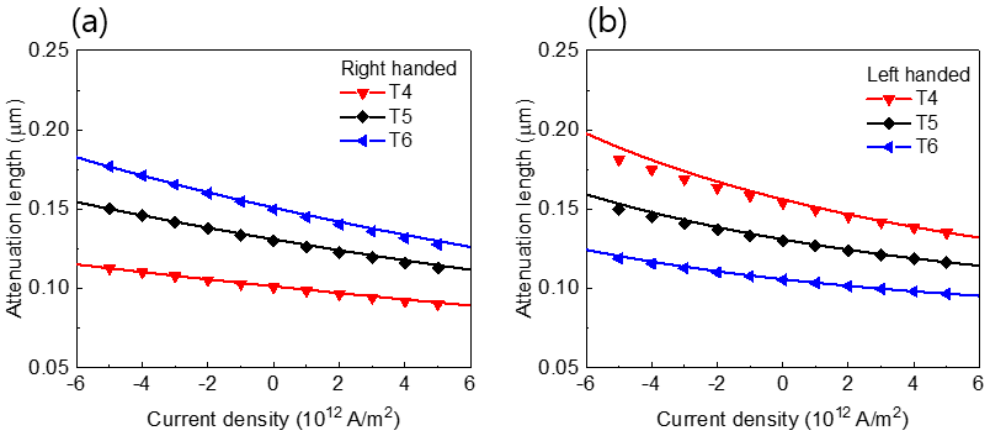

Fig. 2. SW attenuation length for (a) right-handed and (b) left-handed SWs as a function of the current density.

References

[1] V. Vlaminck, and M. Bailleul, Science **322**, 410 (2008).

[2] S.-M. Seo, K.-J. Lee, H. Yang, and T. Ono, Phys. Rev. Lett. **102**, 147202 (2009).

[3] K. Sekiguchi, K. Yamada, S.-M. Seo, K.-J. Lee, D. Chiba, K. Kobayashi, and T. Ono, Phys. Rev. Lett. **108**, 017203 (2012).

Study on the atomic structure and magnetic properties of Mn-doped WS_2 bilayer in first- principles

Tran Van Quang[1,2] and Miyoung Kim[3*]

[1]Institute of Research and Development, Duy Tan University, Da Nang, Vietnam

[2]Department of Physics, University of Transport and Communications, Hanoi, Vietnam

[3]Department of Applied Physics, Sookmyung Women's University, Seoul, Korea

Intriguing physics of graphene with great electrical, thermal, and mechanical properties have stimulated extensive research in two-dimensional (2D) materials. Many attentions have been paid to search for high-quality 2D sheets for forthcoming electronic applications. We carried out first-principles calculation to study the structural and magnetic properties of the Mn doped bilayer WS_2. Number of doping configurations including single and double doping were examined. In general, the most stable structures relate to short bonding length of Mn dopants with W atoms, i.e. either Mn below W or Mn replacing W. In double doped Mn, the stability strongly depends on the ambient environment. The most stable configuration found in the S-rich condition with the substitution of Mn dopants into W sites for both AA and AB stacking configurations. The magnetism is determined mostly by Mn dopants with distinct magnetic moments which is assigned to the charge transfer. All feasibly stable configurations determined by chemical potential are semiconductors with flat spin polarized d-bands localized near Fermi energy. The magnetic semiconducting Mn doped bilayer WS_2 is therefore potential for spintronic applications.

Magnetic property of Fe_3GeTe_2

G. Hye Kim*, Qurat ul Ain, Soon Cheol Hong, and S. H. Rhim
Department of Physics and Energy Harvest-Storage Research Center, University of Ulsan, Republic of Korea
schong@ulsan.ac.kr, sonny@ulsan.ac.kr

In recent years, two-dimensional (2D) materials have received attentions for possible spintronics application. In 2D materials, some physical properties emerge differently from bulk. Conventional wisdom based on Mermin-Wagner theorem stated that the long-range order is impossible in 2D. However, magnetism in 2D has been reported in many places.

Fe_3GeTe_2 (FGT) is intensively studied in the context of 2D magnetism. Ferromagnetism of this material remains when it changes from bulk to single-layer with magnetic moment of 4.7 μ_B [1] and Curie temperature about 220K [2]. Here, magnetic properties of bulk and single-layer Fe_3GeTe_2 are presented in the framework of electric structure: more specifically, spin-orbit coupling related magneto-crystalline anisotropy is tackled using first-principles calculations.

References

[1] Xianqing Lin, and Jun Ni, Phys. Rev. B 100, 085403 (2019)

[2] Bin Chen, JinHu Yang, HangDong Wang, Masaki Imai, Hiroto Ohta, Chishiro Michioka, Kazuyoshi Yoshimura, and Minghu Fang, J. Phys. Soc. Jpn 82, 124711 (2013)

Spin and Anomalous Hall effect in fully Compensated Ferrimagnet Mn_3Al: First-Principles Calculation

Guihyun Han*, Su Yeon An, Soon Cheol Hong, and S. H Rhim
Department of Physics and Energy Harvest-Storage Research Center, University of Ulsan, Republic of Korea
schong@ulsan.ac.kr, sonny@ulsan.ac.kr

Mn_3Al is ferrimagnetic material, whose unit cell contains two inequivalent Mn atoms, where each of moments are opposite but fully compensated as depicted in Figure 1 [1]. This full compensation could be viewed as an antiferromagnetic unit in some sense. In the absence of total magnetization, anomalous Hall effect (AHE) is usually not anticipated. However, non-vanishing AHE has been reported in antiferromagnetic Mn_3Ge [2]. As Mn_3Al behaves somewhat like antiferromagnetic but is ferrimagnetic, an investigation of AHE is the goal of this work. Furthermore, spin Hall effect (SHE) is also studied in the framework of density functional theory using Kubo formula.

References

[1] Michelle E. Jamer et al., Phys. Rev. Applied **7**, 064036 (2017).
[2] Ajaya K. Nayak et al., Sci. Adv. **2**, e1501870 (2016).

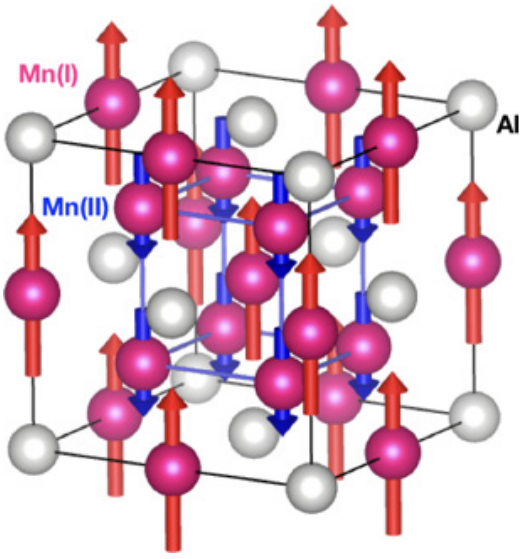

Fig. 1. Crystal structure of Mn_3Al. Red spheres denote for Mn(I) and Mn(II);gray for Al. Red and blue solid arrows represent magnetic moments of Mn(I) and Mn(II), respectively.

Two-dimensional ferromagnetic semiconductors single-layer CrXTe$_3$ (X = Si, Ge, and Sn): Stability and magnetic properties

Won Seok Yun[1*], and J. D. Lee[2]
[1]Convergence Research Institute, DGIST, Daegu 42988, Republic of Korea
[2]Department of Emerging Materials Science, DGIST, Daegu 42988, Republic of Korea

To date, researches on two-dimensional (2D) materials have been actively progressing due to their potential applications in such as nanoscale electronics, photonics, valleytronics, photovoltaics, and so on. Especially, considerable attention has been paid to the magnetic properties of the layered semiconductors for the spintronic applications. Among them, bulk layered transition metal trichalcogenides (TMTCs) $CrSiTe_3$ and $CrGeTe_3$ have been known as ferromagnetic (FM) semiconductors with the Curie temperatures of 32 K and 61 K, respectively. For the bulk phase, each unit cell comprises three TMTCs layers stacked in an ABC sequence. In addition, it has been discovered through the experimental verification that the exfoliated few-layer samples of $CrSiTe_3$ maintained the p-type semiconducting property. Simultaneously, when the number of layers reduces to one, i.e, a single-layer (1L) case, the theoretical studies report that both 1L-$CrSiTe_3$ and 1L-$CrGeTe_3$ are shown to be not only FM, but also semiconducting properties. However, to date there are a few studies focused on the fundamental electronic structures and magnetic properties of 1L-CrXTe$_3$ (X = group IV elements: Si, Ge, and Sn). Therefore, many details about the external carrier, strain, and electric field effects on the electronic and magnetic properties of 1L-$CrXTe_3$ are still lacking. In this study, we have performed the first-principles calculations to scrutinize extensively the electronic and magnetic properties of 1L-CrXTe$_3$. Consequently, we confirm that the considered systems are shown to be FM semiconductors. From the phonon dispersion spectrum, those systems have dynamical stability. In addition, the total magnetic moment of all the systems are shown to be exactly 6.0 μ_B/unit-cell owing to intrinsic semiconducting character. Detailed discussion of strain, carrier doping, and electric field effects on magnetic properties of 1L-CrXTe$_3$ will be given.

Switching Probability Induced by Interfacial Spin Current

Hyun-Jung Hwang[1*], Dong-Kyu Lee[1], and Kyung-Jin Lee[1,2,3]
[1]Department of Materials Science & Engineering, Korea University, Seoul, Republic of Korea
[2]KU-KIST Graduate School of Converging Science and Technology, Korea University, Seoul, Republic of Korea
[3]Department of Nano-Semiconductor and Engineering, Korea University, Seoul, Republic of Korea

Magnetization switching via spin-orbit torque has recently emerged as an efficient method to electrically control magnetization state [1,2]. However, a high current as well as an external magnetic field is required to achieve the deterministic switching of perpendicular magnetization, which is undesirable for practical applications.

One of the suggestions for field-free spin-orbit torque switching is to break the spin current symmetry using another ferromagnet [3] or ferromagnet/normal metal (FM/NM) interface [4,5]. In particular, field-free switching of perpendicular magnetization due to interfacial spin currents generated at the FM/NM interface has been experimentally demonstrated [5]. However, it is unclear how efficiently interfacial spin currents can switch perpendicular magnetization.

In this work, we numerically investigate the switching probability and bit error rate (BER) driven by interfacial spin currents. For an accurate calculation, we use Fokker-Planck calculation that describes a probability distribution of Brownian particles in the presence of thermal effect [9-10]. We find that the interfacial spin current efficiently drives field-free switching with a smaller current density than the conventional spin-transfer torque (STT) switching. We show that the critical current decreases depending on the angle of injected spin polarization and current pulse width.

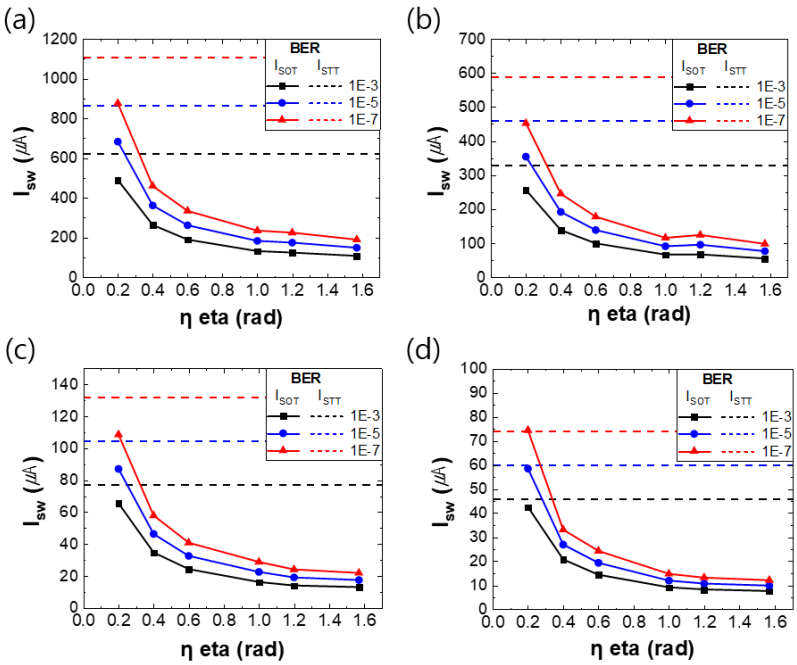

Fig. 1. Critical current for low BER (I_{SW}) as a function of the spin polarization angle η. (a) pulse width = 0.5 ns, (b) 1.0 ns, (c) 5.0 ns, and (d) 10.0 ns.

References

[1] I. M. Miron et al., Nature (London) **476**, 189 (2011).

[2] L. Q. Liu et al., Science **336**, 555-558 (2012).

[3] T. Taniguchi et al., Phys. Rev. Appl. **3**, 044001 (2015).

[4] A. M. Humphries et al., Nat. Commun. **8**, 911 (2017).

[5] S. C. Baek et al., Nat. Mater. **17**, 509 (2018).

[6] W. F. Brown, Phys. Rev., **130**, 1677-1686, (1963).

[7] W. H. Butler et al., IEEE Trans. Magn. **48**, 4684 (2012).

Surface spin wave mode and reversal of gyromagnetic ratio in ferrimagnetic thin film

Changsoo Kim[1,2*], Soogil Lee[2,3], Kyoung-Woong Moon[1], Byong-Guk Park[3], Se Kwon Kim[4], Kab-Jin Kim[2], and Chanyong Hwang[1]

[1]Quantum Technology Institute, Korea Research Institute of Standards and Science (KRISS), Daejeon 34113, Korea
[2]Department of Physics, Korea Advanced Institute of Science and Technology (KAIST), Daejeon 34141 Korea
[3]Department of Materials Science and Engineering, Korea Advanced Institute of Science and Technology (KAIST), Daejeon 34141, Korea
[4]Department of Physics and Astronomy, University of Missouri, Columbia, Missouri 65211, USA

It is well known that spectral asymmetry of Brillouin light scattering (BLS) appears because of localized nature of magnetostiatic surface spin wave and attenuation of light in magnetic thin film. In ferromagnet, a propagating direction of surface spin wave determines at which surface the spin wave is localized. Add to this, our study found that rotational direction of magnetization is also another factor determining bound state of spin waves. To confirm this, we examined the surface spin wave of ferrimagnet, which inversely rotates between the two compensation points (T_M and T_A). We observed that the intensity ratio of surface spin wave modes in Stokes and anti-Stokes is reversed with increase of temperature near T_M and T_A, which is the same as expected in the theory. Also, the high frequency mode was observed and will be discussed here.

The Vortex Core Switching by Bloch Point Pair

Hee-Sung Han*, Sooseok Lee, Dae-Han Jung, Suyeong Jeong, Namkyu Kim, Ki-Suk Lee
School of Materials Science and Engineering, Ulsan National Institute of Science and Technology,
Ulsan, Republic of Korea

In a confined ferromagnetic disk, the magnetic vortex structure, one of magnetic topological texture, has been considered as a good candidate for developing information storage and processing device due to its tiny size and high thermal stability. In addition, its rich dynamic properties, such as gyrotropic mode, azimuthal and radial spin wave modes, shows the potential to develop nano-oscillator. The magnetic vortex is composed of the vortex core at the center and in-plane curling magnetization. There are energetically fourfold states of magnetic vortex with the combination of the vortex core polarization and in-plane curling magnetization. It is well known that the magnetic vortex core can be switched through the injection of the Bloch point on the surface of the disk. In this work, we will report that the vortex core switching by Bloch point pair in the circular shaped permalloy ($Ni_{80}Fe_{20}$, Py) disk through the resonant excitation of a three-dimensional (3D) dynamic mode, a size oscillation of the vortex core. We found that the Bloch point pair is nucleated in the internal region, not surface. Our work provides understanding 3D dynamic nature of magnetic vortex with a method to achieve ultrafast vortex core reversals.

Types of a Magnetic Singularity in an Asymmetric-Shaped Permalloy Disk

Hee-Sung Han[1*], Min-Seung Jung[2], Young-Sang Yu[3], Sooseok Lee[1], Seongsoo Yoon[2], Weilun Chao[4], Peter Fischer[5,6], Jung-Il Hong[2], Mi-Young Im[4], Ki-Suk Lee[1]

[1]School of Materials Science and Engineering, Ulsan National Institute of Science and Technology (UNIST), Ulsan, 44919, Republic of Korea

[2]Department of Emerging Materials Science, Daegu Gyeongbuk Institute of Science and Technology (DGIST), Daegu, 42988, Republic of Korea

[3]Advanced Light Source, Lawrence Berkeley National Laboratory, Berkeley, CA, 94720, USA

[4]Center for X-ray Optics, Lawrence Berkeley National Laboratory, Berkeley, CA, 94720, USA

[5]Materials Sciences Division, Lawrence Berkeley National Laboratory, Berkeley, CA, 94720, USA

[6]Department of Physics, University of California, Santa Cruz, Santa Cruz, CA, 94056, USA

In a ferromagnetic material, a Bloch point is a zero-dimensional singularity. It plays an important role in the switching of a two-dimensional (2D) magnetic structure such as skyrmion and magnetic vortex. The local topological number of the 2D magnetic structure is changed by the injection of the magnetic singularity. Their type is classified by its topological number and shape of the surrounding magnetic configuration.

In this work, we will report the experimental observation of four other energetically equivalent magnetic singularities in an asymmetric-shaped permalloy ($Ni_{80}Fe_{20}$, Py) disk using the magnetic full-field X-ray microscopy (MTXM). The observed structures were reproduced by the micromagnetic simulation. The observed magnetic singularity is shifted in the left or right direction from the center of the disk. It is originated from the symmetry breaking in the asymmetric Bloch walls near the magnetic singularity, which is induced by the geometrical asymmetry. Through the shift direction of magnetic singularity, the three-dimensional (3D) magnetic configuration can be figured out. In this poster, we will discuss detailed configurations of four other energetically equivalent magnetic singularities with understanding the 3D magnetic configuration surrounding the magnetic singularity.

Profile of Pontential Energy of a geometrically confined skyrmion

Dae-Han Jung*, Hee-Sung Han, Namkyu Kim, Gang Hwi Kim, Suyeong Jeong, and Ki-Suk Lee†
School of Materials Science and Engineering, Ulsan National Institute of Science Technology,
Ulsan 44919, Republic of Korea

Magnetic skyrmions, localized swirling spin textures with topologically protection, are of particular interest from fundamentally intriguing physics to new spintronic applications. For the envisioned skyrmion-based applications, the skyrmions are required to be manipulated in geometrically confined structures, instead of infinite sheets of material. Therefore, the interaction between skyrmions and the edge boundaries of the magnetic structure is crucial. In fact, this interaction can prevent skyrmions from being expelled from the track and assist in their propagation velocity with reduced sized, it could be possible to achieve larger data storage densities and faster performance. In this work, we report on a convenient analytical methodology to determine the profile of confining potential of a skyrmion in one-dimensional confined geometries. Our results would be of value in the study of magnetic energetics and could give fresh impetus to the design of skyrmion-based devices.

Bidirectional spin-wave-driven domain wall motion in ferrimagnets

Se-Hyeok Oh[1*], Se Kwon Kim[2], Jiang Xiao[3,4,5], and Kyung-Jin Lee[1,6,7]

[1]Department of Nano-Semiconductor and Engineering, Korea University, Seoul 02841, Korea
[2]Department of Physics and Astronomy, University of Missouri, Columbia, Missouri 65211, USA
[3]Department of Physics and State Key Laboratory of Surface Physics, Fudan University, Shanghai 200433, China
[4]Collaborative Innovation Center of Advanced Microstructures, Nanjing 210093, China
[5]Institute for Nanoelectronics Devices and Quantum Computing, Fudan University, Shanghai 200433, China
[6]Department of Materials Science and Engineering, Korea University, Seoul 02841, Korea
[7]KU-KIST Graduate School of Converging Science and Technology, Korea University, Seoul 02841, Korea

We theoretically and numerically investigate ferrimagnetic domain wall dynamics induced by circularly polarized spin waves in the vicinity of the angular momentum compensation point T_A. We find that the direction of domain wall motion depends on both the circular polarization of spin waves and the sign of net spin density of ferrimagnet.

Figure 1(a)-(c) show the simulation results of DW velocity as a function of the SW frequency. Figure 1(a) represents the results for the case below the angular momentum compensation point T_A. An interesting observation for the DW motion is that the moving direction of DW depends on the circular polarization of SW. Left- (Right-) circularly polarized SW moves the DW towards (away from) the SW source. This bi-directional DW motion is understood by the fact that left- and right-circularly polarized SWs carry the angular momentum with opposite signs. The results for the case above the angular momentum compensation point T_A [Fig. 1(c)] can be understood

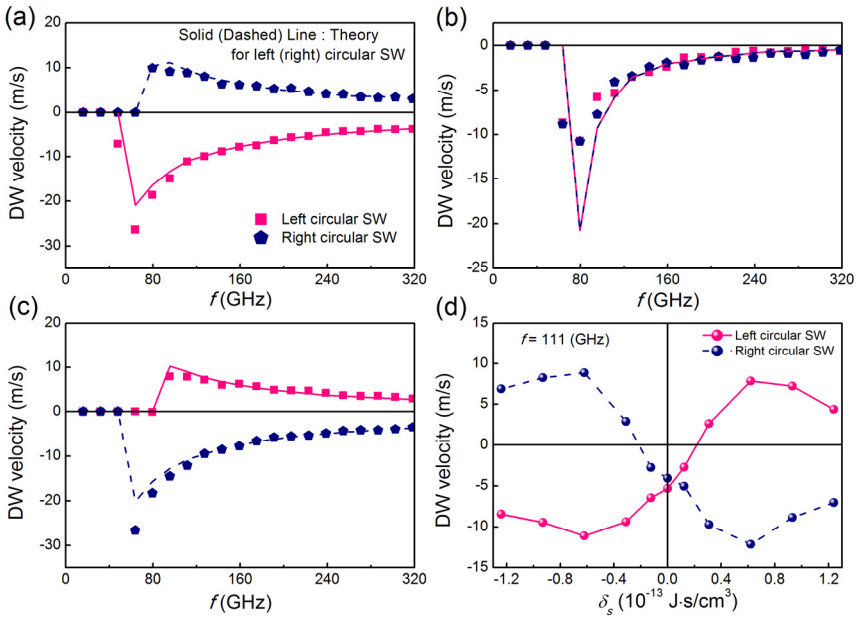

Fig. 1. Calculated domain wall velocity results (a) below T_A, (b) at T_A, and (c) above T_A with various spin-wave frequencies. Symbols are the simulation results and lines are theoretical equations. (d) Domain wall velocity as a function of the net spin density δ_s at a fixed frequency f = 111 GHz.

in a similar way. Contrary to the case below T_A, overall spin moments in the system are reversed so that left-(right-) circularly polarized SW makes DW move away from (towards) the source. For the case at the angular momentum compensation point T_A (i.e., $\delta_s = 0$), both left- and right-circularly polarized SWs drive the DW to the same direction (i.e., towards the SW source) as shown in Fig. 1(b). We note that this DW moving direction at T_A is the opposite to the direction of the DW motion induced by circularly polarized spin waves in true antiferromagnets. Dependence of the DW velocity on the SW circular polarization is summarized in Fig. 1(d), which shows the DW velocity as a function of the net spin density δ_s at a fixed SW frequency (f =111 GHz).

This bidirectional motion originates from the fact that the sign of spin-wave-induced magnonic torque depends on the circular polarization and the subsequent response of the domain wall to the magnonic torque is governed by the net spin density. Our finding provides a way to utilize a spin wave as a versatile driving force for bidirectional domain wall motion.

Logic Devices based on Domain Wall Motion in Chiral-Coupled Nanomagnets

Geun-Hee Lee* and Kab-Jin Kim

Department of Physics, Korea Advanced Institute of Science and Technology, Daejeon 34141, Republic of Korea

Recently, fast data processing and large data storing is becoming more important than ever, because of emerging data science and machine learning. However, modern computer systems, mostly rely on metal-oxide-semiconductor field-effect transistor, have a problem in processing speed and energy, which is known as von-Neumann bottle-neck [1]. One possible solution is a process-in-memory (PiM), which performs basic computing operation inside memories and thus reduces the energy consumption and time delay between processing unit and memory. In this work, we propose domain wall (DW)-based logic devices by employing chiral-coupled nanomagnets, which is applicable to SOT-MRAM and racetrack memory [2,3]. Using micromagnetic simulation, we verified that local modification of magnetic anisotropy[4] and interfacial Dzyaloshinskii-Moriya interaction induce chiral coupling between two different domains[5], resulting a NOT gate logic operation by the spin Hall effect-induced current driven DW motion. In addition, we demonstrated that the NAND or NOR gate can also be developed by assembling our simple NOT gates, enabling a complete logic operation within magnetic memory devices.

Keywords: Micromagnetics, Domain Wall motion, Domain Wall logic

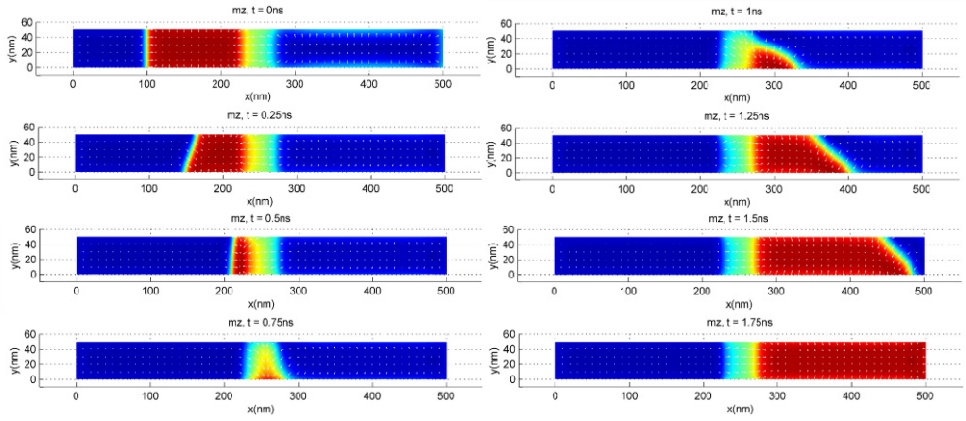

Fig. 1. NOT gate operation

References

[1] K. Takeuchi, Jpn. J. Appl. Phys. **55**, 04EA02 (2016).

[2] G. Yu, Nat. Electron. **1**, 496-497 (2018)

[3] S. S. P. Parkin, et al., Science **320**, 190 (2008)

[4] C. Chappert, et al., Science **280**, 5371 (1998)

[5] Z. Luo, et al., Science **363**, 145 (2019)

Interpretation of skyrmion motions by domain wall motions

Kyoung-Woong Moon*, Jungbum Yoon, Changsoo Kim, and Chanyong Hwang
Korea Research Institute of Standards and Science, Daejeon 34113, Republic of Korea

The magnetic skyrmion is a non-trivial topological magnetization sate and its motions are important issues in development of information processing devices. For the motion of skyrmions, a prominent driving force is the spin-orbit-torque that generated by an electric current flow in the attached heavy metal layer. However, the skymrion motion exhibits a transvers motion from the forced direction known as the skyrmion Hall effect that is an obstacle for skyrmion device. Here, we show that such transverse motions can be eliminated by the other type of spin torque that is generated by the current flow in the magnetic layer. Based on the simplified domain wall motion, we obtain an intrinsic criterion for removing the skyrmion Hall effect and we show another point of view for the skyrmion.

Theory on Spin Torque Ferrimagnetic Resonance

Seok-Jong Kim[1*], Dong-Kyu Lee[2], Se-Hyeok Oh[3], and Kyung-Jin Lee[1,2,3]
[1]KU-KIST Graduate School of Converging Science and Technology, Korea University, Seoul, Republic of Korea
[2]Department of Materials Science & Engineering, Korea University, Seoul, Republic of Korea
[3]Department of Nano-Semiconductor and Engineering, Korea University, Seoul, Republic of Korea

Compensated ferrimagnets have features of both ferromagnets and antiferromagnets, providing fast magnetization dynamics [1-5] and vanishing skyrmion Hall effect [6]. Current-induced spin torque [7, 8] is often used as a driving means. In this respect, it is of crucial importance to find a way of quantifying spin torques in heterostructures containing ferrimagnets. One of the widely employed methods to quantify the spin torque in ferromagnets is the spin torque ferromagnetic resonance (ST-FMR) technique [9, 10]. For ferromagnets, the line-shape analysis of ST-FMR signals provides a way to separately determine the damping-like and field-like torque components. However, it is unclear if this traditional line-shape analysis is valid even for ferrimagnets. In this work, we report a theory on spin torque *ferrimagnetic* resonance. We show that for ferrimagnets, the mixing voltage originating from the damping-like torque can be largely anti-symmetric, in contrast to entirely symmetric signals for ferromagnets. Our result suggests that the line-shape analysis established for ferromagnets cannot be directly applied to ferrimagnets and, instead, a new theory that we provide in this work must be implemented to analyze the spin torque ferrimagnetic resonance.

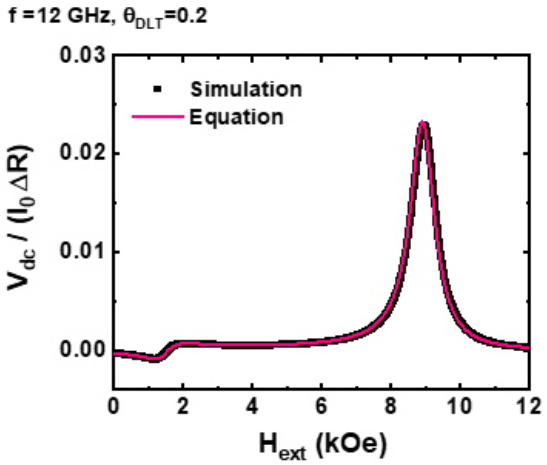

Fig. 1. Spin torque ferrimagnetic resonance signal only with damping-like torque (DLT).

References

[1] K.-J. Kim et al., Nat. Mater. 16, 1187 (2017).
[2] S.-H. Oh et al., Phys. Rev. B 96, 100407(R) (2017).
[3] L. Caretta et al., Nat. Nanotechnol. 13, 1154 (2018).
[4] S. A. Siddiqui et al., Phys. Rev. Lett. 121, 057701 (2018).
[5] S.-H. Oh and K.-J. Lee, J. Magn. 23, 196 (2018).

[6] Y. Hirata et al., Nat. Nanotechnol. 14, 232 (2019).
[7] J. Yu et al., Nat. Mater. 18, 29 (2019).
[8] T. Okuno et al., Nat. Electron. 2, 389 (2019).
[9] A. A. Tulapurkar et al., Nature 438, 339 (2005).
[10] J. C. Sankey et al., Phys. Rev. Lett. 96, 227601 (2006).

Direct observation of domain wall using Scanning Electron Microscopy with Polarization Analysis (SEMPA)

Sang Sun Lee*, Kyung-Woong Moon, Chanyong Hwang
Korea Research Institute of Standards and Science, Daejeon 34113, Republic of Korea

Scanning electron microscopy with polarization analysis (SEMPA) is a technique for observing magnetic domain structures by detecting the spin polarization of secondary electrons [1,2]. Spin-polarized secondary electrons are emitted from a sample is detected by a spin detector and overall scanned image gives magnetic image. SEMPA can be used to image the direction of sample magnetization directly and relative magnitude of sample magnetization can be obtained. Our setup is based on a Schottky type electron source for UHV SEM column with a resolution of 12 nm(expected to be 5 nm at the end of this year), exchange scattering type spin detector and spin switch. This is the most sensitive spin microscope. The spin switch is placed between sample and spin detector, which rotates the polarization vector of secondary electrons by 90 degree. Using the spin switch, three magnetization vectors (Px, Py, Pz) can be measured so that the in-plane and out-of-plane magnetic domain imaging can be possible. We have investigated the magnetic domain by employing SEMPA technique. In this study, we demonstrate that various magnetic domain with domain wall vs film thickness and the spin-reorientation transitions of Co on Pt (111) sample with the use of the spin switch.

References

[1] K. Koike and K. Hayakawa, Jpn. J. Appl. Phys. 23, L187-L188 (1984)
[2] J. Unguris, G. Hembree, R. J. Celotta, and D. T. Pierce, J. Microscopy 139, RP1-RP2 (1985)

Spin-orbit torque switching of perpendicular magnetization in ferromagnetic trilayers

Dong-Kyu Lee[1*], Kyung-Jin Lee[1,2]
[1]Department of Materials Science and Engineering, Korea University, Seoul 02841, Korea
[2]KU-KIST Graduate School of Converging Science and Technology, Korea University, Seoul 02841, Korea

Current-induced magnetization switching is a basic working principle of magnetic random access memories (MRAMs). Previous studies about current-induced magnetization switching have focused on spin-transfer torque (STT) effect in magnetic tunnel junctions or spin-orbit torque (SOT) effect in normal metal/ferromagnet bilayers. SOT switching has advantages over STT switching due to the difference in write-current path. However, there are two critical issues for SOT switching. As compared to STT switching, the switching current is too high and an additional field is required for deterministic switching.

Recent studies found that in ferromagnetic trilayers, a spin-orbit-induced spin current can have a spin polarization deviated from conventional spin-orbit torque (SOT) in bilayers [1-3]. Even though field-free deterministic switching in ferromagnetic trilayers was demonstrated in an experiment [2], the detailed switching dynamics and corresponding analytic expressions of the switching current, which are of crucial for applications based on a tilted spin polarization, has not been explored yet.

In this work, we theoretically and numerically investigate the switching dynamics and switching current for SOT switching of perpendicular magnetization in ferromagnetic trilayers. We find that SOT with a tilted spin polarization is able to achieve field-free deterministic switching at a lower current than conventional SOT or STT switching, offering a possibility for high-density and low-power SOT devices. Moreover, we provide analytical expressions of the switching current for a tilted spin polarization direction [Fig. 1], which will be useful to design SOT devices and to interpret SOT switching experiments. In the presentation, we will discuss the details of switching dynamics, material parameter dependence, and the effect of thermal fluctuation field.

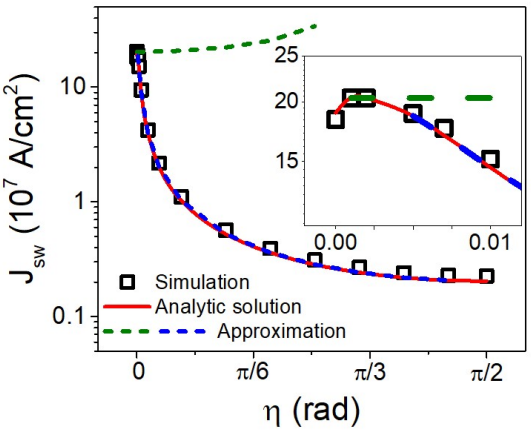

Fig. 1. Switching current density (J_{sw}) induced by a tilted spin polarization direction ($\vec{\sigma} = \cos\eta\hat{y} + \sin\eta\hat{z}$) as a function of η. Inset is J_{sw} at the range from 0 to 0.01 radian. Symbols are macrospin simulation results and lines are analytic solutions.

References

[1] T. Taniguchi et al., Phys. Rev. Applied **3**, 044001 (2015)

[2] S.-h. C. Baek et al., Nat. Mater. **17**, 509 (2018)

[3] V. P. Amin et al., Phys. Rev. Lett. **121**, 136805 (2018)

Ultrafast Spin Precession Frequency Dependence on Pump Intensity: Thermal Energy vs. Magneto-elastic Energy

Yooleemi Shin[1,2,3*], Dong-Eon Kim[2,3*], and Ji-Wan Kim[1,2,3†]

[1]Department of Physics, Kunsan National University, Kunsan 54150, South Korea

[2]Department of Physics and Center for Attosecond Science and Technology, POSTECH, Pohang 37673, South Korea

[3]Max Planck POSTECH/KOREA Research Initiative, Pohang, 37673, South Korea

We demonstrate that the precession frequency of the ultrafast spin dynamics increases with an increase of a femtosecond laser pump intensity in two samples Co(25 nm)/Al_2O_3 and Co(200 nm)/Al_2O_3(15 nm)/Co(25 nm)/Al_2O_3. We ascribe this interesting aspect, opposite to common belief, to the effect of magneto-elastic energy in Ni. Generally, when temperatures of magnetic materials increases by femtosecond pulses, magnetic energy terms, such as a magneto-crystalline, a demagnetizing, and a Zeeman energy, are all reduced resulting in lowering a precession frequency. However, the magneto-elastic energy increases as it is proportional to a lattice expansion, leading to an increase of a precession frequency. This energy term has not been considered so far in analyzing ultrafast spin precession frequency. We also confirm this with the calculation of Landau-Lifshitz-Gilbert equation including the magneto-elastic energy.

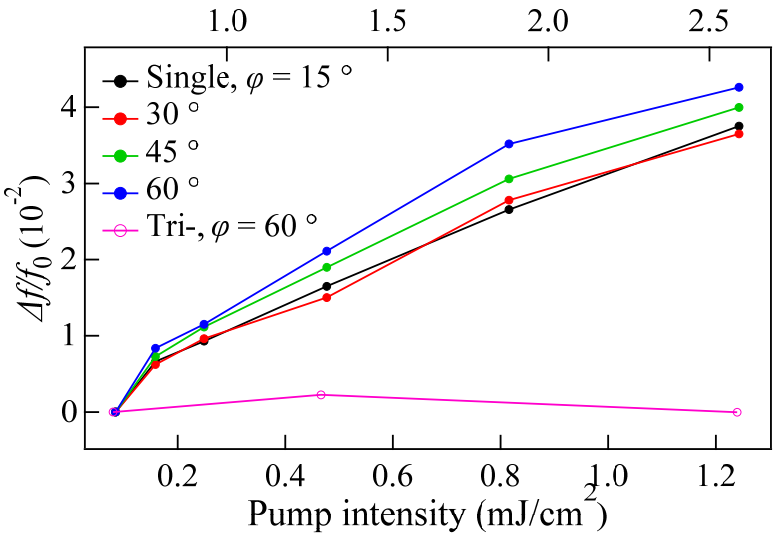

Fig. 1. Pump intensity dependence of spin precession frequencies

Visualization of 1st Order Spin Wave in Au/Co Structure Using Sequential Acoustic Pulses Generated by A Single Femtosecond Optical Pulse

Yooleemi Shin[1,2,3*] and Ji-Wan Kim[1,2,3†]

[1]Department of Physics, Kunsan National University, Kunsan 54150, Korea
[2]Department of Physics and Center for Attosecond Science and Technology, POSTECH, Pohang 37673, Korea
[3]Max Planck POSTECH/KOREA Research Initiative, Pohang, 37673, Korea

We report about the visualization of the first order spin wave mode in the time domain in Au/Co bilayer structures controlled coherently by picosecond acoustic pulses. Two types of acoustic pulses are generated by hot electrons induced by one femtosecond optical pulse in each Co and Au layer leading to a coherent control of spin waves with a time sequence. With varying an angle of external magnetic field and a thickness of Au layer, we finally have revealed the pure motion of a first order spin wave through total suppression of the fundamental spin wave mode. We also provide the simplest way of determining a spin wave exchange stiffness constant using higher order spin wave modes.

Negative spin Hall magnetoresistance due to Spin-Charge Interconversion at Ferromagnet/Oxide Interfaces

Min-Gu Kang[1*], Gyungchoon Go[2], Soogil Lee[1], Kyung-Jin Lee[2,3], and Byong-Guk Park[1]
[1]Department of Materials Science and Engineering, KAIST, Daejeon 34141, Korea
[2]Department of Materials Science and Engineering, Korea University, Seoul 02841, Korea
[3]KU-KIST Graduate School of Converging Science and Technology, Korea University, Seoul 02841, Korea

Interconversion between charge and spin through spin-orbit coupling lies at the heart of condensed-matter physics[1]. Recent studies found that in normal metal (NM)/ferromagnet (FM)/oxide structure, interfacial spin orbit coupling at NM/FM interfaces efficiently converts in-plane charge currents to perpendicular spin currents[2], which is distinct from the Rashba-Edelstein effect, i.e., interfacial spin-density generation. Also, there was theoretical investigation about spin-orbit torque in FM/NM/oxide structure with considering the Rashba interfacial spin-orbit coupling at NM/oxide interface[3]. However, its reciprocal spin-current-to-charge-current conversion at the same interface has yet been proven experimentally.

Here we report the interfacial reciprocal conversion by demonstrating negative spin hall magnetoresistance (SMR) in SiO_2/NiFe/MgO structures. As shown in figure 1. (a), we perform the angle-dependent magnetoresistance measurements using a dc current of 1mA along the *x* direction while rotating the samples on *yz* plane (β) under an external magnetic field of 5T, which is larger than the anisotropy field of NiFe. Figure 1. (b) and (c) show the angular dependence of SMR and its dependence on NiFe thickness (t_{NiFe}) ranging from 1 nm to 50 nm. The observed sign of SMR in NiFe single layer is the opposite to that normally observed in NM/FM bilayers. Moreover, we experimentally demonstrate the generation of spin current in a single FM layer through in-plane harmonic transverse resistance measurements[4]. Figure 1. (d) shows a second harmonic Hall resistances as a function of the azimuthal angle (φ) of the in-plane magnetic field with respect to the current direction, indicating sizable spin-orbit toque-induced effective fields.

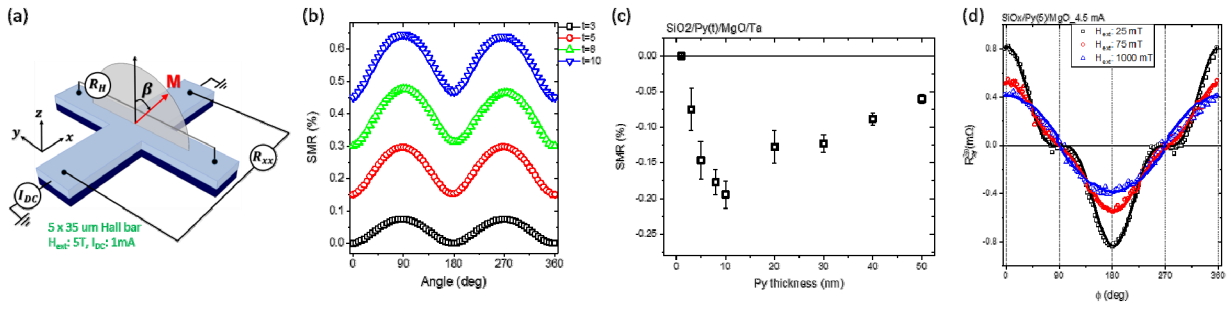

Fig. 1. (a) Schematic of system along y-z plane angle sweep. (b) Angular dependence of negative SMR in SiO_2/NiFe(t)/MgO structure. (c) NiFe thickness dependence of negative SMR. (d) ϕ dependent 2nd harmonic Hall resistance, $R_{xy}^{2w}(\phi)$, with different external field in SiO_2/NiFe(5)/MgO.

Our result demonstrating negative SMR and 2nd Harmonic spin-orbit torque clearly shows that the spin current can be generated even in single FM layer. These cannot be explained by bulk spin Hall effect only, thereby showing the existence of the interfacial spin obit coupling effect.

References

[1] Sinova, J. et al. Spin Hall effects. Rev. Mod. Phys. 87, 1213 (2015).

[2] Baek, S.-h. C. et al. Spin currents and spin–orbit torques in ferromagnetic trilayers. Nat. Mater. 17, 509 (2018).

[3] Eun-Sang Park et al. Effect of Rashba interaction at normal metal/insulator interface on spin-orbit torque of ferromagnet/normal metal/insulator trilayers. Current Applied Physics 19, 1362-1366 (2019)

[4] C.O.Avci. et al. Interplay of spin-orbit torque and thermoelectric effects in ferromagnet/normal-metal bilayers. Phys. Rev. B 90, 224427 (2014)

In-plane direct current probing for spin orbit torque-driven effective fields in heavy metal/ferromagnet/oxide frames

Jinpyo Hong[1†], Jeonghun Shin[1*], Seungmo Yang[2], Jungyup Yang[3]
[1]Division of Nano-scale Semiconductor Engineering Hanyang University, Seoul 133-791, South Korea
[2]Quantum Technology Institute, Korea Research Institute of Standards and Science, Daejeon, Korea
[3]Department of physics, Kunsan national University, South Korea 54150
[†]Fax: +82-(2)-2296-3738 E-mail address: jphong@hanyang.ac.kr

In-plane current-induced magnetization switching in heavy metal/ferromagnet/oxide frames has recently attracted attention as a novel magnetization switching method due to fast switching speed and low power consumption. A great deal of research has been studied on the exact determination of torque, and research on the magnitude of the rashba effect and spin hall effect has continued. As a general method, a harmonic analysis method using AC signal has been proposed. Our experimental results exhibited a strongly polar angular dependency of the spin orbit torque-driven effective fields observed from Ta or W/CoFeM/MgO frames. A new method for analyzing spin orbit torque is presented. We analyze anomalous hall effect in DC current to separate the Rashba effect and the spin hall effect, and present the effective field analysis method.

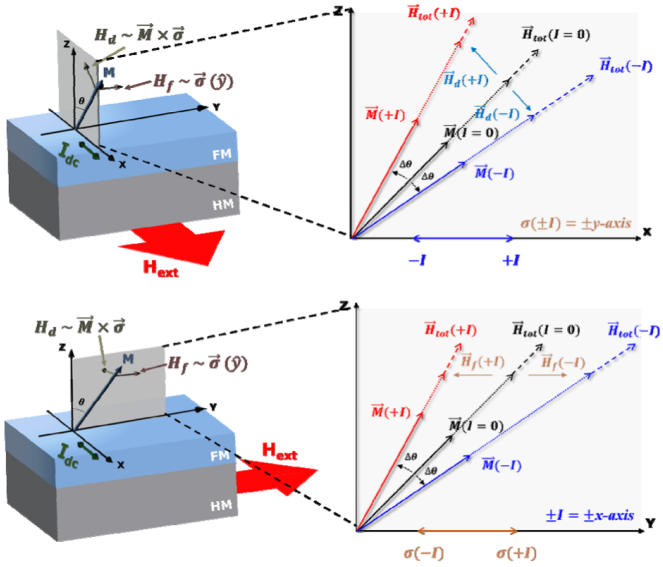

Fig. 1. Parallel and perpendicular to the direct current I_{dc} Sources.

Magnetic domain wall roughness of ferrimagnetic thin films

Kyoung-Hoon Kim* and Kab-Jin Kim
Department of Physics, Korea Advanced Institute of Science and Technology, Daejeon 34141, Republic of Korea

Magnetic domain wall (DW) motion has long been a subject of research in spintronics field because of its fundamental interest as well as technological applications. When the magnetic DW is driven by a weak magnetic field at finite temperature, the motion is generally occurred by successive thermal activation process, which we call DW creep motion. In this creep regime, the DW is considered as an elastic string which has finite roughness due to the quenched disorders. As the roughness governs the scaling law of DW speed, it is highly important to determine the roughness in disordered media. In this study, we investigate the roughness of magnetic domain wall in two different magnetic systems: ferromagnetic Co/Pt and ferrimagnetic GdCo. By developing a program that can automatically analyze the DW roughness from the obtained DW image, we analyze the DW roughness of Co/Pt and GdCo thin films. In the presentation, the result of DW roughness of both systems will be presented with in-depth discussion.

Diode-like manipulation of magnetic skyrmion transmission using an asymmetric modification of edge potential energy surface

Dae-Han Jung*, Hee-Sung Han, Namkyu Kim, GangHwi Kim,
Suyeong Jeong, and Ki-Suk Lee†
School of Materials Science and Engineering, Ulsan National Institute of Science Technology,
Ulsan 44919, Republic of Korea

Magnetic skyrmions, mainly found in a magnetic material with the Dzyaloshinskii-Moriya interaction induced by the spin-orbit coupling, are one of the most promising candidates for future spintronics applications. Due to the demand for device miniaturization, real devices are usually modelled upon confined geometries with edge boundaries. Within this arena, it is essential to manipulate the dynamics of a skyrmion close to the track edge. In this work, we observe two distinct situations where a current-driven skyrmion propagation passes through or pinned at a notch at one of the edges according to the applied current density. This observation can be exploited together with the asymmetrical edge potential energy profile for a skyrmion diode. The phenomenon is explained by a simple model based on the collective coordinates for skyrmion's motion in conjunction with an energy surface corresponding to the boundary force and spin-torque. This work provides an important avenue to design skyrmion-based logic device such as a diode element by manipulating potential energies through the device shape.

Enhancing the coercivity and thermal stability of Nd-Fe-B sintered magnets by grain boundary diffusion process

Sumin Kim[1*], Hyun-Sook Lee[1], Donghwan Kim[2], Jong Wook Roh[3], and Wooyoung Lee[1†]

[1]Department of Materials Science and Engineering, Yonsei University, Seoul 03722, Republic of Korea

[2]R&D center, Star Group, Daegu 42714, Republic of Korea

[3]School of Nano & Materials Science and Engineering, Kyungpook National University, Gyeongsangbuk-do 37224, Republic of Korea

Since their discovery in 1984, high-coercivity sintered Nd-Fe-B magnets have found numerous practical and industrial applications, e.g., as components of actuators, motors, and generators. However, the above applications require long-term magnet operation in high-temperature environments without any coercivity decrease, which is a non-trivial criterion. Generally, the coercivity of Nd-Fe-B magnets can be enhanced by the partial replacement of Nd by Dy, Tb, or both; however, the high cost and scarcity of these rare earths preclude the widespread application of this method and necessitate the development of more economically viable alternatives. One of such alternatives is the reduction of heavy rare earth elements (e.g., Dy and Tb) usage and minimization of remanence and energy product loss via the utilization of the grain boundary diffusion process. The principle of grain boundary diffusion process is to let heavy rare earth elements diffuse along the grain boundaries from the surface to inside of magnet during heat treatment.

In our previous study, we employed consecutive heat treatment-driven Tb-H diffusion to fabricate large-size Nd-Fe-B magnets exhibiting enhanced coercivity without any decrease of remanence (Br) and energy product ((BH)max). However, for application in a high-temperature environment, we should consider both coercivity and thermal stability of Nd-Fe-B magnets such as flux loss, temperature coefficients (β), and squareness.

Herein, for this reason, we enhance the coercivity as well as thermal stability parameter through the changes of heat treatment conditions and diffusion materials.

Epsilon Iron Oxide Nanopowder for the Application of Electromagnetic Wave Absorption

Min Ji Pyo[1,2*], Hee Lack Choi[2], Youn-Kyoung Baek[1†]

[1]Powder and Ceramics Division, Korea Institute of Materials and Science, Chang-won, Korea

[2]Department of Materials Science and Engineering, Pukyong National University, Busan, Korea

Electromagnetic (EM) waves are beginning to be using in electronic devices for high-speed wireless communication such as in local-area networks and radars for the distance between cars. Ferrite magnets with high coercive field (H_c) are expected to show a ferromagnetic resonance for effective suppression of the EM interference and stabilization of the EM transmittance. However, they have limitations in the GHz band application, thus exploring for suitable materials has required. The epsilon iron oxide (ε-Fe_2O_3) has an extremely large H_c value of 20 kOe at room temperature, resulting in zero-field ferromagnetic resonance with a high resonance frequency. Iron oxides (Fe_2O_3) with α or ɣ phases commonly occur in nature. In contrast, ε-Fe2O3 is difficult to synthesize since the metastable phase only can be obtained under the conditions such as limited particle size and annealing temperature. In this study, we developed a scalable method to obtain high purity ε -Fe_2O_3 nanoparticles via an aerosol approach. Moreover, the coercivity of ε-Fe_2O_3 phase can be controlled by substitution of non-magnetic elements, leading to tunable frequency resonance absorption in the region of millimeter wavelengths (30-300 GHz). Thus, our strategy would pave the way for the practical application of ε -Fe_2O_3 as a millimeter-wave absorber.

Keywords: Electromagnetic Wave, Millimeter Wave, Absorber, Aerosol, Epsilon Ferrite

Acknowledgement

This research was supported financially by the Fundamental Research Program (PNK 6530) of Korea Institute of Materials Science.

Determination of Rotor Type considering Magnetization Process

Kyu-Seob Kim*, Kun Woo Ku, Bong-Hyun Lee, Byeong-Hwa Lee
Daegu-Gyeongbuk Division, KATECH, Korea

This paper deals with the post assembly magnetization process of motors using ferrite permanent magnets. In order to meet the needs of mass production, most motors are magnetized post assembly. However, increasingly complex shapes are required to maximize the flux of permanent magnets. As a result, certain locations in the magnet are not fully magnetized by the magnetizing fixture due to insufficient magnetomotive force. Therefore, an analysis concerning the post assembly magnetization is needed. In this paper, the concentrated flux spoke type synchronous motor is analyzed to magnetization process, and then the magnetization level is compared by linkage flux value between post assembly and fully magnetization. Finally, back electromotive force is estimated by post assembly magnetization method the according to the magnet shape.

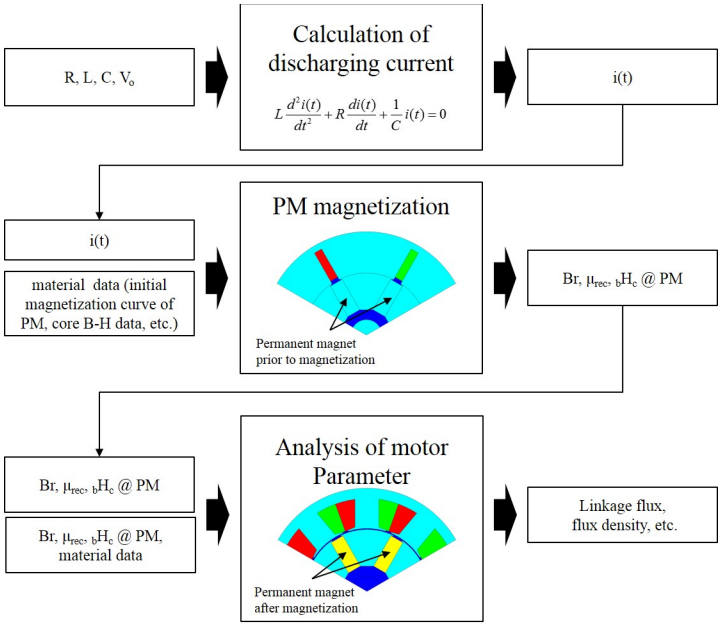

Fig. 1. Post assembly magnetization process

Acknowledgement

This paper was supported by the 2017 Deagu Future Vehicle Leading Technique (Development of electric compressor driving system for air conditioning for semi-mid-class electric vehicles) (DG-2017-02)

Characteristic Comparison of IPM Type Synchronous Motor and Wound Rotor Type Synchronous Motor

Byeong-Hwa Lee*, Su-Chul Kim, Kyu-seob Kim, Kyu-Sik Kim, Bong-Hyun Lee
Electrification System R&D Center, Korea Automotive Technology Institute, Daegu, Korea

Interior Permanent Magnet type Synchronous Motor (IPMSM) has higher torque density and efficiency per unit rotor volume than induction motor and reluctance motor because it can use both magnetic and reluctance torques. Furthermore, wide operating speed range can be obtained with the help of field weakening control. Therefore, their applications are getting widened from small power to large power systems [1]-[3].

However, the rise in the price of rare earth magnet caused by its scarcity becomes a troubling issue which the world is facing nowadays. In this situation, Wound Rotor Synchronous Motor (WRSM) has numerous benefits compared to IPMSM as it does not need magnetic materials and can be operated in a wide range of speeds. So, an alternative solution to IPMSM particularly for the industrial applications is represented by the WRSM [4].

This paper deals with the analysis of characteristics and compares IPMSM with WRSM. First of all, we solve the characteristic equations of motor and propose the efficient control method.

The figure of stator and the stack length are exactly the same for the 2 type and the shapes of designed models and manufactured WRSM rotor are shown, respectively, in Fig. 1, 2, and 3. The parameters are computed by Finite Element Method (FEM) and the characteristic analysis is performed with the values above. Moreover, comparing losses and characteristics which each motor has can be done through the identical method. A total loss is the sum of iron loss, stator copper loss, mechanical loss and rotor losses. The last one is the eddy current loss of permanent magnet for the case of IPMSM, but can be calculated by multiplying wire wound resistance by square of input current for WRSM.

In a complete paper, all the results will be covered and we will propose the efficient control method of IPMSM and WRSM.

References

[1] Ji-Young Lee, Sang-Ho Lee, Geun-Ho Lee, Jung-Pyo Hong, and Jin Hur, “Determination of Parameters Considering Magnetic Nonlinearity in an Interior Permanent Magnet Synchronous Motor”, IEEE Trans. on Magn., vol. 42, no. 4, pp.1303-1306, 2006.

[2] Jin Hur and Byeong-Woo Kim, “Rotor Shape Design of an Interior PM Type BLDC Motor for Improving Mechanical Vibration and EMI Characteristics”, JEET, vol. 5, no. 3, pp.462-467, 2010.

[3] Kyung-Tae Kim, Kwang-Suk, Kim, Sang-Moon Hwang, Tae-Jong Kim, and Yoong-Ho Jung, “Comparison of Magnetic Forces for IPM and SPM Motor with Rotor Eccentricity”, IEEE Trans. on Magn., Vol. 37, No. 5, pp.3448-3451, September 2001.

[4] O. Pyrhonen, M. Niemela, J. Pyrhonen, and J. Kaukonen, “Excitation control of DTC controlled salient pole synchronous motor in field weakening range,” in Proc. 5th Int. Workshop Adv. Motion Control (AMC), 1998, Coimbra, Portugal, pp. 294-298.

This research was supported by the Ministry of Trade, Industry & Energy(MOTIE), Korea Institute for Advancement of Technology(KIAT) through the Encouragement Program for The Industries of Economic Cooperation Region(P006100016).

Zn-doping influence on magnetic and microwave absorption properties of $SrFe_{12}O_{19}$ hexaferrites

H. H. Nguyen*, J. H. Ahn, N. Tran, T. L. Phan and B. W. Lee
Department of Physics and Oxide Research Center, Hankuk University of Foreign Studies, Yongin 17035, South Korea

The crystal structure and magnetic and electromagnetic wave absorption properties of $SrFe_{12-x}Zn_xO_{19}$ (x = 0 - 1) hexaferrites were studied. The analyses of X-ray diffraction patterns indicated that the samples fully crystallized in the *P6₃/mmc* hexagonal structure. The replacement of Zn for Fe in $SrFe_{12-x}Zn_xO_{19}$ enhanced the lattice parameters, meaning that *a* and c decrease with increasing of x, with *a* = 5.884 – 5.879 Å, and *c* = 23.05 – 23.02 Å. The results obtained from magnetization measurements indicated a slight increase of the saturation magnetization (M_s) from 36 emu/g for x = 0 to 40 emu/g for *x* = 0.1, and then a rapid decrease from 40 emu/g for *x* = 0.1 to 30 emu/g for *x* = 1. Meanwhile, excepting for x = 0, the coercivity (Hc) increased from 2.2 kOe for x = 0.05 to 2.8 kOe for x = 0.1, and lightly decreased from 3.3 kOe for x = 0.2 to 3.0 kOe for x = 1. Such changes in M_s and H_c have less influence on the microwave absorption properties. Having studied these properties in the frequency range *f* = 0.1~18 GHz, we have found $SrFe_{12-x}Zn_xO_{19}$ showing a high value of reflection loss *(RL)* with RL > -6 dB. This could be due to the fact that the Zn presence at different polyhedral sites of the M-type hexaferrites structure diluted magnetic interactions between Fe ions and increased magnetocrystalline anisotropy, leading to the increase of Hc and high *(RL)* values.

Automation of dc magnetron sputtering system using real-time thickness monitor

S. H. Lee*, Sug-Bong Choe
Seoul National University Department of physics & Astronomy, Korea

The properties of ultrathin magnetic films are very sensitive to the film thickness. To achieve precise thickness with reasonable reproducibility, here we present a new scheme of thickness control by ditrctly monitoring the deposition thickness in real time. In this scheme, a quartz-crystal-based thickness monitor is employed, whick is interfaced to a computer. Then, a LabView program keeps monitoring the deposition thickness, followed by the shutter control when the deposition thickness reaches to the aiming thickness as shown by Fig. 1. By applying the present scheme, we succeeded to fabricate Ta (5nm)/Pt(2.5nm)/Co(0.25nm)/Pt(1.5nm) films. For comparison, the same films were fabricated by use of the conventional scheme with the deposition time control under priorily-determined deposition rate. The reproducibility will be finally descussed between these two schemes.

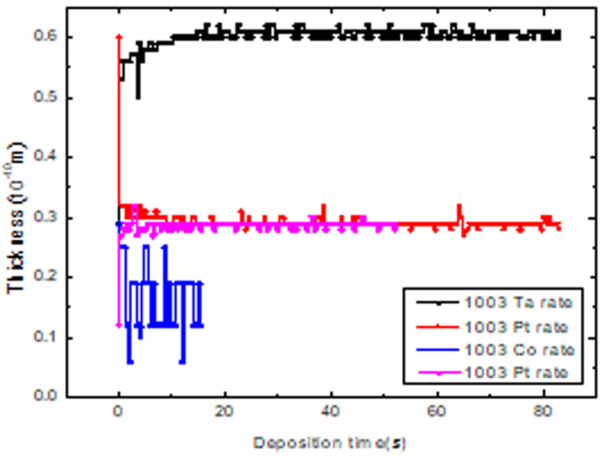

Fig. 1. Deposition rate graph

A study hall effect on CoSiB/Pt/CoSiB structure

Y. K. Kim*, Hana Lee, Minwoo Lee, T. W. Kim
Sejong Univ., Gunja-dong, Gwangjin-gu, KS013, Seoul, Korea

magnetic recording media and magnetic sensors using Magnetic recording films. Magnetic recording films were extensively studied using magnetic recording media and magnetic sensors. Natural hall effects of metal and alloys resulting from spin orbital interaction are much larger than conventional Hall effects due to roundworm forces. Some materials show a wide range of hall effects suitable for Hall sensors. The study conducted an experiment on Hall effect.

The manufacture of the thin film manufacturing equipment was used by the sputtering system, and the deposition conditions were fixed to CoSiB-0.04nm/s, Pt- 0.08-nm/s, Ta-0.05nm/s, and evaporation stacks Ta5 / Pt 3/CoSiB (X)/Pt 3nm. To check the difference between bulk and patterning, 5 inch crome mask was produced and compared. We studies X=2, 2.5, 3nm, Result, V_H(Hall voltage)= 0.15 ~0.175mV, all curve shows clear hysteresis.(PMA). and Pt2nm, Pt2.5nm shows switch surve, and Pt3nm show linear curve.

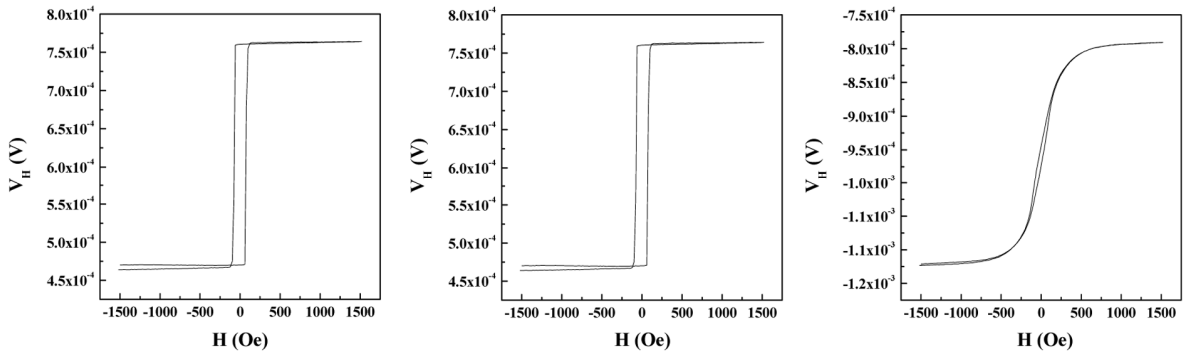

(1) Pt2nm (2) Pt2.5nm (3) Pt3nm

Graph.(1),(2),(3) shows a graph of the variation of Pt(x). X =2nm, 2.5nm, 3nm.
V_H(Hall voltage)= 0.15 ~0.175mV, all curve shows clear hysteresis.

This work was supprted by Ministry of Science and ICT(201900000001268)

Permeability Dependence on Particle Size of Alloy Based FeSiCr Metal Powder

Y. J. Choi*, M. Y. Lee, H. J. Woo, K. W. Cho, B. W. Lee
Department of Physics and Oxide Research Center, Hankuk University of Foreign Studies, Yongin 17035, South Korea

Randomly mixed FeSiCr metal powder was separated in six sections of particle sizes by sieving the metal powder. The six sections are over 63μm, 53-63μm, 45-53μm, 38-45μm, 25-38μm and under 25μm. The X-ray Diffraction (XRD) data shows that the alloy has a simple cubic structure which Si and Cr substituted the Fe site. Scanning Electron Microscope (SEM) image of the powder showed the sphere shape which means that the powder was produced by gas atomization. Energy Dispersive Spectroscopy (EDS) data shows that there are about 87wt% of Fe, 11wt% of Si and 2wt% of Cr in the alloy powder. When we measured the Vibrating Sample Magnetometer (VSM), it showed that the 38-45μm powder has 162.70emu/g for magnetic saturation (M_s), and 7.3428G for coercivity (H_c), and this shows that the particle size with 38-45μm has the most soft magnetic properties among these six sections. Toroidal core with an inner diameter 13mm and outer diameter 20mm was made from each powder. Each powder was mechanically mixed with 3wt% of epoxy resin and pressed by 3 metric tons for 1 minute followed by drying at 150℃ for 2 hours. When measured by the Impedance Analyzer, the inductance of 38-45μm powder, which is expected to show the best soft magnetic properties based on low coercivity and high saturation magnetization. In addition, the highest permeability is over 63μm powder, but there is a drawback that the permeability decreases rapidly as the frequency increases. Looking at the Q-factor data, both the resonant frequency and the Q-factor increase as the powder size decreases.

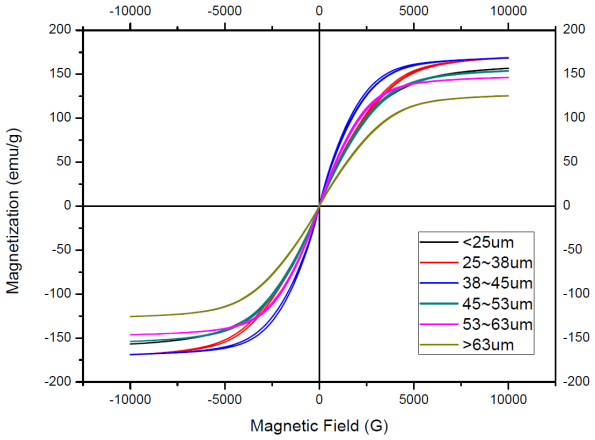

Fig. 1. Hysteresis loop of FeSiCr alloy

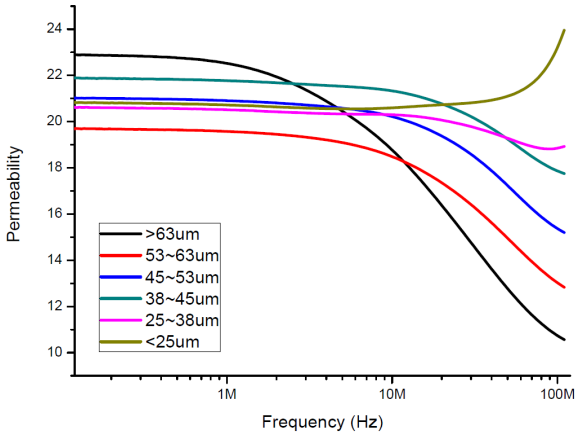

Fig. 2. Permeability dependence on particle size of FeSiCr alloy

SM03

Influence of B/Si content on the soft magnetic properties of annealed FeSiBNbCu alloy system

Jonghee Han*, Seoyeon Kwon and Haein Choi-Yim
Department of Physics, Sookmyung Women's University

Fe-based soft magnet or nanocrystalline alloys have been developed and interested because of their outstanding soft magnetic properties. However, the saturation magnetization (M_s) of these materials is relatively lower than that of Si-steels. Therefore, M_s higher than that of Si-steel materials with a low P_{cv} are required for next generation soft magnetic materials. The purpose of this study is focused on increasing the value of M_s with maintaining low P_{cv} by variation the B or Si contents in FINEMET alloy system. The ribbons of $Fe_{96-x-y}Si_xB_yNb_3Cu_1$ with 2 mm width and 20-30 μm were prepared by using melt-spinning technique. In order to produce nanocrystalline phase and optimize soft magnetic properties of FINEMET system alloys, the ribbons were annealed at the various annealing temperature decided above the crystallization temperature (T_x). The thermal properties of the as-spun ribbons such as T_x were measured by differential scanning calorimetry (DSC). The structural properties were identified by X-ray diffraction (XRD). The magnetic properties of all specimens were measured by using a vibrating sample magnetometer (VSM) and AC B-H loop tracer.

Comparison of Performance for SPMSM using Cobalt Iron and Silicon Steel

Jun-Woo Chin[1*], Min-Ro Park[1], Young-Hoon Jung[1], Chung-Seong Lee[2], and Myung-Seop Lim[1†]
[1]Department of Automotive Engineering, Hanyang University, Seoul 04763, Korea
[2]Central R&D Center, Mando Inc., Seongnam 13486, Korea

Recently, the major topics of the electric machine industry are increasing efficiency and power density. Therefore electric machine designers achieve these goals by parametric design and optimizing the shape of motor [1]. The others are interested in the core materials which have better magnetic properties than the conventional core materials like the silicon steel. So, many new products such as the cobalt iron and the nickel iron were developed for the better magnetic properties [2]. The cobalt iron has better magnetic properties than the silicon steel, especially for B-H characteristic and iron loss, and the nickel iron has lower iron loss than the other materials such as silicon steel and cobalt iron at high frequency [3].

In this paper, the magnetic properties such as B-H characteristic and iron loss are compared according to the core materials, particularly for cobalt iron and silicon steel. Furthermore the performance of the proposed surface-mounted permanent magnet synchronous motors (SPMSM) which employ core materials referred earlier is also compared. The process of iron loss calculation via the 2-D finite element analysis (FEA) is suggested. Also the line-to-line voltage, line current and efficiency at the same load condition are compared.

The proposed core of cobalt iron and silicon steel are Vacoflux48 and 20PNF1500, whose thicknesses are both 0.2 mm. The magnetic properties such as B-H curve and iron loss of the Vacoflux48 and 20PNF1500 were compared as results of the material experiments as shown in Fig. 1. In terms of the B-H characteristic, the cobalt iron has a saturation flux density of 2.1-2.3 Tesla. On the other hand, the conventional silicon steel has a saturation flux density of 1.4-1.6 Tesla. Fig. 1 (b) shows that the iron loss of Vacoflux48 is lower than that of 20PNF1500 at 1000Hz. However, not only for the frequency of 1000Hz, but also for every frequency, the iron losses of Vacoflux48 are lower than those of 20PNF1500.

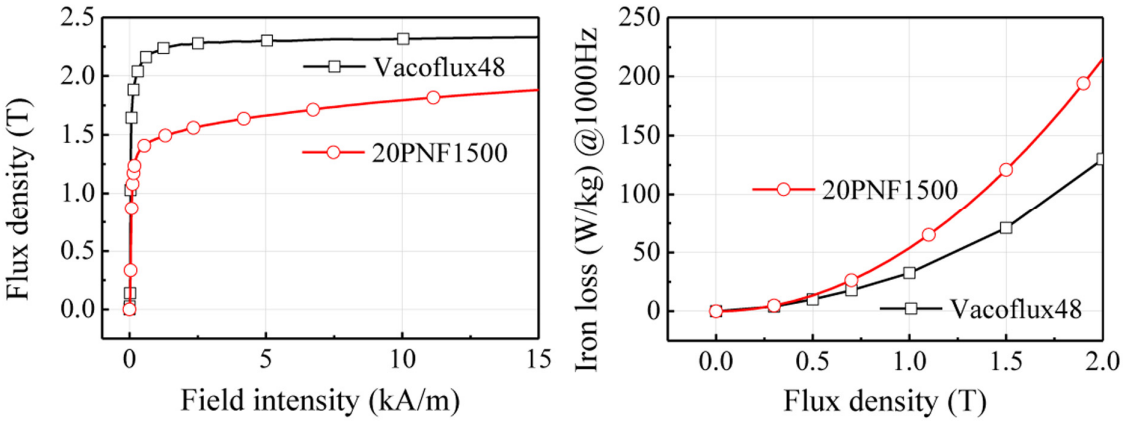

(a) B-H curve (b) Iron loss (@1000Hz)

Fig. 1. Magnetic properties of the cobalt iron and silicon steel

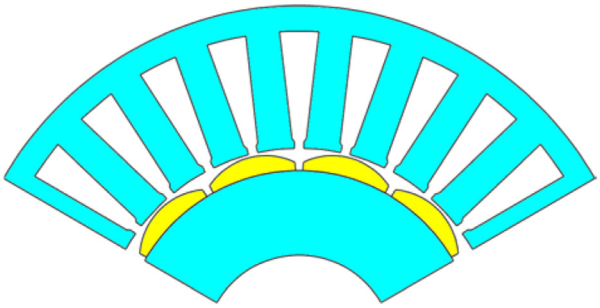

Fig. 2. Shape of proposed SPMSM

To examine and compare the performances of a motor, SPMSM was proposed as an analysis model. An inner-rotor-type SPMSM consists of 12 poles-27 slots, and Nd magnet was used in the rotor. By applying each core material data, the performance and characteristic of SPMSMs were investigated through the 2-D FEA. The process of iron loss calculation through 2-D FEA was proposed. Then the line-to-line voltage, line current and efficiency that can be calculated by d-q axis equivalent circuit were compared.

Development of external field free magnetic biosensor by using self-field

Dong Young Kim[1*], Seok Soo Yoon[1†], Sung-Joon Kim[2], Jae-Hoon Lee[2], Cheol-Gi Kim[2]
[1]Deaperment of Physics, Andong National University, Korea
[2]Department of Emerging Materials Science, DGIST, Korea

The planar Hall resistance (PHR) sensor was fabricated using exchange biased NiFe(20 nm)/Cu(0.5 nm)/MnIr (10 nm) thin film. The magnetic field dependence of Planner Hall (V_{PHR}) and self-field (V_{SF}) signals were measured by using Lock-in Amp. In this works, we used the self-field (V_{SF}) signals (second harmonic signal) in order to detect the magnetic bead. The V_{SF} signal was proportional to the product of sensitivity of V_{PHR} and H_{SF}. The high and stable V_{SF} signals was observed at H=0. Therefore, the magnetic bead detection was also carried out at H=0 by SF method. The bead signal V_{bead} was defined by the voltage difference between output self-field voltage with and without magnetic beads such as $V_{bead} = V_{SFw} - V_{SFwo}$. In order to check the performance of self-field sensor, we made the 6 samples with different concentration (1x is original solution, 100x is 1/100 concentration). The bead signals with bead concentration were measured by SF method at H=0. Bead signal for 1x concentration sample was shown in insert figure of Fig.1. The bead signal detected by using the Self-field sensor operated at H = 0 showed linear behavior up to 1/100 bead concentration as shown in Fig.1. Thus, the self-field sensor can be applied to the external field free biosensor.

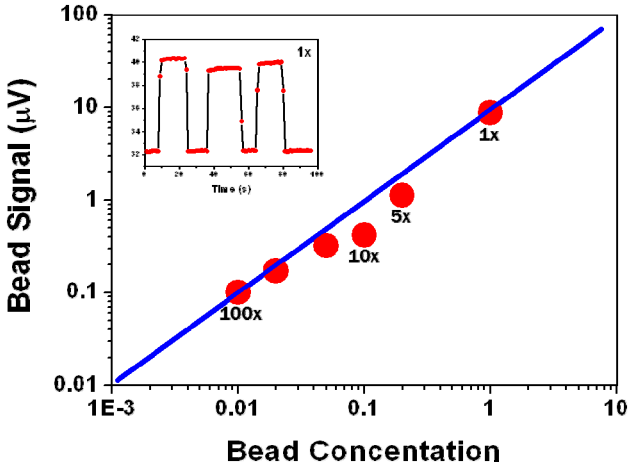

Fig. 1. Bead concentration dependence of bead signal. The insert figure shows the time dependent V_{SF} signal for with and without 1x bead sample

Surface induced ferromagnetism in SnO_2 films

Jiwoong Kim[1*], Sehwan Song[1], Yesul Choi[1], Dooyong Lee[1], Hyegyeong Kim[2], Ho-Sun Lee[2], Jong-Seong Bae[3], Sungkyun Park[1,3]

[1]Department of Physics, Pusan National University, Busan 46241, Korea
[2]Core Research Facilities, Pusan National University, Busan 46241, Korea
[3]Busan Center, Korea Basic Science Institute, Busan 46742, Korea

Thickness-dependent magnetic properties of SnO_2 films were examined. We found that the magnetization in the unit of surface area was consistent with respect to the film thickness, deducing a magnetic moment resides at the film surface or interface. Based on X-ray photoelectron spectroscopy, the amount of oxygen vacancy at the surface was consistent as well as the magnetization, supporting a magnetic ground state is induced at the surface of SnO_2 film by the oxygen vacancy.

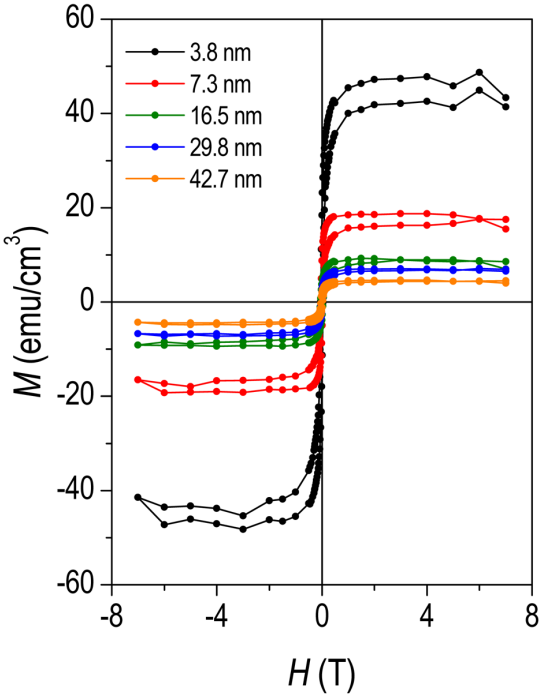

Reference

[1] Jiwoong Kim, et al, "Room temperature ferromagnetism from magnetic ion free binary oxide film "(accepted in J. Magn. Magn. Mater. [https://www.sciencedirect.com/science/article/abs/pii/S0304885319327076])

These works are supported in part by NRF-Korea (NRF-2017K1A3A7A09016305 and NRF-2018R1D1A1B07045663) and Korea Basic Science Institute (KBSI) grant (C38529) to Sungkyun Park.

Switching of Asymmetric Bloch wall in a ferromagnetic rectangular disk

Sooseok Lee[1*], Hee-Sung Han[1], Myeonghwan Kang[1], Hye-Jin Ok[1], Namkyu Kim[1], Mi-Young Im[2], Ki-Suk Lee[1]

[1]Ulsan National Institute of Science and Technology, Korea

[2]Lawrence Berkeley National Laboratory, USA

In a submicron-scaled patterned ferromagnetic thin film, magnetic domain walls (DWs) appear to reduce overall free energy in magnetic films, and they have been identified two types of DWs : In thin and patterned film Neel type domain wall is energetically favored where the spin rotates within plane, and the thicker films have Bloch type domain wall where spins tilt through out-of-plane alignment.[1-4] Such magnetic configurations mainly focused on controlling, manipulating and moving their internal magnetic configuration to develop next generation spintronic devices. In a relatively thick disk, an asymmetric Bloch wall (ABW) with Néel cap forms between two vortex cores to minimize the demagnetization energy along the thickness direction. In this system, there are two degenerate states of ABWs whose rotating orientation is clockwise (CW) or counter-clockwise (CCW) and they are exactly same energy states, they can appear at the same probability within one wall. To switch those states, it is necessary to break the symmetry of two states. For example, asymmetric geometry was utilized for control the ABW states [5]. In this presentation, we propose an efficient way to switch the rotating orientation based on the symmetry breaking of the ABW through the external magnetic field the using micromagnetic simulation and magnetic transmission soft X-ray microscopy, we have observed the switched ABWs in a 100nm thick, rectangular patterned thin permalloy film.

References

[1] A. Hubert and R, Schäfer. Magnetic Domains. (Springer, Berlin, 1999)

[2] Lv, G., Zhang, H., Cao, X., Gao, F. & Liu, Y. Micromagnetic simulations of magnetic normal modes in elliptical nanomagnets with a vortex state. Appl. Phys. Lett. 103, 252404, doi:10.1063/1.4850537 (2013).

[3] Masseboeuf, A. et al. Dimensionality Crossover in Magnetism: From Domain Walls (2D) to Vortices (1D). Phys. Rev. Lett. 104, 127204 (2010).

[4] Hertel, R & Kronmüller, H, Computation of the magnetic domain structure in bulk permalloy, Phys. Rev. B. 60, 7366-7378 (1999)

[5] Cheynis, F. et al. Controlled Switching of Néel Caps in Flux-Closure Magnetic Dots. Phys. Rev. Lett. 102, 107201 (2009).

Current induced switching of magnetization in GaMnAsP film with Perpendicular Magnetic Anisotropy

Seongjin Park[1*], Kyung Jae Lee[1], Seul-Ki Bac[1], Seonghoon Choi, Phunvira Chongthanaphisut[1], Sanghoon Lee[1†], X. Liu[2], M. Dobrowolska[2], and J. K. Furdyna[2]

[1]Physics Department, Korea University, Seoul 136-701, Korea

[2] Physics Department, University of Notre Dame, Notre Dame, IN 46556, USA

We report the observation of current induced switching of magnetization in GaMnAsP film with perpendicular magnetic anisotropy. Crystalline GaMnAsP ferromagnetic semiconductor films were grown by molecular beam epitaxy (MBE) on GaAs (001) substrate. The Hall resistance measured with in-plane and out-of-plane magnetic field revealed that the GaMnAsP film has out-of-plane magnetic easy axis. We have investigated the current dependence of magnetization reversal process of the film by monitoring Hall resistance. The magnetization reversal process shows clear difference between current polarity (i.e., positive and negative currents) with increasing magnitude current indicating the presence of current induced spin-orbit (SO) effective field in the film. We further investigate magnetization switching phenomenon in GaMnAsP film by using current induced effective field. As the magnitude of current increases, the initialized magnetization of GaMnAsP film was reversed at a critical current under in-plane bias field that is collinear to the current direction. The critical current was systematically decreases as the magnitude of in-plane bias field decreases. Even though the presence of current induced SO effective field and magnetization switching was confirmed in our investigation, the experiment involves significant Joule heating owing to the large current, which changes the magnetic anisotropy of the GaMnAsP film. Such Joule heating effect was carefully considered in order to establish current control of magnetization in GaMnAsP film with perpendicular magnetic anisotropy.

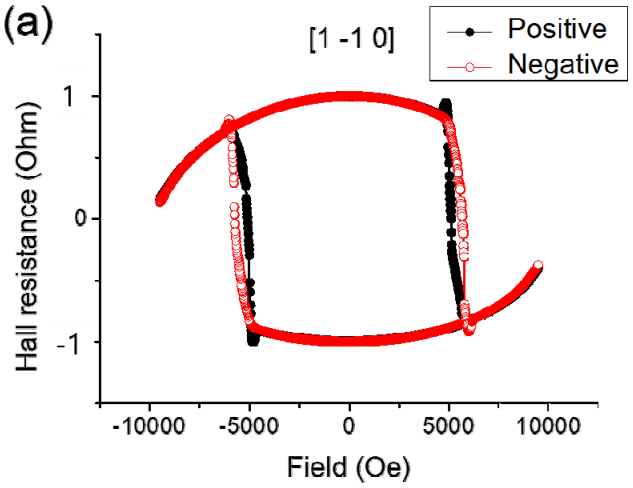

Fig. 1. (a) Magnetic field dependence of Hall resistance at positive and negative current direction along [1 -1 0] in GaMnAsP single layer

Tuning electric- and magneto-resistance by electric field-induced oxygen ion hopping in a single GdO_x wire

Jun-Ho Kang[1*], Soogil Lee[1], Taek-Hyeon Lee[1], Jae Wook Lee[2], Byong-Guk Park[2], and Kab-Jin Kim[1]

[1]Department of Physics, KAIST, Daejeon 34141, Korea

[2]Department of Materials Science and Engineering, KAIST, Daejeon 34141, Korea

Metalic system can be easily controlled by the aid of oxidation modulation. Several studies have been made on the electrical tuning of magnetic properties in metalic devices by controling oxidation [1-3]. However, in the reported ferromagnetic metal/oxide heterostructures, the interface is inevitable and its quality largely affect to the performance of devices. On the contrary, we exploited the oxygen migration effect in a single partially-oxidized-gadolinium (GdO_x) wire, where the oxygen migration occurs toward lateral direction. To probe oxygen migration, we used optical microscope and obtained electric-field polarity dependent optical images. Also, it is obtained that oxygen migration accompanies the resistance change of device. The monotonic resistance change under constant electric field and the bi-directional resistance modulation upon electric field polarity can give opportunity to mimic biological synapse. Furthermore, it is found that a large negative magnetoresistance(MR) appears in our single GdOx wire. We attributes it to the tunneling effect, which comes from the mixture of Gd and GdOx nano-grains. Our results may enable to develop fully functional electro-magnetic devices such as artificial synapse.

References

[1] Baur, U., et al, Nature Materials, **14,** 174-181 (2015)

[2] Huang, M., et al, Scientific reports, **7,** 7452 (2017).

[3] Tan, A. J., et al, Nature Materials, **18,** 35-41 (2019).

Systematic Study for Unidirectional Spin Hall Magnetoresistance in Ferromagnet/Heavy Metal Bilayers with Varying Thickness of Ferromagnetic Layer

Heechan Jang[1*], Eunkang Park[1], Nyun Jong Lee[1,2], Chun-Yeol You[2], Sanghoon Kim[1†]

[1]Department of Physics and EHSRC, University of Ulsan, Ulsan 44610, Korea

[2]Department of Emerging Materials Science, Daegu Gyeongbuk Institute of Science & Technology, Daegu 42988, Korea

[*]Both Mr. Jang and Mr. Park equally contribute to this study.

[†]Corresponding author: sanghoon.kim@ulsan.ac.kr

Unidirectional spin Hall magnetoresistance (USMR) is a new member of the magnetoresistance family arising from the spin current generation in ferromagnet (FM)/non-magnetic heavy metal (HM) bilayers. The USMR shows asymmetric behavior with respect to the current or external magnetic field directions, which makes easy to quantify both spin sign of spin current and amount of charge-to-spin conversion in a system. This can be utilized for quantitative analysis of spin current generation. It is well known that spin current generation gives rise to the USMR, but its mechanism remains under debate. CO Avci et al. firstly reported the USMR and explained the mechanism using spin accumulation concept [1], while electron-magnon scattering has been also reported as a considerable mechanism of the USMR [2,3]. In this study, we observed FM material dependence of the USMR with a fixed HM. Details about our observations will be discussed in this presentation.

References

[1] Can Onur Avci, et al, Nature Physics, 11, 570 (2015).

[2] Kab-Jin Kim, et al, arXiv:1603.08746 (2016).

[3] K. Yasuda, et al, Physical Review Letters, 117, 127202 (2015).

Artifact-free Optical Spin-orbit Torque Magnetometry

Jung-Hyun Park[1*], Joo-Sung Kim[1], Yong-Keum Park[1,2], Hyun-Seok Whang[1], Byoung-Chul Min[2], and Sug-Bong Choe[1]

[1]Department of Physics and Astronomy, Seoul National University, Seoul, 08826, South Korea

[2]Center for Spintronics, Korea Institute of Science and Technology, Seoul, 02792, South Korea

Current control of magnetization via the spin-orbit torque (SOT) has opened a new horizon for magnetic memory devices. SOT causes magnetization switching and domain wall motion that enable read/write operations in spintronic memory devices. For more efficient operation of such spintronic devices and further investigation of underlying SOT mechanisms, a precise and artifact-free SOT quantification method is required. In this circumstance, however, planar Hall effect (PHE) and anomalous Nernst effect (ANE) signals complicate SOT analysis in the electrical harmonic measurement method. Our optical setup utilizes photoelastic modulation (PEM) and balanced detection (BD) to measure the polar magneto-optic Kerr effect (pMOKE) signal exclusively. We demonstrate an optical SOT measurement scheme that is free from artifacts such as the optic PHE and optic ANE. We verified the separation of the pMOKE signal in the Pt/Py bilayer sample with sizable optic PHE. Our method with single measurement principle reduces the analysis complexity, and thus, it could help expand the scope of SOT studies.

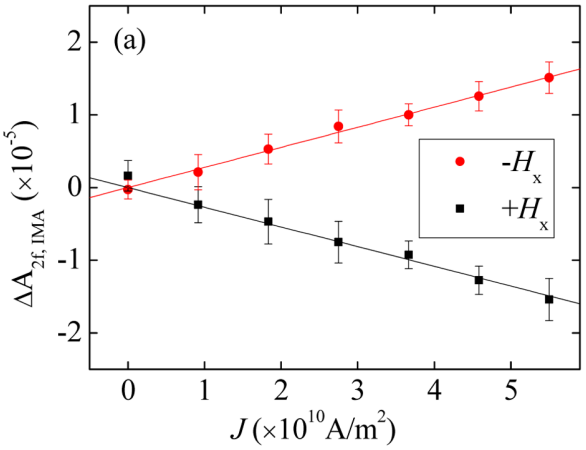

Fig. 1. Linear proportionality of the SOT-induced signal $\Delta A_{2f,\,IMA}$ with respect to current density J at H_x = 100 mT. Red and black lines are linear fits to the data with zero intercept.

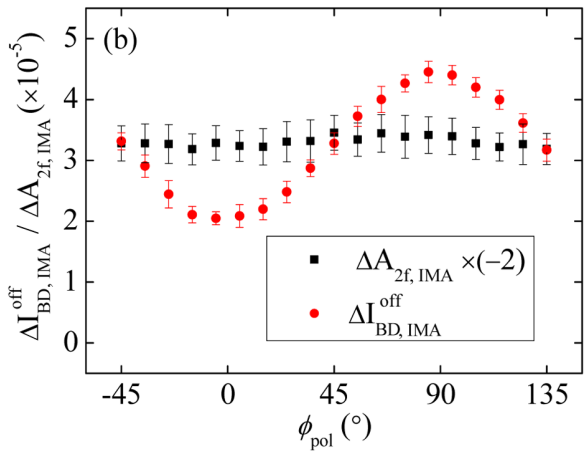

Fig. 2. Comparison of the two SOT-induced signals $\Delta A_{2f,\,IMA}$ and $\Delta I^{off}_{BD,\,IMA}$ with respect to polarization angle ϕ_{pol} at H_x = 8 mT. $\Delta A_{2f,\,IMA}$ has no ϕ_{pol} dependence whereas $\Delta I^{off}_{BD,\,IMA}$ has sinusoidal dependence from optic PHE

Material and thickness investigation in ferromagnet/Ta/CoFeB trilayers for enhancement of spin-orbit torque and field-free switching

Jaimin Kang*, Young-Wan Oh, Jeongchun Ryu, and Byong-Guk Park
Department of Materials Science and Engineering Korea Advanced Institute of Science and Technology (KAIST), Korea

We investigate spin-orbit torques (SOTs) in ferromagnet (FM)/Ta/CoFeB trilayers as a function of Ta thickness (Fig. 1a). Figure 2b describes sign and magnitude of damping-like effective field with respect to Ta thickness (t_{Ta}). When the Ta is thinner than 1.5 nm, the sign of the SOT, exerting on the top perpendicularly magnetized CoFeB, depends on the bottom FM layer; sign is positive for NiFe and negative for CoFeB. As the Ta thickness increases, the sign becomes negative irrespective of the bottom FM, indicating that SOTs are dominated by Ta, which has a negative spin Hall angle. We also observe SOT-induced switching without an in-plane magnetic field in the thickness ranges where the bottom FM or FM/Ta interface-generated SOT is dominant that is illustrated in Figure 1c. Our results demonstrate that proper design of an FM/heavy metal combination and the material thickness can lead to an enhancement of the SOT efficiency and allow us to achieve field-free SOT switching

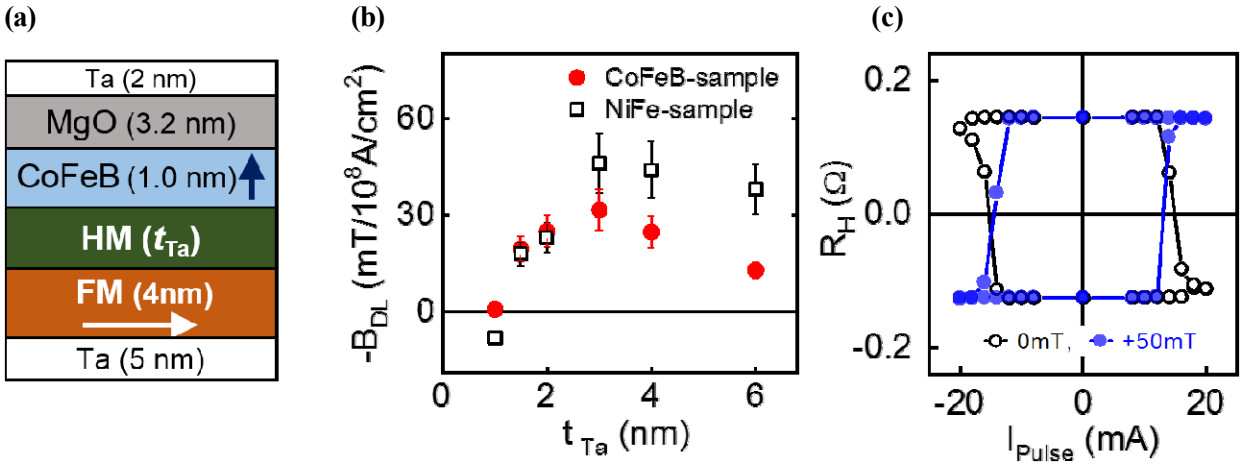

Fig. 1. a) Layer structure of Ta (5 nm)/FM (4 nm)/Ta (t_{Ta})/CoFeB (1.0 nm)/MgO (3.2 nm). b) Damping-like effective field (B_{DL}) induced by SOTs as a function of Ta (t_{Ta}). c) SOT-induced magnetization switching in the CoFeB sample with (blue circle) and without (black open circle) a magnetic field of 50mT along the x-direction.

Gate-tunable nonreciprocal response in noncentrosymmetric $LaAlO_3/SrTiO_3$ interfaces

Daeseong Choe[1*], Mi-Jin Jin[1], Shin-Ik Kim[2], Hyung-Jin Choi[2], Junhyeon Jo[1], Inseon Oh[1], Jungmin Park[1], Hosub Jin[3], Hyun Cheol Koo[4,5], Byoung-Chul Min[4], Suk-Min Hong[4], Hyun-Woo Lee[6], Seung-Hyub Baek[2,7], and Jung-Woo Yoo[1†]

[1]School of Materials Science and Engineering-Low dimensional Carbon Materials Center, Ulsan National Institute of Science and Technology, Ulsan, 44919, Korea

[2]Center for Electronic Materials, Korea Institute of Science and Technology, Seoul, 02792, Korea

[3]Department of Physics, Ulsan National Institute of Science and Technology, Ulsan, 44919, Korea

[4]Center for Spintronics, Korea Institute of Science and Technology, Seoul, 02792, Korea

[5]KU-KIST Graduate School of Converging Science and Technology, Korea University, Seoul, 02481, Korea

[6]Department of Physics, Pohang University of Science and Technology, Pohang, 37673, Korea

[7]Division of Nano & Information Technology, KIST School, Korea University of Science and Technology, Seoul, 02792, Korea

The electrons confined at the interfacial quantum well of a $LaAlO_3/SrTiO_3$(LAO/STO) associated with broken inversion symmetry exhibit various exotic condensed matter phases and rich spin-orbitronic functionalities. This two-dimensional polar conductor may directional propagation of itinerant electrons, *i.e.* the leftward and rightward currents differ from each other, when the time-reversal symmetry is further broken. This potential rectification effect generally was shown to be very weak due to the fact that kinetic energy is much higher than energies associated with symmetry breakings producing weak perturbation. Here, we show giant gate-tunable nonreciprocal charge transport in the $LaAlO_3/SrTiO_3$ conductive oxide interface, where the electrons are confined at two-dimension with low Fermi energy. In addition, the Rashba spin-orbit interaction due to a sub-band hierarchy of this system enables strongly tunable nonreciprocal response through applying a gate voltage. Upon increasing gate voltage, the ratio of resistance change between rightward and leftward currents was increased up to 2.7%. The coefficient γ representing the strength of the magnetochiral anisotropy, was measured to be as high as ~ 10^2 T^{-1} A^{-1}, which is about three order of magnitude higher than those estimated for typical noncentrosymmetric conductors [1]. Moreover, the magnitude of the directional response exhibits additional higher order magnetic-field dependence. The observed behavior of giant directional response in this system is due to the fact that energies associated with the broken inversion symmetry and the broken time-reversal symmetry are comparable to the Fermi energy, which opens a new route to enhance nonreciprocal responses in polar materials.

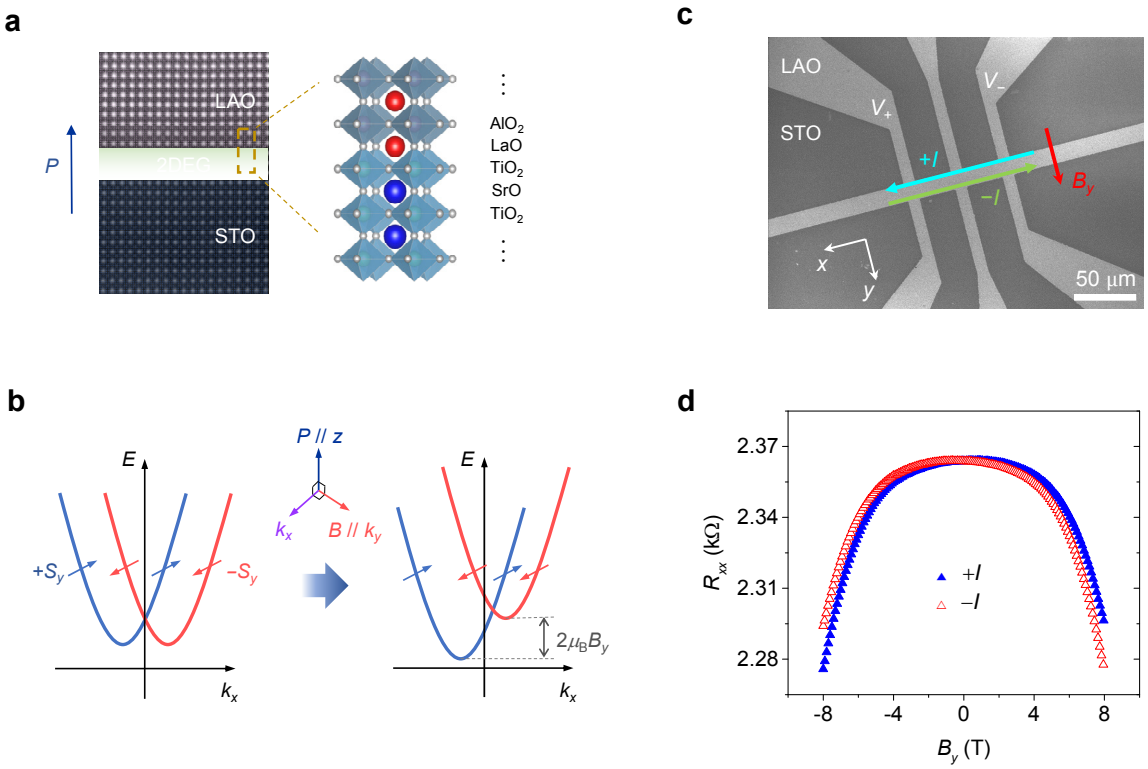

Fig. 1. Nonreciprocal charge transport in the noncentrosymmetric LAO/STO conductive interface. (a) Transmission electron microscopy image and crystal structure of the LAO/STO displaying interface with broken inversion symmetry. (b) Electron dispersion in the presence of the Rashba spin-orbit interaction and the external magnetic field. nonreciprocal charge transport arises when the polarization P, magnetic field B, and the current I are orthogonal to each other. (c) Scanning electron microscopy image of the Hall-bar device fabricated on a 5 mm × 5 mm (001) STO substrate. (d) R_{xx} measured for both direction of currents $+I_x$ and $-I_x$ while sweeping the applied magnetic field B_y.

Reference

[1] D. Choe and M.-J. Jin et al, Nat. Commun. **10**, 4510 (2019)

Enhancement of spin Hall effects inducing damping-like torque in spin-orbit torque using W_3Ta film

Byong Sun Chun*, Seung Mo Yang, Changsoo Kim, Kyoung-Woong Moon, Chanyong Hwang
Quantum Technology Institute, Korea Research Institute of Standards and Science,
Daejeon 305-340, Republic of Korea

In this study, the effects of W_3Ta on the damping-like torque induced by the spin Hall effects (SHE) were investigated. To determine the lower limit of the spin Hall angle in the W_3Ta, the SHE-induced damping-like torque in the sputter-deposited W_3Ta alloy was characterized using ST-FMR. By varying the deposition partial pressure in the sputter-deposited W_3Ta, we could control the crystallographic structure, and obtained a low conductivity of 1.83×10^5 $\Omega^{-1}m^{-1}$ for optimal SHE-induced damping-like torque. In the W_3Ta/CoFeB/MgO/Ta systems, by considering the spin-pumping effect, we obtained an SHE-induced damping-like torque efficiency of -0.678 (± 0.093), which was higher than that of the β-phase W/CoFeB/MgO/Ta structure of -0.477 (± 0.005). In light of this material requirement, W_3Ta, could be suited for the spin current generator, because of their large SHE-induced damping-like torque is promising for applications of SOT-MRAM more effectively and more energy-efficiently.

The Co thickness dependence of the Dzyaloshinskii-Moriya interaction and magnetic anisotropy in Pt/Co/W trilayers

Yong-Keun Park[1,2*], Joo-Sung Kim[1], Yune-Seok Nam[1], Seyyoung Jeon[1], Jung-Hyun Park[1], Kyoung-Whan Kim[2], Hyun-Woo Lee[3], Byoung-Chul Min[2], and Sug-Bong Choe[1†]

[1]Department of Physics and Astronomy, Seoul National University, Seoul, 08826, Republic of Korea

[2]Center for Spintronics, Korea Institute of Science and Technology, Seoul, 02792, Republic of Korea

[3]Department of Physics, Pohang University of Science and Technology, Pohang 790-784, Republic of Korea

The Dzyaloshinskii-Moriya interaction (DMI), one of interesting interfacial phenomena, has been studied due to academic and technological opportunity for generating chiral spin structures in broken inversion symmetry systems. Here, we show the Co thickness tendency of the DMI. We fabricate Pt (3 nm)/Co (t_{Co})/W (5 nm) trilayers with different Co thickness t_{Co} and measure the DMI, D, and effective magnetic anisotropy, K_U^{eff}. The K_U^{eff} is known to have volume contribution K_U^{eff} and surface contribution K_S phenomenologically, with the relation $K_U^{eff} t_{Co} = K_V^{eff} t_{Co} + K_S$ [1]. Since the DMI is sensitive to the interface condition, the D may be linked to the structural condition. In that point, we compare the tendency of K_U^{eff} and D with respect to the $t_{Co}^{eff} (\equiv t_{Co} - t^d)$, where t^d is the dead layer. Like K_U^{eff}, the D may also be presented by the relation $Dt_{Co}^{eff} = D_V t_{Co}^{eff} + D_S$, to decompose the volume contribution D_V and surface contribution D_S.

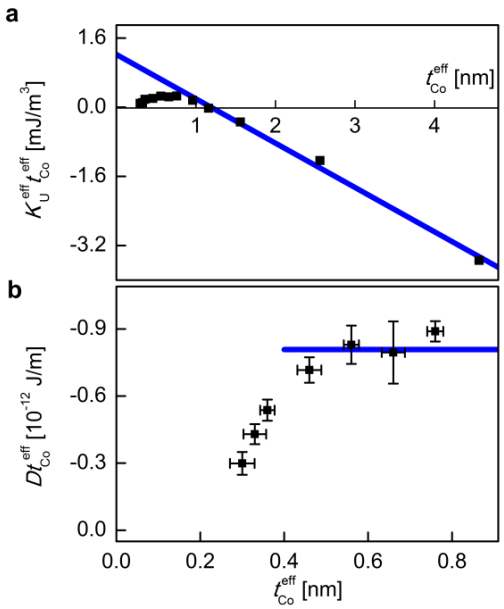

Fig. 1. The $K_U^{eff} t_{Co}^{eff}$ and Dt_{Co}^{eff} with respect to t_{Co}^{eff}. The blue line in (a) is the linear fitting line. The blue horizontal line in (b) shows the average value over the relatively thick t_{Co}^{eff}.

In fig.1(a), the K_U^{eff} deviate from the linear dependence when the t_{Co}^{eff} is thinner than ~ 1 nm, indicating structural conditions begin to change. The Dt_{Co}^{eff} have saturated value in relatively thick t_{Co}^{eff} in fig.1(b), indicating $D_V \cong 0$ and the surface contribution is mostly responsible. Since the tendency of K_U^{eff} and D are not coincident, there may be another magnetic factors affecting the DMI as well as structural factor. Moreover, it is remarkable that the D deviate from the inverse proportionality to the t_{Co}^{eff} in ultrathin t_{Co}^{eff}. This peculiar behaviour of D will be discussed. The t_{Co}^{eff} tendencies of the DMI and SOT, and change of magnetic properties when very thin Cu layer is inserted at Co/W interface will also be discussed. The present observations provide physical understanding for the DMI and a guideline to maximize the DMI for spintronic applications.

Reference

[1] R. Jungblut, M.T. Johnson, J. Stegge, A. Reinders. and F.J.A. Broeder, J. Appl. Phys. **75**, 6424 (1994).

Fast and Energy-effective STT Switching in MTJs with Assistance of SOT

Sachin Pathak* and Jongill Hong
Materials Science and Engineering, Yonsei University, Seoul 03722, Korea

Spin-transfer torque Magnetic Random Access Memory (STT-MRAM) having the building unit of a perpendicular magnetic tunnel junction (p-MTJ) has received a significant attention because it offers not only reduced write current but also strong thermal stability. Despite all these advantages, STT-MRAM also faces various challenges from an industrial point of view such as, reliability of a tunnel barrier, long write latency and high write power. A novel, spin-orbit torque (SOT) switching is gaining interest in order to overcome those problems. Especially, separate read and write lines in SOT-MRAM promises strong reliability, in addition to fast switching speed due to direct switching faster than precession switching in STT-MRAM. In this presentation, we discuss our simulated results showing the significant improvement of both switching speed and power consumption by using STT write pulse (WPSTT) current with additional SOT write pulse (WPSOT) current. We

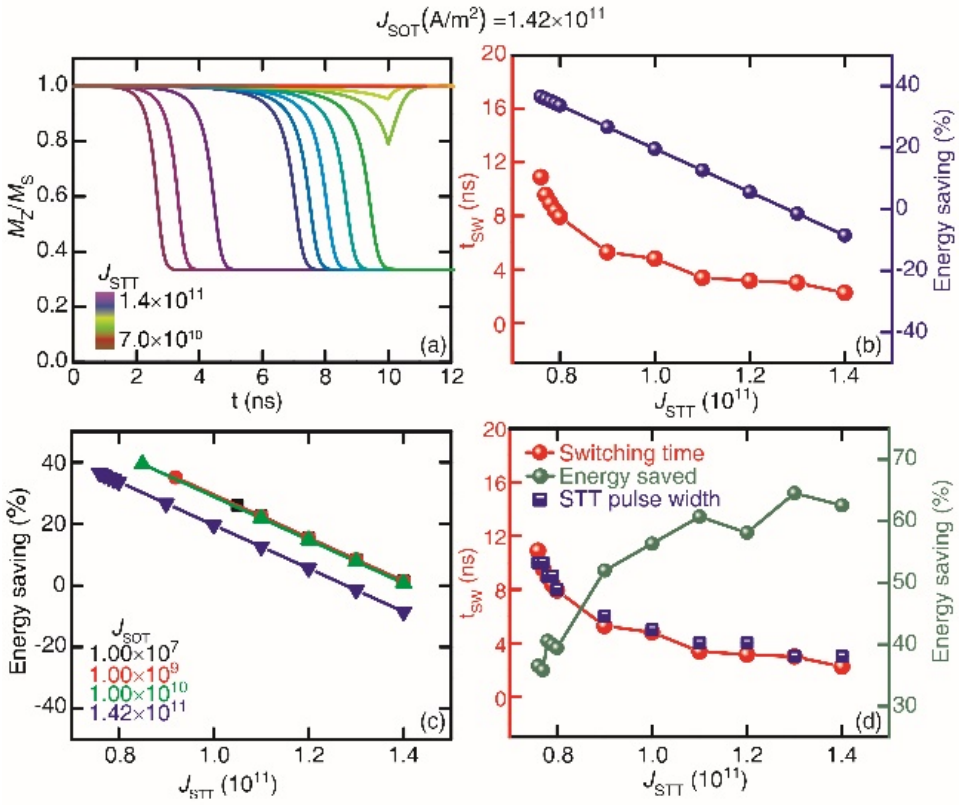

Fig. 1. (a) The magnetization (M_Z/M_S) dynamics as a function of duration under various J_{STT} amplitudes with fixed J_{SOT} (1.42×10^{11} A/m^2) and (b) corresponding switching time (t_{SW}) as a function of J_{STT}. (c) Dependency of energy saving for various J_{SOT} and (d) t_{SW} and energy saving as a function of J_{STT} (J_{SOT}=1.42×10^{11} A/m^2) for STT pulse-cut.

have used OOMMF simulator implemented with an STT-SOT module developed during our study to investigate the switching behavior of a 20 nm cell in a p-MTJ at a WPSTT duration of 10 ns (Fig 1). We found that both amplitude and duration of the WPSOT have a great impact on the switching behavior of the free layer in the p-MTJ. For example, we could dramatically reduce the switching time by 80 % and thereby reduce the write power over 60 % as compared to those in the absence of the WPSOT (Fig 2 (a-d)). Even a very weak SOT current density pulse (of the order of 102 A/m2) significantly reduced the critical current density for switching and thereby decreased the power consumption as well. It is worth to be pointed out that the power can be saved further by tuning the WPSOT parameters i.e. amplitude and duration along at the critical current density of WPSTT. The reduction is closely related to the details of spin precession during switching under the influence of torque due to WPSOT and WPSTT, acting simultaneously. Our finding provides a great impact on the p-MTJ-based memory and logic technology seeking the high speed and low power consumption.

Unconventional Temperature Dependent Magnetoresistance of GdFeCo

Jaehyeon Park[1*], Hirata Yuushou[2], Arata Tsukamoto[3], Teruo Ono[2], Kab-Jin Kim[1]
[1]Department of Physics, Korea Advanced Institute of Science and Technology, Daejeon, Korea
[2]Institute for Chemical Research, Kyoto University, Gokasho, Uji, Kyoto 611-0011, Japan
[3]College of Science and Technology, Nihon University, Funabashi, Chiba 274-8501, Japan

Recently, ferrimagnets have drawn much attention because of their intriguing properties near the compensation temperatures. For example, high domain wall velocity[1] and negligible skyrmion Hall effect[2] have been observed near the angular momentum compensation temperature (T_A), while the enhanced spin orbit torque efficiency has been reported near the magnetization compensation temperature (T_M)[3]. However, the phenomenon mentioned above are all related to the spin dynamics property. There are only few results reported on the spin transport properties which is another important aspect of spintronic research.

In this study, we investigate magnetoresistance (MR) of GdFeCo, a representative rare earth-transition metal ferrimagnetic material. The MR changes linearly to the external magnetic field at high field regime, which seems to be similar to the magnon-based MR[4]. However, the observed MR is in stark contrast to the previously reported magnon-based MR: the magnitude of the MR becomes larger as the temperature decreases, which is opposite to the conventional magnon-based MR. Furthermore, the slope of the MR changes its sign at T_M. These results imply that the observed MR may not caused by magnon, but originates from the ferrimagnetic characteristics.

References

[1] Kim, Kab-Jin, et al. “Fast domain wall motion in the vicinity of the angular momentum compensation temperature of ferrimagnets.” Nature materials 16.12 (2017): 1187.

[2] Hirata, Yuushou, et al. “Vanishing skyrmion Hall effect at the angular momentum compensation temperature of a ferrimagnet.” Nature nanotechnology 14.3 (2019): 232.

[3] Ham, Wooseung, et al. “Temperature dependence of spin-orbit effective fields in Pt/GdFeCo bilayers.” Applied Physics Letters 110.24 (2017): 242405.

[4] Nguyen, V. D., et al. “Detection of domain-wall position and magnetization reversal in nanostructures using the magnon contribution to the resistivity.” Physical review letters 107.13 (2011): 136605.

X-ray Absorption Spectroscopy of the Pb-based Perovskite with Multiferroicity

Nyun Jong Lee[1*], Jae-Hyeon Cho[2], Ju-Hyeon Lee[2], Wook Jo[2], and Sanghoon Kim[1†]
[1]Department of Physics and EHSRC, University of Ulsan, Ulsan 44610, Korea
[2]School of Materials Science and Engineering, Ulsan National Institute of Science and Technology, Ulsan 44919, Republic of Korea
[†]Corresponding author: sanghoon.kim@ulsan.ac.kr

Multiferroicity has great potential for the next generation electronic applications such as ferroelectric photovoltaics, next-generation memory devices. An epitaxially-grown antiferromagnetic $BiFeO_3$ is representative material which shows the multiferroicity with single phase, while a ferromagnetic-electrically coupled material at room temperature has not been reported yet. In this presentation, we show that a Pb-based perovskite is magnetoelectrically coupled above even room temperature. Study on x-ray absorption spectroscopy at both near (XAS) and extended edges (EXAFS) of the perovskite will be discussed to prove that the A-site substitution with Ni induces the ferromagnetic property of the perovskite.

Giant Spin-orbit Torques Induced by Orbital Hall Effect

Soogil Lee[1*], Junho Kang[2], Taekhyeon Lee[2], Jung-Mok Kim[1], Dohyoung Kim[1], Heechan Jang[3], Eun Kang Park[3], Dongwook Go[4], Nyun Jong Lee[3], Yoshinori Kotani[5], Yoichi Shiota[6], Teruo Ono[6], S. Sonny Rhim[3], Kyung-Jin Lee[7], Hyun-Woo Lee[8], Kab-Jin Kim[2], Sanghoon Kim[3], and Byong-Guk Park[1]

[1]Department of Materials Science and Engineering, KAIST, Daejeon 34141, Korea
[2]Department of Physics, KAIST, Daejeon 34141, Korea
[3]Department of Physics, University of Ulsan, Ulsan 44610, Korea
[4]Institute of Physics, FB 08 Physik, Mathematik und Informatik, Johannes Gutenberg-University Mainz, Mainz 55128, Germany
[5]Japan Synchrotron Radiation Research Institute, Sayo, Hyogo 679-5198, Japan
[6]Institute for Chemical Research, Kyoto University, Uji, Kyoto 611-0011, Japan
[7]KU-KIST Graduate School of Converging Science and Technology, Korea University, Seoul 02841, Korea
[8]Department of Physics, Pohang University of Science and Technology, Pohang 37673, Korea

Enhancement of the spin-orbit torque (SOT) in ferromagnet/nonmagnet bilayers is essential for realization of SOT-based devices with low power consumption. Thus, there have been intensive investigations to find suitable materials which exhibit large SOT efficiency, or an effective spin Hall angle (SHA_{eff}). For example, sizable SHA_{eff}s, up to 0.3, have been found with 5*d* transition metals such as β-W. However, much larger SHA_{eff}s are still desired to achieve the low power consumption in SOT-based devices. In this study, we present the giant SOT efficiency of the Gd 10/Cr 5 (nm) bilayer, which is larger than 1. The orbital Hall effect (OHE) can be proposed to explain this giant SOT. That is to say, the large orbital current is generated and injected from Cr into Gd, then converted into the spin current by strong SOC of Gd. In order to prove the orbital accumulation at the Gd/Cr interface from such OHE, current dependence of X-ray magnetic circular dichroism spectra observed with the Gd/Cr device will be also discussed.

Self-Induced Spin-Orbit Torque in TbCo Single Layer

Jae Wook Lee*, Jae Yeol Park, Jong Min Yuk, and Byong-Guk Park
Department of Materials Science and Engineering, KAIST, Daejeon 34141, Korea

Spin-orbit torque (SOT) has been extensively studied in structures involving heavy metal layer, such as heavy metal (HM) / ferromagnet (FM) bilayer and FM / HM / FM trilayer structures, since both the spin Hall effect as well as the Rashba effect are known to arise within the HM layer and the HM / FM interface, respectively. In this study, we report the observation of SOT induced damping-like effective field (H_{DL}) in the absence of HM layer in TbCo single layer structures [Figs. 1(a), 1(b), 1(e), and 1(f)]. As shown in Fig. 1, clear H_{DL} for both the Tb-rich [Fig. 1(a), 1(e)] as well as the Co-rich TbCo single layer [Fig. 1(b), 1(f)] are observed with sign of the harmonic Hall voltage opposite from each other due to the oppositely aligned Co atoms with respect to the external magnetic field. In addition, it is noted that the sign of the H_{DL} is the opposite from that of Pt/TbCo bilayer structures as shown in Figs. 1(c), 1(d), 1(g), and 1(h) suggesting that the effective spin Hall angle is the opposite for the TbCo single layer samples and the Pt/TbCo bilayer samples. Moreover, we performed STEM and EELS analyses for the Tb-rich ($Tb_{35}Co_{65}$) [Figs. 2(a)-2(c)] and the Co-rich ($Tb_{21}Co_{79}$) [Figs. 2(d)-2(f)] TbCo single layer in which we found that the intensities of the Tb and the Co are nearly constant within the TbCo layer suggesting that the compositions of the Tb and the Co are nearly constant within the TbCo layer. Our results suggest that the bulk spin-orbit interaction within the TbCo layer instead of the vertical composition gradient plays a significant role in generating the SOT.

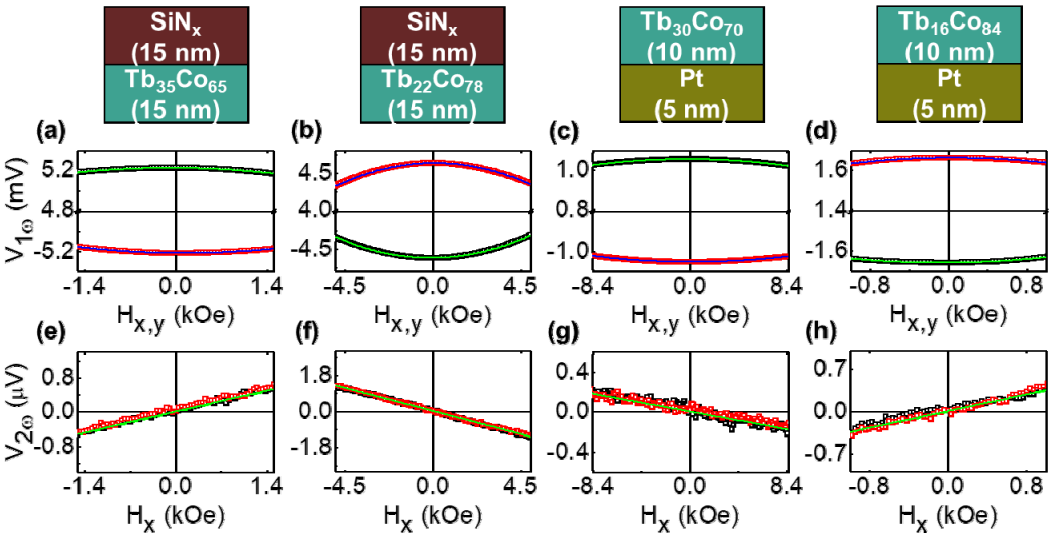

Fig. 1. (a)-(d) First harmonic Hall voltage, (e)-(h) Second harmonic Hall voltage vs. in-plane magnetic field along the current direction, and (i)-(l) Second harmonic Hall voltages vs. in-plane magnetic field perpendicular to the current direction for (a),(e),(i) Tb-rich single layer, (b),(f),(j) Co-rich single layer, (c),(g),(k) Tb-rich bilayer, and (d),(h),(l) Co-rich bilayer.

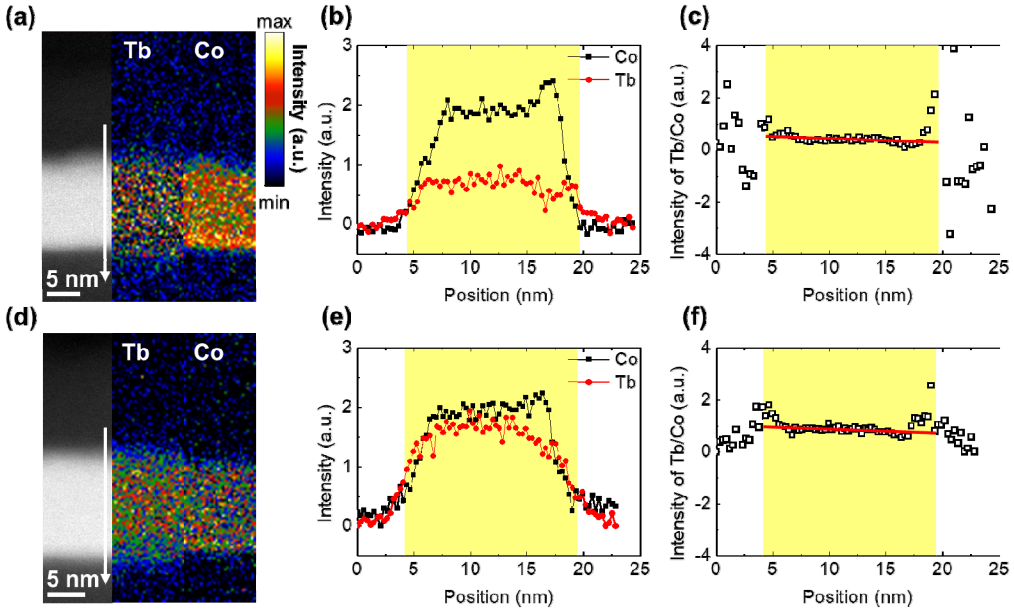

Fig. 2. The annular dark field STEM images as well as the elemental maps of Tb-and Co for (a) Co-rich $Tb_{21}Co_{79}$ and (d) Tb-rich $Tb_{35}Co_{65}$ samples. The intensity of Co and Tb as well as the Tb/Co with respect to the position from the top surface for (b),(c) Co-rich and (e),(f) Tb-rich samples.

Spin-orbit torque induced auto-oscillation in NiFe/heavy metal bilayers

Jong-Guk Choi[1*], Jaehyeon Park[2], Kab-Jin Kim[2], and Byong-Guk Park[1]
[1]Department of Materials Science and Engineering, KAIST, Daejeon 34141, Republic of Korea
[2]Department of Physics, KAIST, Daejeon 34141, Republic of Korea

When a magnetic field is applied to a ferromagnetic material (FM), a damping motion and a precession motion about magnetic field are generated. Similarly, in heavy metal (HM)/FM structures, applying in-plane current produces damping and precession based on the spin injected by the spin Hall effect (SHE). If the damping torque from magnetic field is compensated by the damping torque from injected spin, only precession movement remains, thus enabling stable auto-oscillation (AO) of magnetization.

In this study, we observe the current induced A.O. of magnetization in NiFe/heavy metals (HM), a typical structure of spin-orbit torque (SOT) device. Figure 1 shows the RF spectral density generated by applying in-plane magnetic field and DC current (I_{dc}> 10^{12} A/m^2) to HM/NiFe structures using HM with different spin Hall angles (Pt and W). The A.O. signal is only seen in the in-plane external magnetic field (H_{in}) in a certain direction, because the compensation origin of damping from H_{in} is anti-damping SOT arising from SHE. Fig. 1(a) and Fig. 1(b) show the AO spectral density of Pt/NiFe and its reversed stacking order. The accumulated spin of Pt at top interface and bottom interface are opposite, thus the AO signal occurs in opposite direction of H_{in} for same direction of I_{dc}. Fig. 1(c) shows the case of W/NiFe where the sign of spin Hall angle is opposite to Pt. As expected, the AO signal occurs in different direction of H_{in} than Pt/NiFe. Our experimental results demonstrate that the current induced AO of magnetization in HM/NiFe arises from SOT.

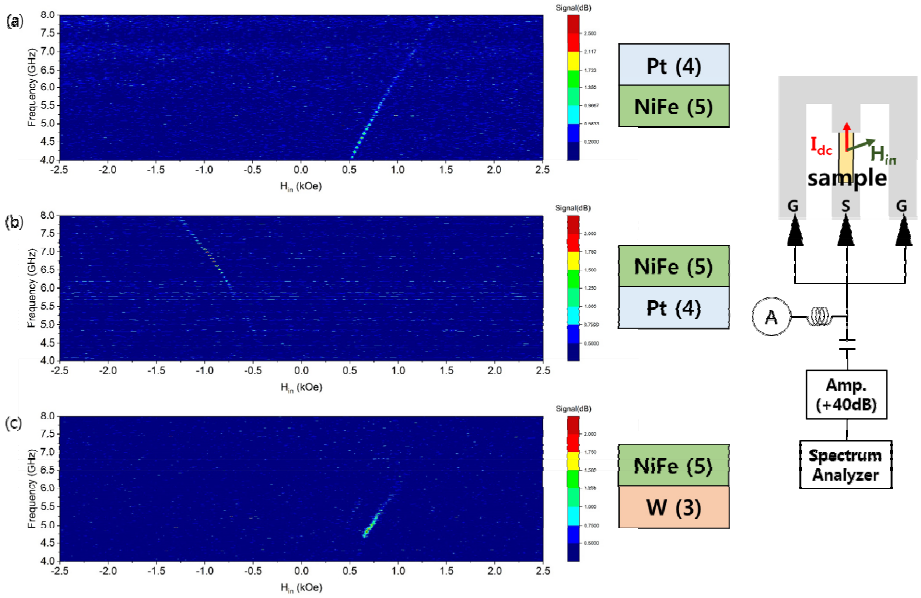

Fig. 1. Auto-oscillation spectral density as a function of external in-plane field in (a) NiFe/Pt, (b) Pt/NiFe, and (c) W/NiFe structures. The angle between I_{dc} and H_{in} is 70^0

Large Magnetoresistance in Two-Dimensional Materials based Heterostructures

Thi Nga Do[1,2*], Hayoung Ko[3], Soo Min Kim[3], and Tae Hee Kim[1,2]

[1]Center for Quantum Nanoscience, Institute for Basic Science, Ewha Womans Unversity, Seoul, 03760, Korea

[2]Department of Physics, Ewha Womans University, Seoul, 03760, Korea

[3]Institute of Functional Composite Materials, Korea Institute of Science and Technology, Jeonbuk, 55324, Korea

Magnetoresistance (MR) behaviors in 12-nm Co/1.6-nm MgO/8-nm Co magnetic tunnel junctions (MTJs) grown on the large-area CVD-grown hexagonal Boron Nitride (h-BN) and graphene films were investigated. Surprisingly, for the MTJs grown on h-BN, we observed MR values larger than 700 % at room temperature with perpendicular magnetic anisotropy. Our results indicate that the spin transport of the perpendicular anisotropy-based magnetic tunnel junctions could be influenced by the 2-D underlayer (h-BN)-ferromagnet (Co) combination. In order to clarify the influences of interface effects between the h-BN and Co layer, the characterization of interface properties was performed by surface sensitive techniques such as Raman and XPS spectroscopy. The microstructural analysis of the interfaces was also carried out using AFM and HR-TEM. Our results can provide more insight into spin transport phenomena in 2-D materials based spintronic devices. In this work, we have highlighted the aspect of interface engineering of 2-D materials with other ferromagnetic materials to develop highly effective spintronic devices with new functionalities.

Temperature and thickness dependence of magnetization switching of Fe_5GeTe_2

Kwangsu Kim[1,2*], Hyobin Anh[3], Kyung Mee Song[2], Changgu Lee[3,4], Tae-Eon Park[2†], Sanghoon Kim[1†]

[1]Depertment of Physics, University of Ulsan, Ulsan 44610, Korea
[2]Center for spintronics, Korea Institute of Science and Technology (KIST), Seoul 02792, Korea
[3]SSKU Advanced Institute of Nanotechnology (SAINT), Sungkyunkwan University, Suwon 16419, Korea
[4]Department of Mechanical Engineering, Sungkyunkwan University, Suwon 16419, Korea

Though magnetic/nonmagnetic heterostructures have attracted much attention for nanoelectronics in recent few years, there are still many uncovered physical phenomena. Especially, transport phenomena, such as magnetoresistance [1], anomalous Hall effect [2], and spin Hall effect [3], related to the interface are puzzling in some systems because of severe intermixing between elements. On the other hands, layered structures of 2D van der Waals Ferromagnet give advantages because such intermixing can be neglected. Most of reported 2D van der Waals ferromagnetic materials have low Curie temperature under 100 K due to their low dimension [4], while the Curie temperature of Fe_5GeTe_2 is near room temperature [5]. Therefore, Fe_5GeTe_2 can be a good template to study and utilize the magnetic property of 2D magnet. In this study, dimensional thermal stability of magnetic properties in Fe_5GeTe_2 will be described by observing magnetic coercivity depending on the thickness and temperature.

References

[1] G. Binasch et al., Phys. Rev. B **39**, 4828 (1989)
[2] L. Liu et al., Science **336**, 6081, pp 555-558 (2012)
[3] S. Emori et al., Nature Materials **12**, 611-616 (2013)
[4] Cheng Gong and Xiang Zhang, Science **363**, eaav4450 (2019)
[5] F. May et al., ACS Nano **13**, 4, 4436-4442 (2019)

Core-shell Ni/$CuSiO_3$ Nanocomposite Nanospheres with Honeycomb Structures for Electromagnetic Wave Absorption

Rambabu Kuchia[1], Taha Latifa[2], Viet Dongquoca[2], Phuoc Cao Vana[2], Jong-Ryul Jeong[2*]

[1]Rare Earth Utilization Technology Department,
Korea Institute of Geoscience and Mineral Research (KIGAM), Daejeon 34132, South Korea

[2]Department of Materials Science and Engineering, Graduate School of Energy Science and Technology,
Chungnam National University, Daejeon 34134, South Korea

In this study, we have investigated the core-shell Ni/$CuSiO_3$ nanocomposite nanospheres by varying the shell ($CuSiO_3$) thickness to control the microwave wave absorption performance. The effects of shell thickness were studied including electromagnetic wave absorption. The electromagnetic absorption analysis shows that the Ni/CuSiO3 core-shell nanospheres (30 wt. %) with shell thickness of 30 nm, show high reflection loss peak of –39.5 dB (9.8 GHz) at the sample thickness of 2.5 mm. It also has a wide effective absorbing bandwidth of 4.8 GHz (7.8–12.6 GHz). It clearly shows that the honeycomb-like core-shell Ni/$CuSiO_3$ composite nanospheres with a proper shell thickness resulting in the high microwave absorption performance. We believe that the absorption mechanisms are related to the novel structure which could enhances the interfacial polarization. The controlled shell thickness results in the good impedance match between EM properties (ε, μ) and magnetic loss from the ferromagnetic Ni. Therefore, we consider that a controlled shell thickness in core-shell Ni/$CuSiO_3$ composite nanospheres establishes a novel approach to achieve the high-performance electromagnetic absorbers in the field of electromagnetic wave absorption.

Observation of Plasmonic Spin Seebeck Effects in Pt/YIG Bilayers with Au Nanoparticles

Phuoc Cao Van, Srivathsava Surabhi, Viet Dong Quoc, Jae Woong Lee,
Cheong Cheon Tae, Rambabu Kuchi, Jong-Ryul Jeong*
Department of Materials Science and Engineering, Graduate School of Energy Science and Technology,
Chungnam National University, Daejeon 34134, South Korea

In this study, we have investigated the variation of longitudinal Spin Seebeck effect (LSSE) in Pt/Y3Fe5O12 (YIG) bilayers with gold nanoparticles (Au NPs) grown on Gd3Ga5O12 {GGG (111)} substrate via rf-sputtering method under the existence of the generation of plasmonic spin current in company with plasmonic heating phenomena induced by continuous laser illumination. The impact of each effect was clarified by using particular samples under different laser power and wavelength. In the Pt/YIG/Au NPs/GGG sample, the relative position of Au NPs to Pt layer makes it generating the inverse thermal gradient (∇T) to the $\nabla T_{external}$ caused by the laser source. When laser wavelength fulfills the SPR condition, there is a breakdown point of the SSE voltage dependence on laser power around 25 mW. The experimental results show the dominance of the plasmonic spin current generation effect over the SSE signal caused by the plasmonic heating effect at the lower laser power region (<25 mW). In contrast, the spin current originated from ∇T_{PH} significantly contributed to the overall SSE voltage signal. On the other hand, at the mismatch condition of SPR and laser wavelength, SSE voltage is linear dependence to the laser power, which confirms the importance of plasmonic heating effect in the spin current generation.

Magneto-optical Properties of Bi-YIG Thin Film using poly[vinylpyrrolidone](PVP) Assisted Metallo-Organic Decomposition Method

Viet Dongquoc, Phuoc Cao Van, Chongchoen Tae, Nguyen Thi Trinh,
Duong Viet Duc, Jong-Ryul Jeong*
Department of Materials Science and Engineering, Graduate School of Energy Science and Technology,
Chungnam National University, Daejeon 34134, South Korea

In this study, we have investigated a bismuth-substituted yttrium iron garnet (Bi-YIG) thin film on a glass substrate with high magneto-optical (MO) performance. The Bi-YIG thin films were fabricated using metallo-organic decomposition (MOD) method. To enhance the MO performance of the as-grown Bi-YIG thin film, different amounts of polyvinylpyrrolidone (PVP) were introduced to a metal nitrate precursor solution as a reducing agent and growth modifier. By using the optimized PVP assisted MOD method, we have obtained a Bi-YIG thin film that exhibited good morphology, high crystallinity, and high saturation magnetization. The Faraday rotation angle of this film reached its highest value of −8.0°/μm, which is close to that of thin films fabricated on gadolinium gallium garnet substrates (−10.5°/μm). Moreover, $BixY_3{-}xFe_5O_{12}$ films with different Bi substitutions were synthesized; these films showed a higher Faraday rotation angle, of up to −12.0°/μm ($Bi_{2.5}Y_{0.5}Fe_5O_{12}$), in which the peak position of the Faraday rotation angle resided in the visible range (505–540 nm). This work reveals that high-quality Bi-YIG thin films on glass substrates via MOD are promising for MO device applications

Controlling of electric and magnetic properties of two-dimensional transition metal dichalcogenides using noble gas ion

Sang Wook Han*, Soon Cheol Hong
University of Ulsan, Korea

After the advent of graphene, a two-dimensional semiconductor, MoS_2, has been studied for the electronics, optoelectronics, catalysis, and energy storage. In particular, it is enabled to fabricate wafer-scale monolayer for practical applications. However, 2D field-effect transistors (FET) composed of MoS_2 monolayer as a fundamental building block of modern devices generally achieve n-type transport despite large on-off ratio and high electron mobility. Mostly, it is known that strong Fermi-level pinning (FLP) at the interface between the contact metal electrode and the MoS_2 channel makes the p-type transport stubborn. Thus, although there were many methods to p-type doping in n-type MoS_2 monolayers such as chemical doping by Nb and Zn, plasma process by P doping, hole injection by inserting MoO_x, which have a high work function, between the MoS_2 monolayer and electrodes of FET, and so on, it is essential to find more effective method without problems caused by doping defects.

Here, we report the polarity switching of the MoS_2 monolayer using noble gas ions. Moreover, we reveal diamagnetic-ferromagnetic transition by the creation of defects. This finding provides a more simple and practical method to control the polarity of the two-dimensional transition metal dichalcogenides without the limit of the area.

Nonuniform magnetic distribution of FeRh films

Sehwan Song[1*], Jiwoong Kim[1], Seojin Yang[1], Yesul Choi[1], Tae-Seong Ju[1], Jong-Seong Bae[2], Brain Kirby[3], Miyata Noboru[4], Sungkyun Park[1†]

[1]Department of Physics, Pusan National University, Busan 46241, Korea

[2]Busan Center, Korea Basic Science Institute, Busan, 46742, Korea

[3]Center for Neutron Research, National Institute Standard & Technology, Gaithersburg, MD 20878, USA

[4]Neutron Science and Technology Center, CROSS-Tokai, 162-1 Shirakata, Tokai, Ibaraki 319-1106, Japan

B2-phase FeRh is well known as metamagnetic transition materials from antiferromagnetic to ferromagnetic above 370 K. During the transition, it shows the volume expansion about 1% and reducing the electrical resistivity due to the increasing density-of-state at Fermi level. However, it exhibits ferromagnetic characteristics at antiferromagnetic region (below transition temperatures) in the film forms due to the presence of the interfacial effect such as strain, capping layer.

In this study, we will provide the depth-dependent magnetic information of FeRh films grown on MgO(100) substrate to understand interface effect of the films above and below the transition temperature. As a result, temperature-dependent magnetic and electrical properties confirmed that the phase transition occurred around T_t ~370 K. Temperature-dependent x-ray diffraction revealed that the lattice parameter increased (~0.5%) after the phase transition. From these results, we confirmed that FeRh film was well fabricated. From analysis of polarized neutron reflectometry, we showed the non-uniform magnetic distribution across the depth direction of the film.

These works are supported in part by NRF-Korea (NRF-2017K1A3A7A09016305 and NRF-2018R1D1A1 B07045663).

Low Current sensing PHR Sensors module for IoT and automobile

J. H. Lee*, S. J. Kim, C. G. Kim
Emerging Materials Science, DGIST, Daegu, Republic of South Korea

Now days, various types of sensors are actively studied in the industrial and medical society. In particular, in the industrial and medical society, studies of magnetic sensors based on magnetic materials are being conducted in a variety of ways. Among these studies, the development of high-resolution sensors is a very important part of signal analysis. Therefore, in this study, we conducted a study on the low current detection module using the PHR (Planar Hall Resistance) [1] sensor, which is a type of magnetic sensor. High resolution low current sensing sensor is fabricated using PHR sensor. The designed PHR sensor is designed to control external magnetic field and use high resolution to detect current. In this study, a three-layer structural(trilayer) [2] was fabricated using a DC magnetron sputter. The PHR sensor used Ta/NiFe/Cu/IrMn/Ta[3]. The fabricated PHR sensor was installed in chip form through calibration circuit and a metal oxide semiconductor (CMOS) process after completion. Manufactured PHR current sensors were designed to measure current at levels 1 to 100 A and measured magnetic resolution 0.14 mG, consumption power 0.5 mA 1% precision and 0.1% nonlinear characteristics.

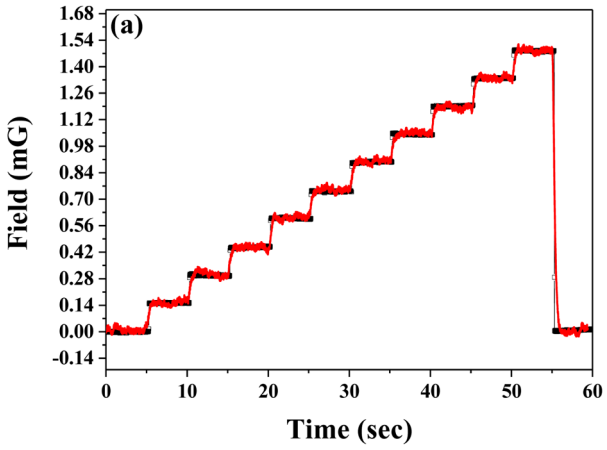

Fig. a. is comparison of sensitivity between flux gate and PHR sensor

References

[1] N. T. Thanh, B. Parvatheeswara Rao, N. H. Duc, and C-G Kim phys. stat. sol. (a) 204, 12, 4053-4057 (2007)

[2] N. J. Gökemeijer, T. Ambrose, and C. L. Chien[3] N. J. Gökemeijer, T. Ambrose, and C. L. Chien, Phys. Rev. Lett. **79**, 4270 (1997).

[3] Christian D. Damsgaard, Susana C. Freitas, Paulo P. Freitas, and Mikkel F. Hansen Journal of Applied Physics **103**, 07A302 (2008)

Controllable Actuation of Magnetic Kirigami Patterns

Trivoramai Jiralerspong[1], Geonhee Bae[2], Sang-Koog Kim[*]
National Creative Research Initiative Center for Spin Dynamics and Spin-Wave Devices, Nanospinics Laboratory, Research Institute of Advanced Materials, Department of Materials Science and Engineering, Seoul National University, Seoul 151-744, Republic of Korea
[1]Current address: 15/2 Montri Road, Tambol TaladYai, Amphur Muang, Phuket, Thailand
[2]Current address: 1, Samsungjeonja-ro, Hwaseong-si, Gyeonggi-do, Republic of Korea
Corresponding author: sangkoog@snu.ac.kr

1. Introduction

The art of paper cutting, kirigami, and its shape transformation capabilities have shown remarkable advancements in the field of science and engineering. A kirigami pattern consists of cuts that are made on a single sheet of material, where planar mechanical deformations could induce shape transformations in both two-dimensional (2D) and three-dimensional (3D) [1]. Due to this remarkable property, kirigami patterns could give rise to complex material properties such as auxetics and mechanical metamaterials where they expand when subjected planar deformations [2]. However, the mechanical deformations of kirigami structures are usually performed physically by hand or machine, and therefore limiting its application in small and tight spaces where access is difficult [3]. To counter this problem, this study proposes a remote-control technique of kirigami patterns using magnetic fields as an external stimulus [4].

2. Method and Results

In this study, the remote control of kirigami patterns in 2D and 3D are achieved by programming the magnetic anisotropy of magnetic nanoparticle (MNP) chains within the magnetic-elastomer composite [5]. The magnetic-elastomer composite is a type of magnetorheological elastomer that is composed of iron oxide (Fe_3O_4) nanoparticles and silicone elastomer. To bring about the 2D and 3D shape transformation, the MNP chains are aligned in-plane and out-of-plane, respectively. The in-plane orientation is performed by aligning the mold and hence the MNP chains along the xy-plane. Likewise, the out-of-plane chain orientation is obtained by placing the mold along the xz-plane by means of a 3D printed jig. The chains are permanently embedded within the composite once the elastomer is cured, even after the removal of the field. The kirigami patterns considered consists of multiple unit shapes that are connected by hinges [6]. Various 2D and 3D shape transformations are produced by changing the magnetic anisotropy within each unit shape and the placement of the hinges. The fabrication and the experimental procedures are performed under a uniform magnetic field that is generated by an electromagnet. The experiment is conducted under a uniform magnetic field of approximately 180 mT that is produced by an electromagnet. Experimental results show that the embedded chains within the kirigami patterns respond quickly to align its magnetic moment along the direction of the applied magnetic field.

3. Discussion

This study has demonstrated the remote 2D and 3D actuation of magnetic kirigami patterns by programming the magnetic anisotropy of each unit shape within the kirigami pattern, which allow the kirigami patterns to be

controllable under an applied uniform magnetic field. In other words, by aligning the MNP chains within each unit shape in-plane and out-of-plane, 2D and 3D shape transformation can be achieved, respectively. Due to magnetic anisotropy, the functionalized unit shapes turn to align the embedded chains with the direction of the applied external magnetic field. Depending on the direction and the angle that the chains make with respect to the applied field, as well as the location of the hinges of the kirigami patterns, a variety of kirigami structures can be fabricated.

4. Conclusion

Remote actuation of kirigami patterns in 2D and 3D can be realized through in-plane and out-of-plane alignment of the MNPs, respectively. It is shown that by aligning the MNP chains in different directions and changing the hinge location within the kirigami pattern, several shape transformation can be obtained. This untethered actuation of kirigami patterns therefore have potential applications in areas such as drug delivery, medical patches, and artificial valves.

References

[1] X. Ren, R. Das, P. Tran, T. D. Ngo, and Y. M. Xie, Smart Mater. Struct. 27, 2018.

[2] A. Rafsanjani and K. Bertoldi, Phys. Rev. Lett. 118, 1, 2017.

[3] K. Bertoldi, V. Vitelli, J. Christensen, and M. Van Hecke, Nat. Rev. Mater. 2, 2017.

[4] R. M. Erb, J. J. Martin, R. Soheilian, C. Pan, and J. R. Barber, Adv. Funct. Mater. 26, 3859, 2016.

[5] Geonhee Bae, “Motion Control of Fractal Structure Magnetic Actuator Embedded with Chained Iron Oxide Nanoparticles”, Master’s thesis, Seoul National University, 2018; Trivoramai Jiralerspong, “Controllable Actuation of Magnetic Kirigami Patterns”, Master’s thesis, Seoul National University, 2019.

[6] V. Kunin, S. Yang, Y. Cho, P. Deymier, and D. J. Srolovitz, Extrem. Mech. Lett. 6, 103, 2016.

This research was supported by the Basic Science Research Program through the National Research Foundation of Korea (NRF) funded by the Ministry of Science, ICT & Future Planning (NRF-2018R1A2A1A05078913).

Calculation of an Equivalent Source for Magnetic Field from a Domestic Induction Cooker

Ji-san Park* and Jin-Kyu Byun
Department of Electrical Engineering, Soongsil University, Korea

I. Introduction

Nowadays, domestic induction cookers are widely used due to their high efficiency, fast heating, and ease of use. Since most induction cookers are operated in the vicinity of the human body, there is a growing public concern about the magnetic field exposure from the induction cookers. Many EMF (electromagnetic field) protection guidelines, such as ICNIRP (International Commission on Non-Ionizing Radiation Protection) guidelines define induced electric field or induced current density in the human body as the basic restrictions (exposure limits based on established health effects). Since it is difficult to measure the basic restrictions inside the human body, they are often calculated using simulations with anatomical human body models. In this paper, a circular current loop is derived as an equivalent source of a domestic induction cooker. The magnetic field from a circular current loop is calculated analytically, and is compared with the measured magnetic field of an induction cooker. The current of the equivalent source is chosen that minimizes the errors between the calculation and the measurement. Using the derived equivalent source, the basic restrictions are calculated by the Sim4Life software.

II. Derivation of the Equivalent Source

The equivalent source is set as a circular current loop in the *x*-*y* plane with its center at the origin. The radial and vertical component of the magnetic flux density (B_r and B_z) from the equivalent source at a point $P(x,y,z)$ can be expressed from the following equations [1]:

$$B_r = \frac{\mu_0 z I}{2\pi r\sqrt{z^2+(a+r)^2}}\left(\frac{a^2+z^2+r^2}{z^2+(r-a)^2}E_2(k)-E_1(k)\right) \tag{1}$$

$$B_z = \frac{\mu_0 I}{2\pi r\sqrt{z^2+(a+r)^2}}\left(\frac{a^2-z^2-r^2}{z^2+(r-a)^2}E_2(k)+E_1(k)\right) \tag{2}$$

where μ_0 is the magnetic permeability of the free space, a is the loop radius, I is the coil current, $r=\sqrt{x^2+y^2}$, $k=\sqrt{\frac{4ra}{z^2+(a+r)^2}}$, and $E_1(k)$ and $E_2(k)$ are the elliptic integrals of the 1st and 2nd kind. For this paper, loop radius of $a = 100$ mm was used that matches the pot location mark on the surface of the induction cooker.

III. Measurement of the Magnetic Field from the Induction Cooker

In the IEC 62233 standard, the distance from the edge of the induction cooker to the probe is given as 30 cm for the magnetic field measurement below 400 kHz [2]. However, the probe distance was set as 20 cm in this paper (Fig. 1) because the distance between the user and the cooker can be less than 30 cm in the actual

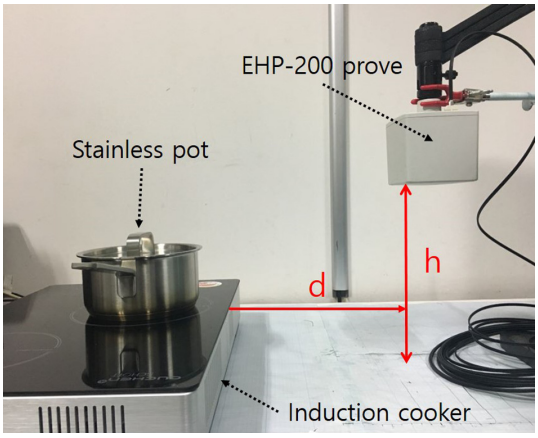

Fig. 1. Induction cooker magnetic field measurement setup (actual measurement distance was $d = 20$ cm).

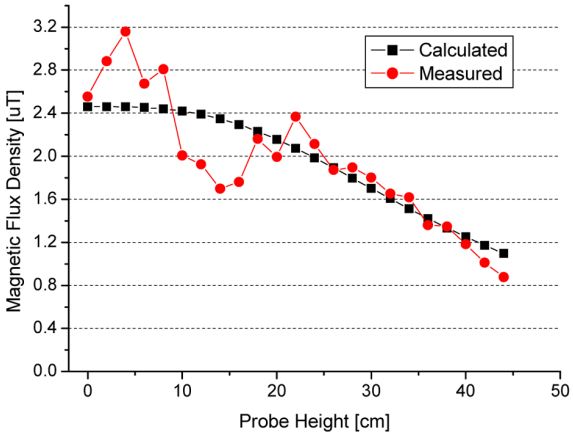

Fig. 2. Magnetic flux density distribution from the induction cooker according to the probe height h.

usage scenario. The vertical position of the probe started from the table surface, and then was increased by 2 cm steps until the height of 44 cm was reached. Narda EHP-200 magnetic field probe was used for the measurement, and the averaging time of the rms magnetic field was 2 minutes. For each probe location, two measurements were made at 2m 20s and 3m 20s after the induction cooker was turned on, and the average value of the two measurements was taken. The cooker was operated at the maximum heating mode with a pot (filled with 800 ml of water) on top of the cooker surface. A wideband measurement was performed (9 kHz – 30 MHz), and the highest magnetic field was found at 28 kHz. Fig. 2 shows the measured magnetic flux density distribution and calculated field from the equivalent source. The equivalent source current of the loop was found that minimizes the squared sum of errors between the calculation and measurement. In the actual operation of the cooker, the coil is periodically turned on and off when the temperature of the coil is too high. Thus, some discrepancies are observed between the measured field values (averaged over 2 minutes) and the calculated ones.

IV. Calculation of the Basic Restrictions in the Human Body Using the Equivalent Source

The equivalent circular loop was used in the Sim4Life software [3] in order to calculate the basic restrictions (induced electric field and induced current density) in the human body. Human model software of IT'IS Foundation (Information Technologies in Society), "Duke" was used in the simulation [4]-[5]. Fig. 3 shows the induced electric field distribution inside the human model. The 99th percentile values of the basic restrictions are summarized in Table I along with their exposure indices with respect to the ICNIRP guidelines.

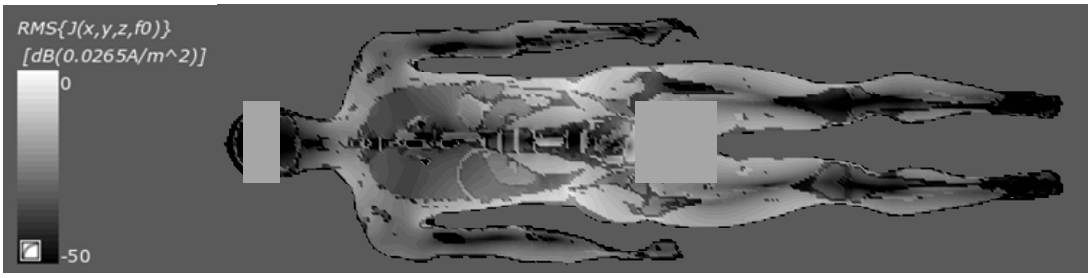

Fig. 3. Induced current density distribution in the human model (Duke) at y-z plane (x=42.8 cm from current loop center).

Table 1. Maximum value and exposure indices of the basic restrictions in the human model (Duke) at 28 kHz.

Basic restrictions	99th percentile value	Exposure limit	Exposure index [%]
Induced electric field E[V/m] (ICNIRP 2010)	0.0342	3.78	0.906
Induced current density J[mA/m^2] (ICNIRP 1998)	9.077	56	16.209

V. Conclusions

The basic restriction values in the human model calculated by the equivalent source were relatively small (0.9-16.2 % of the ICNIRP exposure limits). It is expected that an equivalent source made of multiple concentric circular loops will increase the accuracy of the proposed method.

References

[1] International Standard IEC 62311, IEC, Geneva (2007).

[2] International Standard IEC 62233, IEC, Geneva (2005).

[3] Sim4Life by ZMT (https://www.zmt.swiss).

[4] A. Christ, W. Kainz, E.G. Hahn, K. Honegger, M. Zefferer, E. Neufeld, W. Rascher, R. Janka, W. Bautz, J. Chen, B. Kiefer, P. Schmitt, H.-P. Hollenbach, J. Shen, M. Oberle, D. Szczerba, A. Kam, J. W. Guag, and N. Kuster, Phys. Med. Biol. **55**, N23 (2010).

[5] M.-C. Gosselin, E. Neufeld, H. Moser, E. Huber, S. Farcito, L. Gerber, M. Jedensjö, I. Hilber, F. Di Gennaro, B. Lloyd, E. Cherubini, D. Szczerba, W. Kainz, and N. Kuster, Phys. Med. Biol. **59**, 5287 (2014).

Acknowledgement

This work was supported by the ICT R&D program of MSIT/IITP. [2019-0-00102, A Study on Public Health and Safety in a Complex EMF Environment]

Study of RBCs' Aggregation and Deformability on Pulse Magnetic Field

Seunghwan Bang*, Seonghyun Han, Jinwon Mok, Yukyoung Choi, Minjun Kim, Hyunsook Lee
Department of Oriental Biomedical Engineering, College of Health Science, Sangji University,
Wonju 26339 South Korea

1. Introduction

The human blood circulatory system that supplies nutrients and oxygen are essential for energy metabolism of cells in each tissue. Whole blood is composed of plasma proteins, red blood cells (RBCs), and white blood cell. The aggregation of RBCs (RBCA) and RBCs deformability (RBCD) are morphological features that can facilitate gas exchange as a factor of blood circulation. It is known that many diseases such as angina, myocardial infarction, cardiovascular diseases cause RBCA and RBCD abnormal. [1] Many researches have been done with non-invasive therapies such as electromagnetic field, electrical stimulation, extracorporeal shock waves, and high-intensity focused ultrasound to treat cardiovascular-related diseases. [2] Among them, pulse magnetic field (PMF) stimulation has a positive effect on the improvement of morphological characteristics of RBCs. The purpose of this study is to observe the improvement of RBCA and RBCD according to PMF strength with inducing artificial pathology in RBCs.

2. Method

After the IRB deliberation exemption, whole blood of 3 ml supplied from Gangwon blood bank was centrifuged (3000 rpm, 10 min) twice and only RBCs were extracted with careful removal of plasma and buffy coat. Tert-butyl hydroperoxide (tBHP) to give oxidative stress was used to the extracted RBCs, and verapamil alleviating oxidative stress also was used. Chemically treated RBCs were diluted with plasma protein at hematocrit(Hct) of 45%. PMF stimulus with the intensity of 2700G, 1000G, and 400G was applied to the dilution solution. Erythrocyte sedimentation rate(ESR) is analyzed and compared with various intensity of PMF. In order to observe RBCD, RBCs suspension of 1% Hct using PBS was filtered using pluriStrainer(pluriSelect: Germany) having a pore size of 5μm, and counted the number of RBCs which passed through the filter.

3. Result

In the ESR experiment, distance between the sedimented RBCs and RBC-depleted plasma as a function of time, were measured before and after PMF. It has been found that RBCs exposed to PMF for 3 min. are precipitated slowly. It means that RBCD is improved under PMF exposure with the intensity of 2700G, 1000G, and 400G. In addition, in the filteration experiment, it was confirmed that the number of RBCs passing through the filter increased up to 60% compared to with and without PMF. As a result, PMF stimulation seems to improve RBCA and RBCD. Verapamil treated RBCs has similar effect to the effect of PMF stimulus. The higher PMF strength, the better improvement of RBCA and RBCD. It need more research to determine whether PMF influences the electrical forces between RBCs and plasma proteins based on the experimental results.

References

[1] A.N. Nicolaides, Tikva Horbourne, Rosemary Bowers, P.H. Kidner, E.M. Besterman “Blood viscosity, red-cell flexibility, haematocrit, and plasma-fibrinogen in patients with angina”, (1977).

[2] Kyunghun Shin, Seunghwan Bang, Hyoje Ahn, Hyunsook Lee. “The Change of Capillaroscopic Features under Pulsed Magnetic Field. Journal of Magnetics”, 24(1), 118-122(2019).

A Simulation Study of 3 Dimensional Image Reconstruction for Diabetic Foot imaging based on the Contact Based Near-Infrared Spectroscopy (NIRS)

Mezie Laurence B. Ortiz[1,2,3] and Young-Jin Jung[2,3,4*]

[1]College of Medical Imaging and Therapy, De La Salle Medical and Health Sciences Institute, Cavite 4114, Philippines

[2]Dept. of Multidisciplinary of Radiological Science, Graduate School, Dongseo University, Busan 47011, Republic of Korea

[3]Dept. of Radiological Science, Dongseo University, Busan 47011, Republic of Korea

[4]Center for radiological Environment & Health Science, Dongseo University, Busan 47011, Republic of Korea

E-mail: microbme@outlook.com; Tel. no.: +82-51-320-2871; Fax no.: +82-51-320-2732

Near-Infrared Spectroscopy (NIRS) is an electromagnetic-waves based emerging non-invasive medical imaging technology. NIRS uses non-ionizing radiation to image the soft-tissues in the body focusing on the oxygenated and deoxygenated hemoglobin concentration in the blood. The objective of this study is to show a simulation approach on how to reconstruct a 3-dimensional biological tissue shape models using the contact-based NIRS for Diabetes Mellitus imaging. The result showed that this simulation approach could be of use in the actual reconstruction of a diabetic foot showing absorption coefficient that can serve as biomedical evidence by identifying a hemodynamic response on the diabetic foot tissue. The proposed imaging method can be a useful tool for improving the patient's quality of life.

Keyword: Non-ionizing Electromagnetic wave, Near-Infrared Spectroscopy, Diabetes Mellitus, NIR Tomography, 3D Reconstruction

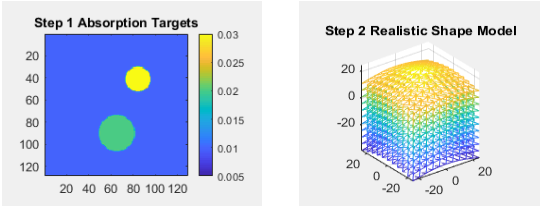

Assumed 2D Biological Tissue Model with Absorption Targets

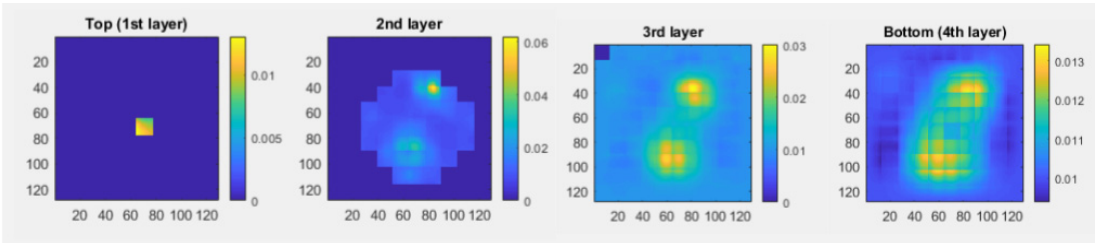

The reconstructed layers of the 3D Biological Tissue Realistic Model with NIR absorption coefficient values (top view)

BM04

Radiation Safety in Videofluoroscopic Swallowing Study: Systematic Review

Jun-Young Hong[1], Ji-Su Park[2*], Gihyoun Lee[3], YoungJin Jung[4]

[1]Department of Multidisciplinary of Radiological Science, Dongseo University, Korea

[2]Advanced Human Resource Development Project Group for Health Care in Aging Friendly Industry, Dongseo University, Korea

[3]Department of Physical and Rehabilitation Medicine, Center for Prevention and Rehabilitation, Samsung Medical Center, Korea

[4]Radiological Science, Dongseo University, Korea

Videofluoroscopic swallowing study (VFSS) is a golden-standard to diagnose dysphagia and oropharyngeal function. Since the VFSS procedure is an X-ray based imaging exam, patients and bolus feeding operators can be irradiated by radiation generated from the X-ray machine as both patient and operator are placed in front of X-ray source. Although the radiation dose from the VFSS procedure is relatively lower than other X-ray imaging modalities, Multiple VFSS procedure may lead to cumulative X-ray irradiation, placing both patient and operator at risk for more radiation induced risk due to increased scan time. Therefore, it is important to summarize procedures radiation safety of the VFSS, and provide it to relevant workers and patients. This study aimed to investigate radiation dose related factors of various protocols, and to summarize dose safety from various VFSS protocols. The PubMed database was explored for relevant publications reporting radiation in the VFSS procedure. 11 articles were selected to be reviewed. This systematic review involved 11 peer-reviewed articles that enunciate the specific dose of the VFSS procedure. The articles were classified into three categories: operator radiation dose, adult patient radiation dose, and pediatric radiation dose. The operator dose reports represented that the operators' scattering exposure, equivalent dose and annual effective dose were significantly lower than the annual dose limit of 20 mSv. Both adult and pediatric patient dose reports represented that the effective dose, which was estimated from recorded dose–area product, was significantly lower than the annual background exposure of 2.4 mSv in various protocols. The present literature review suggested that radiation dose of VFSS by modified barium swallowing is tolerable in both operators and patients. However, various radiation protection strategies should be implemented during the procedure to reduce radiation exposure dose as low as possible.

Keywords: Exposure, Radiation, Videofluoroscopic swallowing study

Fluorescent detection of Bacterial Spores biomarker using Tb^{3+} coordinated Fe_3O_4 Nanoparticles

Thomas Myeongseok Koo[1*], Min Jun Ko[1], Bum Chul Park[2],
Myeong Soo Kim[3], and Young Keun Kim[1*]

[1]Department of Materials Science and Engineering, Korea University, Seoul 02841, Korea
[2]College of Engineering, Research institute of engineering and technology, Korea University, Seoul 02841, Korea
[3]Department of Biomicrosystem Technology, Korea University, Seoul 02841, Korea

Magnetic nanoparticles (NPs) have been widely studied in biomedical applications such as magnetic resonance imaging (MRI), hyperthermia, bio-separation, and diagnosis [1]. In these fields, controllable mobility of the magnetic NPs under the external magnetic field could be a useful tool and low coercivity like superparamagnetism is important to prevent aggregation when the magnetic field is removed [2]. Dipicolinic acid (DPA) is a general biomarker of bacterial spores such as anthracis spore [3]. Lanthanide ions are chelated to DPA easily and the Lanthanide ion-DPA complex has unique and strong fluorescent properties determined by the type of the lanthanide ion [4]. Herein, Fe_3O_4 NPs coordinated by terbium ions (Fe_3O_4-Tb NPs) using carboxyl groups on the surface were used to fluorescent detect DPA. Tb^{3+} are detached from the Fe_3O_4-Tb NPs and chelated with DPA. However, the Fe_3O_4-Tb nanoparticles quenched the fluorescent signal, so we can get the signal using magnetic separation. The used Fe_3O_4-Tb NPs are synthesized by one-pot polyol process and the structure is characterized by transmission electron microscopy (TEM), energy-dispersive X-ray spectroscopy (EDX), X-ray diffraction (XRD), X-ray photoelectron spectroscopy (XPS). Magnetic property is measured by vibrating sample magnetometer (VSM). Above measurements show that the nanoparticles have differences with Fe_3O_4 NPs. Detection limit and specificity to DPA of the Fe_3O_4-Tb NPs are measured using a microplate reader. The Fe_3O_4-Tb NPs have a lower detection limit than the infectious dosage of anthracis.

References

[1] Y. Jun et al., Acc. Chem. Res. 41 (2), 179 (2008)
[2] D. Ling et al., Acc. Chem. Res. 45, 1276 (2015)
[3] X. R. Bai et al., Anal. Chem. 89, 10335 (2017)
[4] M. Donmerz et al., J. Hazard. Mater. 324, 593 (2017)

A study on Performance Test Evaluation of Magnetic and Metal Ceramic Alloy Dental Materials

Seen-Young Kang*, Ji-Min Yu, Hyoung-Sik Kim, Mijung Kim, Ki-Sook Park,
Jae-Won Lee, Seung-Youl Lee†
Medical Device Research Division, National Institute of Food and Drug Safety Evaluation

The purpose of this study is to analyze whether it is possible to scientifically evaluate the safety and performance testing methods associated with the revision of international standards for dental magnetic attachment and metal ceramic alloy items. In this study, we measured the retention force of repeated attachment and detachment of dental magnetic attachments, and measured the physical properties of metal ceramic alloys according to the manufacturing method. As a result, the dental magnetic attachment increased the retention force as the specimen size increased, and the retention force decreased with repeated detachment. Metal ceramic alloys showed a difference in physical properties according to the manufacturing method, and finally, it may be considered that Approval and review can be made through the revised international standard test.

Background

치과용 자성어태치먼트는 수복치의 치관에 고정하거나 가철성 의치를 정확히 안정시키는데 사용된다. 메탈세라믹합금은 손상된 치아의 기능 및 심미성의 회복을 목적으로 심미 보철물의 제작에 사용된다. 본 연구에서는 치과용자성어태치먼트 및 메탈세라믹합금의 국제표준(ISO 13017:2012/Amd1:2015 및 ISO 22674:2016) 개정에 따른 안전성 및 성능시험을 국내 임상환경을 고려한 과학적으로 평가방법을 마련하여 국내 의료기기 허가심사 지원 및 환자의 안전확보를 목적으로 하고자 한다..

Study method

치과용 자성어태치먼트의 시험군 1, 2는 직경 4.4, 4.5 mm 자석구조체와 직경 4.4, 4.5 mm 자석자성재이며, 시험군 3,4,5,6,7은 순서에 따라 4.4, 4.6,4,4.4 mm 자석구조체와 4.2 mm 자석자성재를 준비하였다. 시편은 자성자석구조체와 자석자성재가 접촉하는 면에 접착용 필름을 부착한 뒤, 전용 몰드에 폴리코팅 경화제 혼합용액을 몰드에 부어 경화시킨다. 경화된 시편은 에탄올로 접촉면을 세척하고 접착용 필름 및 잔여물을 제거한다. 유지력 시험은 만능시험기(Instron, Canton, Massachusetts, USA)를 통해 인장력을 인가하여 측정한다. 시험군 1,2,5 는 유사 직경의 치과용 자성어태치먼트 유지력을 비교하였고, 시험군 3,4,5는 접촉면적에 따른 유지력을 비교하였다. 따라서 본 연구에서는 **Fig. 1**과 같은 시험 등을 통하여 안정성과 성능을 검증하였다.

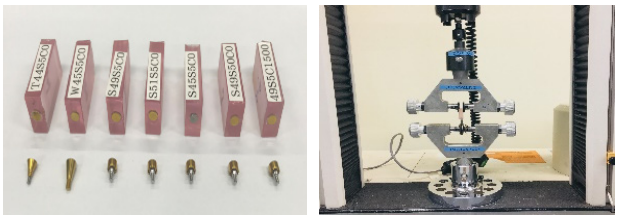

Fig. 1. Test of dental magnetic attachments

메탈세라믹합금의 시편은 ISO 22674:2016을 준용하였으며 STL파일 형식으로 제작하였다. 제조방식은 전통가공 방식, 절삭가공방식, 적층가공방식으로 분류하여 제작하였다. 물리적 특성 시험은 크로스헤드속도 (1.5±0.5) mm/min으로 시편이 파절 될 때까지 인장하중을 가하며, 인장강도, 인장하중, 연신율, 탄성계수를 **Fig. 2.**와 같이 측정하였다.

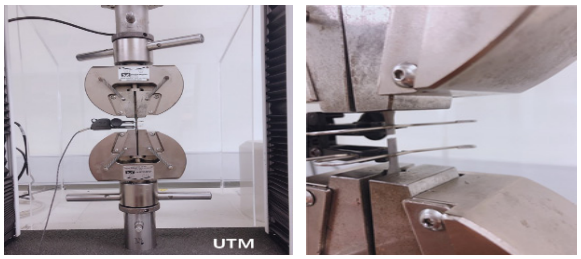

Fig. 2. Test of metal ceramic alloys

Results

치과용 자성어태치먼트의 유지력 시험결과는 **Table 1**과 같다. 시험군 1, 2, 5는 유사 직경의 유지력을 비교하였으며, 시험군 3, 4, 5는 직경의 크기에 따른 유지력을 비교하였다. 시험 간 시편의 크기가 넓어질수록 유지력이 증가하였고, 반복 착탈의 속도에 따라 유지력은 감소하는 것을 나타냈다.

Table. 1 Results of dental magnetic attachment retention force (N/mm^2)

	Retention force (average)	Retention force (size of magnet)
1	1.31±0.20	0.086±0.014
2	1.49±0.17	0.094±0.001
3	2.97±0.88	0.158±0.047
4	3.44±0.97	0.169±0.048
5	2.41±0.75	0.152±0.048
6	1.90±0.23	0.101±0.013
7	3.41±0.73	0.181±0.039

메탈세라믹합금의 연구결과는 **Table 2**와 같이 도출하였다. 전통가공방식과 절삭가공방식의 항복하중, 항복강도, 인장강도는 두 군간의 유의한 차이가 나타나지 않았으나($P>0.05$), 적층가공방식과는 모두 유의한 차이가 나타난다($P<0.05$).

Table. 2 Results according to the manufacturing of metal ceramic alloys.

	Manufacturing methods		
	Traditional method	Subtractive method	Additive method
Yield load [N]	35,841.51	3,152.41	6,387.27
Yield strength [MPa]	500.5	438	966
Tensil strength [MPa]	681	557	1,345
Elongation [%]	10.85	12.50	13.53
Modulus of elasticity [GPa]	226	235	198

Conclusions

치과용 자성어태치먼트는 시편 간의 크기가 넓어질수록 유지력이 증가하고, 반복 착탈의 속도에 따라 유지력 감소를 나타냈다. 또한 메탈세라믹합금은 제조방식에 따라 물리적 특성의 차이가 나타남을 증명하였다. 향후 개정된 시험방법을 통해 향후 허가심사 지원 및 제품의 안전성 및 성능평가에 기여할 것으로 판단된다.

Acknowledgements

본 연구는 식품의약품안전처의 연구개발비(18171MFDS301, 19171MFDS313)로 수행되었으며 이에 감사드립니다.

An InSb-based magnetoresistance biosensor for detecting liver cancer biomaker

Sung Jong Kim[1,2*], Seung-Woo Lee[3], Young-Wan Kwon[1],
Kyung-Jin Lee[1], and Hyun Cheol Koo[1,2]

[1]KU-KIST Graduate School of Converging Science and Technology, Korea University, Korea
[2]Center for Spintronics, Korea Institute of Science and Technology, Korea
[3]Department of Fine Chemistry, Seoul Natinal University of Science and Technology, Korea

The main mechanism of the magnetoresistance sensor is the magnetic field dependence of the resistance and this sensor can be applied to diverse fields. Although the most popular type of magnetoresistance for detecting biomaterial is giant magnetoresistance (GMR) sensor, it has difficulty in mass production due to the complex multilayer structure. In this research, we fabricate the magnetoresistance sensor using InSb semiconductor for diagnosis of liver cancer. InSb is a narrow bandgap semiconductor and has the excellent magnetic properties such as large g-factor and ordinary magnetoresistance. The most fascinating feature of InSb is that the channel resistance is determined by the applied magnetic field as well as the bias current.

In order to detect the antigen, we utilize the sandwich Enzyme-Linked Immunsobant Assay. The detection antibody was covalently paired with Fe_3O_4 nanoparticles, and the capture antibodies were immobilized onto the InSb sensor surface via cross-linkers. After immobilization of the capture antibody on the InSb surface, cancer antigen was carefully placed onto the InSb sensor. After careful washing of the device with deionized water, the detection antibody tagged with Fe_3O_4 nanoparticles was placed on the InSb sensor. Due to the immunospecific binding of the detection antibody to the antigen, the sandwich assay was formed with Fe_3O_4 nanoparticles on the InSb sensor. As the magnetic field is applied, the superparamagnetic Fe_3O_4 nanoparticles, which are attached with sensing area, produce the stray magnetic field. The strength of the stray magnetic field is proportional to the number of nanoparticle which is attached to the antigen. This method is very simple to detect the antigen of any disease and can serve the platform of detecting biomaterials.

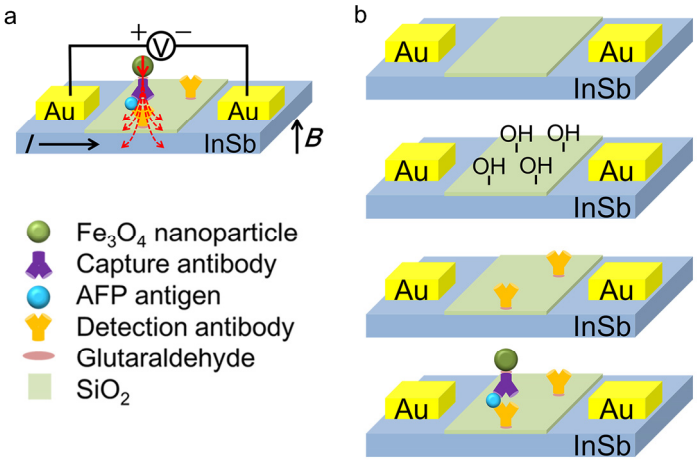

Fig. 1. An InSb-based magnetoresistive biosensor using nanoparticles. (a) Schematic diagram of the biosensor. The curved arrows indicate the stray magnetic field from the nanoparticle. (b) Device fabrication and sensing process.

Performance evaluation of noise reduction algorithms brain T2-weighted magnetic resonance image using newly designed for MRiLab simulation tool

Seong-Hyeon Kang*, Donghyeok Choi, Youngjin Lee
Department of Radiological Science, Gachon University, Korea

The purpose of this study was to investigate the usefulness of the conventional noise reduction algorithms in brain T2-weighted image. To acquire brain T2-weighted image, we used MATLAB software based MRiLab simulation tool, and Gaussian noise was added with standard deviation of 0.005. Then, we modeled conventional noise reduction algorithms, namely, Gaussian filter, Wiener filter, and median filter. In addition, the coefficient of variation (COV) and contrast to noise ratio (CNR) were calculated for quantitatively evaluation. According to the results, the COV and CNR values showed the most improved in the median filter. Especially, COV and CNR values of the reconstructed image with median filter were improved about 1.48 and 1.40 times, respectively, compared to the noisy image. In conclusion, this study has demonstrated that the median filter as conventional noise reduction algorithm can remove the noise efficiency and improve the image characteristics.

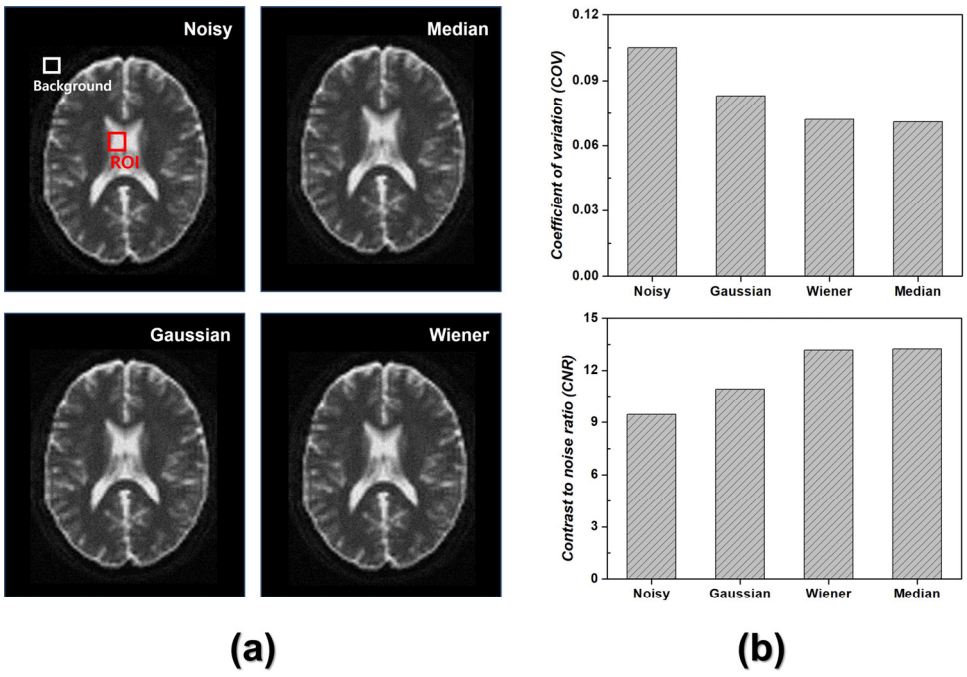

Fig. 1. (a) Reconstructed and noise reduction images by applying various noise reduction algorithms and (b) quantitatively evaluation results

Design and Development of Magnetic Sensor Using a Soft Magnetic Amorphous Wire

Jang-Yeol Kim[1*], Kibeom Kim[2], Hyun Joon Lee[1], Woocheon Park[1], and In-Kui Cho[1]
[1]Radio & Satellite Research Division, ETRI, Daejeon 34129, South Korea
[2]Cho Chun Shik Graduate School of Green Transportation, KAIST, Daejeon 34051, South Korea

Magnetic sensors are the devices that the existence of magnetic field by measuring the absolute value or relative change of the magnitude and the direction of the magnetic field intensity. Nowadays magnetic field sensors are used widely in industry, military, medical treatment, space research, geology, etc [1]. The trend of magnetic sensor development is towards smaller, faster, cheaper, more sensitive and reliable. Among many magnetic sensors, our research group is conducting research to develop the gaint magneto-impedance (GMI) sensor [2,3] and the fluxgate sensor [4,5] for underground or underwater magnetic field communication applications. The proposed GMI sensor has the same structure as fundamental mode-orthogonal fluxgate (FM-OFG) sensor. We are currently conducting research to confirm to possibility of magnetic field communication between GMI sensor and FM-OFG sensor. In this work, we present an off-diagonal GMI sensor and its results for realizing high sensitivity magnetic sensor at receiver unit for magnetic field communication. The GMI sensor is fabricated the soft magnetic material composed Co-Fe-Si-B amorphous ferromagnetic wire of 100μm diameter and the length of 30mm. The solenoid-shaped pickup coil with 250 turns of cu wire with the diameter of 0.1mm was wound around the alumina insulation tube. The amorphous wire was inserted the alumina tube and then it was embedded in PCB substrate. The hysteresis curve experimental result of GMI sensor using the Helmholtz coil at 20MHz showed that the same characteristics as hysteresis curve of soft magnetic material with narrow coercivity of 0.046Oe. The maximum responsivity of GMI sensor was 8.53kV/T of linear range ±100μT with the experimental condition of 20MHz and the excitation AC voltage of $5.5V_{pp}$ and DC bias of $-2.0V_{dc}$. We confirmed the applicability of the GMI sensor for magnetic field communication through the experimental results. Detailed results of the proposed GMI sensor will be presented for a discussion.

Acknowledgements

This work was supported by Institute of Information & communications Technology Planning & Evaluation (IITP) grant funded by the Korea government (MSIT) (No.2019-0-00007, Magnetic Field Communication Technology Based on 10pT Class Magnetic Field for Middle and Long Range)

References

[1] P. Ripka, Magnetic sensors and Magnetometers, Artech House, 2001.
[2] B. Dufay et al, “Characterization of an Optimized Off-Diagonal GMI-Based Magnetometer,” IEEE Sensors J., vol. 13, no, 1, pp. 379-388, 2013.
[3] M. Malátek et al, “Off-diagonal GMI sensor with stress-annealed amorphous ribbon”, Sens. Actuators A: Phys., vol. 164, pp. 41-45, 2010.
[4] S. H. Choi et al, “Orthogonal fluxgate sensor fabricated with a co-based amorphous wire embedded onto surface of alumina substrate”, IEEE Trans. Magn., vol. 47, no. 10, pp. 2573-2576, 2011.
[5] D. Son, “Construction of feed-back type flux-gate magnetometer”, J. Kor. Mag. Soc., vol. 22, no. 2, pp. 45-48, 2012.

Simulation of magnetic field attenuation for telecommunications in water

Jung-Ick Moon*, Sang-Won Kim, Seong-Min Kim, Jaewoo Lee, In-Kui Cho
Electronics and Telecommunications Research Institute, Korea

In this paper, the characteristics of magnetic field attenuation in freshwater and seawater were analyzed for underwater communication using magnetic fields. The attenuation characteristics of the magnetic field were analyzed according to the frequency, salinity, and distance, and the electromagnetic simulation was used for the analysis. In order to improve the accuracy of the simulation, the results were analyzed by comparing the size of the media and the density of mesh element. Therefore, it can be seen that the proper element division and medium size are required as compared with the wavelength for the transmission frequency. It is judged that these results can be used for the design of underwater communication system using magnetic field.

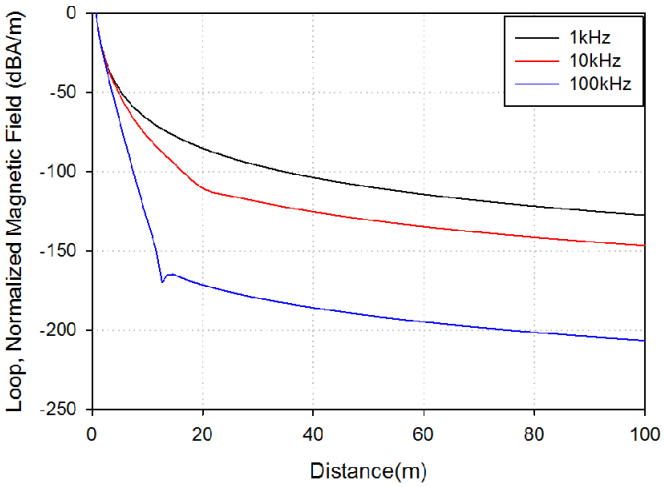

Fig. 1. Normalized magnetic field attenuation in seawater

Acknowledgement

This work was supported by Institute of Information & communications Technology Planning & Evaluation (IITP) grant funded by the Korea government (MSIT) (No.2019-0-00007-001, Magnetic Field Communication Technology Based on 10pT Class Magnetic Field for Middle and Long Range)

Movement detection of magnetic clutch

Kyung-won Kim*, Kwang-ho Shin
Kyungsung University, Korea

A clutch, one of the interior parts of an automobile, serves to transmit or block the power of the engine to the wheels. There are many different types of clutches: friction clutch, fluid clutch, centrifugal clutch and magnetic clutch. In this study, we focused on magnetic clutch. The magnetic clutch operates by generating a corresponding magnetic field when a certain level of current is received. When the magnetic clutch is operated, the physical structure changes. Thus the impedance and inductance of the magnetic clutch also change and we measured this changing impedance and inductance to see if the magnetic clutch is operating. The difference between these impedance and inductance will be electrically checked for the operation of the magnetic clutch.

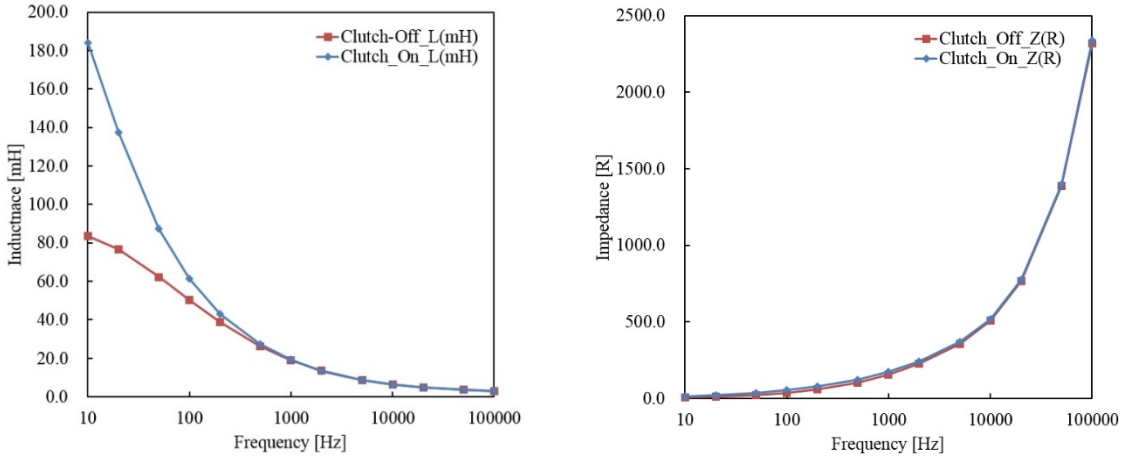

(a) (b)

Fig. 1. The magnetic clutch's (a) Inductance dependence of frequency and (b) Impedance dependence of frequency.

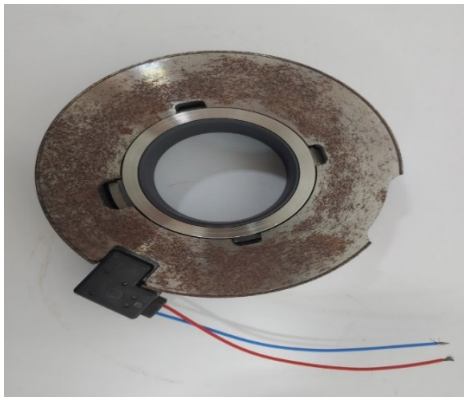

Fig. 2. Magnetic clutch

Wireless power transmission using magnetoinductive wave

Ga-jun Choi*, Kyung-won Kim, Hyeong-geon Kim, Min-seok Kim, Kwang-ho Shin
Kyungsung University, Korea

Wireless power transmission is an energy transmission method that is receiving attention from fourth industrial revolution. These new energy transmission methods include MI wave, MCR, IF, RF and ultrasound. In this study, we investigated MI(magnetoinductive) wave. MI wave could be reducing energy loss when the resonant frequencies were adjusted to be same for all resonators. Fig. 1 shows MI wave circuit diagram in this study. In the case of displacement between the couplings change, the magnetic flux on the coupling also change. This difference will be affective the energy transmission efficiency. Fig. 2 show the measurement of the output voltage by changing the frequency. Fig. 2 (a), (b) and (c) have displacements of 10mm, 15mm and 20mm, respectively. These figures show how energy transmission dependence on displacement of couplings.

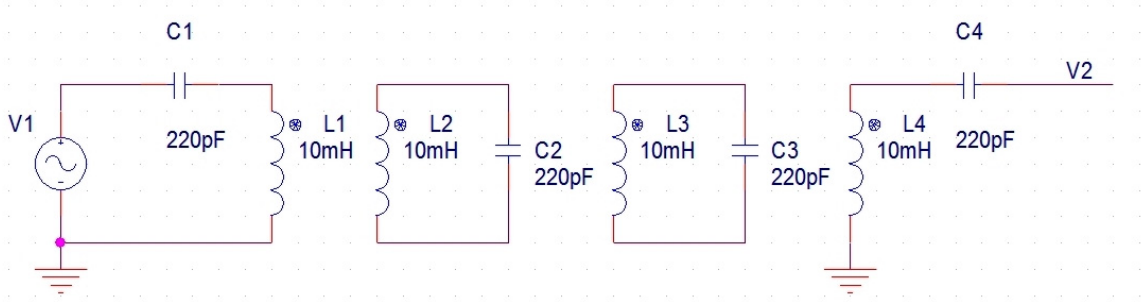

Fig. 1. MI wave circuit diagram.

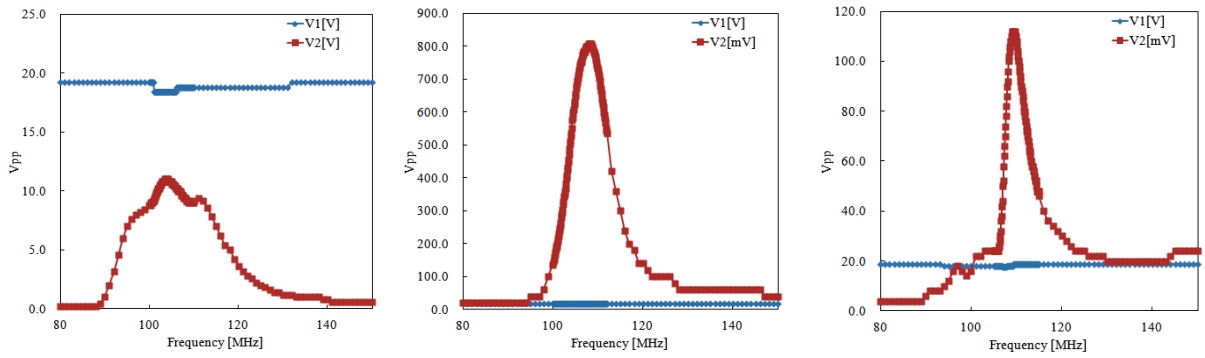

(a) (b) (c)

Fig. 2. Output voltage dependence on fequency.

Fabrication and Analysis of Transferable Planar Hall Magnetoresistance (PHR) Sensor

Taehyeong Jeon*, Mijin Kim, Cheol Gi Kim*
Department of Emerging Materials Science, DGIST, Daegu, 711-873, Republic of Korea

Wearable devices have harvested significant interest over the past decades, because their application range is not only permitted to electrics, electronics and displays but also expanded to bio-applications in implantable types of devices. In particular, manufacturing techniques for wearable devices enable their applicability range in mobile devices, biosensors and soft robots which are the core of information and communication technologies. Recently, commercialized products such as flexible, foldable smart phones and TVs are also emerging.

In addition, as the design of these devices is constantly becoming slimmer and also sensors for mobile electronic components becomes more and more vulnerable to stress or physical deformation. In the future, the flexibility of various sensors such as GPS sensor, geomagnetic sensor, acceleration sensor, gyro sensor is expected to be highly demanded.

In this experiment, we have fabricated transferable magnetic sensors using water soluble polymers as sacrificial substrate. Here, we have transferred magnetic sensor to polymer substrate which has same as human skin and we have also analyzed the performance of magnetic sensors by using the effect on tensile stress due to the curvature of polymer substrates. Furthermore, with simplified models for our transferable magnetic sensors, mechanical and thermal properties were investigated which included measuring stress, reversible bending behavior, and temperature stability.

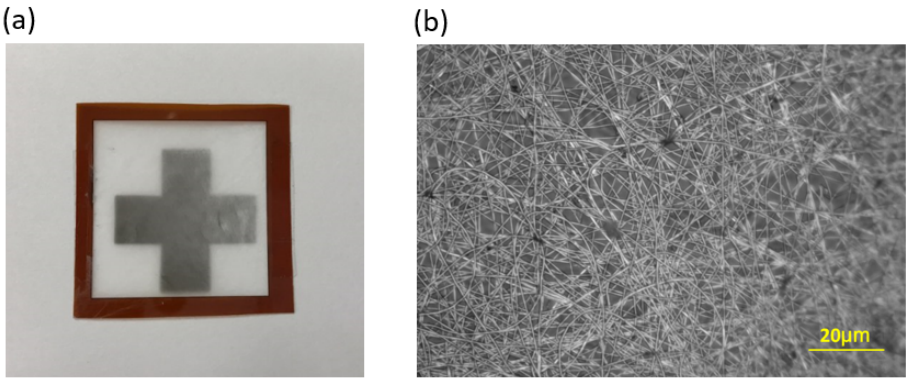

Fig. 1. (a) Image of the transferable magnetic sensor, (b) Microscope image of transferable magnetic sensor.

International Symposium on Magnetism and
Magnetic Materials 2019

Plenary Session II

Present of MRAM development in Samsung

D. S. Kim[1*], K. H. Lee[1], J. H. Lee[1], D. E. Jeong[1], H. C. Shin[1], J. H. Park[1], S. C. Oh[1], J. H. Park[1], S. O. Park[1], B. J. Bae[1], O. I. Kwon[1], K. H. Hwang[1], S. H. Han[2], K. Suh[2], B. Y. Seo[2], Y. K. Lee[2], Y. J. Song[2], S. H. Hwang[2], D. S. Lee[2], Y. S. Ji[2], G. H. Koh[1], G. T. Jeong[2], H. K. Kang[1], and E. S. Jung[2]

[1]R&D Senter, Samsung Electronics Corp, Hwasung, Jorea

[2]S. LSI division, Samsung Electronics Corp, Kiheung, Korea

We recently demonstrated the high manufacturability and robust package level reliability of 8Mb STT-MRAM embedded in 28nm FDSOI logic platform and started mass-production. We will introduce the basic operation and characteristics of STT-MRAM first and the history of MRAM development in Samsung. Also we will present current status of MRAM development and the challenges we have overcome for mass production. Finally near-future technology we have interest in together with the direction of MRAM development will be discussed briefly.

International Symposium on Magnetism and Magnetic Materials 2019

Special Session VI

'Medical Magnetics'

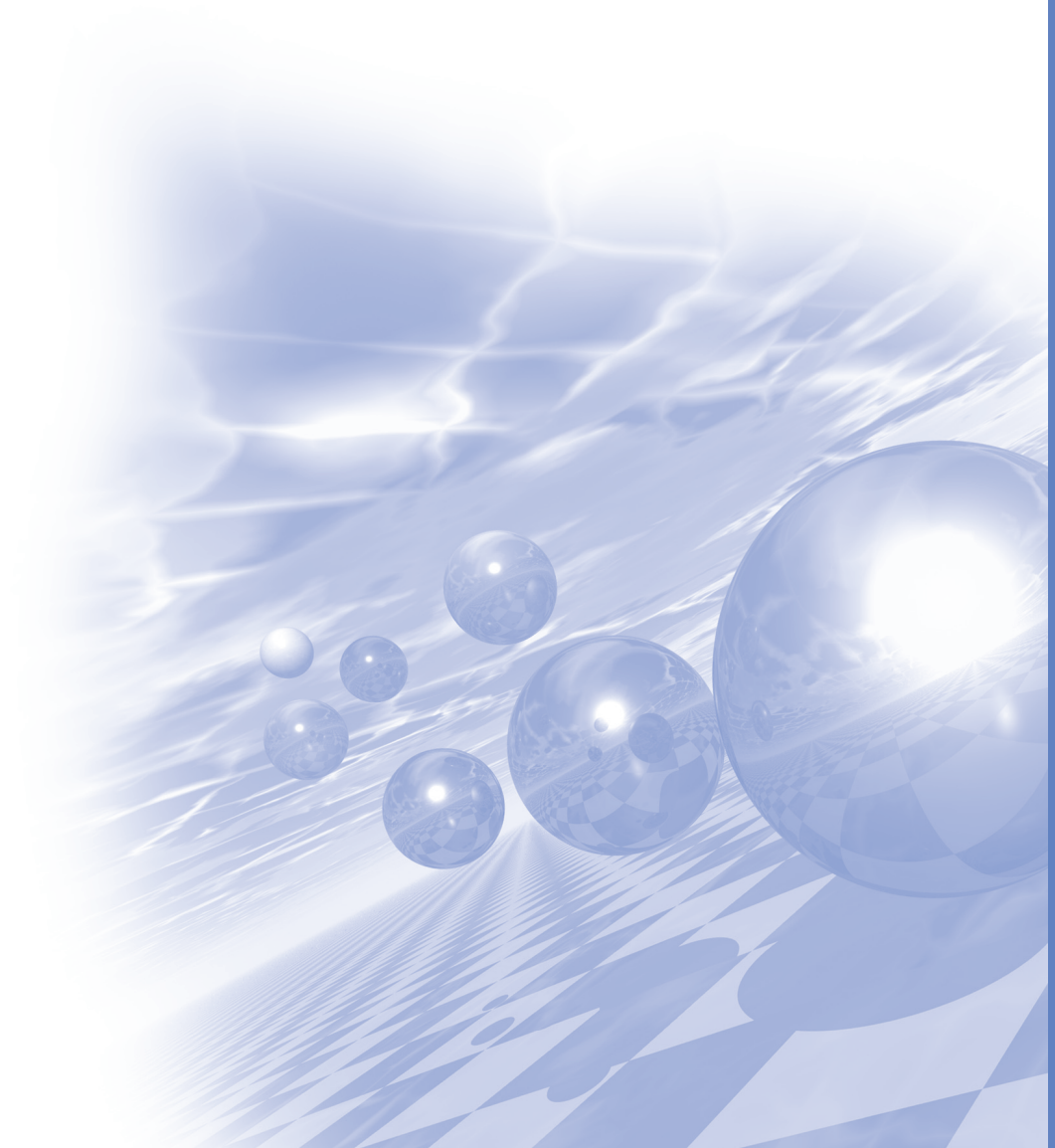

Investigation of transverse magnetic field induced dose effects in inhomogeneous medium on small fields of medical linear accelerator

Woo Sang Ahn[1*], Wonsik Choi[1], Jungwon Kwak[2], In-Hye Jung[1], Seong Soo Shin[1]
[1]Department of Radiation Oncology, Gangneung Asan Hospital,
University of Ulsan College of Medicine, Gangneung 25440, Korea
[2] Department of Radiation Oncology, Asan Medical Center,
University of Ulsan College of Medicine, Seoul 05505, Korea

This work experimentally investigated fluctuations of the dose distributions in inhomogeneous medium in the presence of a transverse magnetic field to the incident photon beam. Two different phantoms consisted of a full water phantom and a water-air-water phantom. The permanent magnets with dimensions of 5 × 5 × 5 cm^3 were arranged on the air region. Depth dose curves with Gafchromic EBT3 self-developing film were measured for 6 and 10 MV photon beams in small fields at SSD (source-to-surface distance) 100 cm with and without a magnetic field of 0.5 T. Depth dose curves showed regions with the enhancement and reduction in the medium. For the field size of 3 × 3 cm^2, the dose to the proximal interface and air region was increased by average 9.8% and 8.9% for 6 and 10 MV photon beams, respectively. The dose to distal air region and interface was decreased by average 5.4% and 5.1% for 6 and 10 MV photon beams, respectively. These dose effects potentially can be used to provide higher doses to the tumor and lower doses to adjacent normal organs in external radiotherapy.

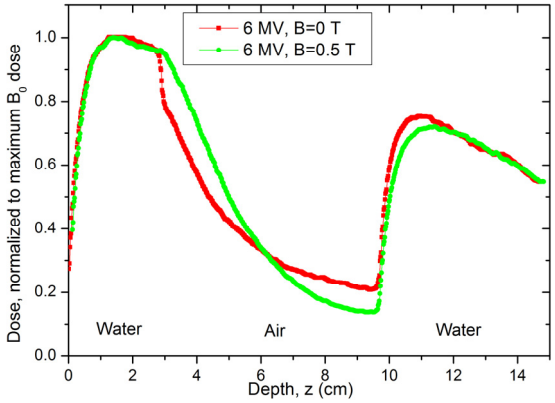

Fig. 1. Depth dose curves on central axis for the field size of 3 × 3 cm^2 of 6 MV photon beam

Fundamental Study on Optimization and Measurement Protocols of Alanine/ESR System

Ki-Tek Han[1*], Woo Sang Ahn[2], Wook Jae Yoo[1], Jeho Min[1], Han-Ki Jang[1†]
[1]Radiation Technology and Research Center, Korean Association for Radiation Application, Korea
[2]Department of Radiation Oncology, Gangneung Asan Hospital, University of Ulsan College of Medicine, Korea

This study is the fundamental research on the development of optimization and measurement protocols of the alanine/ESR system. For accurate and reliable measurement using the alanine/ESR system, the optimization and measurement protocols are necessary. Therefore, we carried out the experiment to develop optimized measurement protocols for the alanine/ESR system. To improve the performance of the alanine/ESR system for dosimetry application, not only the measurement parameters but also the physical conditions, such as a position of sample, must be optimized[1]. Currently, alanine samples manufactured by Bruker and Magnettech are the most widely used in Korea, and thus the experiment for optimizing alanine/ESR system was performed using the alanine samples made by those companies. First of all, the experiment on the optimization of sample position was carried out. Sample position is adjusted by using regulating screw in sample holder. As a result, the optimum locations of alanine sample were 9 mm and 7 mm for the Bruker and the Magnettech samples, respectively. Next, the experiment on the optimization of measurement parameters was performed by adjusting modulation amplitude and sweep time. An increase in modulation amplitude improves SNR but exerts extra burden on the modulation coils and also results in lineshape distortion. To evaluate optimum modulation amplitude, an experiment was performed with varying value from 0.1 to 1 mT at intervals of 0.1 mT. Regardless of the type of alanine sample, when the modulation amplitude value of 0.5 mT was set, it was confirmed that the signal began to be distorted. Therefore, the optimum modulation amplitude was judged by 0.4 mT. In the case of sweep time, the experiment was performed by changing value from 10 to 60 seconds in 10 second increments. As an experimental result, it is appropriate to measure Burker alanine samples for at least 40 seconds and Magnettech alanine samples for at least 50 seconds. In conclusion, the physical conditions and measurement parameters for the optimization of the alanine/ESR system were acquired. Further studies will be carried out to develop the optimization and measurement protocols of the alanine/ESR system using the experimental results of this study.

Acknowledgement

This work was supported by KOREA HYDRO & NUCLEAR POWER Co., LTD (No. 2018-Tech-02).

Reference

[1] R. Ahmad, P. Kuppusamy, Chem Rev. 110(5), 3212 (2010).

Metal artifact reduction of silicon material in head and neck cancer with metal

So Hyun Park*
Department of Radiation Oncology, Jeju National University Hospital,
Jeju University College of Medicine, Jeju, Korea

Purpose: The aim of this study was to investigate materials for reducing metal artifacts in head and neck (H&N) radiotherapy containing high density metals.

Materials and Methods: Computed tomography (CT) images of single and mixed materials used as dental impression materials were acquired, and the hounsfield units (HU) were analysed. Among them, the materials that have been keep same shape and uniformed HU was selected. The dental phantom covered each material which was mixed by the different rates was scanned and the region of interest (ROI) was delineated. The HU of the ROI were evaluated and then, selected material was applied to the simple phantom. In simple phantom, calculated and measured dose were compared for evaluation of the metal artifact reduction material.

Results: When the selected silicon material was covered around the metal, the reduction effect of the metal artifact on the HU value was observed. There were not significant differences between calculation and measurement dose, compared with the homogeneous condition without metal insertion.

Conclusion: Although this study have evaluated the effects of the metal artifact reduction material, further evaluation for the reproducibility and dose accuracy of metal artifact reduction material is needed for clinical use.

A Feasibility Study of Fan-beam DEXA detector based LYSO and GAPD

Jingyu Yang*, Heeseon Heo, Jihoon Kang†
Department of Biomedical Engineering, Chonnam national University

A LYSO-GAPD detector module was proposed for fan-beam DEXA application and was characterized under a variety of conditions. The proposed detector consists of 1 × 8 LYSO array of 3 × 3 × 2 mm^2 discrete crystals and 8 × 8 GAPD array having a 3.07 × 3.07 mm^2 pixels. Energy spectra were acquired using different gamma rays to evaluate the variation of intrinsic energy resolution and photopeak. Dual-energy X-ray spectra were acquired using a K-edge Ce filter and BMD phantom. Also, count rate performance and BMD values were characterized for each step in DEXA phantom. The average photopeaks were 1259 ± 26 and 2603 ± 107 and the average energy resolutions were 25.2% ± 0.5% and 20.1% ± 0.3% for 241Am and 57Co, respectively. The dual energy peaks were located around 32 keV and 65 keV and were clearly isolated. The BMD values for each steps of phantom were clearly identified. These results demonstrate the feasibility of LYSO-GAPD detector allowing more potential merits than conventional CZT detector for fan-beam DEXA application.

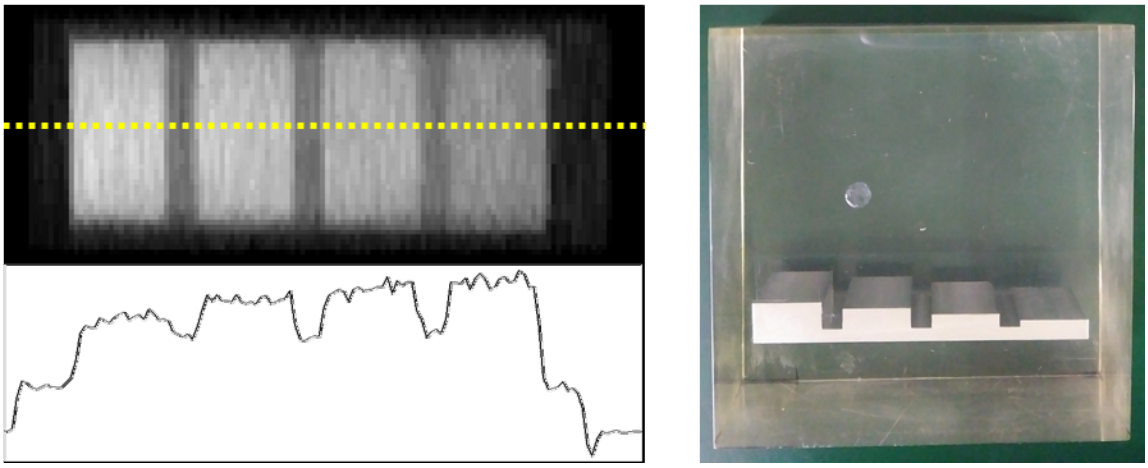

Fig. 1. Acquired DEXA Image (top) and line profile (bottom) for step phantom having different Al thicknesses (right)

Changes according to the lead thickness for Shielding evaluation

Dong-Hee Han[1*], Jong-Hun Won[1], Man-Seok Han[2†], Cheol-Ha Baek[2†]
[1]Department of Health Medical Science, Graduate School, Kangwon National University, Samcheok 25949, Korea
[2]Department of Radiological Science, Kangwon National University, Samcheok 25949, Korea

Radiation is widely used in modern medical and industrial fields. The use of radiation to suit the purpose mainly resulted in benefits. However, there are drawbacks that could affect the human body, which necessitates radiation protection devices, etc. The radiation penetration rate of radiation protection devices used by workers in a wide range of areas where radiation is being used is always an important matter that can affect the human body. In this study, the lead equivalents of the current most commonly used radiation protections devices, 0.25, 0.50, 0.75, 1.00 mmPb, were changed in thickness to 0.02, 0.02, 0.03, and 0.05 mmPb, respectively, to compare differences in radiation penetration rate for each of the leads. Error was confirmed through normalization of results from the Monte Carlo Simulation tool GATE version 8.0 and the results from experiments with lead sheets. As a result, most of the experimental results tended to have greater experimental value than the simulated results, with an average error of 2.004%, with a maximum error of 5.711% at 100 kVp, 0.21 mmPb, and a minimum error of 0.157% at 110 kVp and 0.19 mmPb. It is expected that simulation tools will be available when applying a wider range of energy as well as diagnostic areas in the future to check radiation penetration rates by microlayer thickness and to present the criteria for lead equivalents in the manufacture and sale of radiation protection devices.

Keywords: Radiation Shielding Devices, Microlayer Thickness, Radiation Penetration Rate, Monte Carlo Simulation

Acknowledgement

This research was supported by a grant (19171MFDS337) from Ministry of Food and Drug Safety in 2019.

The effects of motor imagery combined with functional electrical stimulation on cerebral cortex excitability in stroke patients

Jong-Bae Choi[1*], Bo-Kyoung Song[2], Man-Seok Han[3]

[1]Department of Occupational Therapy, KyungHee University Medical Center, Republic of Korea
[2]Department of Occupational Therapy, Kangwon National University, Samcheok, Republic of Korea
[3]Department of Radiological Science, Kangwon National University, Samcheok, Republic of Korea

Purpose: The purpose of this study was to investigate the effect of motor imagery combined with functional electrical stimulation (MI-FES) on cerebral cortex excitability in stroke patients.

METHED: We examined the effect of MI-FES on cerebral cortex excitability using transcranial magnetic stimulation (TMS) of motor evoked potential (MEP) amplitude and latency, quantitative electroencephalography (QEEG) of delta alpha ratio (DAR) and power ratio index (PRI) assessments.

This study was to evaluate 30 stroke patients who were satisfied the selection criteria of the study. Experiments were divided into MI-FES group, motor imagery (MI) group. Following the pre-test, all subjects participating in the study were given traditional physical therapy and occupational therapy for 30 minutes, 5 times weekly, and MI-FES in the experimental group, MI in control group were carried out twice for 20 minutes per day, 5 days a week, for 6 weeks, followed by a post-test.

To evaluate the effects of intervention, a Wilcoxon signed-rank test was used to compare pre- and post-intervention results in each group. The Mann-Whitney *U* test was used to compare changes in outcome measures between the groups.

Results: The results of the pre-test and post-test follow-up prior were evaluated and the following conclusions were drawn.

This study showed that there was a significant difference for all evaluations within the MI-FES group, with significant differences in MEP amplitude and latency, QEEG DAR, and PRI index values in the comparison that those of the MI group.

Conclusions: MI-FES therapy is suggested to be an effective treatment for cerebral cortex excitability and upper extremity recovery in stroke patients.

Keywords: Motor imagery combined with functional electrical stimulation, Motor imagery, Motor evoked potential amplitude, Motor evoked potential latency, Quantitative electroencephalography.

Interplay Effect in Proton Scanning Therapy by Magnetic Scanner

Jeongmin Seo*
Dept. of Radiological Science, Catholic University of Pusan, Korea

Proton therapy is cutting edge technology in clinical radiation oncology. Especially Proton pencil beam spot scanning is one of most advanced techniques in radiation therapy. Proton therapy have two types of shooting radiation. One is scattering type which performed by scatterers, other is scanning type performed by control magnetic scanner. Scanning type use pencil beams which do not consider the movements of organs and targets from breathing.

Radiation therapy planning systems do not properly reflect the interplay effect caused by the independent movement of the beam and the target in the patient. Thus, the interplay effect may cause the delivered radiation dose to deviate from the planned one. This effect has emerged as a topic of significant interest in the field of proton therapy. Previous studies used 10 phases or less of 4D plan were used to represent the continuous respiratory motion, making these dose calculations questionable. It has never been confirmed if these discrete phases properly represent a patient's actual/continuous movement of respiratory motion.

In this study, the respiratory motion was simulated using phantoms and fast 4D dose calculation was performed using a kernel method for investigating proper temporal resolution of 4D calculation in spot scanning by magnetic scanner.

The results of this study suggest a paradigm to reason the appropriate temporal resolution, depending on factors such as amplitudes, for evaluation of interplay effect in spot scanning by magnetic scanner.

International Symposium on Magnetism and
Magnetic Materials 2019

Special Session VII

'High Clarke number element based Supermagnet'
(Closed Session)

The Practical Energy Product of Hard- and Soft-magnetic Core/Shell Cylinder

Namkyu Kim, Hee-Sung Han, Soo Seok Lee, and Ki-Suk Lee*
School of Materials Science and Engineering, Ulsan National Institute of Science and Technology, Ulsan 44919, Republic of Korea

Recently, as the demand for devices using magnetic energy of permanent magnets such as electric cars and wind power generators has increased, research to develop new high-efficiency and low-cost permanent magnets is actively underway. Exchange-coupled magnets are good candidate for high-efficiency permanent magnet by exchange-coupling high anisotropic magnets having low magnetization (hard magnet) with high saturation magnet despite low anisotropy (soft magnet). Such structures are expected to improve energy product as a combination of high coercive force of the hard phase and high saturation magnetization of the soft magnet. In order to apply this advantage to high performance permanent magnets, various types of exchange-coupled magnet have been investigated including multi-layer, mixture, core/shell structure, and so on. Cylindrical core/shell structure is particularly advantageous due to its large interface and versatility at controlling composition and demagnetization factor by dimension. Since the energy product corresponds to the energy stored in the stray field generated by the magnet itself, it must be measured from H_d and B at the remanent state. Thus, we investigated the energy product of the cylindrical core/shell structure considering the demagnetization field, which affect not the maximum energy product, but the practical energy product at zero external field. In this work, we adopted cylindrical core/shell structure composed of the soft magnetic shell (FeCo) and the hard-magnetic core (Sm_2Co_{17}) as a model system. With the model system, we computed minimization of the Gibbs free energy of the model system made up with $2\times2\times2$ nm^3 sized cell, which is smaller than the exchange length of two materials, by using a finite differential micromagnetic solver. To estimate the energy product, the hysteresis loops were calculated by applying external magnetic field ranging from -10 T to 10 T along easy axis and B- and H- fields were obtained directly from them. The model consists of a hard-magnetic core having the dimension of maximizing the theoretical energy product is enveloped by diverse thickness of the soft magnetic shell, and the energy product and nucleation field calculated. We finally expanded the model to array structure of the cylindrical core/shell, and the results show great prospect for applying to bulk permanent magnet with high value of energy product at sophisticatedly controlled dimension.

First-Principles Materials Design of Rare-Earth Free Permanent Magnets with High Energy Product and Good Thermal Stability

D. Odkhuu[1,2*], T. Ochirkhuyag[1], and S. C. Hong[3†]

[1]Department of Physics, Incheon National University, Incheon 22012, South Korea

[2]Institute of Physics and Technology, Mongolian Academy of Sciences, Ulaanbaatar, Mongolia

[3]Department of Physics, University of Ulsan, Ulsan 44610, South Korea

[*]odkhuu@inu.ac.kr

[†]schong@ulsan.ac.kr

The α"-phase $Fe_{16}N_2$ has received intensive attention since the first report on its giant magnetic moment of 3 m_B per Fe in 1972 [1]. This surprisingly large magnetic moment, in addition to high Curie temperature (T_c) and cheap materials price, would make it a potential candidate for rare-earth (RE) free permanent magnet applications. However, there are two major obstacles that hamper practical implementation of α"-$Fe_{16}N_2$: (1) Poor thermal stability and small uniaxial magnetic anisotropy (K_u). Herein, employing first-principles prediction and rigid-band analysis, we demonstrate an extremely large K_u up to 3 MJ·m^{-3} in α"-$Fe_{16}N_2$ by replacing Fe with Zn, a value more than 60% of K_u (4.9 MJ·m^{-3}) attained for RE-included best permanent magnet $Nd_2Fe_{14}B$ [2], while improving thermal stability. Such a supreme K_u can be attributed to the mutual mechanisms of the Jahn-Teller orbital splitting and excess electron-induced energy level changes in the rigid-band selection rule. Moreover, we reveal that the replacement by Ti in addition to Zn can improve the thermal stability further by an order of magnitude in terms of the standard enthalpy of formation without much suppressing K_u. We will also discuss on possibilities of simultaneous improvement of the thermal stability and K_u with the replacement by the other 3*d*-metal and metalloid elements, where Al and Si replacement elements are in particular emphasize. These results provide an instructive guideline for simultaneous improvements of the thermal stability and energy product in 3*d*-only permanent magnets without RE or heavy-metal elements.

References

[1] T. K. Kim, M. Takahashi, Appl. Phys. Lett. 20, 492 (1972).

[2] M. Sagawa, S. Fujimura, H. Yamamoto, Y. Matsuura, and S. Hirosawa, J. Appl. Phys. 57, 4094 (1985).

This research was supported by Future Materials Discovery Program through the National Research Foundation of Korea (NRF) funded by the Ministry of Science and ICT (2016M3D1A1027831).

The effect of grain size, grain boundary materials, and grain boundary thickness on the magnetic properties of Fe-based magnetic materials

Ho-Sup Kim*, Sang-Soo Oh, Jeong-Hyeon Jo
Korea Electrotechnology Research Institute, Changwon, Kyungnam, 641-120, Korea

The effects of grain boundary material, grain size and grain boundary thickness on magnetic materials were investigated. The magnetic material FeCo was deposited on a MgO-IBAD substrate using a co-evaporation method. In order to control grain size and grain boundary thickness, experiments were conducted using substrate temperature, composition ratio as process variables. It was confirmed that the grain size decreases as the deposition temperature increases for the same thickness. Also, the lower the deposition temperature, the smaller the grain boundary spacing was. The results showed a similar tendency regardless of the composition ratio. We investigated the effect of grain boundary material on the magnetic properties. Samples with different FeCo grain size and grain boundary spacing were prepared on the IBAD substrate. Each Cu, SmCu, Mg, Al material was deposited on the sample as a grain boundary material and then heat-treated at 800 degrees. The surface morphologies of samples were measured using SEM, and the cross-sectional images were measured using TEM. In addition, magnetic properties were measured using PPMS. Through the above measurements, it was confirmed that the grain boundary material, grain size and grain boundary thickness had a significant influence on the coercive force of the magnetic material.

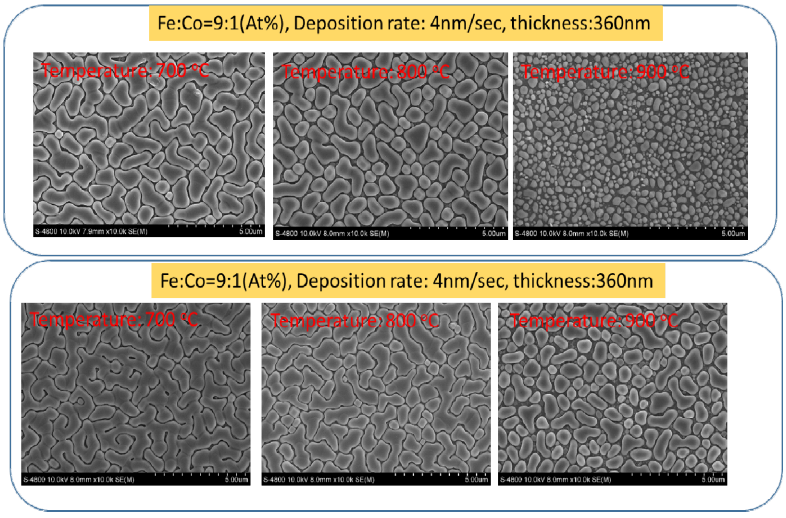

Fig. 1. Grain size and grain boundary thickness depending on the deposition rate and substrate temperature of FeCo thin film

Synthetic methods for magnetically enhanced rare-earth free MnBi magnets

Jong-Woo Kim[1*], Yang Yang[1,2], Jihoon Park[1], Jung Tae Lim[1], Chul-Jin Choi[1]
[1]Powder & Ceramics Division, Korea Institute of Materials Science (KIMS), Republic of Korea
[2]School of Materials Science and Engineering, Pusan National University, Republic of Korea

Recent research on developments of new permanent magnets, especially rare-earth free candidates are current emerging issues of industry as well as academic research for the growing market demands. Among the rare-earth free permanent magnets, MnBi have attracted tremendous attention for its strong magnetocrystalline anisotropy and high energy product [1]. In addition, the intermetallic MnBi compound in its low-temperature phase (LTP) shows high uniaxial positive temperature coefficient of coercivity. At high temperature, MnBi LTP shows higher coercivity as compared with other rare-earth magnets. Therefore, MnBi is referred as a potential candidate for high-temperature application [2].

In this study, a novel fabrication method for MnBi alloys and its advantages will be discussed. A detailed optimization process and mass synthetic process of MnBi powder via 'bottom-up' process which has advantages for industrial applications will be emphasized. In addition, structural and magnetic property variations according to the elements doping to enhance MnBi's magnetic property will be shown [3]. Furthermore, effective post processing method for control of microstructure, grain-boundary diffusion and finally, enhancement of magnetic property will also be discussed. The optimized process for remarkably high maximum energy product, $(BH)_{max}$ of more than 13 MGOe, which is reasonable value for permanent magnet applications will be emphasized in a perspective of next generation permanent magnet markets.

References

[1] J. Cui et al., Acta Materialia **158** (2018) 118-137
[2] J. Park et al., Metals **4** (2014) 1-11
[3] Y. Yang et al., J. Alloys and Compounds **769** (2018) 813-816

Fabrication of Powder Making and Bulk Process for Fe Rich Magnetic Compound with $ThMn_{12}$ Structure

Jihoon Park*, Hui-Dong Qian, Jung Tae Lim, Jong-Woo Kim, and Chul-Jin Choi†
Powder & Ceramic Division, Korea Institute of Materials Science, Changwon, Gyeongnam, 51508, South Korea

Fe-rich compound with tetragonal $ThMn_{12}$ structure have been extensively studied as a potential high performance permanent magnetic material due to its high saturation magnetization of 1.43 T, anisotropy field of 10.9 T and Curie temperature of 800 K [1]. D However, its low intrinsic coercivity, its use as a permanent magnetic material is limited. Therefore, in this work, we have developed a new fabrication method to produce microstructure refined high density $Sm(Fe_{0.8}Co_{0.2})Ti$ bulk magnet.

Virgin alloys by prepared by arc-melting, followed by melt-spinning the alloys to produce amorphous $Sm(Fe_{0.8}Co_{0.2})_{11}Ti$ ribbons. The ribbons pressed to produce green bodies, and the green bodies were annealed at 800 ^{o}C for times ranging from 10 to 20 min.

The fabricated $Sm(Fe_{0.8}Co_{0.2})_{11}Ti$ bulk sample exhibits coercivity of 3912 Oe and maximum energy product $(BH)_{max}$ of 8.65 MGOe, as shown in Fig. 1, which is much higher than the reported 5 MGOe [2]. By microstructure analysis, it was found that the enhanced coercivity and $(BH)_{max}$ are originated from the precisely controlled grains which is close to single domain size. The details of the fabrication procedure, microstructure and magnetic properties will be discussed.

References

[1] Y. Hirayama, Y. K. Takahashi, S. Hirosawa, and K. Hono, Scr. Mater. **138**, 62 (2017).

[2] Tetsuji Saito, Fumiya Watanabe, and Daisuke Nishio-Hamane, J. Alloys Compd. **773**, 1018 (2019)

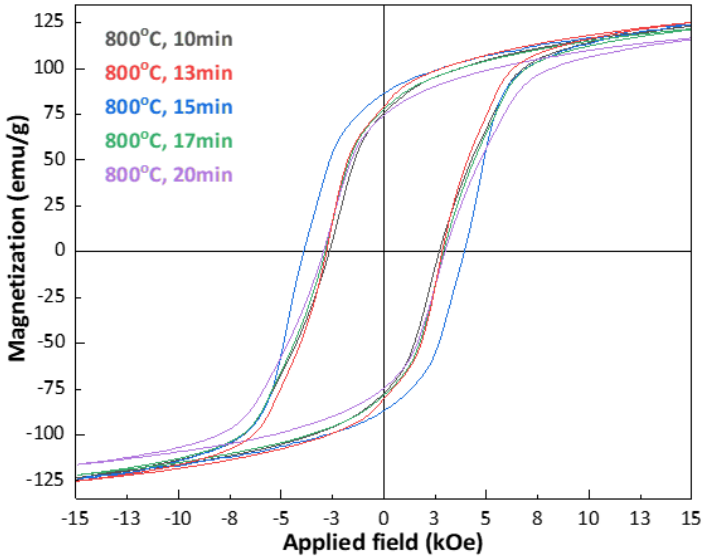

Fig. 1. Magnetic hysteresis loops of $Sm(Fe_{0.8}Co_{0.2})_{11}Ti$ bulk samples with different annealing time.

Synthesis and Characterization of $ThMn_{12}$-type by nitridation reaction

Kang-Hyuk Lee, and Sang-Im Yoo*
Department of Material Science and Engineering, Research Institute of Advanced Materials (RIAM),
Seoul National University, Seoul, Korea

The $ThMn_{12}$-type structure has attracted attention as permanent magnetic material due to the high anisotropy field, saturation magnetization (M_s), and Curie temperature (T_C). The Sm-Fe-Co-Ti materials have been intensively studied in an effort to synthesize high permanent magnets by controlling the doping element. In this study, we tried to investigate B and N doped Sm-Fe-Co-Ti materials prepared by nitridation reaction. we prepared the $Sm(Fe_{0.8}Co_{0.2})_{11}Ti$ ribbons were used high-purity Sm (99.95%), Fe (99.99%), Co (99.95%), and Ti (99.95%) as starting materials and were prepared by using arc-melting and melt spinning methods. The as-prepared ribbons were heat-treated at 800-900 ℃ for 10 - 20 min in Ar gas. The as-crystallized ribbons were heated at 450 - 700 ℃ for 10 - 20 min in 1% H2/N2 gas. Samples were characterized by using x-ray diffractometer (XRD) with Cu-Kα radiation source, vibrating sample magnetometer (VSM) and scanning electron microscopy (SEM). The samples were obtained $ThMn_{12}N$-type phase at 450 ℃ for 10 - 20 min in 1% H_2/N_2 gas. Detailed microstructures and magnetic properties of Sm-Fe-Co-Ti-N(BN) will be presented for a discussion

Acknowledgements

This research was supported by Future Materials Discovery Program through the National Research Foundation of Korea(NRF) funded by the Ministry of Science and ICT (2016M3D1A1027835).

Control of morphology in hard magnetic Sm-Co nanofibers

Minkyu Kang, Jimin Lee, Gyutae Lee, EunJae Lee, Yong-Ho Choa and Jongryoul Kim*
Department of Materials Science and Chemical Engineering, Hanyang University, Ansan, 15588, South Korea

Recently, attention has been focused on improving the magnetic properties of permanent magnet materials for miniaturization and high efficiency of equipment. In order to improve the energy product ($(BH)_{max}$) of permanent magnet materials, high coercivity and remanence magnetization properties are required. Therefore, it is necessary to develop the rare earth hard magnetic material having high magnetic moment and magnetocrystalline anisotropy properties. Recent permanent magnet studies have focused on Nd-Fe-B and Sm-Co having high energy. In addition, In order to improve the magnetic properties, studies are being actively made to produce single domain size one-dimensional structures using shape anisotropy as well as magnetic anisotropy of materials. We also tried to fabricate meso-scale Sm-Co one-dimensional structure, but there was no dramatic improvement was seem because of the random distribution of crystal grains in the Sm-Co nanofibers and the nanofibers were entangled. Thus, we aimed the aspect ratio and shape control of Sm-Co nanofibers.

Sm-Co nanofibers are fabricated by electrospinning process, calcination and reduction-diffusion process. The prepared nanofibers were analyzed for magnetic properties and morphology according to pulverization conditions.

As a result, aggregation of nanofibers was solved without loss of saturation magnetization of Sm-Co. These results clearly demonstrated the possibility of improving the properties of multilayered one-dimensional structures under the control of morphology of nanofibers.

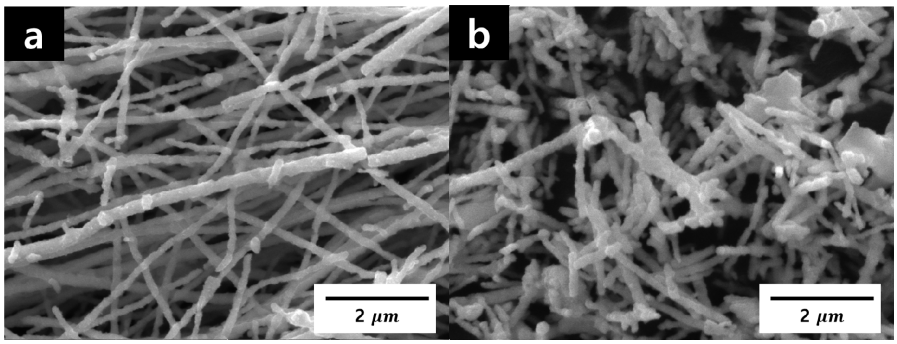

Fig. 1. FE-SEM micrographs of (a) as and (b) pulverized Sm-Co nanofibers

Author Index

Digests of the International Symposium on Magnetism and Magnetic Materials 2019

The Korean Magnetics Society

International Symposium on Magnetism and Magnetic Materials 2019 Vol. 29, No. 2.

#905 KSTC, (Yeoksam-dong) 22, 7gil, Teheran-ro, Gangnam-gu, Seoul 06130, Korea

TEL. (02)3452-7363, **FAX.** (02)3452-7364

E-mail. komag@unitel.co.kr, **Home-page.** www.komag.org